THEORETICAL AND EXPERIMENTAL STUDIES OF MICELLIZATION AND PHASE BEHAVIOR OF AQUEOUS SOLUTIONS OF SINGLE AND MIXED SURFACTANTS

by

SUDHAKAR PUVVADA

B. Tech., Chemical Engineering,
Indian Institute of Technology, Madras (1986)

M.S. in Chemical Engineering Practice
Massachusetts Institute of Technology (1989)

Submitted to the
Department of Chemical Engineering
in partial fulfillment of the requirements for the degree of

DOCTOR OF SCIENCE
IN CHEMICAL ENGINEERING

at the

MASSACHUSETTS INSTITUTE OF TECHNOLOGY

JANUARY 1992

Signature of Author _____
Department of Chemical Engineering

Certified by _____
Professor Daniel Blankschtein
Thesis Supervisor

Accepted by _____
Professor William M. Deen
Chairman, Departmental Graduate Committee

THEORETICAL AND EXPERIMENTAL STUDIES OF MICELLIZATION AND PHASE BEHAVIOR OF AQUEOUS SOLUTIONS OF SINGLE AND MIXED SURFACTANTS

by

SUDHAKAR PUVVADA

Submitted to the Department of Chemical Engineering on
January 9, 1992 in partial fulfillment of the requirements for the
Degree of Doctor of Science in Chemical Engineering

ABSTRACT

A molecular-thermodynamic approach to describe and predict micellization and phase behavior of aqueous micellar solutions is presented. The theoretical approach consists of blending a thermodynamic theory, that describes the salient features of micellar solutions at the macroscopic level, with a molecular model of micellization that describes the essential physical factors controlling micelle formation and growth at the molecular level.

The thermodynamic theory consists of evaluating the Gibbs free energy of the micellar solution and incorporates the salient characteristics of these complex fluids including (i) the self-assembling and dynamic nature of micellar aggregates, (ii) the broad micellar size and composition distribution, (iii) intermicellar entropic contributions, and (iv) intermicellar interactions which drive phase separation phenomena.

The molecular model of micellization incorporates the effects of solvent properties and surfactant molecular structure on the numerical magnitude of the various intramicellar contributions which control micelle formation and growth. These contributions include (i) the hydrophobic effect, (ii) conformational effects associated with packing of the surfactant hydrophobic moieties in the micellar core, (iii) curvature-dependent interfacial

effects at the micellar core-water interface, (iv) steric and electrostatic interactions between the surfactant hydrophilic moieties, and (v) intramicellar entropic contributions associated with mixing the various surfactant species in a mixed micelle.

The molecular-thermodynamic approach is then utilized to predict a broad spectrum of micellar solution properties as a function of surfactant type, concentration and composition, as well as temperature and the presence of solution modifiers such as urea. The predicted properties include (i) the critical micellar concentration, (ii) the micellar size and composition distribution and its characteristics including the weight-average aggregation number and the relative variance, (iii) the average micellar composition, (iv) the micellar shape, (v) the coexistence curve bounding the two-phase region of the phase diagram including the critical concentration, and (vi) other thermodynamic properties such as the osmotic pressure and the osmotic compressibility.

The theoretical approach provides an accurate description of a wide range of experimental findings in aqueous solutions of (i) single nonionic surfactants belonging to the alkyl polyethylene oxide (C_iE_j) family, (ii) the nonionic surfactant $C_{12}E_6$ in the presence of urea, and (iii) binary mixtures of C_iE_j nonionic surfactants. The theoretical approach is also utilized to make qualitative predictions of micellar properties for various other aqueous solutions containing binary mixtures of nonionic-ionic, zwitterionic-ionic, anionic-cationic, and hydrocarbon-fluorocarbon surfactants.

Finally, in a related investigation, the peculiarities of osmotic pressure measurements of self-assembling micellar solutions have been examined. Specifically, it has been shown that traditional methods of measuring and analyzing osmotic pressure of micellar solutions yield the weight-average micellar aggregation number rather than the generally accepted number-average aggregation number. The implications of this surprising new result regarding the extent of micellar growth have been examined.

Thesis Supervisor: Dr. Daniel Blankschtein

Title: Associate Professor of Chemical Engineering

ACKNOWLEDGEMENTS

I thank my advisor, Professor Blankschtein, for his support, criticism, and guidance during my stay here at MIT. His enthusiasm was a constant source of inspiration during the difficult periods of this thesis. He has been most willing to spend time with me; he gave me an opportunity to get a glimpse of his way of thought, his diligence, and his approach to research and writing papers.

I also thank Profs. Benedek, Hatton and Merrill for their insightful suggestions and helpful comments. They patiently listened to my long talks, asked the right questions and guided me in the right direction.

I owe a lot of thanks to Prof. Giuseppe Briganti for patiently teaching me about the various laboratory equipment. My discussions with him were very useful in generalizing and extending the scope of my research.

I thank Doo Soo Chung and Henry Thomas for teaching me the art of light scattering.

To Leah Abraham, I owe special thanks for the careful and detailed phase diagram measurements.

I thank Prof. Overbeek for the quick understanding and the subsequent insightful questions about various aspects of my research.

Without the help of Igal Szleifer, I would have spent a lot of time calculating the effects of chain conformations.

I owe special thanks to Chia-Li, Claudia, Leo, Mark, Nick, Pak, Teresa, and Yvonne who have been more my friends than my colleagues. Our discussions ranging from the origin of the universe to cooking brought some sense of order and balance in my thoughts. They have been very supportive and helpful throughout my stay here. From each one of them, I learnt some invaluable aspect of life and research which I will treasure through my life.

I also owe thanks to lots and lots of people, both here and at home, for their affection and support during the last five years. But for them, this thesis would not have

been completed. I take this opportunity to thank them in some random order:
my wife, Veena for her love, support and encouragement, the great food, and for tolerating my poor correspondence before our marriage,
my father and mother, for their encouragement, guidance and concern,
my brother Krishna and sister Padma for their affection and encouragement,
Suresh for being a very good friend and for his support and help at those difficult times,
Raghu and Nandini for their encouragement, timely advice and the relaxing christmas parties,
Subodh and Aparna for the great dinner parties and for their advice, both technical and personal,
Paul for all the jokes and the squash games,
David for being a great roommate, a very good friend, and for all the innumerable discussions we have had,
Dipak and Sunita for their help with Sangam and being such good friends,
Varda, Ramprasad and Prasanna for helping me adjust to the culture shock,
Ganesh and Vishak for their good humor,
Bhavik for teaching me that life is not just research alone,
Laxman for keeping me in touch with India and its culture,
Nishikanth for all the "discuss anything and everything" sessions,
the Basketball Gang for letting me throw bricks,
Kanth and Shaku for their support and advice,
Joy and Gordon for all those inspiring after-hour discussions,
Surya, Bhava, and Ashok for being such good friends and for the memories of our drive from Texas to California,
John Cremin for teaching me my way around the machine shop, and
Finally, I would like to acknowledge the financial support from the Center for Materials Science and Engineering at MIT which funded the work leading to this thesis.

To my Parents and my wife Veena
for their love, patience, and support.

All actions take place in time by the interweaving of the forces of nature, but the man lost in selfish delusion thinks that he himself is the actor.
But the man who knows the relation between the forces of nature and actions, sees how some forces of Nature work upon other forces of Nature, and becomes not their slave.

From the Gita

TABLE OF CONTENTS

LIST OF FIGURES

LIST OF TABLES

CHAPTER 1

INTRODUCTION

1.1 UNIQUE CHARACTERISTICS OF SURFACTANT SOLUTIONS

Surfactants are molecules composed of a hydrophilic moiety (*head*) which is soluble in water and a hydrophobic moiety (*tail*) which is not. This unique duality towards an aqueous environment leads to a rich spectrum of complex self-association phenomena which simpler solute molecules do not exhibit (for comprehensive experimental and theoretical surveys see Mittal, 1977; Mittal and Lindman, 1984; Corti and Degiorgio, 1985). This spectrum includes monolayer formation at air-water, air-oil, and oil-water interfaces, micelle formation in surfactant-water mixtures, and microemulsion formation in surfactant-water-oil mixtures.

In polar solvents such as water surfactant molecules initially migrate to the air-water interface where they collect to form a monolayer in which the hydrophobic tails are oriented away from the aqueous phase (to reduce the unfavorable contact with water) while the hydrophilic heads are immersed in it. Because of their ability to concentrate at interfaces, as monolayers, surfactants are capable of reducing both surface and interfacial tensions. Furthermore, surfactants are also capable of emulsifying nonpolar organic compounds, for

example, oils, in aqueous solutions, or vice-versa, because of their ability to reduce interfacial tensions between oil and water.

As the surfactant concentration is increased, the interfaces become saturated with surfactant molecules, and consequently it becomes thermodynamically favorable for these molecules to self-associate, within the bulk of the solution, into colloidal aggregates called micelles. In these aggregates, the hydrophilic heads remain exposed to water and shield the hydrophobic tails in the interior from the unfavorable contact with water. Micelle formation is typically accompanied by a large decrease in the free energy of the solution. However, localization of the surfactant molecules in a micelle reduces the entropy of the solution. The competition between these two effects gives rise to a threshold concentration called the critical micellar concentration (CMC), below which surfactant molecules are predominantly dispersed as monomers and above which they predominantly form micelles. The onset of micellization at the CMC is marked by a sudden change in many physical properties of the solution including surface tension, electrical conductivity, optical turbidity, and osmotic pressure.

Micelles can appear in sizes ranging from tens to thousands of monomers. Typically, the smaller micelles are spheroidal in shape while the larger ones grow into one-dimensional cylindrical aggregates or into two dimensional discoidal aggregates or bilayers. A salient feature of micellar aggregates is that their shape and size are not necessarily fixed, and significant morphological changes can be induced by varying the total surfactant concentration, surfactant composition, temperature, pressure, ionic strength, pH, and other solution conditions. Furthermore, micelles are dynamic entities which are continually and

reversibly exchanging monomers with one another, a process that can generate an entire distribution of micellar sizes and compositions. The resulting distribution and any equilibrium property derived from it can respond in a reversible manner to changes in solution conditions.

Another important characteristic of many surfactant solutions is that they exhibit the phenomenon of phase separation at relatively low surfactant concentrations above the CMC. In this phenomenon, a single isotropic micellar phase (characterized by no positional or orientational long-range order) separates into two isotropic micellar phases which have different surfactant concentrations and, in the case of mixed micellar solutions, can also have different surfactant compositions. Phase separation can be induced by varying solution conditions such as temperature, pressure, surfactant composition, or surfactant concentration. The resulting coexistence curves (binodals) usually exhibit a pronounced asymmetry between the concentrated micellar-rich and dilute micellar-poor branches.

Surfactants used in commercial applications essentially always consist of a mixture of two or more surfactants. This is because of the higher cost associated with producing isomerically pure surfactants and also because surfactant mixtures often exhibit properties which are superior to those of the constituent single surfactants. Indeed, the CMC's of certain surfactant mixtures have been found to be substantially smaller than the CMC's of the constituent single surfactants due to synergistic (attractive) interactions between the surfactants. Antagonistic (repulsive) interactions between surfactants in certain mixtures lead to mixture CMC's which are larger than the constituent single surfactant CMC's. In general, synergistic and antagonistic interactions between the various surfactant species

present in the mixture can modify significantly the solution properties of the surfactant mixture, including their ability to reduce interfacial tensions, the characteristics of the micellar size and composition distribution, and the phase behavior and phase equilibria associated with these complex fluids.

The unique characteristics of micellar solutions, as described above, arise because weak physical forces, rather than the strong valence forces that lead to chemical bonding, are primarily responsible for micelle formation. These forces include hydrophobic interactions, hydrogen bonding and hydration, interfacial interactions, steric repulsions, and electrostatic interactions. Typically, the magnitudes of these forces, and thus the characteristic properties of micellar solutions, can be easily altered by modifying solution conditions, for example, by changing temperature, pressure, surfactant concentration and composition, or by adding solution modifiers such as salts and urea.

1.2 SURFACTANT APPLICATIONS

The many unique features of surfactant solutions are reflected and exploited in a wide range of industrial and technological applications. Surfactants are among the most versatile products of the chemical industry, and are utilized in such diverse applications as detergency, wetting, flotation, enhanced oil recovery, emulsification, lubrication, and surfactant-based separation processes. They are also widely used in the pharmaceutical industry and in the fields of chemical kinetics and biochemistry. As such they appear in diverse products ranging from detergents and other cleansing agents, motor oils, drilling

muds and flooding agents used in the petroleum industry, and flotation agents used in the mining industry. The global consumption of surfactants in 1990 has been estimated to be about 16.3 billion pounds. In addition, surfactants occur naturally in the human body and are essential in many biomedical processes including cholesterol solubilization and transport, and cell membrane formation.

1.3 BRIEF THEORETICAL BACKGROUND

A theoretical understanding of the rich variety of micellar solution phenomena described above represents an outstanding problem. To date, all theoretical advances have proceeded along two very different, seemingly unrelated, directions.

On the one hand, significant efforts have been devoted to understand micelle formation and micelle structure. In particular, for single-surfactant solutions, the phenomenological theory of micellization (Tanford, 1980), the geometric packing theory (Israelachvili et al., 1976), the molecular theory (Nagarajan and Ruckenstein, 1977), and the mechanical theory (Eriksson et al., 1985a; Eriksson and Ljunggren, 1985b) have contributed significantly to our understanding of micellization. For mixed surfactant solutions, the mixture critical micellar concentration (CMC) has been described (Lange, 1953; Shinoda, 1954; Clint, 1975; Holland and Rubingh, 1983) in the context of the regular solution theory (Guggenheim, 1952) using an empirical interaction parameter. A better understanding of the molecular origin of the interaction parameter was provided by the molecular theory of Nagarajan (1985). Although the approaches described above have contributed to a better

understanding of micellization, they were developed for concentrations near the CMC, where intermicellar interactions are negligible, and are thus these approaches are incapable of describing the phase behavior and phase separation phenomena observed at higher surfactant concentrations, where intermicellar interactions play a dominant role. In addition, these theoretical approaches are not predictive and utilize empirical parameters obtained from the measured CMC values.

On the other hand, very little effort has been devoted to understand the solution behavior at higher surfactant concentrations where, as stated above, intermicellar interactions become increasingly important and can induce phase separation. In particular, thermodynamic phenomenological theories (Blankschtein et al., 1985 and 1986; Kjellander, 1982) and statistical liquid-state theories (Reatto and Tau, 1984) have been developed for this purpose. These approaches successfully *describe* the phase behavior characteristics of micellar solutions, but cannot describe the solution behavior near the CMC. More importantly, these approaches are not *predictive* in nature and utilize empirical parameters obtained by fitting to experimental data.

Additional theoretical background will be presented in the Introductions of each of the following chapters.

1.4 MOTIVATION AND RESEARCH GOALS

It is evident that, so far, there has been no attempt to develop a *unifying* theoretical approach capable of *self-consistently* describing the two, seemingly disparate, phenomena of

micellization and phase behavior within a *single coherent computational framework*. This immediate need, coupled with the tremendous practical importance of micellar solutions, has motivated and guided the direction of the investigation reported in this thesis. Specifically, this investigation constitutes an effort to understand and systematically calculate the *numerical magnitude* of micellar solution properties as a function of (i) the molecular structure and composition of the surfactants, (ii) solution conditions such as temperature, and (iii) the presence of solution modifiers such as urea.

To this end, we have developed a molecular-thermodynamic approach which consists of blending a *molecular model of micellization* (Puvvada and Blankschtein, 1990a and 1990b), which captures the essential physical factors controlling micelle formation and growth at the *molecular level*, with a *thermodynamic theory* (Blankschtein et al., 1985 and 1986; Puvvada and Blankschtein, 1991a), which captures the salient features of these complex fluids at the *macroscopic level*. The molecular model of micellization utilizes information, which is readily available experimentally or can be estimated using *statistical mechanics* or *scaling-type arguments* (Puvvada and Blankschtein, 1990a), about surfactant molecules, water, and additives. This information includes the chemical nature and size of the surfactant hydrophilic and hydrophobic moieties, values of interfacial tensions between hydrocarbon and solvent (water and any additives), and values of the transfer free energies of hydrocarbons from solvent to bulk hydrocarbon. In addition, the value of the free-energy change associated with hydrocarbon-chain packing inside the micellar core is needed.

To test the validity and range of applicability of the proposed theoretical approach, we have compared its predictions with experimental measurements. These measurements

include (a) the critical micellar concentration (CMC) using surface tension, (b) the average micellar hydrodynamic radius using dynamic light scattering, and (c) cloud-point temperatures and coexistence curves using a thermo-regulated optical cell and chromatography. The proposed molecular-thermodynamic approach provides an excellent description of a wide range of experimental findings in aqueous solutions of (i) single nonionic surfactants belonging to the alkyl polyethylene oxide (C_iE_j) and glucoside families (see Chapter 2), (ii) the nonionic surfactant $C_{12}E_6$ in the presence of urea (see Chapter 3), and (iii) binary mixtures of C_iE_j nonionic surfactants (see Chapter 5). Furthermore, the theoretical approach is also utilized to make qualitative predictions (see Chapter 4) of micellar properties for various other aqueous solutions containing binary mixtures of nonionic-ionic, zwitterionic-ionic, and anionic-cationic surfactants, as well as hydrocarbon-fluorocarbon based surfactants. In addition, aspects of the theoretical framework are utilized to rationalize some unexpected findings regarding osmotic pressure measurements of self-assembling micellar solutions (see Chapter 6).

Finally, it is important to stress how the philosophy behind the theoretical formulation described in this thesis differs from earlier investigations of aqueous micellar solutions. First, contrary to most previous studies in this field, in this investigation we have stressed the importance of providing *self-consistent quantitative predictions* of a broad spectrum of micellar properties over a wide range of solution conditions. Indeed, we have made predictions for surfactant mole fractions ranging from 10^{-6} to 10^{-2}, and temperatures ranging between 0-100°C for a number of surfactant systems (Puvvada and Blankschtein, 1990a and 1990b). Second, the theoretical framework has been utilized (Briganti et al.,

1991) to understand and quantitatively predict the effect of solution modifiers, such as, urea (up to 6M) on micellar properties of aqueous solutions of the nonionic surfactant $C_{12}E_6$. Finally, for the first time, the theoretical approach has also been used (Puvvada and Blankschtein, 1991a and 1991b, Puvvada et al., 1991c) to understand and quantitatively predict the behavior of aqueous solutions of binary surfactant mixtures as a function of (i) the nature of the surfactants comprising the binary mixture, (ii) the mixture composition, and (iii) temperature.

The remainder of the thesis is organized as follows. In Chapter 2, we describe the molecular-thermodynamic theory for single-surfactant solutions, and then utilize this theory to predict and compare, with experimental data, micellar properties of aqueous solutions of nonionic surfactants belonging to the alkyl polyethylene oxide (C_iE_j) and glucoside families. In Chapter 3, we describe and predict the effect of urea on micellar properties of aqueous solutions of $C_{12}E_6$. Subsequently, in Chapter 4, we extend the thermodynamic theory to describe micellar solutions of binary surfactant mixtures. The generalized theory is then utilized to make qualitative predictions of the effects of surfactant type and composition on the properties of mixed micellar solutions. In Chapter 5, we extend the molecular model of micellization to describe mixed micelle formation in aqueous solutions of surfactant mixtures. Subsequently, we blend the molecular model of mixed micellization with the thermodynamic theory of mixed micellar solutions described in Chapter 4, and the resulting generalized molecular-thermodynamic theory is utilized to predict and compare, with experimental data, micellar properties of aqueous solutions of binary mixtures of nonionic surfactants belonging to the C_iE_j family. In Chapter 6, we examine the peculiarities of

osmotic pressure measurements of self-assembling micellar solutions, and discuss how our findings impact the interpretation of these measurements in the context of micellar growth. Finally, in Chapter 7, we present some concluding remarks. A list of cumulative references for this thesis is presented in Chapter 8.

1.5 REFERENCES TO CHAPTER 1

Blankschtein, D.; Thurston, G.M.; Benedek, G.B. *Phys. Rev. Lett.* **1985**, *54*, 955.

Blankschtein, D.; Thurston, G.M.; Benedek, G.B. *J. Chem. Phys.* **1986**, *85*, 7268.

Briganti, G.; Puvvada, S.; Blankschtein, D. *J. Phys. Chem.* **1991**, *95*, 8989.

Clint, J.H. *J. Chem. Soc. Faraday Trans. 1*, **1975**, *71*, 1327.

Corti, M.; Degiorgio, V.; Cantu, L. *in Physics of Complex and Supermolecular Fluids*, Safran, S., Clark, N.; Eds.; Wiley: New York, **1987**, p. 463.

Eriksson, J.C.; Ljunggren, S.; Henriksson, U. *J. Chem. Soc. Faraday Trans. 2*, **1985a**, *81*, 833.

Eriksson, J.C.; Ljunggren, S. *J. Chem. Soc. Faraday Trans. 2*, **1985b**, *81*, 1209.

Goldstein, R.E. *J. Chem. Phys.* **1986**, *84*, 3367.

Guggenheim E.A. *Mixtures: The Theory of the Equilibrium Properties of Some Simple Classes of Mixtures, Solutions and Alloys*; Clarendon:Oxford, **1952**.

Holland, P.M.; Rubingh, D.N. *J. Phys. Chem.* **1983**, *87*, 1984.

Israelachvili, J.N.; Mitchell, D.J.; Ninham, B.W. *J. Chem. Soc. Faraday Trans. 2*, **1976**, *72*, 1525.

Kjellander, R.; *J. Chem. Soc. Faraday Trans. 2*, **1982**, *78*, 2025.

Lange, V.H. *Kolloid, Z.* **1953**, *96*, 131.

Mittal, K.L., Ed.; *Micellization, Solubilization and Microemulsions*, Plenum: New York, 1977, Vols. 1 and 2.

Mittal, K.L.; Lindman, B. Eds.; *Surfactants in Solution*, Plenum: New York, **1984**, vols. 1, 2, and 3.

Nagarajan, R.; Ruckenstein, E. *J. Colloid Interface Sci.* **1977**, *60*, 221.

Nagarajan, R. *Langmuir*, **1985**, *1*, 331.

Puvvada, S.; Blankschtein, D. *J. Phys. Chem.* **1989**, *93*, 7753.

Puvvada, S.; Blankschtein, D. *J. Chem. Phys* **1990a**, *92*, 3710.

Puvvada, S.; Blankschtein, D. *Proceedings of the 8th International Symposium on Surfactants in Solution*; Mittal, K.L., Shah, D.O., Eds.; Plenum: New York, **1990b**, in press.

Puvvada, S.; Blankschtein, D. *J. Phys. Chem.* **1991a**, *submitted.*

Puvvada, S.; Blankschtein, D. *J. Phys. Chem.* **1991b**, *submitted.*

Puvvada, S.; Chung, D.S.; Thomas, H.; Blankschtein, D.; Benedek, G.B. *J. Phys. Chem.* **1991c**, in preparation.

Reatto, L.; Tau, M. *Chem. Phys. Lett.* **1984**, *108*, 292.

Shinoda, K. *J. Phys. Chem.* **1954**, *58*, 541.

Tanford, C. *The Hydrophobic Effect*, Wiley:New York, **1980**.

CHAPTER 2

THEORETICAL ANALYSIS OF SINGLE-SURFACTANT SOLUTIONS

2.1 INTRODUCTION

As described in Chapter 1, aqueous micellar solutions of single surfactants are currently the subject of intense experimental study (Mittal, 1977; Mittal and Lindman, 1984; Degiorgio and Corti, 1985). Consequently, a growing body of detailed information is becoming available on micelle formation and growth, micellar size distribution, critical micellar concentration, and micellar phase behavior including phase separation. In view of these experimental developments it becomes increasingly necessary to construct a theoretical approach capable of unifying the rich variety of seemingly unrelated experimental findings into a single coherent computational framework. The central aim of this thesis, as stated in Chapter 1, has been to contribute to this much needed theoretical unification.

In spite of recent significant advances in our understanding of the nature of intermolecular forces (Israelachvili, 1985), we do not yet possess all the required microscopic information to carry out a purely statistical-mechanical calculation of the partition function

and associated free energy of a micellar solution. Needless to say, such a calculation would also involve formidable computational challenges.

Instead of following a purely microscopic route, we have developed a new theoretical approach which consists of blending a molecular model of micellization (Puvvada and Blankschtein, 1990; Blankschtein and Puvvada, 1990), which captures the essential physical factors that drive micellization at the molecular level, with a thermodynamic theory of phase behavior and phase separation of single-surfactant micellar solutions (Blankschtein et al., 1985 and 1986), which captures the salient features of the micellar solution at the macroscopic level. The resulting molecular-thermodynamic approach provides a powerful computational tool which can be used to predict a broad spectrum of equilibrium thermodynamic properties of aqueous micellar solutions over a wide range of surfactant concentrations and other solution conditions such as temperature. These predictions range from individual micellar properties such as the CMC and the micellar size distribution, to collective micellar properties reflected in the phase behavior and phase separation phenomena.

The molecular model of micellization, inspired by the work of Tanford (1974 and 1980) and Nagarajan and Ruckenstein (1977 and 1979), constitutes an effort to systematically calculate the magnitude and temperature dependence of the essential physical factors involved in the process of micellization. For this purpose, we have extended previous work by including the following important new elements:

(1) A detailed multi-step thought process to "visualize" micellization (see Figure 2.1), which permits a clear identification, description and calculation of the free-energy changes

associated with each intermediate step of the process, and therefore provides a convenient tool to evaluate the free energy of micellization.

(2) A systematic quantitative account of curvature effects on the interfacial component of the free energy of micellization.

(3) A numerical evaluation of the free-energy change associated with hydrocarbon-chain packing for different micellar shapes.

(4) An explicit calculation of the "optimum" equilibrium values of the micellar-core minor radius, l_c^*, and the free energy of micellization, g^*_{mic}, for a given micellar shape, which requires minimizing g_{mic} with respect to l_c.

(5) A computational procedure to determine whether the micelles exhibit two-dimensional, one-dimensional, or no growth, and an interpolation scheme to evaluate the free energy of micellization associated with the deduced form of growth.

(6) A capability to predict the temperature variation of micellar solution properties including the CMC and the micellar size distribution.

In addition, we have developed simple scaling-type arguments to evaluate the magnitude and temperature dependence of the molecular parameters which characterize the architecture of the surfactant molecule, for example, the conformation adopted by the hydrophilic chain-like moiety of alkyl polyethylene oxide (C_iE_j) nonionic surfactants.

The proposed molecular-thermodynamic approach is capable of predicting (1) the critical micellar concentration and its dependence on temperature, (2) the micellar size distribution as a function of temperature, (3) the critical surfactant concentration for phase separation, and (4) other thermodynamic properties such as the osmotic compressibility. All

these predictions have been tested in aqueous solutions of several nonionic surfactants belonging to the C_iE_j and glucoside families over a wide range of surfactant concentrations (typically, CMC < X < 500CMC) and temperatures, and were found to be in excellent agreement with the experimental data.

The remainder of this chapter is organized as follows. In Section 2.2 we review the central elements of a recently developed thermodynamic theory of phase behavior and phase separation of isotropic single-surfactant micellar solutions. In Section 2.3 we present a detailed description of the molecular model of micellization. In Section 2.4 we blend the molecular model of micellization with the thermodynamic theory to obtain the proposed molecular-thermodynamic approach, and describe the evaluation of equilibrium thermodynamic properties. Section 2.5 presents a comparison of the theoretical predictions with experiments conducted in aqueous solutions of several nonionic surfactants. Finally, Section 2.6 presents our concluding remarks.

2.2 THERMODYNAMIC THEORY OF SINGLE-SURFACTANT MICELLAR SOLUTIONS

In this section we review a recently proposed thermodynamic theory of phase behavior and phase separation of isotropic micellar solutions (Blankschtein et al., 1985 and 1986). Consider a solution of N_s surfactant molecules and N_w water molecules in thermodynamic equilibrium at temperature T and pressure P. If the concentration of surfactant exceeds the critical micellar concentration (CMC), then, due to surfactant association, a distribution of micellar sizes $\{N_n\}$ is formed, where N_n denotes the number

of n-type micelles (n-mers). In the spirit of the multiple-chemical equilibrium model (Corkill et al., 1969; Mukerjee, 1972), different micellar sizes are treated as distinct chemical species in equilibrium with each other and with the monomers. The total Gibbs free energy of the solution, G, is modelled as the sum of three contributions: the free energy of formation G_f, the free energy of mixing G_m, and the free energy of interactions between the various components G_i, that is,

$$G = G_f + G_m + G_i \ . \tag{2.1}$$

The total Gibbs free energy can then be analyzed using the methods of equilibrium thermodynamics to predict a broad spectrum of thermodynamic properties of the micellar solution. Below we briefly describe each contribution to the total Gibbs free energy.

2.2.1 Free Energy of Formation

The free energy of formation is expressed as

$$G_f = N_w \mu_w^o + \sum_n N_n \mu_n^o \ , \tag{2.2}$$

where μ_w^o(T,P) is the free-energy change of the solution when a water molecule is added to pure water, and μ_n^o(T,P,sh,l_c) reflects the free-energy change of the solution when a single aggregate characterized by shape sh, aggregation number n, and micellar-core minor radius l_c, is placed at a given position in bulk water. Note that μ_w^o and μ_n^o are commonly referred

to as the standard-state chemical potentials of water and n-mers, respectively. Using the surfactant material balance equation, $\Sigma_n nN_n = N_s$, Eq. (2.2) can be rewritten as

$$G_f = N_w\mu_w^o + N_s\mu_1^o + \sum_n nN_n g_{mic}(sh,n,l_c), \tag{2.3}$$

In Eq. (2.3), $g_{mic}(sh,n,l_c) = (\mu_n^o/n - \mu_1^o)$, represents the change in free energy when a surfactant molecule is transferred from a given position in bulk water to a stationary micelle, characterized by sh, n, and l_c, in bulk water, and thus reflects the propensity of a micelle to form and then grow. In this thesis, this free-energy change will be referred to as the *free energy of micellization*. For notational convenience we will omit hereafter the arguments sh, n, and l_c appearing in g_{mic}, unless it is explicitly required. Note that g_{mic} summarizes the many complex physico-chemical factors that are responsible for micelle formation and growth including (Tanford, 1980; Nagarajan and Ruckenstein, 1977; Ben-Shaul et al.; 1985; Gruen, 1985) hydrophobic, steric and electrostatic interactions, and conformational and interfacial effects which are described in more detail in Section 2.3. Note that g_{mic} does not include contributions from the solution entropy of mixing and intermicellar interactions.

2.2.2 Free Energy of Mixing

The free energy of mixing is modelled as

$$G_m = kT\,[N_w \ln(X_w) + \sum_n N_n \ln(X_n)], \tag{2.4}$$

where $X_w = N_w/(N_w+N_s)$ is the mole fraction of water, $X_n = N_n/(N_w+N_s)$ is the mole fraction of n-mers, and k is the Boltzmann constant. $-G_m/T$ models the entropy of mixing of the formed micellar aggregates, the monomeric surfactant molecules, and the solvent. The expression in Eq. (2.4) reflects the number of geometric configurations that describe the positions of micelles, monomers and water molecules in the solution as a function of the relative proportions of each of these constituents. These relative proportions are represented by the mole fractions X_w and $\{X_n\}$. The expression for G_m in Eq. (2.4) does not reflect explicitly the shape and flexibility of the micellar aggregates.

2.2.3 Free Energy of Interaction

A mean-field type expression is adopted to model interactions between the formed micellar aggregates, monomeric surfactant molecules and water molecules, and is given by

$$G_i = -\frac{1}{2} C N_s \phi, \tag{2.5}$$

where ϕ is the total volume fraction of surfactant and C(T,P) is a phenomenological parameter that reflects the magnitude of the effective intermicellar attraction. The interactions summarized in G_i drive phase separation. In essence, G_i represents the free-energy change when a micelle is removed from pure water, which is the reference solution for defining G_f, and placed in the presence of other micelles and monomeric surfactant molecules in the solution. This mean-field type approximation neglects the details of the local environment seen by a micelle and therefore, as can be seen from Eq. (2.5), does not depend explicitly on micellar shape and size.

The thermodynamic consequences of adopting the Gibbs free-energy model reviewed above have been examined (Blankschtein et al., 1985 and 1986; Thurston et al., 1986). Using the necessary expressions derived from Eqs. (2.1)-(2.5) it was possible to predict a broad spectrum of equilibrium thermodynamic properties which includes (i) the micellar size distribution, (ii) the spinodal curve including the critical point, (iii) the coexistence curve, and (iv) the osmotic compressibility.

It is essential to emphasize that all these predictions depended explicitly on the values of the free energy of micellization, g_{mic}, and the phenomenological interaction parameter, C. These two *unknown* contributions were obtained by *fitting* the predicted coexistence curve to an experimentally measured coexistence curve. Subsequently, these fitted numerical values were used to self-consistently predict other micellar solution properties such as the average micellar size and the osmotic compressibility. Excellent agreement was found with independently conducted experiments (Blankschtein et al., 1986).

It is quite clear that the thermodynamic theory described above could become even

more valuable if we could minimize the need to fit the theory to experiments in order to obtain the two unknown contributions, g_{mic} and C. Indeed, it would be highly desirable to develop molecular models to evaluate g_{mic} and C utilizing available information about surfactant molecular architecture and solvent properties. We have begun the first step in this direction by developing a molecular model for g_{mic}. A detailed description of this model is presented in the next section.

2.3 MOLECULAR MODEL OF MICELLIZATION

2.3.1 General Considerations

As stated in Section 2.2.1 the free energy of micellization, $g_{mic}(sh,n,l_c)$, represents the free-energy change (per monomer) required to form an n-mer, having shape sh, core minor radius l_c, from n individual monomers in water. Its magnitude reflects many complex physico-chemical factors such as the hydrophobic effect, hydrogen bonding, conformational free-energy changes associated with hydrocarbon-chain packing, and steric and electrostatic interactions between the hydrophilic surfactant moieties (head groups) (Tanford, 1974; Nagarajan and Ruckenstein, 1977; Israelachvili et al., 1976).

Significant progress has been made over the last two decades in our fundamental understanding and capability to model micellization (for a comprehensive review see Mittal, 1977; Mittal and Lindman, 1984; Corti and Degiorgio, 1985). Of most pertinence to the

present work are the phenomenological theory of Tanford (1974 and 1980) and the statistical-thermodynamic theory of Nagarajan and Ruckenstein (1977 and 1979).

In his seminal work, Tanford (1974) decomposed the free energy of micellization into an attractive contribution associated with the hydrophobic effect, and a repulsive contribution associated with head-group repulsions. The attractive contribution was evaluated from available experimental data on the free energy of transfer of an alkyl chain from water to bulk hydrocarbon. To this attractive contribution was added a repulsive correction reflecting the partial contact of the hydrocarbon chains with water. The attractive contribution was further adjusted, to improve agreement with experimental CMC values, by assuming that the micellar-core minor radius, l_c, was approximately 0.8 times the fully extended hydrocarbon-chain length, l_{max}. Head-group repulsions of ionic surfactants were modelled explicitly using the Debye-Huckel equation. Other repulsive contributions, for example, steric, present in both ionic and nonionic surfactants, were estimated empirically using either experimental CMC values or monolayer-compression data. Using this semi-empirical approach it was possible to predict the observed trends in surfactant solution characteristics including CMC's and aggregation numbers.

Nagarajan and Ruckenstein (1977) extended Tanford's phenomenological approach by formulating a statistical-thermodynamic theory which clarified the physical origin of the various attractive and repulsive contributions to the free energy of micellization. In particular, they stressed the essential role of non-electrostatic steric head-group repulsions in micellization of nonionic surfactants. They modelled this repulsive contribution using an excluded-volume type description. In addition, they included an empirical

correction,obtained by fitting to CMC data, to account for contributions due to hydrocarbon-chain packing. The same empirical correction was used regardless of micellar shape. Using this formulation they were able to predict the CMC and characteristics of the micellar size distribution, such as, the average micellar aggregation number, for a variety of aqueous surfactant systems with or without added electrolyte.

It is important to emphasize that the two approaches described above were aimed primarily at describing individual micellar properties in the vicinity of the CMC. Consequently, the micellar solution was modelled as being ideal, that is, intermicellar interactions were neglected. In order to model the collective micellar solution phase behavior at higher surfactant concentrations, where the micellar solution can exhibit phase separation, it is essential to incorporate the previously neglected intermicellar interactions.

Our approach to model the free energy of micellization extends previous work by including a number of important new elements which we summarize below:

(1) A detailed thought process to "visualize" micellization as a series of reversible steps, each associated with a well defined physico-chemical factor (see Figure 2.1). This convenient scheme permits a calculation of the free energy of micellization through a clear identification of the basic underlying assumptions, and an unambiguous account of the free-energy contributions associated with each step of the thought process (see also Farrell, 1988; Ljunggren and Eriksson, 1987).

(2) A systematic quantitative account of the effect of curvature on the interfacial component of the free energy of micellization.

(3) A free-energy contribution, associated with hydrocarbon-chain packing, which is calculated for different micellar shapes. As stated above, in previous quantitative studies of micellization this contribution was either ignored, or assumed to be independent of micellar shape and parametrized empirically by fitting it to experimentally measured CMC values. We have explicitly evaluated this free-energy contribution as a function of l_c and sh. The calculations were done numerically in the context of the recently developed single-chain mean-field model (Ben-Shaul et al., 1985, Szleifer et al., 1985 and 1986; Gruen, 1985).

(4) An "optimum" micellar-core minor radius, l_c^*, for a given shape, sh, which is determined by calculating the free energy of micellization, g_{mic}, for different values of l_c and subsequently minimizing it with respect to l_c. This procedure allows for the fact that, due to geometrical constraints, l_c need not be equal to the length of a fully extended hydrocarbon chain, l_{max}.

(5) A procedure to determine the micelles which exhibit two-dimensional, one-dimensional or no growth. The procedure involves identifying the optimum shape, sh^*, for which g_{mic} exhibits its absolute minimum.

(6) The temperature variation of (i) the transfer free energy of an alkyl chain from water to bulk hydrocarbon, (ii) the hydrocarbon-water interfacial tension, and (iii) the average cross-sectional area of the hydrated hydrophilic head groups of some nonionic surfactants studied. This has enabled us to predict the temperature variation of micellar solution properties, such as, the CMC and characteristics of the micellar size distribution.

Our molecular model of micellization is based on the following description of a model micelle. The micelle consists of a "dry" core whose uniform density is assumed to be equal to that of bulk liquid n-alkane. This assumption is supported by measurements of the partial molar volumes and compressibilities of n-alkanes dissolved in micelles (Vikingstad and Hoiland, 1978), and of the partial molar volumes of lipid chains in bilayers (Nagle and Wilkinson, 1978), where the measured values are very close to those of bulk liquid n-alkanes. The micellar core is separated from bulk water by a micelle-water interface which is assumed to consist of two regions: an outer layer which contains hydrophilic head groups, hydrated counterions, if any, and water, and an inner layer containing hydrated CH_2 groups. It is well known that the micelle-water interface exhibits fluctuations, and that the amplitude of these fluctuations is on the order of 1-2 Å, that is, about one C-C bond length -- namely, an order of magnitude less than the minor radius of a typical micelle (Ben-Shaul and Gelbart, 1985). By modelling the micelle as consisting of an inner hydrated layer we believe that we can "capture" these surface "roughness" fluctuations in a semi-quantitative manner. NMR studies of aqueous nonionic (Podo et al., 1973) and ionic (Cabane, 1981) surfactant solutions also seem to indicate that the thickness of the inner hydrated layer is on the order of a C-C bond length. We have therefore assumed that the thickness of the inner hydrated layer is equal to the length of one CH_2 group. In other words, we have assumed that the CH_2 group adjacent to the hydrophilic head group lies within the hydration sphere of the head group, and therefore does not have any hydrophobic properties (Tanford, 1974).

Accordingly, in the remainder of this thesis we denote by *head*, the surfactant hydrophilic head group and the CH_2 group adjacent to it, and by *tail*, the rest of the

surfactant molecule comprising (n_c-2) CH_2 groups and a terminal CH_3 group, that is a total of (n_c-1) carbon atoms. Note that although in general the molecular model of micellization can be used to treat both single-tail and double-tail surfactants, in the present thesis we only discuss the single-tail case.

2.3.2 Description of Thought Process

Based on the description of the model micelle presented above, we have developed a thought process to "visualize" the reversible formation of an n-mer (final state) from n individual monomers (initial state) in water, see Figure 2.1. Since the value of the free-energy change associated with this reversible process, that is, the free energy of micellization, g_{mic}, should be independent of the path connecting the initial and final states, we have chosen a series of convenient intermediate states to calculate g_{mic}. Each individual step, connecting these intermediate steps, contributes to g_{mic} a free-energy change that can be evaluated using a simple statistical-thermodynamic approach, and/or available experimental data (see below).

The various steps of the proposed thought process involve:

(1) Breaking the bond between the head and the tail.

(2) Discharging the head, if it is charged (ionic) or is dipolar (zwitterionic). The counterions are simultaneously discharged.

(3) Transferring the tail from water to bulk hydrocarbon.

(4) Creating an interface separating a hydrocarbon core from water.

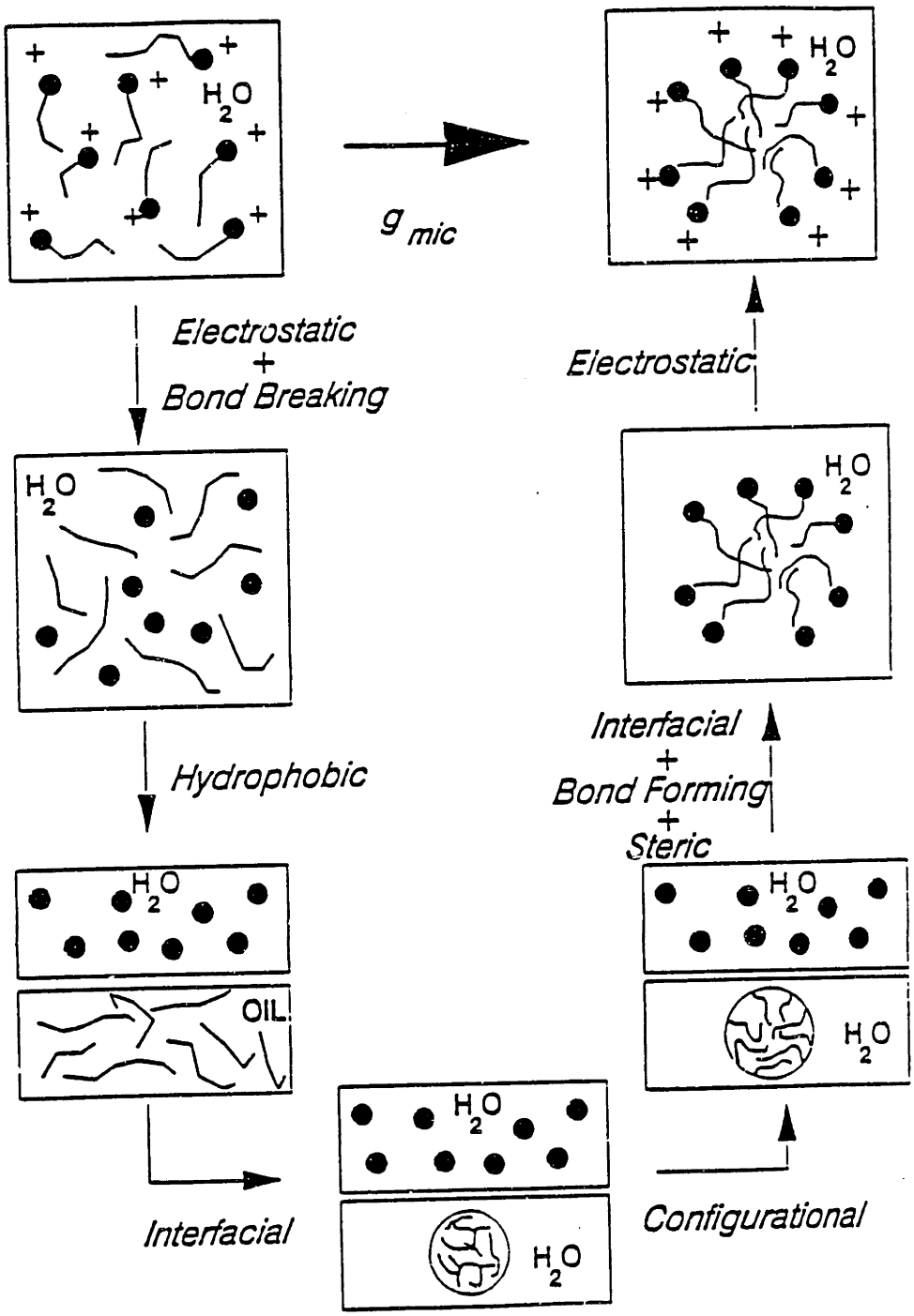

Figure 2.1: Schematic representation of thought process to "visualize" micellization.

(5) Anchoring one end of the tail, present in the hydrocarbon core, at the interface created in step (4).

(6) Placing the head at that interface. This would require (a) reforming the bond broken in step (1) between the head and the tail, (b) screening part of the micellar core from water, and (c) introducing possible non-electrostatic interactions, for example, steric, between the heads.

(7) Recharging the head of ionic and zwitterionic surfactants, which was discharged in step (2), at the interface. The counterions are simultaneously charged.

The contributions to the free energy of micellization listed above can be conveniently divided into those associated with the tail and those associated with the head. Sections 2.3.2.1 and 2.3.2.2 below discuss these contributions in more detail. A computational scheme to evaluate the free energy of micellization for various micellar shapes and sizes is presented in Section 2.3.3. Note that in Sections 2.3.2.1 and 2.3.2.2 the free energy of micellization is evaluated, per surfactant molecule, for a particular micellar shape, sh, and micellar-core minor radius, l_c. The resulting "optimum" equilibrium shape, sh^*, and corresponding "optimum" equilibrium micellar-core minor radius, l_c^*, are determined by minimizing the free energy of micellization with respect to l_c and sh. This procedure is discussed in more detail in Section 2.3.3.

2.3.2.1 Tail Effects

These effects reflect the free-energy change associated with transferring the tail from water to the micellar core. The transfer is modelled by a three-step process:

(1) Transfer the Tail from Water (w) to Bulk Hydrocarbon (hc): This is an attractive contribution, $g_{w/hc}$, that can be evaluated using experimental data for the solubility of hydrocarbons in water. The resulting temperature-dependent expression is given by (Abraham, 1984)

$$g_{w/hc} = h_{w/hc} - Ts_{w/hc} , \tag{2.6}$$

where the enthalpic contribution, $h_{w/hc}$, is given by

$$h_{w/hc} = [3.04 - 1.05(n_c - 1)]kT , \tag{2.7}$$

and the entropic contribution, $s_{w/hc}$, is given by

$$s_{w/hc} = [5.06 + 0.44(n_c - 1)]k \tag{2.8}$$

(2) Create a Hydrocarbon Core-Water Interface: This contribution, g_σ^t, is evaluated using the concept of a macroscopic interfacial free energy of a hydrocarbon-water interface, including its dependence on interfacial curvature. Since the heads have not yet been placed

at the interface, the entire hydrocarbon surface is exposed to water and must be used to evaluate the interfacial free-energy contribution. The free-energy change per monomer is therefore given by

$$g_o^t = \sigma a, \tag{2.9}$$

where σ is the interfacial free energy per unit area (interfacial tension) characterizing the curved hydrocarbon core-water interface, and $a = Sv/l_c$ is the interfacial area per monomer, where S is a shape factor (3 for spheres, 2 for cylinders, and 1 for discs or bilayers), $v = 27.4 + 26.9(n_c-1)$ (in $Å^3$) is the volume of the tail[2], and l_c is the micellar-core minor radius. For a disc or a bilayer l_c corresponds to the half-thickness of the hydrocarbon core.

We believe that it is necessary to introduce the curvature dependence of σ because micelles are small objects (the minor radius of the micellar core is typically 10-20Å) and can form in a variety of shapes. Surprisingly, such a dependence has not been systematically included in previous quantitative treatments of micellization.

In this thesis the curvature dependence of σ is approximated using the well known Gibbs-Tolman-Koenig-Buff equation (Gibbs, 1961; Tolman, 1948 and 1949; Koenig, 1950; Buff, 1951), that is,

$$\sigma = \sigma_o[1-(S-1)\delta/l_c], \tag{2.10}$$

where δ is the Tolman distance (Tolman, 1948 and 1949), S was defined above, and σ_o is the interfacial tension of a planar hydrocarbon-water interface (typical value of 50

ergs/cm^2). For our calculations we have included (Aveyard et al., 1972) the variation of σ_o with the number of carbon atoms in the tail, n_c-1, and with temperature.

Equation (2.8) indicates that the curvature dependence of σ is proportional to δ/l_c, which represents only the first term in a more general Taylor series expansion (Buff, 1960; Goodrich, 1968) in powers of δ/l_c. Theoretical analyses (Ono and Kondo, 1960; Rowlinson and Widom, 1982; Fisher and Wortis, 1984) of the interfacial region separating a liquid drop and a vapor phase indicate that the Tolman distance δ scales as the average radius of the molecules present in the liquid. In analogy, for a hydrocarbon-water interface, with hydrocarbon playing the role of "liquid" and water the role of "vapor", it can be shown that δ scales as the radius of a hydrocarbon molecule. Since a hydrocarbon molecule adopts an extended conformation in bulk hydrocarbon (Kimura and Nakano, 1977), we have taken δ to scale as the fully extended length, l_{max}, of the tail. In particular, to obtain best agreement with experimental results we have assumed a value $\delta = 2.25$Å for a C_{11} tail (or $n_c = 12$), and estimated δ for other C_n tails using the scaling assumption

$$\delta(n) = \delta(11)\frac{l_{max}(n)}{l_{max}(11)}, \qquad (2.11)$$

where (Tanford, 1974) $l_{max}(n) = 1.54 + 1.265n$ (in Å).

That the chosen value $\delta = 2.25$Å is a reasonable one can be seen from the following crude analysis which utilizes the known solubility data of hydrocarbons in water (McAuliffe, 1966). Hermann (1972) and Reynolds et al. (1974) analyzed the available solubility data using estimated molecular areas, and found that the free energy per unit area of the

"hydrocarbon-water interface", corresponding to a single hydrocarbon molecule, was approximately 18-25ergs/cm^2. At the maximum solubility of hydrocarbon in water, the hydrocarbon is dispersed as single chains. Consequently, if we approximate a single hydrocarbon chain as a cylinder having a radius of 2.5Å (this corresponds to a typical hydrocarbon-chain cross-sectional area of 20.4Å^2), the "hydrocarbon-water interface" will correspond to a concentric cylinder having a radius exceeding that of the first one (the hydrocarbon molecule) by tnat of a water molecule, (typical value (Reiss, 1965) of 1.5Å). This would correspond to a radius of 4Å for the cylindrical "hydrocarbon-water interface". Using the value $l_c = 4$Å in Eq. (2.8), with $S = 1$ and $\sigma = 18\text{-}25$ergs/cm^2, we obtain $\delta = 1.9\text{-}2.5$Å. This compares favorably with the value $\delta = 2.25$ Å that we have adopted for a C_{11} chain.

The limitations of the Gibbs-Tolman-Koenig-Buff equation in the limit of very small minor radii, where the applicability of thermodynamic concepts becomes questionable, have been addressed (Defay and Prigogine, 1966). In addition, the uncertainty in the expansion of σ in powers of δ/l_c for cylindrical interfaces has been recently discussed (Henderson and Rowlinson, 1984). In this respect, we view Eqs. (2.8) and (2.9) as an approximate computational tool to estimate the systematic variation of σ with l_c. In other words, we assign a broader meaning to the parameter δ viewing it primarily as a convenient correction factor used to model the effect of l_c on σ.

(3) Anchor the Tail at the Interface: In the micellar core the tail is attached to the head which lies at the interface, and therefore one end of the tail must be positioned at the micellar core-water interface. Due to this positional constraint the tail loses some of its

conformational degrees of freedom within the micellar core. The associated loss in conformational free-energy can depend strongly on the shape of the micelle (Ben-Shaul et al., 1985; Szliefer et al, 1985 and 1986). To evaluate this free-energy change per surfactant molecule, $g_{hc/mic}$, we have followed Ben-Shaul et al. (1985) and Gruen (1985) who utilized the single-chain mean-field model (Ben-Shaul and Gelbart, 1985) and the rotational isomeric state approximation (Flory, 1969). Note, however, that these earlier treatments of chain conformations were concerned primarily with calculating and comparing with experiments the bond-orientational order parameters of the tails, and not with predicting thermodynamic properties of surfactant solutions.

The rotational isomeric state approximation (Flory, 1969) assumes that each bond of a normal alkane chain can exist in three discrete rotational states: a ground state, denoted trans (t), in which two consecutive bonds are staggered in the same plane making an angle of 112°, and two excited states, denoted gauche ($g^{\pm}$), in which the consecutive bonds are rotated out of that plane by approximately $\pm 120°$. The energy of the gauche state relative to the trans state is approximately 1kT. In addition, sequences ($g^{+}g^{-}$) or (g^{-g+}) on successive bonds have an excess energy on the order of 3kT because of steric hindrances between the CH_2 groups. All such conformations are very unfavorable and therefore, following common practice (Szleifer et al, 1985 and 1986; Gruen, 1985), have been eliminated in our calculations.

In the single-chain mean-field model the constraints imposed by the neighboring chains on a central chain are taken into account in a "mean field" approach. The "mean field" generated by the neighboring chains is evaluated by generating and averaging over all

conformational degrees of freedom within the micellar core. The associated loss in conformational free-energy can depend strongly on the shape of the micelle (Ben-Shaul et al., 1985; Szliefer et al, 1985 and 1986). To evaluate this free-energy change per surfactant molecule, $g_{hc/mic}$, we have followed Ben-Shaul et al. (1985) and Gruen (1985) who utilized the single-chain mean-field model (Ben-Shaul and Gelbart, 1985) and the rotational isomeric state approximation (Flory, 1969). Note, however, that these earlier treatments of chain conformations were concerned primarily with calculating and comparing with experiments the bond-orientational order parameters of the tails, and not with predicting thermodynamic properties of surfactant solutions.

The rotational isomeric state approximation (Flory, 1969) assumes that each bond of a normal alkane chain can exist in three discrete rotational states: a ground state, denoted trans (t), in which two consecutive bonds are staggered in the same plane making an angle of 112°, and two excited states, denoted gauche ($g^{\pm}$), in which the consecutive bonds are rotated out of that plane by approximately ± 120°. The energy of the gauche state relative to the trans state is approximately 1kT. In addition, sequences (g^+g^-) or (g^-g^+) on successive bonds have an excess energy on the order of 3kT because of steric hindrances between the CH_2 groups. All such conformations are very unfavorable and therefore, following common practice (Szleifer et al, 1985 and 1986; Gruen, 1985), have been eliminated in our calculations.

In the single-chain mean-field model the constraints imposed by the neighboring chains on a central chain are taken into account in a "mean field" approach. The "mean field" generated by the neighboring chains is evaluated by generating and averaging over all

possible conformations of the central chain. This implicitly assumes that all possible conformations of the neighboring chains are identical to those of the central chain. In other words, the mean-field approach assumes that the shape, sh, seen on average by each monomer in the micelle is the same for all monomers. Such a condition is only satisfied by the three regular shapes of spheres, infinite-sized cylinders and infinite-sized discs or bilayers. Therefore, we have calculated the conformational (packing) free-energy contribution only for these three regular shapes.

The methodology used in calculating the conformational free-energy of a micelle of shape, sh, and core minor radius, l_c, involves the generation of a large number of conformations for a single chain. Each conformation is specified by the bond sequence (the number of gauche and trans bonds and their positions), the overall rotational orientation of the chain, and the distance of the first CH_2 group in the tail from the interface. For each bond sequence that is generated, the first CH_2 group in the tail is placed randomly over three different positions in a layer 1.53Å (the length of a C-C bond) from the interface, and then the entire chain is rotated randomly over 12 different orientations. Consequently, for a single tail with (n_c-1) carbon atoms this procedure generates $3^{(n_c-3)}$ bond sequences, 12 rotational orientations, and 3 positional orientations. For each one of these conformations, we determine the positions of the (n_c-2) CH_2 groups and of the terminal CH_3 group, and then exclude all conformations in which some of these groups are exposed to water outside the micellar core. The energy of each conformation is then evaluated from the number of gauche-trans bonds present, and the excess energy of a gauche bond over that of a trans bond (approximately 1kT). Once all conformations and their corresponding energies have

been computed, the resulting partition function and associated free energy, $g_{hc/mic}$, can be evaluated, in conjunction with the assumption that the density in the micellar core is uniform and equal to that of bulk hydrocarbon.

2.3.2.2 Head Effects

Once the micellar core is formed, the uncharged heads are placed back at the interface and subsequently recharged along with the counterions. The entire procedure can be conveniently divided into three major contributions:

(1) Interfacial Free-Energy Contribution: When the heads are placed back at the interface, they screen a fraction of the interfacial area from contact with water. The screened interfacial area per monomer can be estimated from the area, a_o, corresponding to the chemical bond between the head and the tail (typical value of 21Å^2). Because of this screening, the interfacial free energy per monomer is effectively reduced by an amount, g_σ^h, given by

$$g_\sigma^h = \sigma a_o, \tag{2.12}$$

where, as before, σ is given by Eq. (2.8).

Hence, the total interfacial free-energy contribution per monomer, g_σ, is given by subtracting Eq. (2.10) from Eq. (2.7), that is, by

$$g_\sigma = g_\sigma^t - g_\sigma^h = \sigma(a - a_o). \tag{2.13}$$

(2) Steric Contribution: The presence of the heads at the interface results in steric and other non-electrostatic interactions. In this step, electrostatic interactions are not included because the heads (if charged) have been discharged in step (2) of the thought process. As a first approximation we have considered only steric repulsions between the heads which, in the case of nonionic surfactants, are believed to be the most important non-electrostatic head-head interactions (Nagarajan and Ruckenstein, 1977). The free energy associated with these steric repulsions is calculated by treating the heads present at the interface as an ideal-localized monolayer (Fowler and Guggenheim, 1965). The use of a localized monolayer model reflects the fact that each head is physically attached to a tail at the interface. The resulting free-energy contribution, g_{st}, can be expressed as

$$g_{st} = -kT\ln\left(1 - \frac{a_h}{a}\right), \tag{2.14}$$

where a_h, the average cross-sectional area of the head has been estimated from the ratio v_h/l_h, where v_h and l_h are the volume and end-to-end length of the head, respectively. The volume of the head can be estimated from known molecular volumes of the individual groups comprising the head. Recall that the head includes one CH_2 group from the

hydrocarbon chain. The length, l_h, of the head, however, depends on the particular conformation that the head adopts. Since $a_h = v_h/l_h$, it follows that a head adopting an extended conformation will have smaller values of a_h, whereas a head adopting a compact conformation will have larger values of a_h. For more details on the estimation of a_h for nonionic surfactants see Section 2.5.1.

(3) Electrostatic Contribution: In this chapter we focus on nonionic surfactants. Because the dipole moments of the nonionic head groups are rather small and the dielectric constant of the aqueous medium is large, the electrostatic dipole-dipole interaction in aggregates of nonionic surfactants is on the order of 0.03kT, and thus it is negligible compared to the other contributions to the free energy of micellization (Nagarajan and Ruckenstein, 1977) (see Table 2.1). However, for aqueous solutions of ionic or zwitterionic surfactants electrostatic interactions can play a very important role in determining the equilibrium micellar shape and size. For these systems we propose to calculate the free-energy change associated with electrostatic interactions using the Poisson-Boltzmann equation (Mitchell and Ninham, 1983; Missel et al., 1989) with appropriate boundary conditions. In calculating this free-energy change we propose to discharge all heads and associated counterions, and subsequently recharge them so as to describe the actual distribution of counterions around the micelle[34].

2.3.3 Free Energy of Micellization for Non-Regular Finite-Sized Micelles

Based on the description of the model micelle presented in Section 2.3.1, the equilibrium state of a micelle can be fully described by specifying the time-averaged magnitudes of three variables: (i) the minor radius of the micellar core l_c, (ii) the number of surfactant molecules, n, in the micelle, and (iii) the geometrical shape, sh, of the micelle. Note that it is the time-averaged magnitudes of these three variables that must be specified since micelles are fluctuating entities. In addition, in the context of the proposed molecular model (see Section 2.3.2.1) the contribution of hydrocarbon-chain packing to the free energy of micellization can only be computed exactly for the three regular shapes of spheres, infinite-sized cylinders, and infinite-sized discs or bilayers.

For each of these three regular micellar shapes we calculate and subsequently minimize the free energy of micellization, g_{mic}, with respect to l_c to determine the minimum free-energy value, $g^*_{mic}(sh)$, and the corresponding micellar-core minor radius, l_c^*, for that particular shape, sh, of the micelle. In the absence of entropy of mixing contributions, the "optimum" shape sh^* that the micelle would adopt (based on the free energy of micellization alone) can be estimated by minimizing $g^*_{mic}(sh)$ with respect to sh. That is, if sh^* corresponds to a sphere, then finite-sized spherical micelles will be favored. However, if sh^* corresponds to an infinite-sized cylinder or disc, then infinite-sized ($n=\infty$) cylinders or discs, respectively, will be favored. When entropy of mixing contributions are included the surfactant solution will typically consist of a distribution of finite-sized micelles, since a large number of small micelles is entropically favored over a small number of larger ones.

Consequently, even if sh^* corresponds to an infinite-sized cylinder, the solution will actually consist of a distribution of finite-sized cylindrical micelles (*one-dimensional growth*). Similarly, if sh^* corresponds to an infinite-sized disc the surfactant solution will actually consist of a distribution of finite-sized disc-like micelles (*two-dimensional growth*). Finally, if sh^* corresponds to a sphere we model the micellar solution as consisting of spherical micelles which do not grow at all. To summarize, we calculate g_{mic} for the three regular micellar shapes, then identify sh^*, which determines whether the surfactant solution consists of micelles which exhibit two-dimensional, one-dimensional, or no growth.

In this thesis, the free energy of micellization, $g_{mic}(n)$, associated with non-regular finite-sized micelles is estimated by linearly interpolating between the "optimum" free energies of micellization corresponding to the limiting regular shapes. For example, $g_{mic}(n)$ for a micelle that grows in one dimension is estimated by linearly interpolating between the "optimum" free energies of micellization of an infinite-sized cylindrical micelle, $g^*_{mic}(cyl)$, and a finite-sized spherical micelle, $g^*_{mic}(sph)$: see the full straight line in Figure 2.2. The actual value of $g_{mic}(n)$ could deviate from this "ideal" straight-line behavior, as shown by the dotted line in Figure 2.2. We speculate that this deviation from "ideality" would be larger for micelles which exhibit little growth. This is suggested by experimental measurements (Degiorgio, 1985) in which the observed minimum size of the micelles is considerably larger than that corresponding to the largest possible spherical micelle (whose size is estimated using the geometrical packing constraints developed by Israelachvili et al., 1976). In view of this deviation, we anticipate that our molecular model will predict larger values of the CMC (since we predict larger values of g_{mic}), and smaller aggregation numbers for micellar

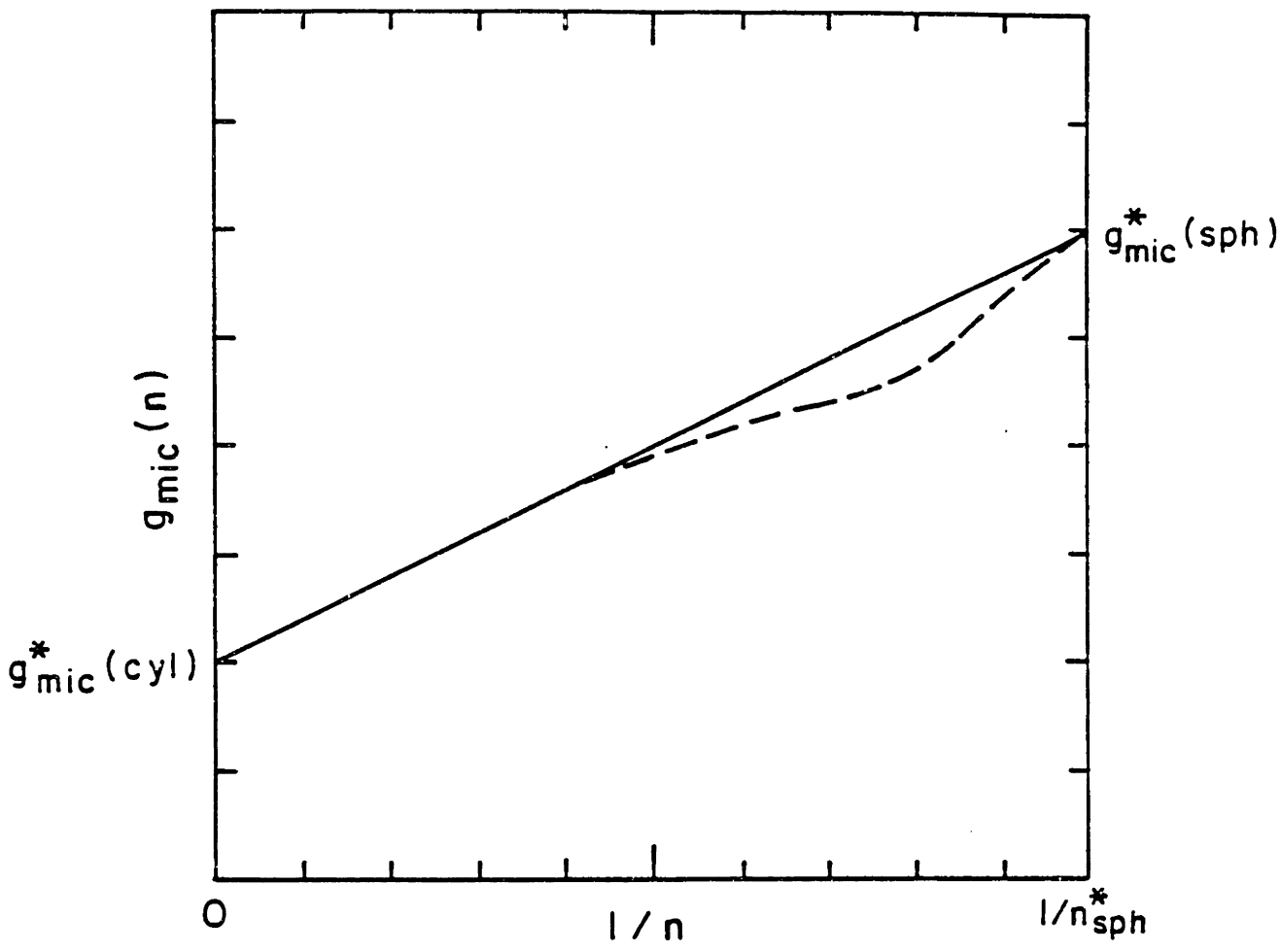

Figure 2.2: Schematic plot of the free energy of micellization, $g_{mic}(n)$, as a function of the inverse aggregation number, n, for a micelle which exhibits one-dimensional growth. The solid line represents a linear interpolation between g^*_{mic}(cyl) and g^*_{mic}(sph), and the dashed line could represent the actual free energy of micellization (see Section 2.2.3).

systems which do not exhibit micellar growth (see also the discussion in Section 2.5.2).

Using the above mentioned interpolation scheme, $g_{mic}(n)$ can be estimated as a function of n for the cases of one-dimensional and two-dimensional micellar growth. In particular, for the case of one-dimensional growth, a linear interpolation between $g^*_{mic}(cyl)$ and $g^*_{mic}(sph)$ leads to

$$g_{mic}(n) = g^*_{mic}(cyl) + \frac{n^*_{sph}}{n}[g^*_{mic}(sph) - g^*_{mic}(cyl)], \qquad (2.15)$$

where n^*_{sph} is the aggregation number of the "optimum" spherical micelle. The expression in Eq. (2.13) is identical to one derived previously by Missel et al. (1980).

The proposed molecular model of micellization, Eqs. (2.6)-(2.12) together with $g_{hc/mic}$, contains three molecular parameters: n_c, δ and a_h. n_c is a known property of the hydrocarbon chain, δ is evaluated using Eq. (2.9), and a_h can be estimated as explained in Section 2.3.2.2 (see also the discussion in Section 2.5.1). Typical values of these parameters for various nonionic surfactants are presented in Table 2.1. For a given surfactant, utilizing the values of these parameters, we have evaluated the four contributions ($g^*_{w/hc}$, $g^*_{hc/mic}$, g^*_{σ} and g^*_{st}) to $g^*_{mic}(sh)$ for the three regular shapes of spheres, infinite-sized cylinders and infinite-sized discs. For all the surfactants presented in Table 2.1 we have found that $g^*_{st}(disc)=\infty$, thus making disc-shaped micelles totally unfavorable. Therefore, in Table 2.1 we present the calculated values of the "optimum" micellar-core minor radius l^*_c, and the corresponding contributions $g^*_{w/hc}$, $g^*_{hc/mic}$, g^*_{σ}, g^*_{st} to g^*_{mic}, for both spherical and infinite-sized cylindrical micelles. From the values presented in Table 2.1 one can make the follow-

TABLE 2.1. Values of the three molecular parameters n_c, a_h, and δ; the four free-energy contributions $g^*_{w/hc}$, g^*_{st}, $g^*_{hc/mic}$, and g^*_{σ} to g^*_{mic}, for spherical and infinite-sized cylindrical micelles at their "optimum" micellar-core minor radius l^*_c, evaluated at 25°C, for aqueous solutions of several nonionic surfactants.

Surfactant	n_c	a_h ($Å^2$)	δ (Å)	$g^*_{w/hc}$ (kT)	g^*_{st} (kT)		$g^*_{hc/mic}$ (kT)		g^*_{st} (kT)		g^*_{mic} (kT)		l^*_c (Å)	
					Sph	Cyl	Sph	Cyl	Sph	Cyl	Sph	Cyl	Sph	Cyl
$C_{12}E_4$	12	27	2.25	-18.46	0.56	0.91	1.51	1.53	3.78	2.69	-12.61	-12.61	15.4	14.0
$C_{12}E_6$	12	38	2.25	-18.46	0.93	1.45	1.51	1.35	3.78	3.03	-12.24	-12.24	15.4	13.0
$C_{12}E_8$	12	48	2.25	-18.46	1.35	2.60	1.48	1.33	3.89	3.20	-11.74	-11.74	15.0	12.5
$C_{10}E_6$	10	38	1.90	-15.47	0.93	1.50	1.32	1.24	3.73	2.92	-9.49	-9.49	12.8	11.0
C_8 Glucoside	8	43	1.50	-12.48	1.16	1.59	1.28	1.15	3.66	3.32	-6.38	-6.38	10.3	8.0
C_{12} Glucoside	12	43	2.25	-18.46	1.15	1.78	1.51	1.30	3.78	3.20	-12.02	-12.02	15.4	12.5
C_8 Glyceryl Ether	8	24	1.50	-12.48	0.48	0.81	1.28	1.35	3.66	2.33	-7.06	-7.99	10.3	10.0

ing observations:

(1) The largest contribution to g^*_{mic} is $g^*_{w/hc}$, the free-energy change associated with transferring the tail from water to bulk hydrocarbon.

(2) As a_h increases there is an increase in the magnitude of g^*_{st}, this increase being larger for cylindrical micelles. This is in agreement with the well-accepted view (Israelachvili et al., 1976) that surfactant molecules possessing large heads will favor the formation of spherical micelles rather than cylindrical ones.

(3) The value of $g^*_{hc/mic}$ increases with increasing n_c, and is larger for spherical micelles than for cylindrical ones.

(4) The numerical magnitude of g^*_{σ}, for a given shape, is relatively constant.

(5) The "optimum" micellar-core minor radius, l_c^*, is larger for spherical than for cylindrical micelles. In addition, the value of l_c^* decreases with increasing a_h.

Figure 2.3 shows predicted values of g_{mic} as a function of l_c for aqueous solutions of $C_{12}E_6$ at 285K and 310K, for spherical and infinite-sized cylindrical micelles. The figure illustrates vividly that the numerical magnitude of the free energy of micellization, g_{mic}, varies with both micellar shape and temperature. The figure also indicates that at these two temperatures infinite-sized cylindrical micelles are favored over spherical ones, which as explained above implies one-dimensional growth. Note that the numerical magnitude of the free-energy minimum, corresponding to g^*_{mic} for the given shape, decreases with temperature. In addition, the value of the "optimum" micellar-core minor radius, l_c^*, at which the minimum value, g^*_{mic}, occurs (indicated by the arrows) varies with temperature. The maximum value of l_c in the figure corresponds to the fully extended tail length (16.7Å).

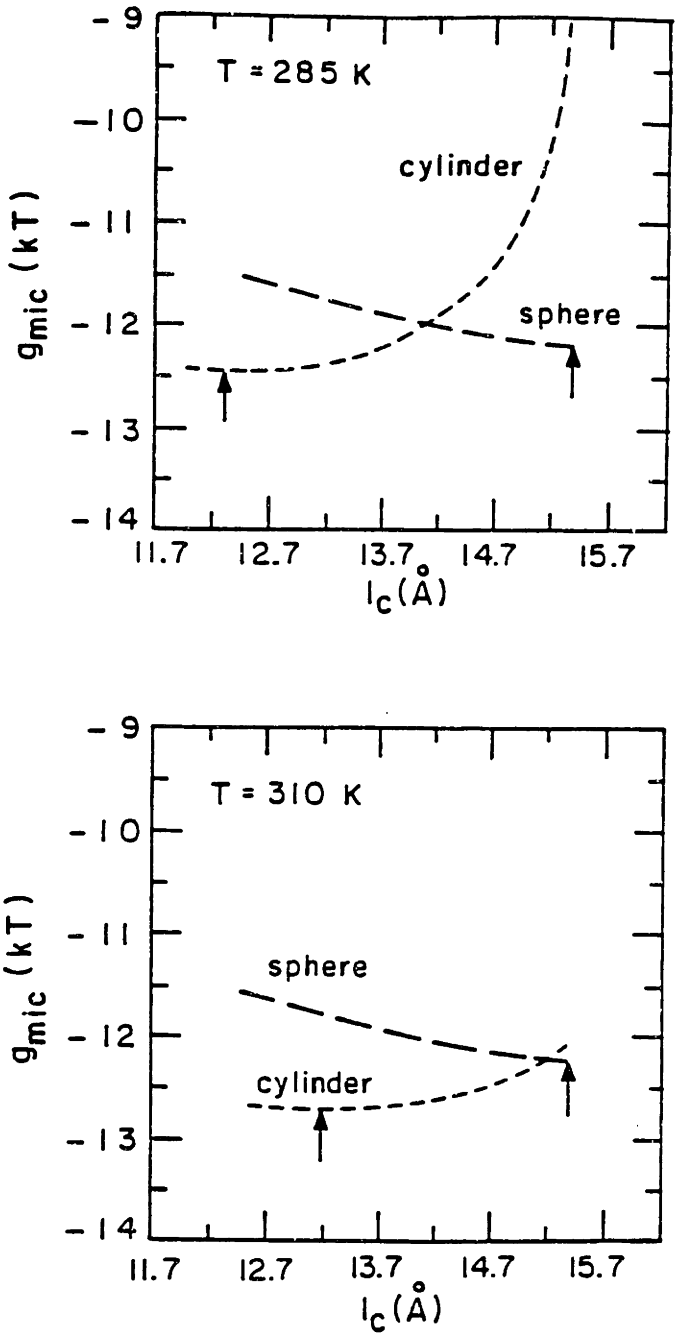

Figure 2.3: Predicted free energy of micellization for aqueous solutions of $C_{12}E_6$ as a function of the minor radius l_c of the micellar core for infinite-sized cylindrical (- - -) and spherical (—— ——) micelles at 285K and 310K. Arrows indicate the value of the "optimum" free energy of micellization, g^*_{mic}, at the "optimum" micellar-core minor radius, l_c^*, for each shape. Clearly, infinite-sized cylindrical micelles are favored at both temperatures, which implies one-dimensional micellar growth (see Section 2.3.3).

2.4 EVALUATION OF THERMODYNAMIC PROPERTIES

Using the free-energy expressions, Eqs. (2.1)-(2.5), the chemical potentials of water and n-mers can be calculated (Blankschtein et al., 1985 and 1986; Thurston et al., 1986). The resulting expressions are

$$\mu_w = \mu_w^o + kT\left[\ln(1-X) + X - \sum_m X_m\right] + \frac{1}{2}\frac{C\phi^2}{\gamma}, \qquad (2.16)$$

and

$$\mu_n = \mu_n^o + kT\left[\ln X_n + 1 + n(X-1-\sum_m X_m)\right] + \frac{1}{2}nC\left[(1-\phi)^2-1\right], \qquad (2.17)$$

where $X = N_s/(N_w+N_s)$ is the total mole fraction of surfactant, ϕ is the total volume fraction of surfactant, C(T,P) is the phenomenological interaction parameter, $\gamma = \Omega_S/\Omega_W$ is the ratio between the volume of a surfactant molecule, Ω_S, and the volume of a water molecule, Ω_W, and X_m is the mole fraction of an m-mer, defined as $N_m/(N_w+N_s)$.

Using the principle of multiple chemical equilibrium (Corkill et al., 1969; Mukerjee, 1972) between micelles of different sizes and monomers, that is, $\mu_n = n\mu_1$, the following expression for the micellar size distribution $\{X_n\}$ is obtained

$$X_n = \frac{1}{e} X_1^n \, e^{-n[\beta g_{mic}(n)-1]}, \qquad (2.18)$$

where $\beta = 1/kT$, and X_1 is the mole fraction of monomer which can be evaluated using Eq. (2.18) in the surfactant mass balance equation, $X = X_1 + \Sigma_n nX_n$. Note that Eq. (2.18) does not depend explicitly on the value of the interaction parameter C. This can also be seen immediately from Eq. (2.5), since G_i does not depend explicitly on either the shape or the size of the micelles. Clearly, other choices of G_i may lead to distributions which will depend explicitly on intermicellar interactions (Corti and Degiorgio, 1981; Ben-Shaul and Gelbart, 1982).

The characteristics of the micellar size distribution including the weight-average aggregation number, $<n>_w$, and the relative variance, V, can be evaluated using Eq. (2.15) and are given by

$$<n>_w = \frac{\sum_n n^2 X_n}{\sum_n nX_n}, \qquad (2.19)$$

and

$$V = \frac{<(n-<n>_w)^2>_w}{<n>_w^2}. \qquad (2.20)$$

The critical micellar concentration (CMC) of the surfactant solution is defined as that concentration where a plot of the monomer concentration, X_1, as a function of total surfactant concentration, X, exhibits a break.

The critical point, which signals the onset of phase separation, is characterized by the critical surfactant concentration, X_c, and the critical temperature, T_c. At the critical point thermodynamic stability requires that the two conditions, $(\partial^2 g/\partial X^2)_{T,P} = 0$ and $(\partial^3 g/\partial X^3)_{T,P} = 0$, should be satisfied, where $g = X\mu_1(X,T,P) + (1-X)\mu_w(X,T,P)$. By simultaneously solving these two conditions one can evaluate the values of X_c and of the critical interaction parameter C_c, corresponding to the value of C at T_c.

The osmotic pressure of the solution, π, is related (Guggenheim, 1952) to the solvent chemical potential by $\pi = -(\mu_w - \mu_w^0)/\Omega_w$, where $(\mu_w - \mu_w^0)$ is given in Eq. (2.14a). This expression is derived under the assumption that the effective volumes of water and surfactant molecules Ω_w and Ω_s, respectively, are independent of concentration X and pressure P. The osmotic compressibility of the solution, $(\partial\pi/\partial X)^{-1}_{T,P}$, can then be obtained by differentiating the osmotic pressure π with respect to X at constant T and P. In the context of the present mean-field type theory, the osmotic compressibility as a function of temperature along the critical isochore, X_c, diverges at T_c with a mean-field critical exponent of 1.

As stated in the Introduction, aqueous solutions of many nonionic surfactants exhibit the phenomenon of phase separation when they are heated above a certain temperature (Degiorgio and Corti, 1985). In this phase separation two coexisting liquid micellar phases,

having different surfactant concentrations Y and Z, form. Thermodynamic equilibrium between these phases requires (Guggenheim, 1952) that temperature, pressure, and chemical potential of each different chemical species be the same in the two phases. In particular, this implies that (i) $\mu_w(Y,T,P) = \mu_w(Z,T,P)$, and (ii) $\mu_1(Y,T,P) = \mu_1(Z,T,P)$. Since $\mu_n = n\mu_1$, the equality in (ii) guarantees that $\mu_n(Y,T,P) = \mu_n(Z,T,P)$. A simultaneous solution of the two conditions (i) and (ii) yields the two coexisting concentrations Y(T,P) and Z(T,P), and hence the entire coexistence curve delineating the boundary between the one-phase and two-phase regions. The actual calculation of these two concentrations (Blankschtein et al., 1986) requires knowledge of the two contributions $g_{mic}(T,P)$ and C(T,P).

2.5 THEORETICAL PREDICTIONS AND COMPARISON WITH EXPERIMENTS

2.5.1 Parameter Estimation

The molecular-thermodynamic approach presented in Sections 2.2, 2.3 and 2.4 enables us to predict a broad spectrum of equilibrium thermodynamic properties of aqueous surfactant solutions over a wide range of surfactant concentrations (CMC < X < 500CMC) and temperatures. These properties include (i) the critical micellar concentration (CMC) as a function of temperature, (ii) the micellar size distribution, $\{X_n\}$, including the relative variance of the distribution and the weight-average micellar aggregation number, as a function of surfactant concentration and temperature, (iii) the critical surfactant concentration, X_c, signalling the onset of phase separation, and (iv) the osmotic

compressibility, as well as other thermodynamic properties, as a function of temperature and surfactant concentration.

All these predictions depend explicitly on the values of the free energy of micellization, g_{mic}, and the interaction parameter C. In addition, the molecular parameter γ, the ratio between the volumes of a surfactant molecule and a water molecule, needs to be specified. This can be done in a straightforward manner using known densities of surfactant and water. The value of g_{mic} can be computed using the molecular model of micellization presented in Section 2.3.

On the other hand, we currently do not have a similar molecular description to evaluate the interaction parameter C. It is interesting to note, however, that in the context of the proposed molecular-thermodynamic approach the value of C is not actually needed to predict many of the important properties of the micellar solution, which include the CMC and the micellar size distribution along with all its characteristics (see Eqs. (2.15)-(2.18)).

It is also interesting to observe, that in some cases the parameter C was found to be approximately temperature independent (Blankschtein et al., 1986). In such cases, it is possible to evaluate the magnitude of C by simply fitting the theoretically predicted critical temperature, T_c, to the experimentally measured T_c. That is, when C does not vary much with temperature one only requires knowledge of the experimentally accessible quantity T_c, in conjunction with the molecular model of micellization, to predict the entire spectrum of thermodynamic properties of the micellar solution.

In general, however, and in particular for some of the nonionic surfactants studied in this chapter, one expects that C will be a strong function of temperature (Blankschtein

et al., 1986; Kjellander, 1982). In that case, we have determined the temperature variation of C by fitting the theoretically predicted coexistence curve to the experimentally measured one. It should be stressed however, that even in this case one only requires knowledge of the experimentally measured T_c, in conjunction with the molecular model of micellization, to predict the critical surfactant concentration X_c (see Section 2.5.4 and Table 2.2). Furthermore, we have found that the predicted osmotic compressibility as a function of temperature along the critical isochore, X_c, is mostly determined by the value of C_c and not by the variation of C with temperature (see Section 2.5.4 and Figure 2.8). Thus, once again, it appears that in the context of the present approach knowledge of the experimentally determined T_c is the most important experimental input needed, in conjunction with the molecular model of micellization, to make a broad range of predictions of the thermodynamic properties of aqueous surfactant solutions.

Most of the predictions which follow have been made for aqueous solutions of nonionic surfactants belonging to the polyoxyethylene glycol monoether family (C_iE_j). These surfactants have a polar head group comprising j ethylene oxide (EO = CH_2CH_2O) units, and a hydrocarbon tail group comprising i carbon atoms. We have also predicted CMC's of aqueous solutions of alkyl glucosides, alkyl glyceryl ethers and alkyl glycol ethers.

As stated in Section 2.3.3 the value of the average head cross-sectional area, a_h, is an important molecular parameter which controls the magnitude of the steric contribution, g^*_{st}, to the free energy of micellization, g^*_{mic} (see Table 2.1). In the case of C_iE_j nonionic surfactants, the conformation adopted by the j (EO) units in the surfactant molecule determines the value of a_h. To estimate a_h in this case we have borrowed concepts from the

scaling theory of polymer solutions (Flory, 1969). For a "real" polyethylene oxide (PEO) polymer, comprising a large number of monomeric EO units, the end-to-end length of the polymer, l_h, increases with the number of monomeric units, j, according to some power-law, j^x, with x typically in the range 0.5-0.7, depending on the affinity between polymer and solvent (Flory, 1969).

As stated in Section 2.3.2.2, we have assumed that $a_h = v_h/l_h$, where v_h is the volume of the head, and l_h is the end-to-end length of the head. Since v_h increases linearly with j, one would conclude that a_h should be proportional to j^z, with z in the range 0.3-0.5. This type of behavior is expected for randomly coiled polymers having large values of j. However, for the short chains comprising the surfactant head group, $3 < j < 10$, this limiting form of a randomly coiled polymer does not apply, and the end-to-end length of the head increases more slowly with j. This is because the smaller head groups ($j \leq 10$) are in a more extended zig-zag conformation, whereas the longer head groups are in a more compact meander conformation (Rosch, 1967). In our calculations we have adopted the value $z = 0.8$, which reflects the slower increase of l_h with j ($x = 0.2$), and is also suggested by the experimental work of Mitchell et al. (1983).

In addition, because the EO units of C_iE_j surfactants are hydrated, with the hydration number decreasing with increasing temperature (Nilsson and Lindman, 1983), we expect that the average cross-sectional area of the head will decrease with temperature. In this thesis, we have assumed that a_h varies linearly with temperature, that is,

$$a_h = a_{ho}\left[1 - H(T - 298)\right], \tag{2.21}$$

where a_h is the average cross-sectional area of the head at temperature T, a_{ho} is the average cross-sectional area of the head at 298K, and H reflects the decrease in hydration with temperature. For the predictions made in this thesis, H was estimated to be 0.0075 for $C_{12}E_6$, by fitting the theoretical predictions to the temperature variation of the CMC, and this value of 0.0075 was subsequently used, without further adjustments, to predict the temperature-dependent properties of other C_iE_j surfactants. It is interesting to note that if one assumes that the conformation of the head does not change much with temperature, then a value of 0.0075 for H would correspond to a dehydration of 0.020 water molecules per EO unit per °C. This compares favorably with the experimental value of 0.017 water molecules per EO unit per °C measured using electrical conductivity (Bordi et al., 1988).

Below, we use the proposed molecular-thermodynamic approach to predict a broad spectrum of micellar solution thermodynamic properties.

2.5.2 Critical Micellar Concentration

Utilizing Eq. (2.18), we have been able to predict the critical micellar concentration (CMC) of aqueous micellar solutions of a number of nonionic surfactants. In particular, Figure 2.4 shows predictions of the CMC of aqueous solutions of C_iE_j surfactants as a function of ethylene oxide content (j), for i=8, 10 and 12. Figure 2.5 shows predictions of the CMC of aqueous solutions of C_iE_6 as a function of temperature, for i=10 and 12. To the best of our knowledge this is the first quantitative prediction of the variation of CMC with temperature for nonionic surfactants. The various symbols in Figures 2.4 and 2.5

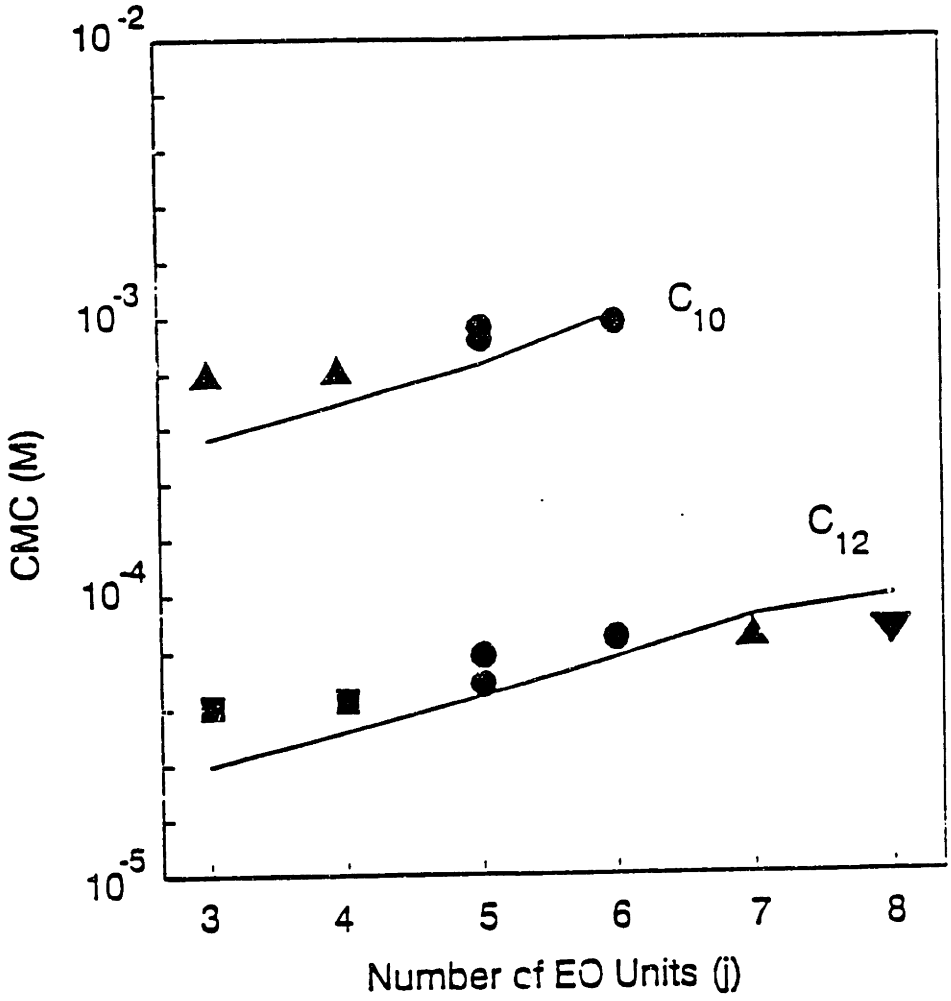

Figure 2.4: Critical micellar concentration (CMC) of aqueous solutions of $C_{10}E_j$ and $C_{12}E_j$ as a function of the number of ethylene oxide (EO) units, j, at 25°C. The solid lines represent theoretical predictions. The experimental points are (▲) Mukerjee and Mysels, 1971; (●) Becher, 1967; (▼) Meguro et al., 1981; and (■) Jiding and Zhengyu, 1986.

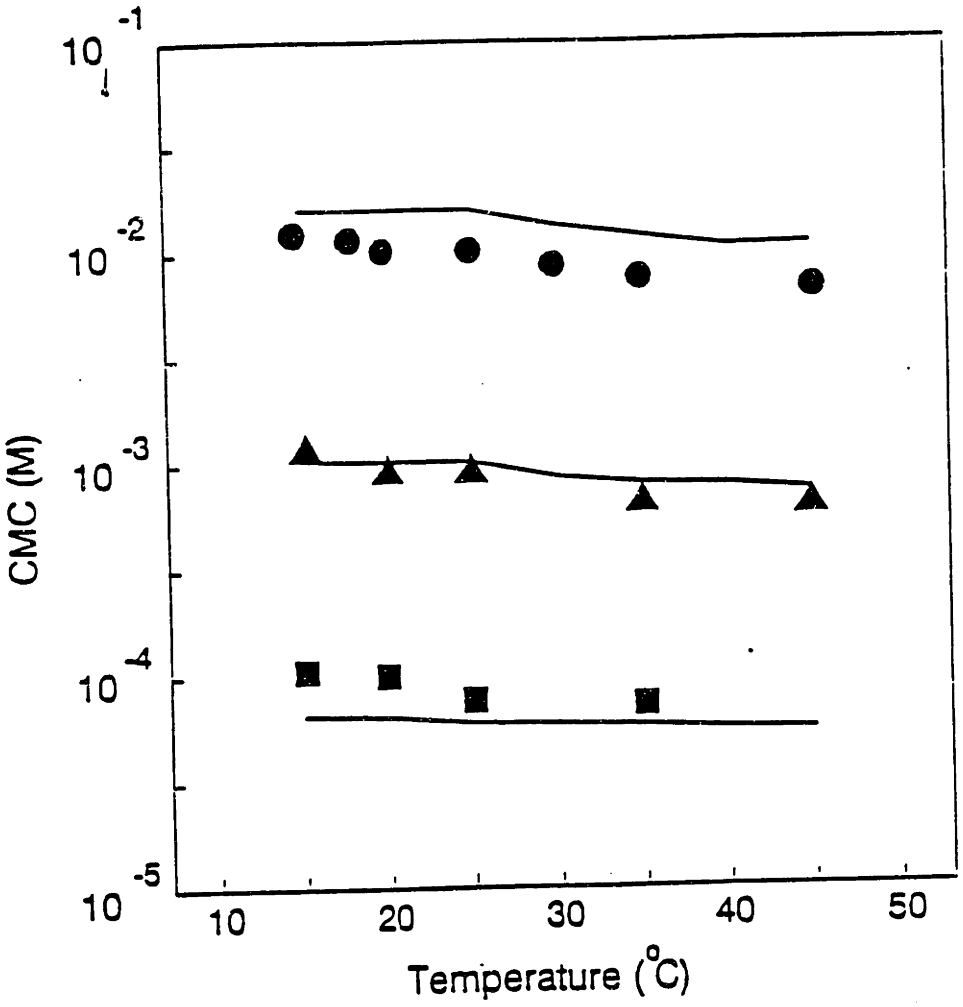

Figure 2.5: Predicted (solid line) critical micellar concentration (CMC) of aqueous solutions of $C_{12}E_6$ (■), $C_{10}E_6$ (▲) and C_8E_6 (●) as a function of temperature. The experimental points are from Mukerjee and Mysels (1971).

denote experimental points (Mukerjee and Mysels, 1971; Becher, 1967; Meguro et al., 1981; Jiding and Zhengyu, 1986), and as can be seen the theoretical predictions are in good agreement with experiments. Note that for some surfactants, for example, $C_{10}E_5$ in Figure 2.4 and $C_{12}E_6$ in Figure 2.5, we have included more than one experimental CMC value to indicate the magnitude of the uncertainty of reported experimental values.

Figures 2.4 and 2.5 indicate that the molecular model predicts larger values of the CMC for some surfactants, for example, C_8E_6, $C_{10}E_8$ and $C_{12}E_8$. Using the procedure described in Section 2.3.3, we have found that aqueous solutions of these surfactants consist of micelles which do not grow. Accordingly, we believe that the predicted larger values reflect the deviation from "ideality" of the free energy of micellization that has been described in Section 2.3.3, see also Figure 2.3.

Figure 2.6 shows the predicted CMC's of aqueous solutions of alkyl glucosides and alkyl glyceryl ethers as a function of n_c, the number of carbon atoms per chain. The glucoside head group is known to form a cyclic structure (Morrison and Boyd, 1983), for which we have estimated the average head cross-sectional area, a_h, to be approximately 43Å^2. Once again, there is very good agreement with experimental results (Shinoda et al., 1961).

CMC's of aqueous solutions of octyl glyceryl ether and octyl glycol ether have been estimated to be 7.0×10^{-3}M and 6.0×10^{-3}M, respectively. This compares very favorably with the experimental values (Shinoda et al., 1959) of 5.8×10^{-3}M and 4.9×10^{-3}M, respectively. Both octyl glyceryl ether and octyl glycol ether have small heads, and their average head cross-sectional areas were estimated to be 24Å^2 and 21Å^2, respectively.

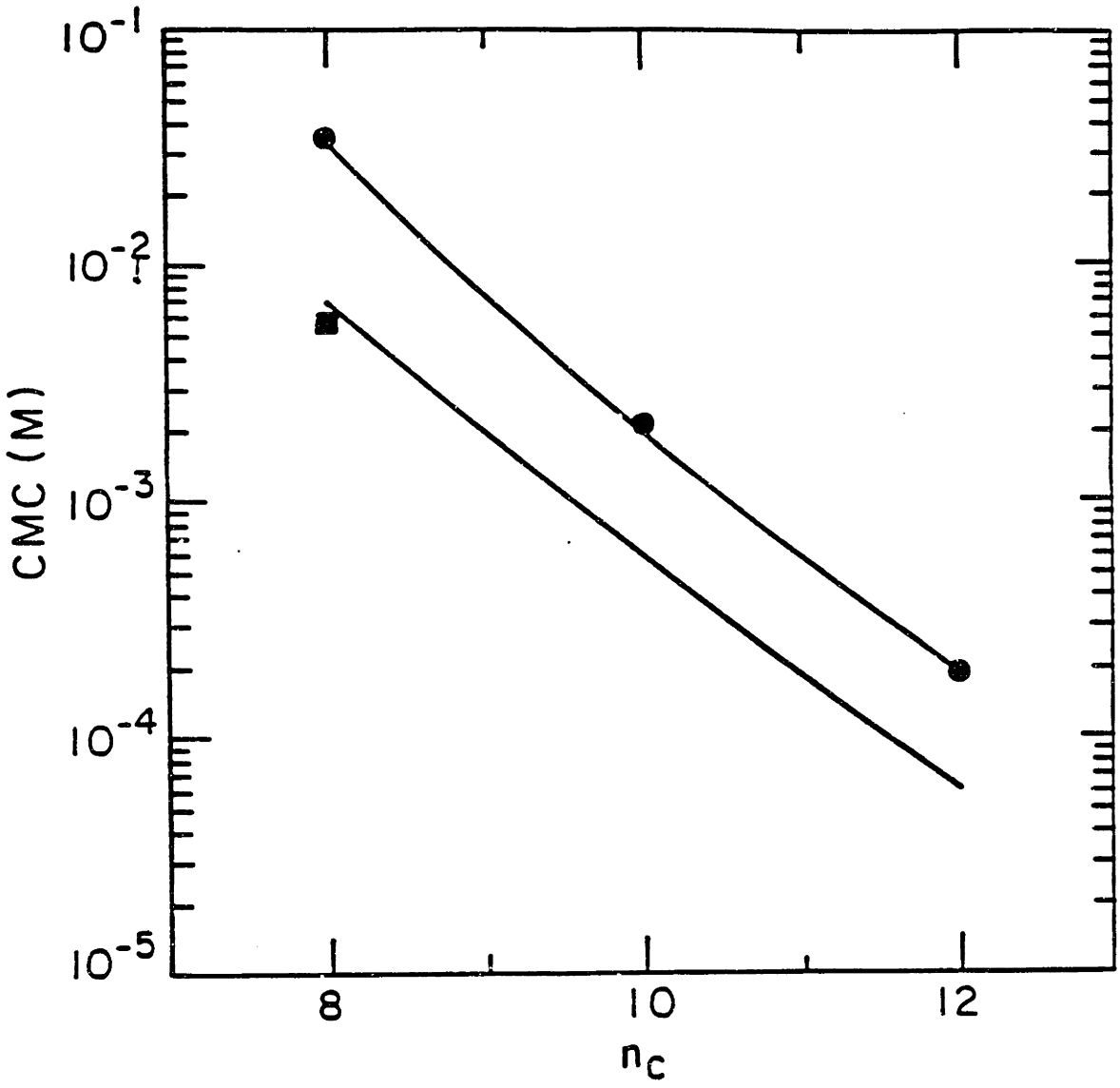

Figure 2.6: Predicted (solid line) critical micellar concentration (CMC) of aqueous solutions of alkyl glucosides (●) and alkyl glyceryl ethers (■) as a function of n_c, the chain-carbon number, at 25°C. The experimental points are from Shinoda et al. (1961).

2.5.3 Characteristics of the Micellar Size Distribution

A very challenging and still controversial aspect of micellar solution phase behavior deals with the extent of micellar growth and associated degree of polydispersity of C_iE_j nonionic surfactants in aqueous solutions (Degiorgio, 1985). The relative variance of the micellar size distribution, V, constitutes a measure of polydispersity. In particular (Mukerjee, 1972; Blankschtein et al., 1986), large polydisperse cylindrical-like micelles are characterized by V = 0.5, whereas small monodisperse micelles are characterized by V=0.

To gain some insight on this important issue we have used Eqs. (2.15)-(2.17) to predict the temperature variation of V (at a fixed surfactant concentration of 1 wt%) for a series of four nonionic surfactants $C_{12}E_5$, $C_{12}E_6$, $C_{12}E_7$, and $C_{12}E_8$, see Figure 2.7. This figure shows that there is a narrow predicted temperature range in which micelles grow from small monodisperse micelles (V=0) to large polydisperse cylindrical-like micelles (V=0.5), and that this temperature range differs from surfactant to surfactant. Thus, while micelles of $C_{12}E_5$ remain polydisperse at all temperatures above 0°C, micelles of $C_{12}E_6$, $C_{12}E_7$, and $C_{12}E_8$ are monodisperse until about 15°C, 35°C and 50°C, respectively, and then begin to grow. This predicted transition from a solution composed of monodisperse micelles to one composed of polydisperse micelles has been experimentally verified by a number of studies (Nilsson et al., 1983; Lindman and Karlstrom, 1987; Corkill and Walker, 1972; Brown and Rymden, 1987; Fujimatsu et al., 1988; Zana and Weill, 1985). The reported experimental transition temperatures are 15-18°C (Corkill and Walker, 1972; Brown and Rymden, 1987), 34°C (Fujimatsu et al., 1988) and 50°C (Zana and Weill, 1985) for $C_{12}E_6$, $C_{12}E_7$ and $C_{12}E_8$,

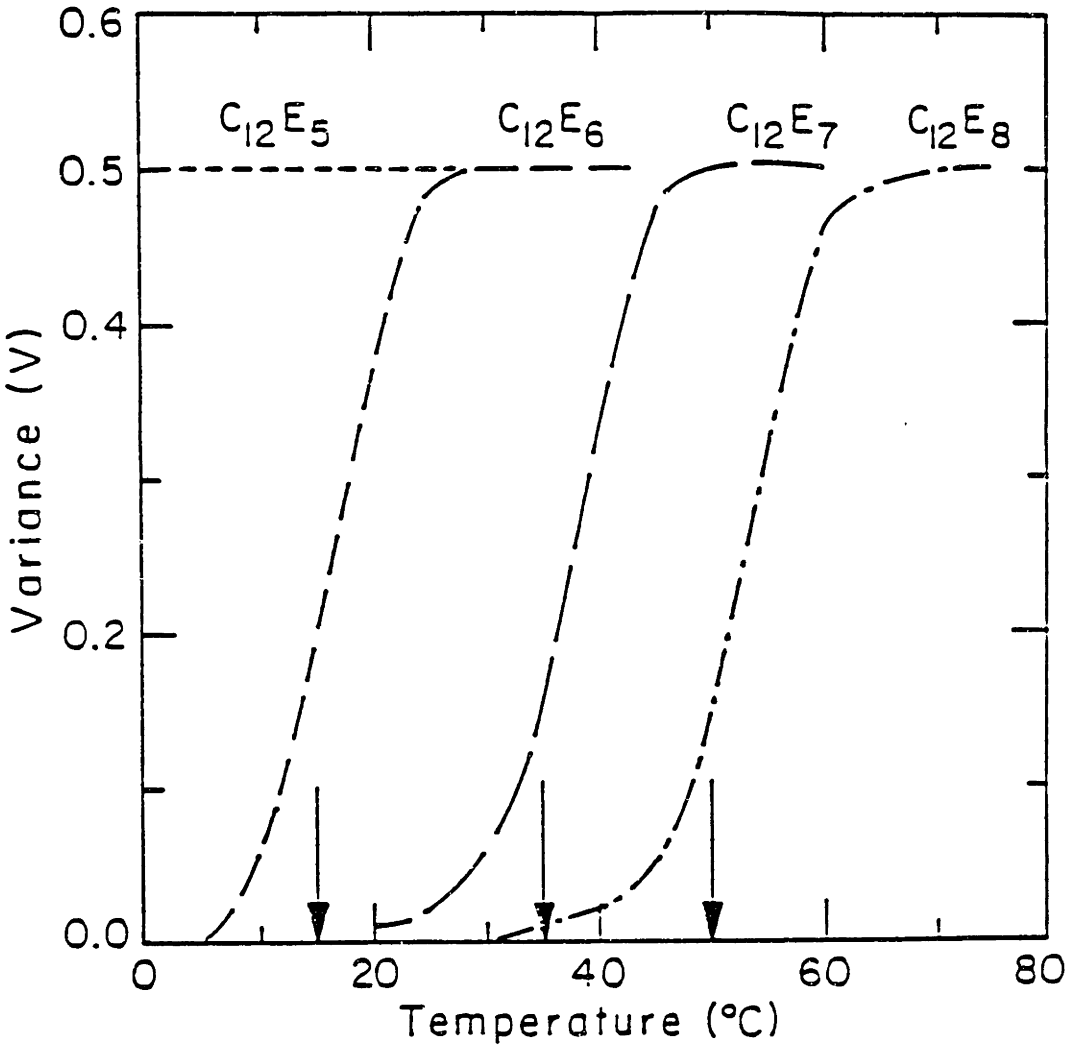

Figure 2.7: Predicted variance (V) of the micellar size distribution as a function of temperature for aqueous solutions of $C_{12}E_5$, $C_{12}E_6$, $C_{12}E_7$, and $C_{12}E_8$. The theoretical predictions were made at a surfactant concentration of 1wt%. The experimental transition temperatures are 15-18°C for $C_{12}E_6$ [Corkill and Walker, 1972; Brown and Rymden, 1987), 34°C for $C_{12}E_7$ [Fujimatsu et al., 1988), and 50°C for $C_{12}E_8$ [Zana and Weill, 1985). The predicted transition temperatures are indicated by the arrows.

respectively, and compare very favorably with our theoretical predictions (see the arrows in Figure 2.7).

2.5.4 Critical Surfactant Concentration For Phase Separation

Another important micellar solution property is the critical surfactant concentration, X_c, at which the system exhibits phase separation. Beyond its fundamental importance, the ability to predict X_c should be of value to the surfactant technologist, since this concentration signals the entrance into the sometimes undesirable two-phase region, where the surfactant solution ceases to be uniform and separates into two coexisting phases. Utilizing the molecular-thermodynamic approach (see Section 2.4) we have been able, to the best of our knowledge for the first time, to predict X_c for various aqueous solutions of C_iE_j nonionic surfactants.

Table 2.2 shows values of the predicted and experimental (Mulley and Metcalf, 1962; Lang and Morgan, 1980; Corti, et al., 1984; Mulley, 1967; Evans et al., 1987; Strey and Pakusch, 1986) critical concentrations of aqueous solutions of several C_iE_j surfactants. There is very good agreement with the experimental data. As explained in Section 2.5.1, for these predictions we have used the experimentally reported critical temperatures, T_c, in conjunction with our molecular model of micellization. Note that in Table 2.2 we have presented a number of experimental values of the critical concentration and temperature for a given surfactant, because the reported values of T_c and X_c vary from author to author, and between different batches of surfactant. The observed range of experimental values

Table 2.2. Comparison of theoretical and experimental values of critical concentrations of aqueous solutions of nonionic surfactants.

Surfactant	Critical Concentration (wt%)	
	Experimental ±0.5 wt%	Theoretical
$C_{12}E_4$	0.7[a]	0.4
$C_{12}E_5$	1.0[b]	1.3
$C_{12}E_6$	2.3[c],2.6[b]	2.2
$C_{12}E_7$	3.2[b]	3.3
$C_{12}E_8$	3.2[d],4.3[b]	3.9
$C_{10}E_4$	2.1[e]	2.9
$C_{10}E_5$	3.5[e]	4.9
$C_{10}E_6$	8.0[f]	8.5

(a) Evans et al., 1987; (b) Fujimatsu et al., 1988; (c) Strey and Pakusch, 1986; (d) Corti et al., 1984; (e) Lang and Morgan, 1980; (f) Mulley and Metcalf, 1962;

could reflect differences in surfactant purity.

2.5.5 Osmotic Compressibility

The osmotic compressibility is a very useful equilibrium property in the study of solution thermodynamics. In particular, in the case of micellar solutions measurements of this property can be used to learn about (i) the shape and average size of micelles, (ii) the nature of intermicellar interactions, and (iii) the universality class associated with the deduced critical exponent.

Utilizing the molecular-thermodynamic approach (see Section 2.4), we have been able to predict the osmotic compressibility along the critical isochore, X_c, as a function of reduced temperature, $\epsilon = (T_c - T)/T_c$, for aqueous solutions of $C_{12}E_8$ (see the full curve in Figure 2.8). For this prediction, we have used the concentration variable c, the weight of $C_{12}E_8$ per unit volume of solution, which is related to X by $c = (M_s/\Omega_s)\gamma X/[1+(\gamma-1)X]$, where M_s and Ω_s are the molecular weight and volume of the surfactant, respectively. As explained in Section 2.5.1 for this prediction it was necessary to use the temperature variation of C, as deduced by fitting the predicted coexistence curve to an experimentally measured[74] one in aqueous solutions of $C_{12}E_8$. However, as stressed above, we have found that the numerical magnitude of the predicted osmotic compressibility is not very sensitive to the deduced temperature variation of C, and is mainly determined by the value of C at the critical temperature T_c, that is, by C_c. The theoretical prediction over 2.5 decades of osmotic compressibility and reduced temperature compare very favorably with the experimental measurements of Dietler and Cannell (1988) (full circles) and Corti et al. (1987) (full inverted triangles). For this prediction we have used the reduced temperatures as reported by these authors instead of the actual temperature values, because the critical temperature reported by Dietler and Cannell (1988) ($T_c = 79.2°C$) is different from that reported by Corti et al. (1987) ($T_c = 75.5°C$). In order to estimate C_c we have used the value T_c = 79.2°C reported by Dietler and Cannell (1988).

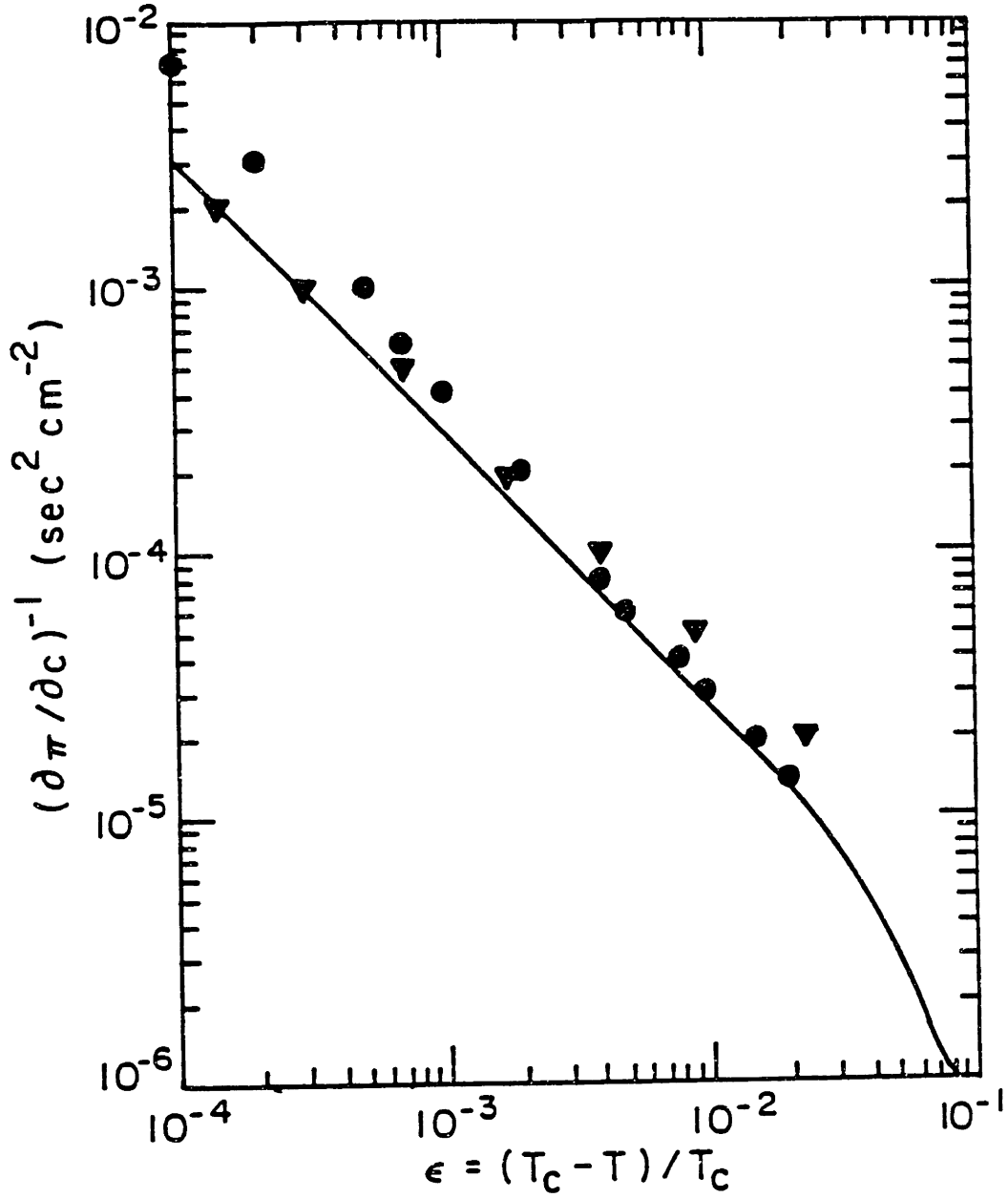

Figure 2.8: Predicted (solid line) osmotic compressibility versus reduced temperature along the critical isochore for aqueous solutions of $C_{12}E_8$. The experimental points are: (▼) Corti et al., 1987; (●) Dietler and Cannel, 1988.

2.6 CONCLUDING REMARKS

We believe that beyond its fundamental value, the molecular-thermodynamic approach for aqueous solutions of single surfactants, presented in this chapter, could become a valuable computational tool for the surfactant technologist. Indeed, using the procedures described in this chapter the surfactant technologist could identify, select and possibly even tailor aqueous solutions of single surfactants for a particular application without the need of performing routine measurements of a large number of equilibrium properties, thus making his work more efficient and productive.

A number of very important and challenging fundamental issues need further clarification and development. First, the microscopic origin and associated theoretical modelling of the intermicellar attraction, leading to the observed phase separation in aqueous solutions of C_iE_j nonionic surfactants, deserve further attention. In this chapter we have captured this attraction empirically in terms of the phenomenological parameter C, without providing a detailed molecular description of its magnitude and temperature dependence.

Second, the conformation adopted by the hydrated polyoxyethylene hydrophilic moiety of C_iE_j nonionic surfactants, both as a function of ethylene oxide content (j) and temperature, represents another unresolved problem. In the present work, we have developed a simple scaling-type argument, in conjunction with an assumed linear temperature variation of the extent of hydration, to model these complex effects.

Finally, the evaluation of interfacial effects occurring at the micellar level needs further clarification. Can one retain the concept of a macroscopic hydrocarbon-water interfacial tension? Is it possible to model the curvature dependence of the interfacial tension using concepts such as the Tolman distance? In this chapter we have assumed, as has been done in most previous theories of micellization, that these concepts remain approximately valid.

The approach presented in this chapter can be extended to treat similar phenomena in other, more complex, self-assembling surfactant systems. It is clear that by including electrostatic interactions our analysis can be implemented to describe solutions of ionic and zwitterionic surfactants, with or without added electrolytes.

By incorporating the effects of solution modifiers, such as urea, on the free energy of micelliization, the theory can be used to describe and model the variation of micellar properties as a function of the solution modifier. Indeed, in Chapter 3, we describe the effect of urea on micellar properties of aqueous solutions of $C_{12}E_6$.

By extending the thermodynamic theory (see Chapter 4) and the molecular model of micellization (see Chapter 5) to include more than one type of surfactant, it is possible to study the solution properties of mixed micellar solutions.

2.7 REFERENCES TO CHAPTER 2

Abraham, M.H. *J. Chem. Soc. Faraday Trans. 1,* **1984**, *80*, 153.

Aveyard, R.; Briscoe, B.J.; Chapman, J. *J. Chem. Soc. Faraday Trans. 1*, **1972**, *68*, 10.

Becher, P. *in Nonionic Surfactants*, Shick, M.J., Ed.; Arnold: London, **1967**, p. 478.

Ben-Shaul A.; Gelbart, W.M. *J. Phys. Chem.* **1982**, *86*, 316.

Ben-Shaul, A.; Gelbart, W.M. *Ann. Rev. Phys. Chem.* **1985**, *36*, 179.

Ben-Shaul, A.; Szleifer, I.; Gelbart, W.M. *J. Chem. Phys.* **1985**, *83*, 3597.

Blankschtein, D.; Thurston, G.M.; Benedek, G.B. *Phys. Rev. Lett.* **1985**, *54*, 955.

Blankschtein, D.; Thurston, G.M.; Benedek, G.B. *J. Chem. Phys.* **1986**, *85*, 7268.

Bordi, F.; Cametti, C.; Di Biasio, A. *J. Phys. Chem.* **1988**, *92*, 4772.

Brown, W.; Rymden, R. *J. Phys. Chem.* **1987**, *91*, 3565.

Buff, F.P. *J. Chem. Phys.* **1951**, *19*, 1591.

Buff, F.P. *in Handbuch der Physik*, Flugge, S. Ed.; Springer:Berlin, **1960**, vol 10, p. 1.

Cabane, B. *J. Physique.* **1981**, *42*, 847.

Corkill, J.M.; Goodman, J.F.; Walker, T.; Wyer, J. *Proc. R. Soc. London Ser. A* **1969**, *312*, 243.

Corkill, J.M.; Walker, T. *J. Colloid Interface Sci.* **1972**, *39*, 621.

Corti M.; Degiorgio, V. *J. Phys. Chem.* **1981**, *85*, 711.

Corti, M.; Minero, C.; Degiorgio, V. *J. Phys. Chem.* **1984**, *88*, 309.

Corti, M.; Degiorgio, V.; Cantu, L. *in Physics of Complex and Supermolecular Fluids*, Safran, S., Clark, N., Eds.; Wiley: New York, **1987**, p. 463.

Defay R.; Prigogine, I. *Surface Tension and Adsorption*, Longmans: London, **1966**.

Degiorgio, V.; Corti, M., Eds.; *Proceedings of the International School of Physics Enrico Fermi - Physics of Amphiphiles: Micelles, Vesicles and Microemulsions*, North-Holland Physics Publishing: The Netherlands, **1985**.

Degiorgio, V. *in Proceedings of the International School of Physics Enrico Fermi - Physics of Amphiphiles: Micelles, Vesicles and Microemulsions*, Degiorgio, V.; Corti, M. Eds.; North-Holland Physics Publishing: The Netherlands, **1985**. p. 303.

Dietler, G.; Cannell, D.S. *Phys. Rev. Lett.* **1988**, *60*, 1852.

Evans, H.; Tildesley, D.J.; Leng, C.A. *J. Chem. Soc. Faraday Trans.* **1987**, *83*, 1525.

Farrell, R.A. *Ph.D. Dissertation*, University of Florida **1988**.

Fisher, M.P.A.; Wortis, M. *Phys. Rev. B* **1984**, *29*, 6252.

Flory, P.J. *Statistical Mechanics of Chain Molecules*, Wiley: New York, **1969**.

Fowler R.; Guggenheim, E.A. *Statistical Thermodynamics*, Cambridge: London, **1965**.

Fujimatsu, H.; Ogasawara, S.; Kuroiwa, S. *Coll. Polym. Sci.* **1988**, *266*, 594.

Gibbs, J.W. *The Scientific Papers of J.W. Gibbs*, Dover: New York, **1961**, Vol. 1, p. 219-258.

Goldstein, R.E. *J. Chem. Phys.* **1986**, *84*, 3367.

Goodrich, F.C. *Trans. Faraday Soc.* **1968**, *64*, 3403.

Gruen, D.W.R. *J. Phys. Chem.* **1985**, *89*, 146, 153.

Guggenheim, E.A. *Mixtures: The Theory of the Equilibrium Properties of Some Simple Classes of Mixtures, Solutions and Alloys*, Clarendon: Oxford, **1952**.

Henderson J.R.; Rowlinson, J.S. *J. Phys. Chem.* **1984**, *88*, 6484.

Hermann, R.B. *J. Phys. Chem.* **1972**, *76*, 2754.

Israelachvili, J.N.; Mitchell, D.J.; Ninham, B.W. *J. Chem. Soc. Faraday Trans. 2*, **1976**, *72*, 1525.

Jiding, X.; Zhengyu, H. *in Surfactants in Solution*, Mittal, K.L., Bothorel, p., Eds.; Plenum: New York, **1986**, vol. 5, p. 1055.

Kimura, H.; Nakano, H. *J. Phys. Soc. Japan*, **1977**, *43*, 1477.

Koenig, F.O. *J. Chem. Phys.* **1950**, *18*, 449.

Lang, J.C.; Morgan, R.D. *J. Chem. Phys.* **1980**, *73*, 5849.

Leng, C.A. *J. Chem. Soc. Faraday Trans. 2* **1985**, *81*, 145.

Lindman, B,; Karlstrom, G. *Z. Phys. Chem. Neue Folge* **1987**, *155*, 199.

Ljunggren S.; Eriksson, J.C. *Prog. Coll. Polym. Sci.* **1987**, *74*, 38.

McAuliffe, C. *J. Phys. Chem.* **1966**, *70*, 1267.

Meguro, K.; Takasawa, Y.; Kawahashi, N.; Tabata, Y.; Ueno, M. *J. Colloid Interface Sci.* **1981**, *83*, 50.

Missel, P.J.; Mazer, N.A.; Carey, M.C.; Benedek, G.B. *to be published.*

Missel, P.J.; Mazer, N.A.; Benedek, G.B.; Young, C.Y.; Carey, M.C. *J. Phys. Chem.* **1980**, *84*, 1044.

Mitchell, D.J.; Tiddy, G.J.T.; Waring, L.; Bostock, T.; McDonald, M.P. *J. Chem. Soc. Faraday Trans. 1*, **1983**, *79*, 975.

Mitchell, D.J.; Ninham, B.W. *J. Phys. Chem.* **1983**, *87*, 2996.

Mittal, K.L., Ed.; *Micellization, Solubilization and Microemulsions*, Plenum: New York, 1977, Vols. 1 and 2.

Mittal, K.L.; Lindman, B. Eds.; *Surfactants in Solution*, Plenum: New York, **1984**, vols. 1, 2, and 3.

Morrison, R.T.; Boyd, R.N. *Organic Chemistry* Allyn and Bacon: Boston, **1983**.

Mukerjee, P.; Mysels, K.J. *Critical Micelle Concentration of Aqueous Surfactant Systems*, NSRDS-NBS 36, U.S. Dept. of Commerce: Washington, D.C. **1971**.

Mukerjee, P. *J. Phys. Chem.* **1972**, *76*, 565.

Mulley, B.A.; Metcalf, A.D. *J. Colloid Sci.* **1962**, *17*, 523.

Mulley, B. *in Nonionic Surfactants* Shick, M.J., Ed.; Arnold: London, **1967**, p. 421.

Nagarajan, R.; Ruckenstein, R. *J. Colloid Interface Sci.* **1977**, *60*, 221.

Nagarajan, R.; Ruckenstein, E. *J. Colloid Interface Sci.* **1979**, *71*, 580.

Nagle, F.F.; Wilkinson, D.A. *Biophys. J.* **1978**, *23*, 159.

Nilsson, P.G.; Wennerstrom, H.; Lindman, B. *J. Phys. Chem.* **1983**, *87*, 1377.

Nilsson, P.G.; Lindman, B. *J. Phys. Chem.* **1983**, *87*, 4756.

Ono S.; Kondo, S. *in Handbuch der Physik*, Flugge, S. Ed.; Springer:Berlin, **1960**, vol. 10, p. 134.

Podo, F.; Ray, A.; Nemethy, G. *J. Am. Chem. Soc.* **1973**, *95*, 6164.

Reatto, L.; Tau, M. *Chem. Phys. Lett.* **1984** *108*, 292.

Reiss, H. *in Advances in Chemical Physics*, Prigogine, I., Ed.; Interscience: London, **1965**, Vol. 9, p. 1.

Reynolds, J.A.; Gilbert, D.B.; Tanford, C. *Proc. Nat. Acad. Sci. U.S.A.* **1974**, *71*, 2925.

Rosch, M. *in Nonionic Surfactants*, Shick, M.J., Ed.; Arnold: London, **1967**, p. 753.

Rowlinson, S.; Widom, B. *Molecular Theory of Capillarity*, Clarendon: Oxford, **1982**.

Shinoda, K.; Yamaguchi, T.; Hori, R. *Bull. Chem. Soc. Japan* **1961**, *34*, 237.

Shinoda, K.; Yamanaka, T.; Kinoshita, K. *J. Phys. Chem.* **1959**, *63*, 648.

Strey, R.; Pakusch, A. *in Surfactants in Solution*, Mittal, K.L., Bothorel, P., Eds.; Plenum: New York, **1986**, Vol. 4, p. 465.

Szleifer, I.; Ben-Shaul, A.; Gelbart, W.M. *J. Chem. Phys.* **1985**, *83*, 3612.

Tanford, C. *J. Phys. Chem.* **1974**, *78*, 2649.

Tanford, C. *The Hydrophobic Effect*, Wiley: New York, **1980**.

Tolman, R.C. *J. Chem. Phys.* **1948**, *16*, 758.

Tolman, R.C. *J. Chem. Phys.* **1949**, *17*, 333.

Thurston, G.M.; Blankschtein, D.; Fisch, M.R.; Benedek, G.B. *J. Chem. Phys.* **1986**, *84*, 4558.

Vikingstad, E.; Hoiland, H. *J. Colloid Interface Sci.* **1978**, *64*, 510.

Zana R.; Weill, C. *J. Physique. Lett.* **1985**, *46*, L-953.

CHAPTER 3

EFFECT OF UREA ON $C_{12}E_6$-H_2O SOLUTIONS

3.1 INTRODUCTION

As described in Chapter 1, aqueous solutions of surfactants including nonionic ones are widely used as detergents, solubilizers, and emulsifiers. Their practical importance has triggered a significant effort to gain a fundamental understanding of their micellization characteristics, as well as their phase behavior in both aqueous and nonaqueous media (Shick, 1967).

The unique chemical structure of nonionic surfactants belonging to the alkyl polyethylene oxide (C_iE_j) family offers a convenient model system to study how systematic variations in the hydrophobic/hydrophilic character of the surfactant affects micellar solution properties (Shick, 1967; Mitchell et al, 1983). In particular, in aqueous solutions, the hydrophobic/hydrophilic character can be altered by (a) varying the number of methylene groups, i, or the number of ethylene oxide groups, j, of the surfactant, (b) varying the temperature of the solution, and (c) modifying the properties of the aqueous solvent.

A common method to modify the solvent consists of adding electrolytes, such as simple salts, or nonelectrolytes, such as urea. In particular, urea and its derivatives are well-

known denaturants of proteins and this has been attributed to the isothermal unfolding of the protein molecule (a change in conformation) due to weaker hydrophobic interactions in the presence of urea (Tanford, 1964). Several studies have been conducted to probe the effect of urea on the properties of aqueous micellar solutions (Shick, 1964; Emerson and Holtzer, 1967; Franks, 1978). Two different mechanisms for urea action have been proposed: (i) an indirect mechanism, where urea decreases the "structure" of water to facilitate the hydration of the nonpolar solute (Wetlaufer et al., 1964; Franks and Franks, 1968), and (ii) a direct mechanism, where urea replaces some of the water molecules in the hydration shell of the solute (Nozaki and Tanford, 1963; Roseman and Jencks, 1975; Enea and Jolicoeur, 1982). The indirect mechanism has been widely accepted (Franks, 1978), and many experimental results seem to support the hypothesis that urea acts as a "water-structure breaker". However, most of the experimental techniques used in these studies did not provide information at a molecular level, and conflicting interpretations of urea action have been proposed (Subramanian et al., 1971; Swenson, 1966). Recent computer simulations (Kuharski and Rossky, 1984a and 1984b) as well as some studies using electron-spin resonance spectroscopy (Baglioni et al., 1990), which have probed the system at a molecular level, seem to indicate that urea has a negligible effect on water structure and mainly replaces some water molecules in the hydration shell around the solute. These new findings appear to support the direct mechanism.

Since the properties of micellar solutions are determined by a delicate balance of hydrophobic/hydrophilic interactions of the surfactant with water (Tanford, 1980; Israelachvili, 1985), one expects that urea may have a profound effect on these properties.

Indeed, urea has been shown to (i) increase the critical micellar concentration (CMC) of ionic (Corkill et al., 1967; Hamdiyyah and Mansour; 1979; Das Gupta and Moulik, 1989) and nonionic (Shick, 1964) surfactants, (ii) decrease the mean-micellar hydrodynamic radius of ionic micelles (Mazer et al., 1979), and (iii) raise the cloud-point temperatures of aqueous solutions of nonionic surfactants (Han et al., 1988 and 1989), and lower the cloud-point temperatures of aqueous solutions of zwitterionic surfactants (Carvalho et al., 1989). The observed effects were rationalized qualitatively in terms of the properties of urea-water solutions. For example, (i) the increase in the CMC was explained in terms of the enhanced solubility of the surfactant hydrophobic moiety in the presence of urea (Wetlaufer et al., 1964), (ii) the reduction in the mean-micellar hydrodynamic radius was attributed to a lowering of the interfacial tension between hydrocarbon and water in the presence of urea (Missel et al., 1982), and (iii) the decrease in cloud-point temperatures of zwitterionic surfactants was rationalized by the fact that urea increases the dielectric constant of water (Carvalho et al., 1989). However, a quantitative understanding of these effects remains a challenging unsolved problem.

Accordingly, the aim of the present work is two-fold: (1) to conduct a systematic experimental study of the effect of urea on various micellar solution properties, such as (a) CMC, (b) micellar shape and size, and (c) phase separation behavior, in aqueous solutions of $C_{12}E_6$; (2) to provide a quantitative interpretation of the experimental results in the context of a recently developed molecular-thermodynamic theory of micellar solutions. We have chosen $C_{12}E_6$ because aqueous solutions of this nonionic surfactant offer a number of convenient experimental features which are described in Sec. 3.3.

The remainder of this chapter is organized as follows. Sec. 3.2 describes the theoretical approach used to model the effect of urea on micellar properties of aqueous solutions of $C_{12}E_6$. Sec. 3.3 presents a description of the materials and experimental methods used to determine the various properties. Sec. 3.4 discusses the estimation of the various molecular parameters which appear in the theoretical approach presented in Sec. 3.2. Sec. 3.5 compares the theoretical predictions with the experimental results, and discusses possible mechanisms for the observed effect of urea. Finally, Sec. 3.6 presents some concluding remarks.

3.2 THEORETICAL APPROACH

In this section we briefly review the molecular-thermodynamic approach presented in Chapter 2 (Puvvada and Blankschtein, 1990a and 1990b; Blankschtein and Puvvada, 1990) to predict micellar solution properties. The new approach consists of blending a molecular model of micellization (Puvvada and Blankschtein, 1990a), which captures the essential physico-chemical forces operating at the micellar level, with a thermodynamic framework for micellar solutions (Blankschtein et al., 1985 and 1986), which captures the salient features of the solution at the macroscopic level.

The theoretical formulation has been successfully utilized to predict micellar properties of aqueous solutions of nonionic surfactants, belonging to the alkyl polyethylene oxide and glucoside families, as a function of surfactant molecular architecture, surfactant concentration, and temperature (Puvvada and Blankschtein 1990a). The predicted

properties, which compare favorably with available experimental data, include (i) CMC, (ii) micellar size distribution and its characteristics, (iii) micellar shape, (iv) coexistence curves, including the critical surfactant concentration, and (v) other thermodynamic properties such as the osmotic compressibility. The thermodynamic framework has also been successfully utilized to describe the phase behavior of aqueous solutions of zwitterionic surfactants, in the presence of added electrolytes (Huang et al., 1990) and urea (Carvalho et al., 1989), over a wide range of surfactant concentrations and temperatures.

The encouraging results obtained so far have motivated us to implement the molecular-thermodynamic approach to describe the effect of urea on micellar properties of aqueous solutions of $C_{12}E_6$. Below, we present the modifications that need to be implemented in the molecular model of micellization to account for the presence of urea, as well as briefly describe the thermodynamic framework and the calculation of micellar solution properties. A complete account of the molecular-thermodynamic formulation can be found in Chapter 2.

3.2.1 Molecular Model of Micellization

As descibed in Chapter 2, the molecular model is used to estimate the magnitude of the free energy of micellization, $g_{mic}(n,l_c,sh)$, from the molecular characteristics of the surfactant and the solvent. Note that g_{mic} represents the free-energy change when a surfactant molecule is transferred from bulk solvent (which includes water and any additives such as urea) to a micelle (characterized by an aggregation number, n, core-minor radius,

l_c, and shape, sh) present in the same solvent. The numerical magnitude of g_{mic}, which reflects the propensity for micelles to form and subsequently grow, summarizes the many physico-chemical forces responsible for micelle formation.

The free-energy contributions associated with the various forces are evaluated using a thought process to "visualize" the formation of a micelle from individual monomers as a series of reversible steps. The free energy of micellization, g_{mic}, is then evaluated by summing the free-energy changes associated with each step of the thought process. Below, we describe the various steps of the thought process needed to estimate g_{mic} for the $C_{12}E_6$-water-urea system.

(a) After breaking the bond between the hydrophilic moiety ("head") and the hydrophobic moiety ("tail") of each $C_{12}E_6$ molecule, the tails are transferred from the urea-water(uw) solution to bulk hydrocarbon(hc). This gives rise to an attractive contribution, $g_{uw/hc}$, that can be conveniently evaluated using a two-step transfer process. First, the tails are transferred from the urea-water solution to pure water(w). This gives rise to a repulsive contribution, $g_{uw/w}$, since urea enhances the solubility of the hydrocarbon tails in water. Subsequently, the tails are transferred from pure water to bulk hydrocarbon, which gives rise to an attractive contribution, $g_{w/hc}$. While $g_{w/hc}$ can be evaluated from the known solubilities of hydrocarbons in pure water (Abraham, 1984), the evaluation of $g_{uw/w}$ is more problematic because solubility data of n-alkanes in urea-water solutions are limited to those between methane and butane. To obtain a more accurate estimation of $g_{uw/w}$ for the longer tails, we have used the available solubility data for the shorter chains in conjunction with a recently proposed hydration-shell hydrogen-bond model (Muller, 1990a and 1990b) (see Sec. 3.4 for

more details). We find that $g_{uw/w} \approx (0.3U)$ kT, where U is the molarity of urea, k is the Boltzmann constant, and T is the absolute temperature.

(b) The next step involves the creation of an interface separating a hydrocarbon core (characterized by minor radius, l_c, and shape, sh) from the urea-water solution. This step reflects the repulsive interfacial contribution to g_{mic}, and the resulting free-energy change per monomer is evaluated by

$$g_\sigma = \sigma_o \left[1-(S-1)\delta/l_c\right] (a-a_o) , \qquad (3.1)$$

where σ_o is the interfacial tension between bulk hydrocarbon and the urea-water solution, δ is the Tolman distance which was estimated (see Sec. 2.2.2) to be 2.25Å for $C_{12}E_6$ and assumed to be independent of urea concentration, a_0 is the interfacial area screened from contact with water by the head, and $a = Sv/l_c$ is the total interfacial area per monomer which is exposed to water, where S is a shape factor (3 for spheres, 2 for cylinders, and 1 for discs or bilayers), and v is the volume of the tail estimated (see Sec. 2.2.2) to be 323 A^3. The dependence of σ_o on urea concentration is given by $\sigma_o = \sigma_o(U=0) - \sigma_u U$, with $\sigma_u \approx 1.5$ dyne/cm (see Sec. 3.4 for details on the estimation procedure).

(c) The next step involves estimating the free-energy change associated with the loss in conformational degrees of freedom of the tails inside the micellar core. This repulsive contribution, $g_{hc/mic}$, is calculated by utilizing a single-chain mean-field model described in Sec. 2.2.2 (Ben-Shaul et al., 1985; Szliefer et al., 1985; Gruen, 1985). This involves the generation of a large number of conformations of the tail inside the micellar core, in the context of the rotational isomeric state approximation, and the evaluation of the partition

function and associated free energy. Note that this free-energy contribution is independent of urea concentration.

(d) After reforming the bond between the head and the tail at the interface between the micellar core and the urea-water solution, the final step involves evaluating the free-energy change associated with steric interactions between the uncharged surfactant heads. This repulsive contribution, g_{st}, is calculated by treating the heads present at the interface as an ideal-localized monolayer, which reflects the fact that each head is physically attached to a tail at the interface. The resulting free-energy contribution is given by

$$g_{st} = -kT \ln\left(1-\frac{a_h}{a}\right), \tag{3.2}$$

where a_h is the average cross-sectional area of the head. This important molecular characteristic reflects the interactions of the ethylene oxide head with the urea-water solution, and consequently is expected to vary both with temperature and the concentration of urea (for details on the estimation of these variations see Sec. 3.4).

The four contributions, $g_{uw/hc}$, g_{σ}, $g_{hc/mic}$, g_{st}, to g_{mic} are calculated for the three regular shapes of spheres, infinite-sized cylinders, and infinite-sized discs as a function of the micellar core-minor radius, l_c. The total free energy, $g_{mic}(l_c,sh)$, is then minimized with respect to l_c in order to obtain the optimum values of the micellar core-minor radius, $l^*_c(sh)$, and the free energy of micellization, $g^*_{mic}(sh)$, for that shape. Subsequently, the optimum shape of the micelle, sh^*, is determined by minimizing $g^*_{mic}(sh)$ with respect to sh. This procedure allows us to predict whether the micelles that form exhibit two-dimensional, one-

dimensional, or no growth. However, since entropic considerations limit the size of micelles, g_{mic} for the intermediate non-regular finite-sized micelles needs to be estimated. This is done by linearly interpolating between the optimum free energies corresponding to the limiting regular shapes. For example, g_{mic} for a micelle that exhibits one-dimensional growth is estimated by linearly interpolating between the free energies of micellization of an infinite-sized cylindrical micelle and a finite-sized spherical micelle. For additional details see Sec. 2.2.3.

3.2.2 Thermodynamic Framework

It is well established that over the range of urea concentrations of interest in this work (0-6M), urea mixes ideally with water (Stokes, 1967; Grant et al., 1972). Therefore, we expect urea to distribute uniformly in the solution. There is also evidence that when a urea-water micellar solution undergoes liquid-liquid phase separation, the urea concentrations in the two coexisting phases do not differ significantly (Carvalho et al., 1989). This seems to suggest that, as a first approximation, it is reasonable to treat the ternary system $C_{12}E_6$-water-urea as a pseudobinary system of $C_{12}E_6$ in an effective solvent, whose properties depend on the concentration of urea.

With this in mind, we use a thermodynamic description of the micellar solution which incorporates the following features: (i) the free energy of micellization, g_{mic}, (ii) a distribution of micelles in chemical equilibrium with each other, (iii) the entropy of mixing micelles, monomers, and solvent, and (iv) a mean-field interaction potential between the

micelles. The total Gibbs free energy of the solution, G, is given by (see Chapter 2)

$$G = N_w\mu_w^o + N_s\mu_1^o + \sum_n nN_n g_{mic}(n,l_c,sh) + kT\left[N_w lnX_w + \sum_n N_n \ln X_n\right] - \frac{1}{2}CN_s\Phi, \quad (3.3)$$

where N_n and N_w are the number of n-mers and solvent molecules respectively, X_n and X_w are the corresponding mole fractions, N_s is the total number of surfactant molecules, ϕ is the total surfactant volume fraction, μ°_1 and μ°_w are the standard-state chemical potentials of surfactant and solvent, respectively, and C is a mean-field interaction parameter that reflects the magnitude of the effective intermicellar attraction. Note that the presence of urea can modulate the effective value of C.

Using the free-energy expression given in Eq. (3.3), and imposing the conditions of chemical equilibria between micelles having different aggregation numbers, the following expression for the micellar size distribution, $\{X_n\}$, was obtained in see Sec. 2.3

$$X_n = \frac{1}{e} X_1^n e^{-\beta n[g_{mic}(n)-1]}, \quad (3.4)$$

where X_1 is the monomer mole fraction, and $\beta = 1/kT$. All equilibrium properties associated with the distribution, including the CMC, and characteristics of the distribution, can be computed by solving Eq. (3.4) in conjunction with the material balance equation, $X = \Sigma nX_n$, where X is the total surfactant mole fraction.

In particular, we have evaluated the CMC by plotting the monomer mole fraction, X_1, as a function of the total surfactant mole fraction, X, and identifying the concentration

where the plot exhibits a break.

We have also computed the relative variance, V, of the micellar size distribution,

$$V = \frac{\langle (n - \langle n \rangle_w)^2 \rangle_w}{\langle n \rangle_w^2}, \qquad (3.5)$$

where $\langle n \rangle_w$ is the weight-average micellar aggregation number. Note that the relative variance reflects the polydispersity and shape of the micelles.

The critical point, which signals the onset of phase separation, is characterized by the critical surfactant concentration, X_c, and the critical temperature, T_c. At the critical point, thermodynamic stability requires that the two conditions, $(\partial^2 g/\partial X^2)_{T,P} = 0$ and $(\partial^3 g/\partial X^3)_{T,P} = 0$ should be satisfied, where $g = G/(N_w+N_s)$. By simultaneously solving these two equations we have evaluated the values of X_c, and of the critical interaction parameter, C_c, corresponding to the value of C at T_c.

In addition, the entire cloud-point (coexistence) curve can be calculated by demanding the simultaneous equalities of the monomer and solvent chemical potentials in the two coexisting phases. For additional details see Sec. 2.3.

3.3 MATERIALS AND EXPERIMENTAL METHODS

We have chosen $C_{12}E_6$ because aqueous solutions of this nonionic surfactant offer a number of convenient experimental features: (i) the CMC is very low (6.7×10^{-5}M), thus

providing a broad dilute concentration range to study micellar solution properties in the absence of significant intermicellar interactions, (ii) the solution exhibits a cloud-point (coexistence) curve with a lower consolute (critical) temperature of $T_c \approx 51°C$, thus allowing a convenient temperature range over which the phase separation behavior can be studied as a function of urea concentration under atmospheric pressure, and (iii) the micelles in this system exhibit a "sphere-to-rod" shape transition as the temperature is increased beyond approximately 18°C, and this temperature is sufficiently below the critical temperature so that shape transitions can be studied using light scattering measurements without the complicating influence of critical fluctuations.

3.3.1 Materials and Sample Preparation

Homogeneous $C_{12}E_6$ was obtained from Nikko Chemicals, Tokyo, (Lot No. 7008) and used without any further purification. The high purity of the surfactant was confirmed by the absence of any detectable minimum in the measured surface tension versus surfactant concentration curves, as well as by comparing our measured value of $T_c \approx 51.14°C$ for the $C_{12}E_6$-water system with values reported in the literature from highly purified samples (Strey and Pakusch, 1986; Fujimatsu et al., 1988). In addition, to ensure uniformity in the results, all our measurements were conducted using the same lot of surfactant. Urea was obtained from Merck with a nominal purity of 99.5% and was used without any further purification. All solutions were prepared using deionized water which had been fed through a Milli-Q ion-exchange system.

3.3.2 Critical Micellar Concentration Measurement

The critical micellar concentration (CMC) was obtained by the surface-tension method. This method is based on the fact that the surface tension decreases quite rapidly with increasing surfactant concentration until the CMC, above which it remains practically constant. By plotting the measured surface tension as a function of the logarithm of the surfactant concentration, the CMC was estimated from the break in the surface tension curve. A Wilhelmy-Plate Tensiometer (Kruss K10T) was used to measure the surface tensions. All measurements were carried out in a thermostated device maintained at 25°C.

3.3.3 Coexistence Curve Determination

Coexistence curves for liquid-liquid phase separation were determined by the cloud-point method. In the case of $C_{12}E_6$ in water, this method consists of visually identifying the temperature at which solutions of known concentration become cloudy, upon raising the temperature. Each sample was placed in a transparent thermo-regulated device whose temperature was controlled to within 0.01°C. Initially, each sample was cooled to a temperature low enough so that it exhibited a single, clear, homogeneous phase. The temperature was then raised in small steps until the solution started to cloud at a temperature T_u. As soon as clouding was observed, the temperature was lowered in small steps until the cloudiness disappeared at a temperature T_d. T_{cloud} was then determined by taking the average of T_u and T_d. Note that at each step the sample was first stirred

thoroughly, using a magnetic stirrer, to ensure temperature homogeneity, and subsequently observed for any signs of cloudiness with the stirrer shut off. The entire procedure was repeated several times with smaller steps in temperature. This cycling procedure was adopted to ensure reproducibility and reversibility in the observed clouding behavior. All measurements were reproducible to within 0.05°C.

3.3.4 Light Scattering Measurements

Dynamic light scattering and intensity measurements were performed using a He-Ne laser (λ = 6328 Å) in a 90° configuration, and a home-made correlator with 128 channels. These measurements were performed as a function of temperature (5-65°C) and urea concentration (0, 2, 4, and 6M urea) at a fixed surfactant mole fraction of 10^{-3}. At this surfactant concentration both intensity and scattering-correlation functions have been shown (Brown and Rymden, 1987) to be independent of scattering angle in $C_{12}E_6$-D_2O solutions. The dynamic light scattering data were interpreted using a cumulants analysis (Koppel, 1972; Mazer et al., 1976). The mean-micellar hydrodynamic radius was calculated, in the context of the Stokes-Einstein relation, from the first cumulant using available (Venkatesan and Suryanarayana, 1956) viscosity data for urea-water solutions.

3.4 ESTIMATION OF MOLECULAR PARAMETERS

As discussed in Sec. 3.2, the molecular-thermodynamic approach can be used to predict various properties of micellar solutions using molecular information about the surfactant and the solvent. The important molecular parameters involved, including the effect of urea on them, are described below.

In Sec. 3.2.1 we saw that the solubility of the surfactant tail in the solvent is an important molecular parameter which needs to be adequately described. Indeed, the increased solubility of the tail in water in the presence of urea is captured by the free-energy contribution, $g_{uw/w}$. Recall that this contribution represents the free-energy change associated with transferring the tail from the urea-water solution to pure water. Since solubility data of n-alkanes in urea-water solutions are only available for those between methane and butane (Wetlaufer et al., 1964), the required extrapolation to the longer tail of $C_{12}E_6$ seems questionable. We have therefore estimated this contribution using a recently proposed (Muller, 1990a and 1990b) hydration-shell hydrogen-bond model. This is a two-state model, where the hydrogen atom of a water molecule is either hydrogen-bonded or not, and the average fraction of broken and intact hydrogen bonds are calculated through a knowledge of the bond-breaking enthalpies and entropies (the adjustable parameters of the model). Using this simple model, it was possible to reproduce measured values of excess heat capacities, enthalpies, entropies and free energies of transfer from pure hydrocarbon to aqueous solutions with and without added urea. The model could also explain the very puzzling trends in water proton NMR chemical shifts for solutions of polar

molecules with large hydrophobic groups. Using this model and a cavity surface area of 530 $Å^2$ for the C_{12} tail, we estimate a value of approximately 0.3 kT per molar urea for the free-energy change, $g_{uw/w}$. Note that a value of 530 $Å^2$ for the cavity surface area of a C_{12} chain was obtained by extrapolating the values reported (Amidon et al, 1975) for shorter (up to C_{10}) n-alkanes.

A second important molecular feature is the value of the interfacial tension between bulk hydrocarbon and the urea-water solution, σ_o. In this respect, interfacial tensions between heptane and water in the presence of 1M and 2M urea were recently measured (Gabrielli, 1989). The measured values indicate that in the presence of urea σ_o is lowered by approximately 1.5 dyne/cm per molar urea. This value was linearly extrapolated up to 6M urea and used in all our calculations. Note that the linear extrapolation is reasonable since, as mentioned earlier, urea-water solutions exhibit ideal behavior over this range of urea concentrations (Stokes, 1967; Keefe and Shack, 1972).

The third important molecular characteristic of the surfactant is the average cross-sectional area of the head, a_h. Indeed, the magnitude of a_h determines the value of the steric contribution, g_{st}, to the free energy of micellization. As stated earlier, the hydrophobic/hydrophilic character of the surfactant can be altered by varying temperature. Thus, on increasing temperature $C_{12}E_6$ becomes less hydrophilic Nilsson and LIndman, 1983). The precise mechanism leading to the observed temperature dependence is still a topic of active research (Kjellander and Florin, 1981; Goldstein, 1984; Karlstrom, 1985). One explanation which has been suggested (Mitchell et al., 1983; Nilsson and Lindman, 1983) is that the ethylene oxide groups of $C_{12}E_6$ hydrate in the presence of water, with the

hydration number decreasing with increasing temperature. Consequently, we expect a_h to decrease as the temperature is increased. In addition, according to the direct mechanism (Nozaki and Tanford, 1963) described earlier, urea perturbs the hydration shell of the head by replacing some of the water molecules. Since an urea molecule is approximately 2.5 times larger than a water molecule, we expect a_h to increase with the addition of urea at a fixed temperature. Note that the larger size of the urea molecules also implies that a_h will decrease at a faster rate with increasing temperature in the presence of urea. These qualitative arguments are summarized by the following empirical expression for the dependence of a_h on temperature and urea concentration

$$a_h = a_{ho}\{1 - H(T-298)\} , \tag{3.6}$$

with $a_{ho} = (38.1 + 0.8U)$ Å^2 and $H = (7.5 + 0.57U)\times10^{-3}$ per °C, where U is the molarity of urea. Note that the values of a_{ho} and H at 0M urea are the same as those used to predict the properties of $C_{12}E_6$ in pure water (see Sec. 2.3). The values used to describe the dependence of a_{ho} and H on urea concentration have been adjusted to best fit experimental results. Work is currently in progress to validate these numbers using other independent measurements.

Below, we use the molecular-thermodynamic theory described in Sec. 3.2, with the three molecular parameters estimated in this section, to predict and interpret a broad spectrum of micellar solution properties as a function of urea concentration and temperature.

3.5 RESULTS AND DISCUSSIONS

Figure 3.1 shows predictions of the CMC of aqueous solutions of $C_{12}E_6$ as a function of urea concentration at 25°C. The predicted values are in good agreement with our measured values at 0, 2, and 4M urea concentrations. The estimated experimental uncertainties, shown by the error bars, reflect the error in determining the CMC from the measured surface-tension curve. Note that as the concentration of urea was increased, the measured surface-tension values were more scattered, and as a result the CMC could only be determined with a larger uncertainty. Measurements could not be performed at 6M urea because of the precipitation of a white solid, presumably urea or an urea complex, on the Wilhelmy plate and on the sides of the sample container. The observed increase in the CMC with increasing urea concentration is consistent with the enhanced solubility of the nonpolar tail, and the increased hydration of the ethylene oxide (EO) head in the presence of urea. In the context of the molecular model of micellization, we find that the enhanced solubility of the tail in urea-water solutions is the dominant factor in determining the CMC.

Figure 3.2 shows the measured intensity of scattered light (in arbitrary units) as a function of temperature for 0, 2, 4, and 6M urea concentrations at a fixed surfactant mole fraction of 10^{-3}. The figure clearly indicates that, at fixed urea concentration, the scattering intensity remains approximately constant up to a certain temperature T^* (T^* = 15, 22, 28, and 37°C for 0, 2, 4, and 6M urea concentrations, respectively), beyond which it increases rapidly. In each case, T^* is sufficiently below the critical temperature (T_c-T $\approx$ 37°C) that critical-fluctuation effects should be minimal. Consequently, it is reasonable to associate the

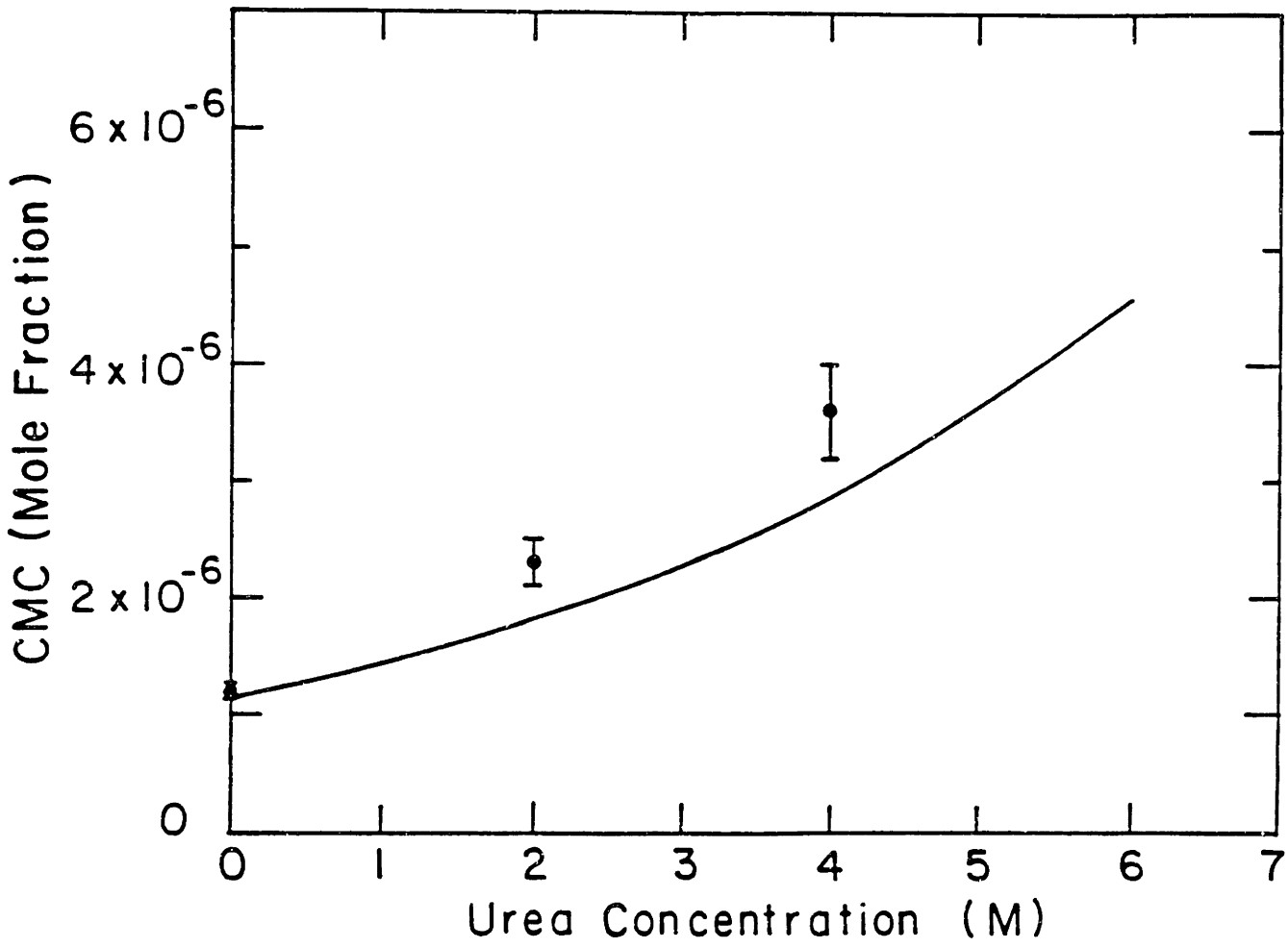

Figure 3.1. Measured critical micellar concentration (CMC) of aqueous solutions of $C_{12}E_6$ for 0, 2, and 4M urea concentrations. The solid line represents the theoretical prediction.

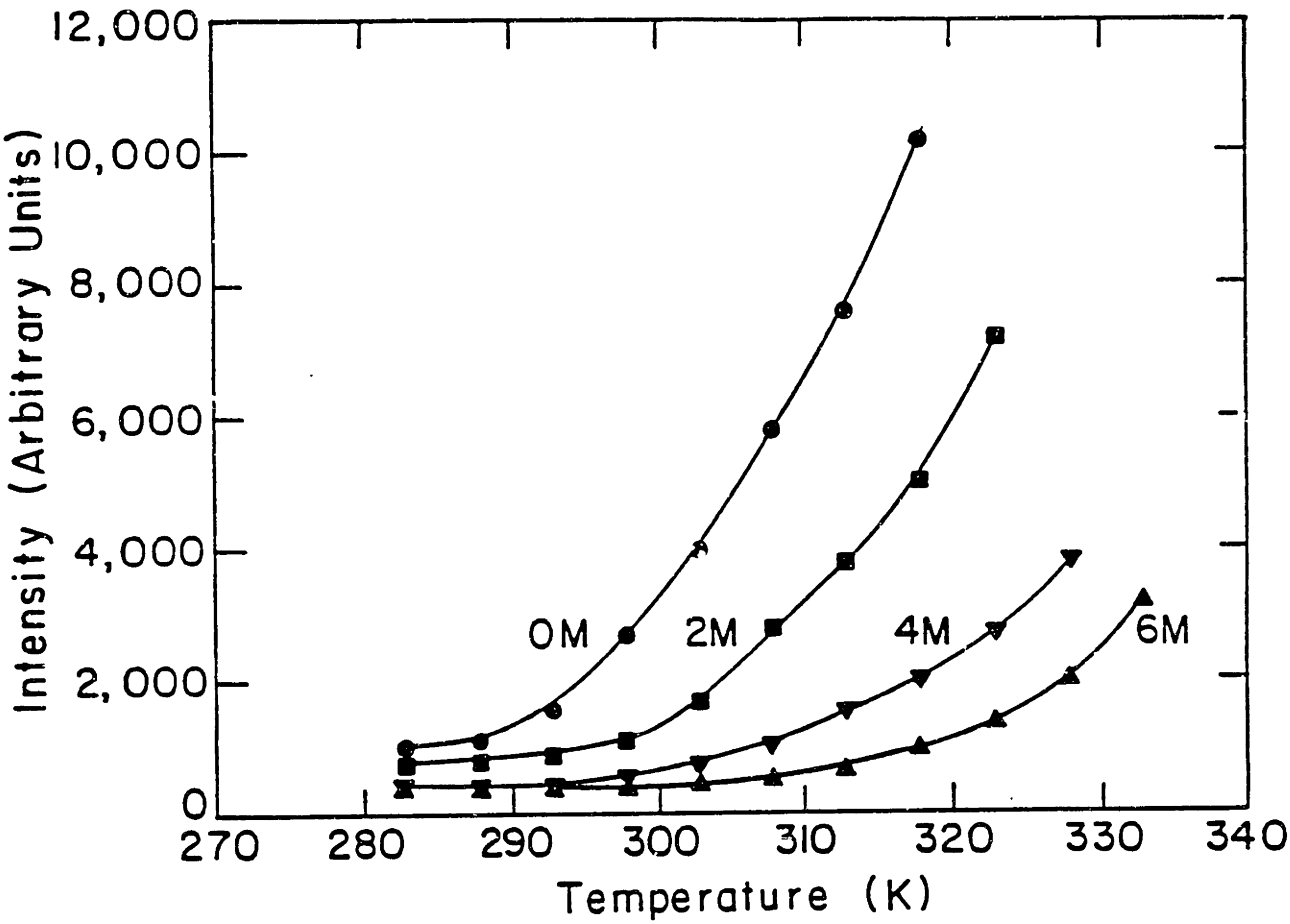

Figure 3.2. Measured intensity of scattered light (in arbitrary units) as a function of temperature for 0, 2, 4, and 6M urea concentrations. The various symbols represent experimental points. The solid lines are drawn to guide the eye.

increase in intensity with an increase in micellar size. With this in mind, the picture that seems to emerge is one in which, for $T<T^*$, the micelles are relatively small with their size approximately constant, and for $T>T^*$, the micelles exhibit growth. In addition, urea is seen to have a significant effect on T^*, shifting it to higher values. These conclusions are supported by the measured values of the mean-micellar hydrodynamic radius, R_h, as a function of temperature and urea concentration reported in Fig. 3.4 (see discussions below). The observed experimental trends can be rationalized in terms of interactions between the ethylene oxide (EO) heads and water in the presence of urea. As described in Sec. 3.4, the EO heads of $C_{12}E_6$ dehydrate with increasing temperature. This reduces the value of a_h and associated steric repulsions between the heads, thus enabling the micelles to grow from spheroidal structures (characterized by a larger curvature) into rod-like structures (characterized by a smaller curvature) as temperature is increased. However, addition of urea at fixed temperature increases the value of a_h, thus effectively increasing steric repulsions. This, in turn, implies smaller micelles, and a shift in the "sphere-to-rod" transition temperature, T^*, to higher values.

The postulated "sphere-to-rod" transition occurring at T^*, as well as the shift in T^* to higher temperatures upon adding urea, can be predicted in the context of the molecular-thermodynamic theory. For this purpose, it is convenient to consider the relative variance of the micellar size distribution, V, which constitutes a measure of polydispersity and micellar shape. In particular, small monodisperse spheroidal micelles are characterized by $V=0$, whereas large polydisperse rod-like micelles are characterized by $V=0.5$ (see Sec. 2.3). We have therefore used Eq. (3.5) to predict the temperature variation of V (at a fixed

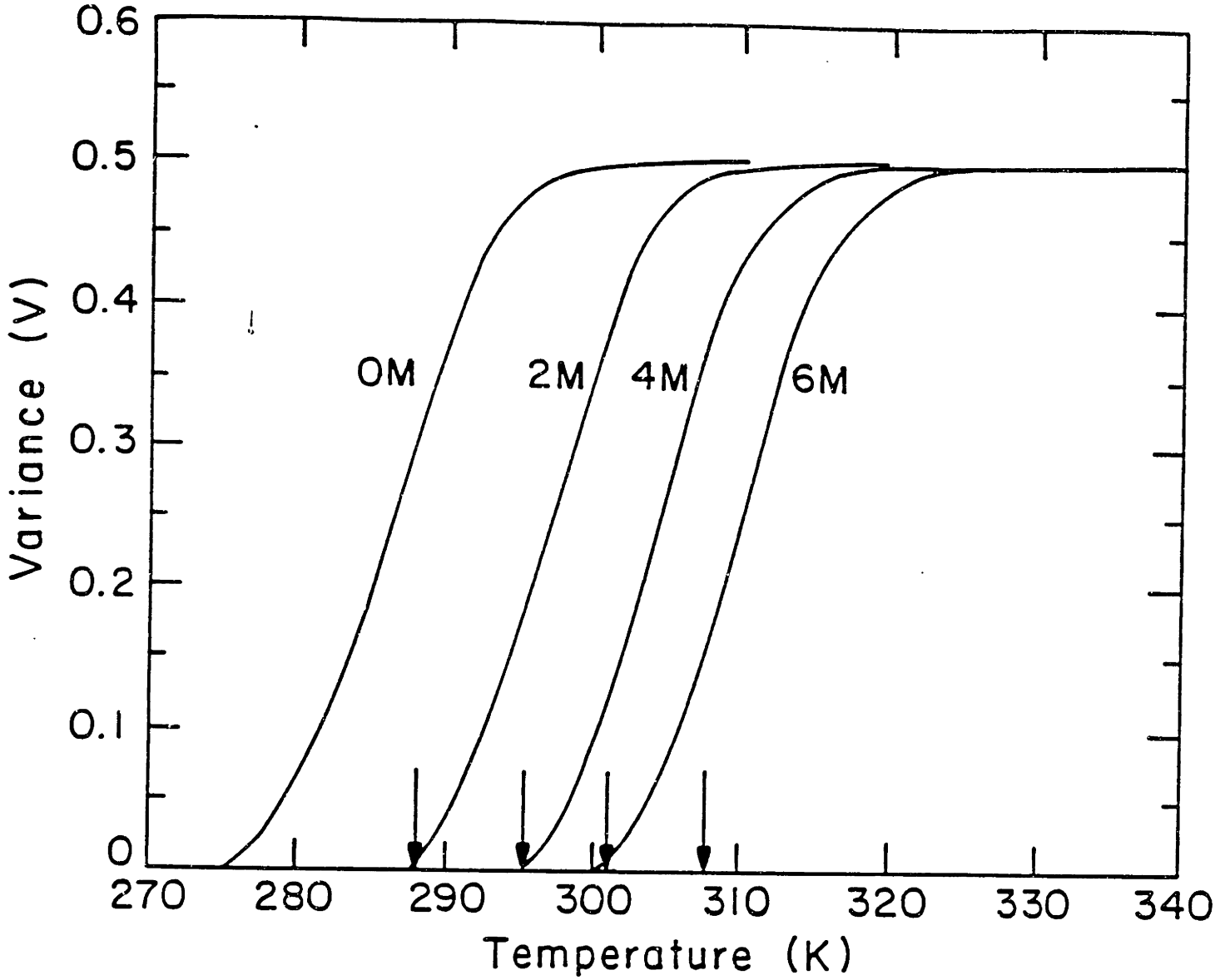

Figure 3.3. Predicted variance (V) of the micellar size distribution as a function of temperature for aqueous solutions of $C_{12}E_6$ at 0, 2, 4, and 6M urea concentrations. The theoretical predictions were made at a surfactant mole fraction of 10^{-3}. The arrows represent the experimentally determined "sphere-to-rod" shape transition temperatures obtained from the break in the intensity versus temperature curves shown in Fig. 3.2.

surfactant mole fraction of 10^{-3}) for 0, 2, 4, and 6M urea concentrations, see Figure 3.3. The figure shows that there is a narrow temperature range in which micelles grow from small monodisperse spheroidal micelles (V=0) to large polydisperse rod-like micelles (V=0.5), and that this transition temperature is shifted to higher values with increasing urea concentration. The theoretical predictions of the transition temperatures are in very good agreement with the experimentally determined T^* values shown by arrows in Fig. 3.3, obtained from the break in the intensity versus temperature curves shown in Fig. 3.2.

Figure 3.4 shows the measured mean-micellar hydrodynamic radius, R_h, as a function of temperature for 0, 2, 4 and 6M urea concentrations. Note that the results are presented as $\log(R_h)$ versus T_c-T, the difference between the critical temperature, T_c, and the actual temperature, T. We have used this representation to illustrate the rather remarkable fact that the curves for all urea concentrations overlap, and that the behavior of R_h exhibits a pronounced change at a value of T_c-T $\approx$ 37°C for all urea concentrations. This behavior seems to suggest a strong correlation between micellar shape and size and phase separation. We will comment further on this correlation after discussing the effect of urea on phase separation (see below).

Figure 3.5 shows the predicted variation of the critical concentration for phase separation, X_c, as a function of urea concentration. For these predictions, we have used the measured values of T_c in conjunction with the molecular-thermodynamic theory. The predicted values are in excellent agreement with our experimental values at 0, 2, 4, and 6M urea concentrations. Note that the experimental critical concentration values were determined from the minima of the measured cloud-point curves. The estimated

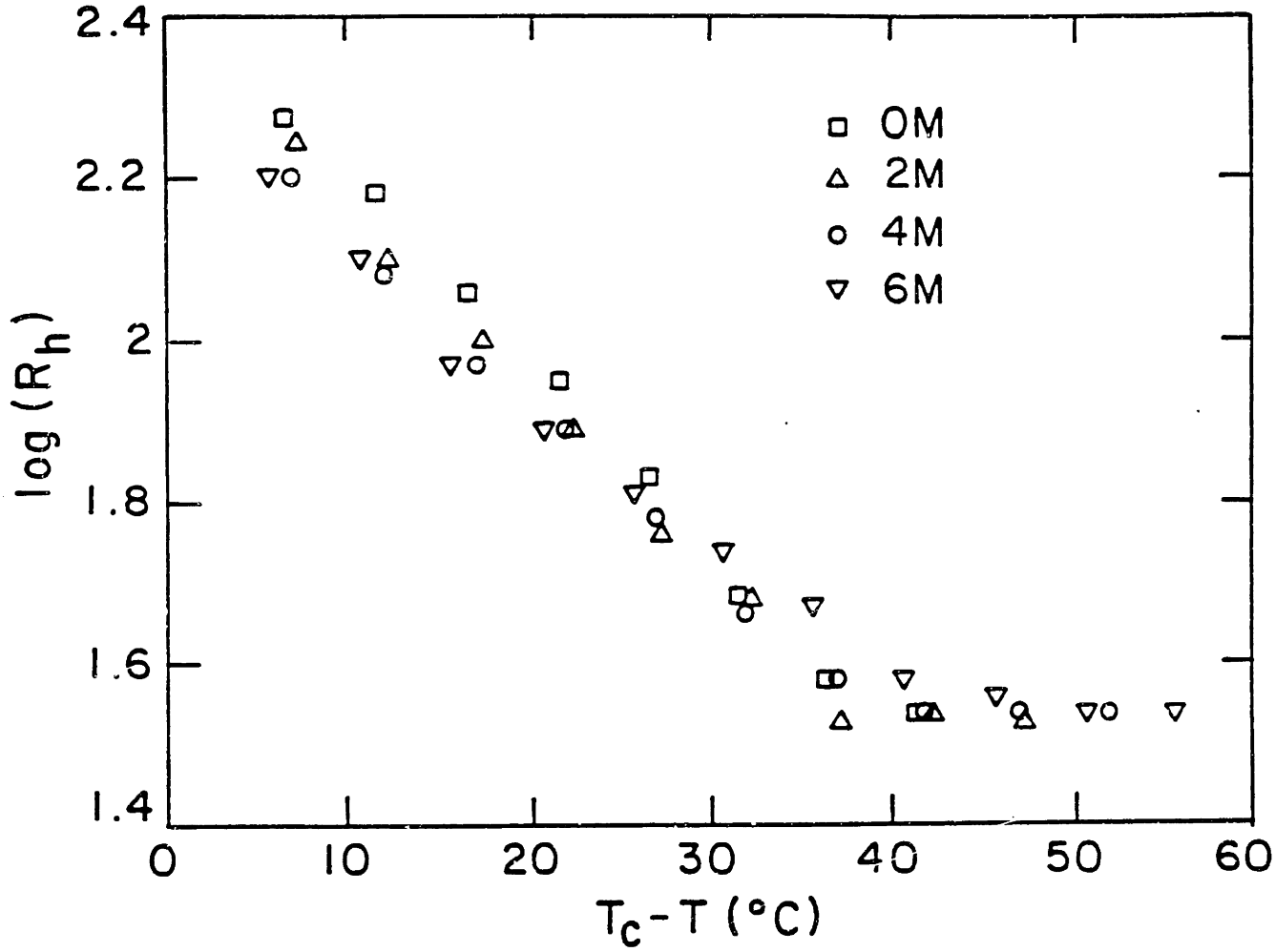

Figure 3.4. Measured mean-micellar hydrodynamic radius, R_h, as a function of T_c-T for aqueous solutions of $C_{12}E_6$ at 0, 2, 4, and 6M urea concentrations. The resulting universal curve exhibits a break at a value of T_c-T ≈ 37°C.

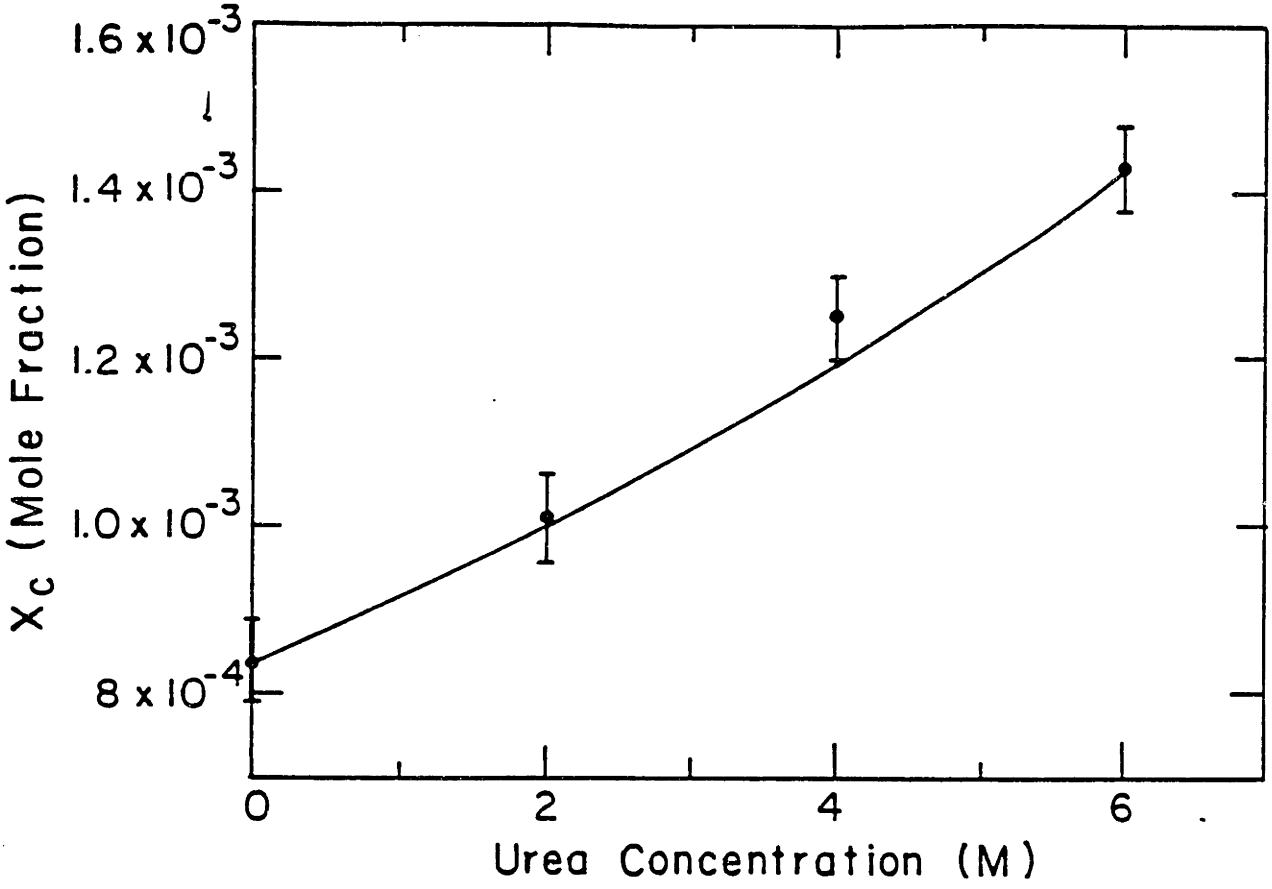

Figure 3.5. Measured critical concentration for phase separation, X_c, of aqueous solutions of $C_{12}E_6$ for 0, 2, 4, and 6M urea concentrations. The solid line represents the theoretical prediction.

experimental uncertainties, shown by the error bars, reflect the error in determining the minima.

Figure 3.6 shows the measured cloud-point temperatures (various symbols) for 0, 2, 4, and 6M urea concentrations (the solid lines are drawn to guide the eye). Using the measured values, in the context of the molecular-thermodynamic theory, it is possible to evaluate the effective mean-field intermicellar attraction parameter, C, as a function of temperature and urea concentration. Figure 3.7 shows that, at a fixed temperature, the effective intermicellar attraction, captured by C, decreases with increasing urea concentration. Furthermore, the value of C increases linearly with temperature with the slope, dC/dT, increasing with increasing urea concentration. This dependence of C on temperature and urea concentration can be rationalized in terms of competing attractive van der Waals and repulsive steric interactions between the hydrated micelles (Mitchell et al., 1983; Israelachvili, 1985). Indeed, if one envisions that the addition of urea results in a thicker hydration layer (because urea is larger than water, and according to the direct mechanism it replaces some of the water molecules in the hydration layer of the micelle), steric repulsions between micelles would increase in the presence of urea at a fixed temperature. Furthermore, since urea increases the static dielectric constant of water (Stokes, 1967; Keefe and Shack, 1972), the strength of the attractive van der Waals interactions would also increase in the presence of urea at a fixed temperature. However, since the overall effect of adding urea is a reduction in the effective intermicellar attraction parameter, C, it appears that urea has a larger effect on the steric repulsions than on the van der Waals attractions between the hydrated micelles. Similarly, as temperature is

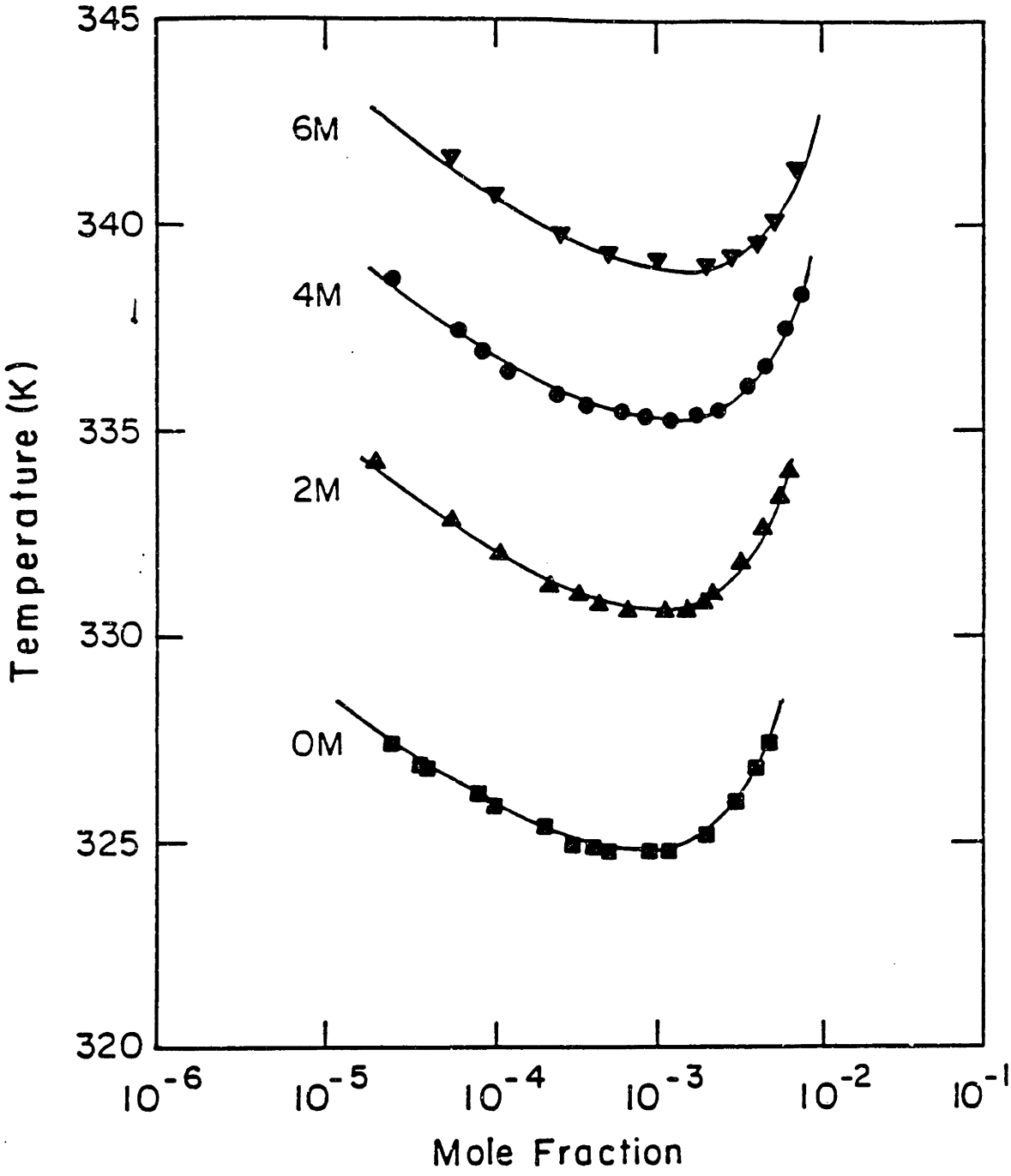

Figure 3.6. Measured cloud-point temperatures (various symbols) for 0, 2, 4, and 6M urea concentrations. The solid lines are drawn to guide the eye.

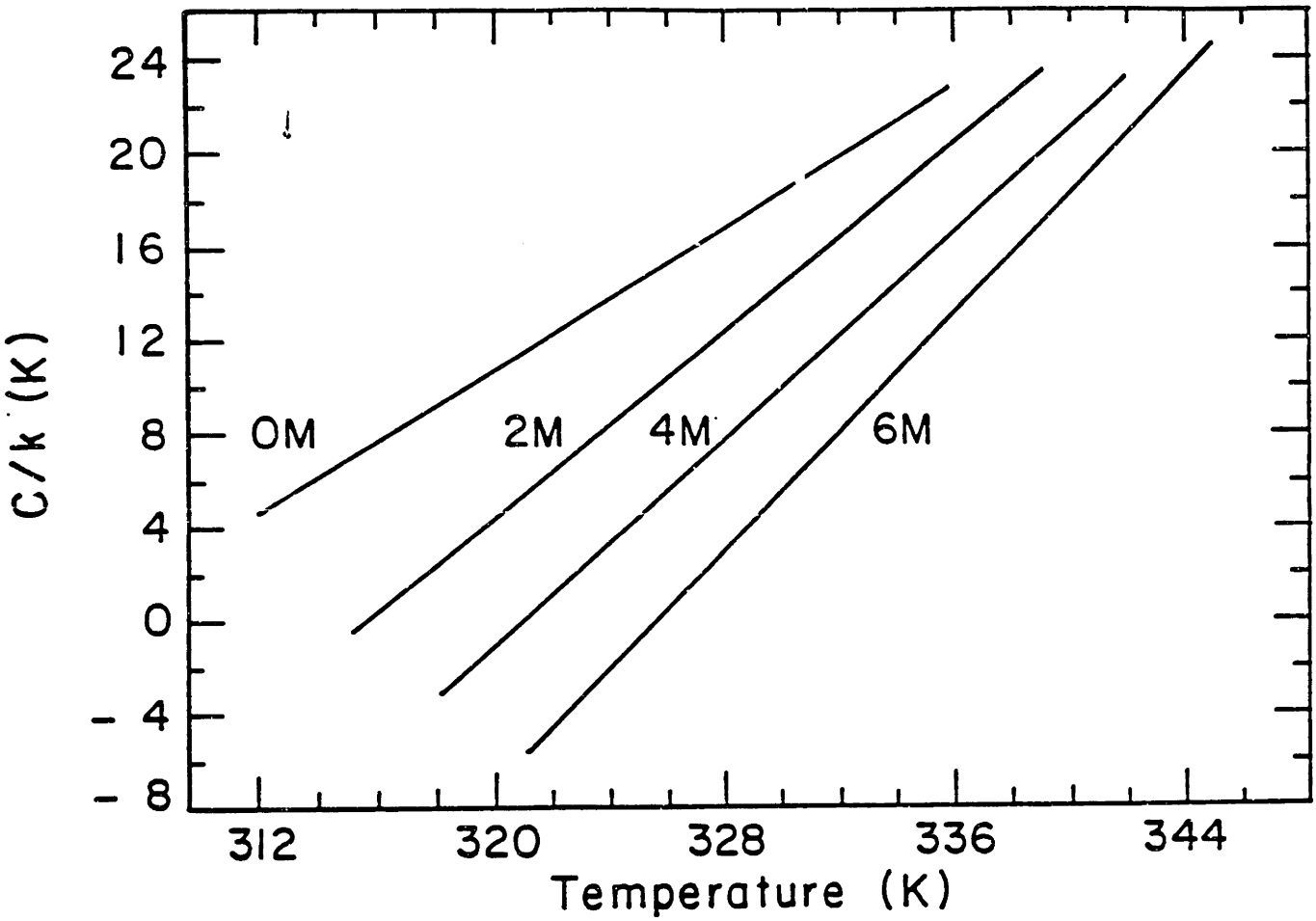

Figure 3.7. Calculated values (solid lines) of the effective intermicellar attraction parameter, C, as a function of temperature for 0, 2, 4, and 6M urea concentrations.

increased at fixed urea concentration, the dehydration of the EO heads (giving rise to a thinner hydration layer) will decrease steric repulsions between the hydrated micelles, thus contributing to an increase in the value of C. Since the EO head dehydrates at a faster rate in the presence of urea (see Sec. 3.4), and the temperature dependence of the van der Waals attraction is independent of urea concentration (because the change in the dielectric constant of water in the presence of urea is weakly dependent on temperature(Stokes, 1967)), dC/dT would increase with increasing urea concentration.

We return next to the possible correlation between micellar shape and size and phase separation suggested by the data in Fig. 3.4. It is tempting to speculate that the link between these two features is provided by the hydration characteristics of the EO heads. Indeed, this determines (1) the magnitude of a_h, which controls the magnitude of intramicellar steric repulsions, and is primarily responsible for the evolution in micellar shape and size with increasing temperature and urea concentration, and (2) the magnitude of C, through changes in intermicellar steric repulsions, responsible for changes in phase separation characteristics, such as T_c, with urea concentration.

Finally, Figure 3.8 shows the experimental cloud-point (coexistence) curves plotted in reduced coordinates, T/T_c, and, X/X_c, where T_c and X_c are the critical temperature and concentration, respectively. It is apparent that all the experimental points, corresponding to 0, 2, 4, and 6M urea concentrations, collapse onto a single universal curve. Further work is needed to understand the origin of this very interesting phenomenon.

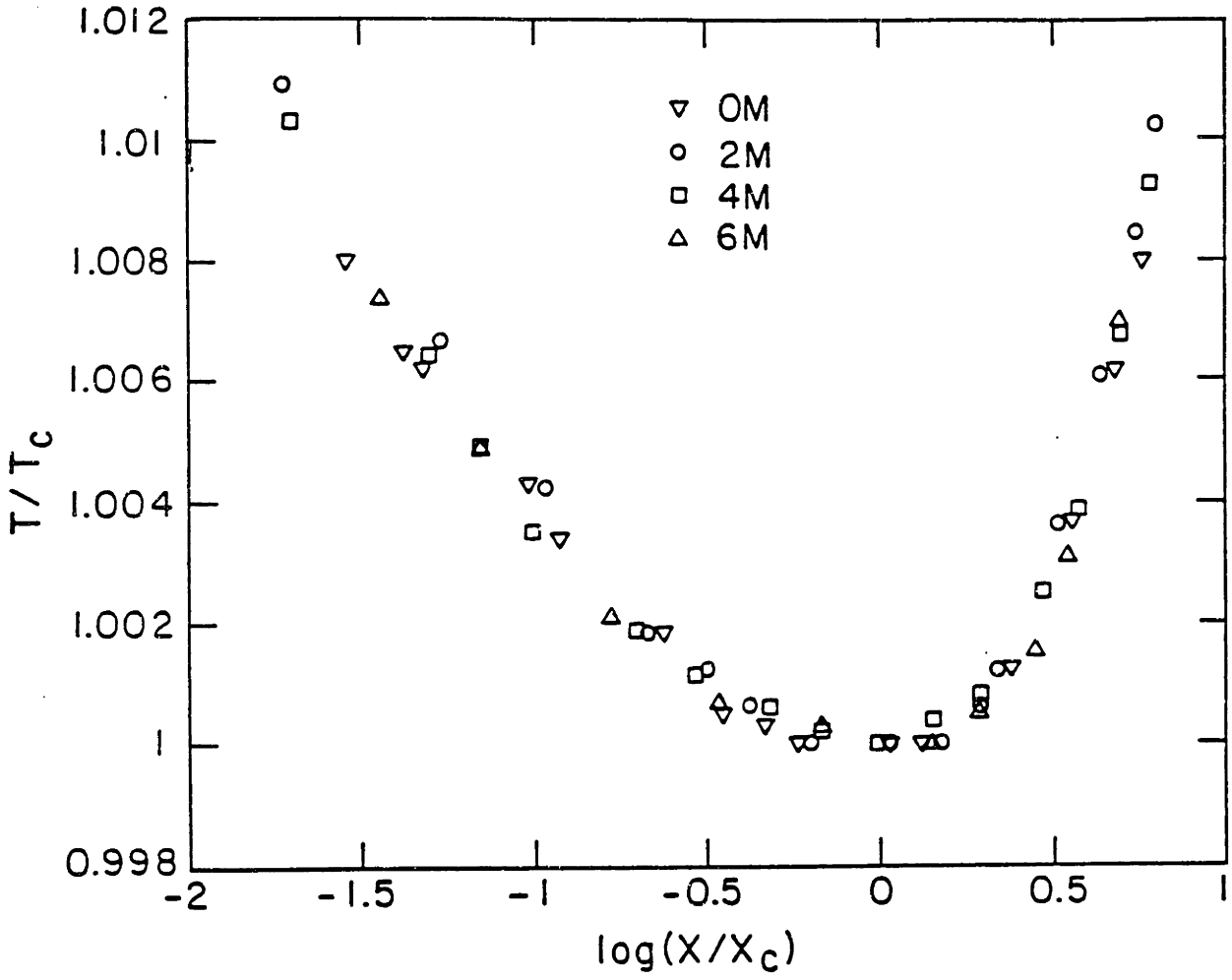

Figure 3.8. Experimental cloud-point curves (from Fig. 3.6) plotted in reduced coordinates, T/T_c, and, X/X_c, where T_c and X_c are the critical temperature and concentration, respectively. The collapse onto a single universal curve is apparent.

3.6 CONCLUDING REMARKS

The data presented in this chapter clearly shows that urea has a significant effect on the properties of aqueous micellar solutions of $C_{12}E_6$. In particular, we find that the addition of urea, (i) increases the value of the CMC, (ii) decrease micellar size, (iii) shifts the "sphere-to-rod" transition temperature to higher values, and (iv) shifts the critical point, associated with the coexistence curve, to a higher temperature and concentration. A very interesting observation is that the coexistence curves, at 0, 2, 4, and 6M urea concentrations, collapse onto a single universal curve when plotted in reduced coordinates. A similar behavior is observed for plots of the mean-micellar hydrodynamic radius, R_h, versus temperature at 0, 2, 4, and 6M urea concentrations. In addition, we have shown that it is possible to quantitatively rationalize these effects in the context of the molecular-thermodynamic theory presented in Chapter 2.

A number of important issues need further clarification and development. In particular, the hydration characteristics of the ethylene oxide headgroups seems to play a very important role in determining the magnitudes of both the intermicellar and intramicellar steric repulsions, through C and a_h, respectively. An understanding of the microscopic origin of hydration, including its dependence on the concentration of urea and temperature, can provide a link between the inter- and intra- micellar repulsions. A microscopic description of hydration could also facilitate the description of the origin of the observed collapses of the various coexistence curves and R_h onto single universal curves.

3.7 REFERENCES TO CHAPTER 3

Abraham, M.H. *J. Chem. Soc., Faraday Trans. 1*, **1984**, *80*, 153.

Abu Hamdiyyah, M.; Al Mansour, L. *J. Phys. Chem.* **1979**, *17*, 2236.

Amidon, G.L.; Yalkowsky, S.H.; Anik, S.T.; Valvani, S.C. *J. Phys. Chem.* **1975**, *79*, 2239.

Baglioni, P.; Ferroni, E.; Kevan, L. *J. Phys. Chem.* **1990**, *94*, 4296.

Ben-Shaul, A.; Szleifer, I.; Gelbart, W.M. *J. Chem. Phys.* **1985**, *83*, 3597.

Blankschtein, D.; Thurston, G.M.; Benedek, G.B. *Phys. Rev. Lett.* **1985**, *54*, 955.

Blankschtein, D.; Thurston, G.M.; Benedek, G.B. *J. Chem. Phys.* **1986**, *85*, 7268.

Blankschtein, D.; Puvvada, S. *MRS Symposium Proceedings* **1990**, *177*, 129;

Brown, W.; Rymden, R. *J. Phys. Chem.* **1987**, *60*, 775.

Carvalho, B.L.; Briganti, G.; and Chen, S-H. *J. Phys. Chem.* **1989**, *93*, 4282.

Corkill, J.M.; Goodman, J.F.; Harrod, S.P.; Tate, J.R. *Trans. Faraday Soc.* **1967**, *63*, 2460.

Das Gupta, P.K.; Moulik, S.P. *Coll. Polym. Sci.* **1989**, *267*, 246.

Emerson, M.F.; Holtzer, A. *J. Phys. Chem.* **1967**, *71*, 3320.

Enea, O.; Jolicoeur, C. *J. Phys. Chem.* **1982**, *86*, 3370.

Franks, F., Ed.; *Water: A Comprehensive Treatise*; Plenum: New York, **1978**; Vol. 4; and references therein.

Franks, H.S.; Franks, F. *J. Chem. Phys.* **1968**, *48*, 4746.

Fujimatsu, H.; Ogasawara, S.; Kuroiwa, S. *Coll. Polym. Sci.* **1988**, *266*, 594.

Gabrielli, G. *Personal Communication.*

Goldstein, R.E. *J. Phys. Chem.* **1984**, *80*, 5340.

Grant, E.H.; Keefe, S.K.; Shack, R. *Advan. Mol. Relaxation Processes* **1972**, *4*, 217.

Gruen, D.W.R. *J. Phys. Chem.* **1985**, *89*, 146, 153.

Han, S.K.; Lee, S.M.; Schott, H. *J. Colloid Interface Sci.* **1988**, *126*, 393.

Han, S.K.; Lee, S.M.; Kim, M.; Schott, H. *J. Colloid Interface Sci.* **1989**, *132*, 444.

Huang, Y.X.; Thurston, G.M.; Blankschtein, D.; Benedek, G.B. *J. Chem. Phys.* **1990**, *92*, 1956.

Israelachvili, J.N. *Intermolecular and Surface Forces*; Academic: New York, **1985**.

Karlstrom, G. *J. Phys. Chem.* **1985**, *89*, 4962.

Kjellander, R.; Florin, E. *J. Chem. Soc., Faraday Trans. 1*, **1981**, *77*, 2053.

Koppel, D.E. *J. Chem. Phys.*, **1972**, *57*, 4814.

Kuharski, R.A.; Rossky, P.J. *J. Am. Chem. Soc.* **1984**, *106*, 5786, 5794.

Mazer, N.A.; Benedek, G.B.; Carey, M.C. *J. Phys. Chem.*, **1976**, *80*, 1075.

Mazer, N.A.; Carey, M.C.; Kwasnick, R.F.; Benedek, G.B. *Biochemistry* **1979**, *18*, 3064.

Missel, P.J.; Mazer, N.A.; Carey, M.C.; Benedek, G.B. In *Solution Behavior of Surfactants*, Vol. 1; Mittal, K.L., Fendler, E.J., Eds.; Plenum: New York, **1982**; pp. 373.

Mitchell, D.J.; Tiddy, G.J.T.; Warring, L.; Bostock, T.; McDonald, M.P. J. Chem. Soc., Faraday Trans. 1, **1983**, *79*, 975; and references therein.

Muller, N. *J. Phys. Chem.* **1990a**, *94*, 3856.

Muller, N. *Acc. Chem. Res.* **1990b**, *23*, 23.

Nilsson, P.G.; Lindman, B. *J. Phys. Chem.* **1983**, *87* 4756.

Nozaki, Y.; Tanford, C. *J. Biol. Chem.* **1963**, *238*, 4074.

Puvvada, S.; Blankschtein, D. *J. Chem. Phys.* **1990a**, *92*, 3710.

Puvvada, S.; Blankschtein, D. *Proceedings of the 8th International Symposium on Surfactants in Solution*; Mittal, K.L., Shah, D.O., Eds.; Plenum: New York, **1990b**, in press.

Roseman, M.; Jencks, W.P. *J. Am. Chem. Soc.* **1975**, *97*, 631.

Shick, M.J. *J. Phys. Chem.* **1964**, *68*, 3585.

Shick, M.J. *J. Phys. Chem.* **1967**, *68*, 3585.

Shick, M.J. Ed.; *Nonionic Surfactants;* Arnold: London, **1967**; and references cited therein.

Stokes, R.H. *Aust. J. Chem.* **1967**, *20*, 2087.

Strey, R.; Pakusch, A. In *Surfactants in Solution*, Vol. 4, Mittal, K.L., Bothorel, P., Eds.; Plenum: New York, **1986**; pp. 465.

Subramanian, S.; Sarma, T.S.; Balasubramanian, D.; Ahulawalia, J.C. *J. Phys. Chem.* **1971**, *75*, 815.

Swenson, C.A. *Arch. Biochem. Biophys.* **1966**, *117*, 494.

Szleifer, I.; Ben-Shaul, A.; Gelbart, W.M. *J. Chem. Phys.* **1985**, *83*, 3612.

Tanford, C. *J. Am. Chem. Soc.* **1964**, *86*, 2050.

Tanford, C. *The Hydrophobic Effect*; Wiley: New York, **1980**.

Venkatesan, V.K.; Suryanarayana, C.V. *J. Phys. Chem.* **1956**, *60*, 775.

Wetlaufer, D.B.; Malik, S.K.; Stoller, L.; Coffin, R.L. *J. Am. Chem. Soc.* **1964**, 86, 508.

CHAPTER 4

THERMODYNAMIC THEORY OF MIXED SURFACTANT SOLUTIONS

4.1 INTRODUCTION

As mentioned in Chapter 1, surface-active compounds used in commercial applications typically consist of a mixture of surfactants because they can be produced at a relatively lower cost than that of isomerically pure surfactants. In addition, in many surfactant applications, mixtures of dissimilar surfactants often exhibit properties superior to those of the constituent single surfactants due to synergistic interactions between the surfactant molecules (Scamehorn, 1986). Indeed, in solutions containing mixtures of surfactants, the tendency to form aggregated structures (mixed micelles) can be substantially different than in solutions containing only the constituent single surfactants. For example, the critical micellar concentration (CMC) of a mixture of anionic and cationic surfactants in aqueous solution is considerably lower than the CMC's of each individual surfactant (Rosen and Hua, 1982b). On the other hand, antagonistic interactions, in mixtures of hydrocarbon-based and fluorocarbon-based surfactants in aqueous solution, result in mixture CMC's that can be considerably higher than the CMC's of the constituent single surfactants

(Mukerjee and Handa, 1981; Handa and Mukerjee, 1981). In general, specific interactions (synergistic or antagonistic) between surfactants result in solutions of surfactant mixtures having micellar and phase behavior properties which can be significantly different from those of the constituent single surfactants. Consequently, understanding specific interactions between the various surfactant species present in the solution is of central importance to the surfactant technologist. Indeed, in order to tailor surfactant mixtures to a particular application, the surfactant technologist has to be able to predict and manipulate (i) the tendency of surfactant mixtures to form monolayers, micelles, and other self-assembling aggregates in solution, (ii) the properties of the formed aggregates such as their shape and size, (iii) the distribution of the various surfactant species between monomers and aggregates, and (iv) the phase behavior and phase equilibria of solutions containing surfactant mixtures.

In spite of their considerable practical importance, solutions of surfactant mixtures (mixed micellar solutions) have not received the full attention that they deserve. To date, considerable experimental and theoretical effort has been devoted to determine and predict the CMC (Scamehorn, 1986). On the other hand, very few systematic studies have been conducted to study micelle shape and size (Attwood et al., 1975), phase equilibria (Ali and Mulley, 1978; Yoesting and Scamehorn, 1986; Marszall, 1988; Souza et al., 1986; Valaulikar and Manohar, 1985; Sadaghiania, 1991), and thermodynamic properties (Holland, 1984) of mixed micellar solutions. Below, we briefly highlight some of the theoretical studies of mixed micellar solutions which are particularly relevant to the present thesis. A comprehensive overview of theoretical and experimental aspects of mixed micellar solutions

can be found in Scamehorn (1986).

The first attempts to describe the CMC of solutions of surfactant mixtures were the ideal-mixing models (Lange, 1953; Lange and Beck, 1973; Shinoda, 1954; Clint, 1975). These models assume that the different surfactants mix ideally in a mixed micelle, and that micellization can be described using the pseudo-phase separation model (Stainsby and Alexander, 1950). Recall that the pseudo-phase separation model treats micellar aggregates as a separate thermodynamic pseudo-phase, and thus assumes that the micelle size approaches infinity. The CMC in this model represents that concentration at which the pseudo-phase (mixed micelle) first forms through a process analogous to phase separation. In the ideal-mixing models, the mixture CMC was found to be only a function of the CMC's of the constituent single surfactants and the composition of the mixture. Ideal-mixing models have been quite successful in predicting the CMC of aqueous solutions of binary nonionic (Lange, 1953; Shinoda, 1954; Barry et al., 1970) and binary ionic (Lange and Beck, 1973; Clint, 1975; Nishikido et al., 1975) surfactants that belong to an homologous series. On the other hand, in solutions which contain two or more non-homologous surfactant species, the measured CMC's were often found to be substantially lower (negative deviations) than those predicted by the ideal-mixing models (Rosen and Hua, 1982b; Funasaki and Hada, 1979; Jost et al., 1988). The observed deviations from ideality were attributed to nonideal mixing effects arising from specific interactions between the different surfactants present in the mixed micelle. This led naturally to the development of nonideal-mixing models (Rubingh, 1979; Holland and Rubingh, 1983), where the nonidealities were captured using activity coefficients calculated in the context of the regular solution theory

(Guggenheim, 1952) in terms of an empirical surfactant-surfactant specific interaction parameter ϵ. The empirical parameter ϵ constitutes a measure of the synergistic (attractive, for $\epsilon < 0$), or antagonistic (repulsive, for $\epsilon > 0$) interactions between two different surfactants, and has been determined (Rosen and Hua, 1982a; Kamrath and Frances, 1983; Zhu and Rosen, 1984) for numerous mixed surfactant systems by fitting to experimental CMC data. The interaction parameters determined from binary surfactant mixtures have also been used (Holland, 1986) to predict CMC's of ternary and other multicomponent surfactant mixtures, and the predictions have been found to be in good agreement with experimental values. As noted above, the nonideal-mixing models have been adequate to describe the CMC of surfactants mixtures. However, model predictions for the enthalpy change associated with mixing two or more surfactants in aqueous solution were found to be much larger than those obtained using calorimetric measurements (Holland, 1984). In addition, all mixing models (both ideal and nonideal) described above treat micellization in the context of the pseudo-phase separation model, and consequently are incapable of describing micellar shape, micellar size and composition, micellar size polydispersity, phase behavior, and phase equilibria of mixed micellar solutions.

Micellar size was explicitly taken into account in the molecular model developed by Nagarajan (1985). This model, based on an earlier one for single-surfactant solutions (Nagarajan and Ruckenstein, 1977), incorporates many of the relevant physical factors responsible for micelle formation, and was able to predict the mixture CMC as well as micellar size and composition for a number of aqueous solutions of binary surfactant mixtures. The model is also able to describe the observed nonidealities without the use of

an empirical specific interaction parameter. However, this model cannot be used to describe phase behavior and phase equilibria of mixed micellar solutions because it does not incorporate free-energy contributions due to intermicellar interactions.

The effect of alcohols on the stability of surfactant micelles has been studied (Ljunggren and Eriksson, 1977) using a mechanical theory in the context of small-systems thermodynamics (Hall and Pethica, 1984). Using this theory it was possible to predict the CMC and the micellar size as a function of added alcohol concentration. As in the previous studies, this theory cannot be used to describe phase behavior and phase equilibria because it does not incorporate contributions from intermicellar interactions.

The average micellar size and the composition distribution of mixed micelles were analyzed theoretically by Ben-Shaul et al. (1986). In particular, they treated the case of mixed micelles that exhibit one-dimensional growth into long cylindrical micelles, and found that the weight-average aggregation number of a linearly growing mixed micelle varies as $X^{0.4}$, where X is the total surfactant mole fraction. Note that this result is different from that obtained (Missel et al., 1980) for linearly growing single-surfactant micelles, where the variation of the weight-average micelle aggregation number on total surfactant mole fraction is proportional to $X^{0.5}$. To the best of our knowledge, this interesting theoretical prediction has not yet been tested experimentally.

An approach based on a variational principle has been developed to study the micellar distribution properties of binary mixed micellar solutions (Stecker and Benedek, 1984). In this approach, the micellar solution free energy is expressed as a function of the micellar distribution function, and subsequently various trial distribution functions are

examined. The distribution function which minimizes the solution free energy, while satisfying the surfactant conservation equations, is chosen as the optimal one. This optimal distribution function can then be used to determine the average micellar shape and size as a function of concentration, composition, and other solution conditions. The model predictions depend on two phenomenological parameters, $\Delta\mu_A$ and $\Delta\mu_B$, which reflect the free energy required to transfer a surfactant A or a surfactant B molecule, respectively, from water into a mixed micelle. Since a molecular model for determining the values of these two parameters has not yet been developed, *a-priori* predictions of the micellar properties cannot be made. In addition, since free-energy contributions due to intermicellar interactions were not included, this approach cannot be used to describe phase behavior and phase equilibria of mixed micellar solutions.

Phase separation of aqueous solutions of mixed nonionic-ionic surfactant solutions was modelled (Meroni et al., 1987) assuming the presence of monodisperse micelles interacting through two-body intermicellar potentials. The spinodal and the coexistence surfaces were determined from the interaction potentials using the mean-spherical approximation in the context of liquid state theory. This approach, which has been previously used to describe coexistence curves of aqueous solutions of single nonionic surfactants (Reatto and Tau, 1984), was extended to describe the effect of adding ionic surfactants on the coexistence curves of a single nonionic surfactant in aqueous solutions. The model successfully predicted that the closed-loop coexistence curve present in the nonionic surfactant solution would shrink and finally vanish upon the addition of an ionic surfactant. However, the model requires as inputs the measured values of the micellar size

as well as the critical temperature and concentration associated with the lower consolute (critical) point of the pure nonionic surfactant in aqueous solution. Accordingly, this approach cannot be used to describe and predict characteristics of the micellar size and composition distribution or the CMC of the mixed micellar solution.

The highlights of previous theoretical work in the area of mixed micellar solutions presented above clearly indicate that, so far, the theoretical advances have proceeded along two very different, seemingly unrelated, directions. On the one hand, significant efforts have been devoted to understand mixed micellization and growth, mixed micellar structure, micellar size and composition distribution, and mixed CMC characteristics. On the other hand, very little effort has been devoted to understand the solution behavior at higher surfactant concentrations where intermicellar interactions become increasingly important and can affect the phase behavior and induce phase equilibrium phenomena. It is evident that, so far, there has been no attempt to formulate a theoretical approach capable of *unifying* the previously disconnected treatments of micellization and phase behavior, including phase equilibria, into a *single* coherent computational framework. As described in Chapter 1, it is the purpose of this thesis to contribute to this much needed *theoretical unification*.

The theoretical approach that we propose, inspired by our work on single-surfactant solutions described in Chapter 2 (Puvvada and Blankschtein, 1990a and 1990b; Blanskchtein and Puvvada, 1990), consists of blending a thermodynamic theory of micellar solutions, which captures the salient features of mixed micellar solutions at the macroscopic level, with a molecular model of mixed micellization, which captures the essential physical factors at the micellar level. The resulting molecular-thermodynamic approach provides a valuable

tool to predict solution properties of mixed surfactant systems using molecular parameters that reflect (i) the nature of the surfactant molecules involved in the micellization process, and (ii) solution conditions such as temperature, pH, ionic strength, and the presence of additives such as salts. As such, the molecular-thermodynamic approach may be utilized to design surfactant mixtures for a particular application, as well as to modify and control the resulting micellar solution properties.

In this chapter, we formulate the thermodynamic theory and develop expressions relating micellar solution properties to molecular characteristics such as the free energy of micellization. We subsequently use these expressions, in the context of a simple analytical phenomenological model for the free energy of micellization, to make *qualitative* predictions of the effect of surfactant type and composition on the properties of the mixed micellar solution. In Chapter 5, we will present a detailed molecular model of mixed micellization which can be used in conjunction with the thermodynamic framework developed in this chapter to make *quantitative* predictions of micellar solution properties. Note that the theoretical approach presented in this and the following chapter differs from previous ones in that it is capable of describing and predicting self-consistently a broad spectrum of micellar solution properties ranging from the CMC and the micellar size and composition distribution to the phase behavior and phase equilibria of mixed micellar solutions. In addition, our theoretical approach clarifies the molecular basis of a number of empirical parameters introduced in some of the earlier studies of mixed micellization.

The remainder of the chapter is organized as follows. In Sec. 4.2 we formulate the general thermodynamic framework to describe mixed micellar solutions. Specifically, in

Sec. 4.2.1 we present the mathematical structure of the various contributions to the Gibbs free energy of the mixed micellar solution, and derive expressions for the chemical potentials of the various solution components. In Sec. 4.2.2 we derive expressions for the micellar size and composition distribution and its moments, and in Sec. 4.2.3 we analyze the phase behavior and phase separation phenomena. An important contribution to the micellar solution Gibbs free energy is the free energy of mixed micellization, and a simple analytical phenomenological model to compute this contribution is developed in Sec. 4.2.4. In Sec. 4.3 we present and discuss the predictions of the thermodynamic framework for aqueous solutions containing binary mixtures of nonionic-nonionic, nonionic-ionic, zwitterionic-ionic, anionic-cationic, and nonionic hydrocarbon-nonionic fluorocarbon surfactants. The theoretical predictions include (i) the CMC variation with surfactant monomer composition, (ii) the variation of micellar composition with surfactant monomer composition at the CMC, (iii) the variation of the weight-average mixed micelle aggregation number with total surfactant composition, and (iv) the effects of adding small quantities of a second surfactant on the phase separation characteristics of the micellar solution, including the shift in the critical temperature as well as the distribution of the two surfactant species between the coexisting micellar-rich and micellar-poor phases. Finally, in Sec. 4.4 we present some concluding remarks.

4.2 THERMODYNAMIC FRAMEWORK

4.2.1 Gibbs Free Energy and Chemical Potentials

The thermodynamic formulation used to describe the free energy of a mixed surfactant solution constitutes a generalization of the one developed in Chapter 2 to describe single-surfactant solutions (Blankschtein et al., 1985 and 1986). For the sake of clarity, in this chapter we present a theoretical description of aqueous solutions of a mixture of *two* surfactants. Extension of the formalism to describe solutions containing additional surfactant species is conceptually similar, and therefore will not be discussed.

Consider a solution of N_w water molecules, N_A surfactant A molecules, and N_B surfactant B molecules in thermodynamic equilibrium at temperature T and pressure P. If the concentration of the surfactant mixture exceeds its CMC, the surfactant molecules will self-assemble to form a distribution of mixed micelles $\{N_{n\alpha}\}$, where $N_{n\alpha}$ is the number of mixed micelles having aggregation number n and composition α. Note that in such a mixed micelle, there are $n\alpha$ surfactant A molecules, and $n(1-\alpha)$ surfactant B molecules. Note also that $N_A=\Sigma_{n,\alpha}\, n\alpha N_{n\alpha}$, and $N_B=\Sigma_{n,\alpha}\, n(1-\alpha)N_{n\alpha}$. In the spirit of the multiple-chemical equilibrium description (Corkill et al., 1969), mixed micelles of different sizes and compositions are treated as distinct species in chemical equilibrium with each other as well as with the free monomers in the solution.

The Gibbs free energy of the mixed surfactant solution G is modelled as the sum of three contributions: the free energy of formation G_f, the free energy of mixing G_m, and the

free energy of interaction G_i. These contributions, as in the single-surfactant case, are chosen to provide a heuristically appealing identification of the various factors responsible for micelle formation and growth, on the one hand, and for phase behavior and phase equilibria, on the other.

The free energy of formation is expressed as

$$G_f = N_w\mu_w^o + N_A\mu_A^o + N_B\mu_B^o + \sum_{n,\alpha} nN_{n\alpha}g_{mic}(sh,n,\alpha), \qquad (4.1)$$

where $\mu_w^o(T,P)$, $\mu_A^o(T,P)$, *and* $\mu_B^o(T,P)$ are the standard-state chemical potentials of water, surfactant A monomers, and surfactant B monomers, respectively, at the solution temperature T and pressure P, and $g_{mic}(sh,n,\alpha)$ is the free energy of micellization, which represents the free-energy change per monomer associated with transferring $n\alpha$ surfactant A monomers and $n(1-\alpha)$ surfactant B monomers from water into a mixed micelle of shape sh, aggregation number n, and composition α. The numerical magnitude of g_{mic}, which reflects the propensity of a mixed micelle to form and subsequently grow, summarizes the many complex physico-chemical factors responsible for mixed micelle formation such as the hydrophobic effect, hydrogen bonding, conformational changes associated with hydrophobic-tail packing in the micellar core, steric and electrostatic interactions between the hydrophilic head groups, and the entropy of mixing the two surfactants in the mixed micelle (see also Chapters 2 and 5).

The free energy of mixing the formed mixed micelles, free monomers, and water is modelled by an expression of the form

$$G_m = kT\left[N_w \ln X_w + \sum_{n,\alpha} N_{n\alpha} \ln X_{n\alpha}\right], \tag{4.2}$$

where $X_w = N_w/(N_w+N_A+N_B)$, $X_{n\alpha} = N_{n\alpha}/(N_w+N_A+N_B)$, k is the Boltzmann constant, and T is the absolute temperature. $-G_m/T$ is an entropic contribution which reflects the number of ways in which the distribution of mixed micelles, the free monomers, and the water molecules can be positioned in the solution as a function of the solution concentration and composition. The free energy of mixing, as expressed in Eq. (4.2), opposes the tendency to form micelles because monomer aggregation reduces the total number of available spatial configurations. The entropy of mixing also opposes the tendency of the micellar solution to phase separate, because of the loss in available spatial configurations associated with this phenomenon. Note that Eq. (4.2) is a generalization of the expression used with considerable success to describe (Puvvada and Blankschtein, 1989, 1990a and 1990b; Blankschtein et al., 1985 and 1986; Briganti et al., 1991; Carale and Blankschtein, 1992; Carvalho et al., 1989) micellization, phase behavior, and phase separation in single-surfactant solutions.

The free energy of interaction reflects interactions between mixed micelles, water molecules, and free monomers in the solution. At the level of a mean-field type quadratic expansion, in Appendix A we show that this free-energy contribution takes the following form

$$G_i = -\frac{1}{2} C_{eff}(\alpha_{soln})(N_A+N_B)\phi, \tag{4.3}$$

where $\phi=\phi_A+\phi_B$ is the sum of the volume fractions, ϕ_A and ϕ_B, of surfactants A and B, respectively, $\alpha_{soln} = N_A/(N_A+N_B)$ is the composition of the surfactant mixture, and $C_{eff}(\alpha_{soln})$ is an effective mean-field interaction parameter for the mixture which is related to the single-surfactant interaction parameters, C_{AW} and C_{BW}, and a specific interaction parameter C_{AB} through the following expression (see Appendix A)

$$C_{eff}(\alpha_{soln}) = C_{AW}\alpha_{soln} + C_{BW}(1-\alpha_{soln}) - C_{AB}\alpha_{soln}(1-\alpha_{soln})\frac{\sqrt{\gamma_A\gamma_B}}{\gamma_{eff}} . \tag{4.4}$$

In Eq. (4.4), $\gamma_A=\Omega_A/\Omega_w$ and $\gamma_B=\Omega_B/\Omega_w$, where Ω_w, Ω_A, Ω_B are the effective molecular volumes of water, surfactant A and surfactant B, respectively, and $\gamma_{eff} = \alpha_{soln}\gamma_A + (1-\alpha_{soln})\gamma_B$.

The two interaction parameters, C_{AW} and C_{BW}, reflect interactions in aqueous solutions of surfactant A and surfactant B, respectively (see Eqs. (A6) and (A7) in Appendix A), and consequently can be obtained from experiments conducted in the corresponding single-surfactant solutions. Fositive values of C_{AW} (or C_{BW}) indicate net attractive interactions between the surfactant molecules, while negative values indicate net repulsive interactions. Note that net attractive interactions can induce phase separation, while net repulsive interactions oppose phase separation (Guggenheim, 1952). More specifically, note that, to leading order in surfactant concentration, $\gamma_A C_{AW}/k$ and $\gamma_B C_{BW}/k$, are equal to the critical temperatures, T_c^A and T_c^B, of the corresponding single-surfactant solutions (Blankschtein et al., 1986). In particular, many nonionic surfactants in aqueous solution

exhibit (Mitchell et al, 1983) phase separation between 0 and 100°C, and thus have $\gamma_A C_{AW}/k$ (or $\gamma_B C_{BW}/k$) values of approximately 300K. More generally, any surfactant in aqueous solution which exhibits phase separation between 0-100°C, for example, a zwitterionic surfactant such as C_8-lecithin (Blankschtein et al., 1986), will have $\gamma_A C_{AW}/k$ (or $\gamma_B C_{BW}/k$) values of approximately 300K. On the other hand, aqueous solutions of ionic surfactants in the absence of salt typically do not exhibit phase separation because of the long-range electrostatic intermicellar repulsions. Therefore, we expect ionic surfactants to have large negative C_{AW} (or C_{BW}) values. In Table 4.1, we list typical values of C_{AW} for nonionic, zwitterionic, and ionic surfactants.

As described in Appendix A, the interaction parameter C_{AB} describes specific interactions that may exist between surfactants A and B, and therefore constitutes a measure of the synergistic (attractive, for $C_{AB}<0$), or antagonistic (repulsive, for $C_{AB}>0$) interactions between the two surfactant molecules. Note that mixtures of nonionic surfactants usually form ideal mixtures, and therefore are expected to have $C_{AB}\approx 0$. On the other hand, mixtures of dissimilar surfactants (for example, ionic-nonionic or anionic-cationic surfactants)

Table 4.1. Typical values of the interaction parameter C_{AW}, and $\partial C_{AW}/\partial T$ for various types of surfactants.

Surfactant Type	C_{AW}/k (K)	$\partial(C_{AW}/k)/\partial T$
Nonionic	+O(10)	+O(1)
Zwitterionic	+O(10)	≈ 0
Ionic	$<< 0$	≈ 0

usually form nonideal mixtures with expected non-zero values of C_{AB}. From the discussion in Appendix A, we expect C_{AB} to become increasingly negative (increased synergism) in the sequence nonionic-nonionic, anionic-anionic, nonionic-ionic, and anionic-cationic surfactant mixtures. Mixtures of hydrocarbon-based and fluorocarbon-based surfactants are expected to have C_{AB} values greater than zero because the two surfactants exhibit repulsive (antagonistic) interactions (Mukerjee and Handa, 1981). In Table 4.2, we list typical values of C_{AB} for various surfactant mixtures.

The thermodynamic consequences of the proposed free-energy formulation are described below. The properties examined include the CMC, the micellar size and composition distribution and its moments, and the phase behavior and phase equilibria. All these properties are governed by the proposed Gibbs free energy model through the chemical potential of water μ_w, and the chemical potential of a mixed micelle, of aggregation number n and composition α, $\mu_{n\alpha}$, which are obtained by differentiating the Gibbs free energy, Eqs. (4.1)-(4.3), with respect to N_w and $N_{n\alpha}$, respectively. The resulting expressions

Table 4.2. Typical values of the specific interaction parameters C_{AB} and C.

Surfactant Mixture	C_{AB}/kT	C/kT
Nonionic-Nonionic	~0	~0
Monovalent Anionic-Monovalent Anionic	≤0	~0
Nonionic-Monovalent Ionic	<0	2-6
Monovalent Anionic- Monovalent Cationic	<< 0	10-25
Hydrocarbon-Fluorocarbon (Nonionics)	>0	<0

are given by

$$\mu_w = \mu_w^o + kT\left[\ln(1-X)+X-\sum_{n,\alpha} X_{n\alpha}\right] + C_{eff}(\alpha_{soln})\frac{\phi^2}{2\gamma_{eff}}, \tag{4.5}$$

$$\mu_{n\alpha} = n\alpha\mu_A^o + n(1-\alpha)\mu_B^o + (ng_{mic}+kT) + kT\left[\ln X_{n\alpha} + n\left(X-1-\sum_{n\alpha} X_{n\alpha}\right)\right] + n\alpha\mu_A^i + n(1-\alpha)\mu_B^i, \tag{4.6}$$

where $X = X_A + X_B$, with $X_A = N_A/(N_W+N_A+N_B)$ and $X_B = N_B/(N_W+N_A+N_B)$, is the total mole fraction of surfactant in the solution, and the interaction (i) contributions to the monomer chemical potentials are given by

$$\mu_A^i = -\frac{\phi}{2}\left[C_{AW} + \frac{\gamma_A}{\gamma_{eff}}\left[\alpha_{soln}C_{AW}+(1-\alpha_{soln})C_{BW}\right](1-\phi) - (1-\alpha_{soln})\frac{\sqrt{\gamma_A\gamma_B}}{\gamma_{eff}}C_{AB}(1-\phi_A)\right], \tag{4.7}$$

and

$$\mu_B^i = -\frac{\phi}{2}\left[C_{BW} + \frac{\gamma_B}{\gamma_{eff}}\left[\alpha_{soln}C_{AW}+(1-\alpha_{soln})C_{BW}\right](1-\phi) - \alpha_{soln}\frac{\sqrt{\gamma_A\gamma_B}}{\gamma_{eff}}C_{AB}(1-\phi_B)\right]. \tag{4.8}$$

The chemical potentials of surfactant A and surfactant B monomers can be obtained from Eq. (4.6) by substituting n=1, and α=1 (for A) or 0 (for B), respectively, that is,

$$\mu_A = (\mu_A^o + kT) + kT\left[\ln X_{1A} + X - 1 - \sum_{n\alpha} X_{n\alpha}\right] + \mu_A^i, \tag{4.9}$$

$$\mu_B = (\mu_B^o + kT) + kT\left[\ln X_{1B} + X - 1 - \sum_{n\alpha} X_{n\alpha}\right] + \mu_B^i , \tag{4.10}$$

where X_{1A} and X_{1B} are the mole fractions of free surfactant A and surfactant B monomers, respectively. Using Eqs (4.5)-(4.10) for the chemical potentials, below we predict various properties of the mixed micellar solution.

4.2.2 Micellar Size and Composition Distribution and its Moments

When the mixed micellar solution is in thermodynamic equilibrium, the chemical potential $\mu_{n\alpha}$ of a mixed micelle of aggregation number n and composition α is related to the chemical potentials of the free monomers through the constraints imposed by the conditions of multiple chemical equilibrium, that is,

$$\mu_{n\alpha} = n\alpha\mu_A + n(1-\alpha)\mu_B . \tag{4.11}$$

Eq. (4.11) implies that the chemical potential of a mixed micelle having aggregation number n and composition α is equal to the sum of the chemical potentials of its constituent $n\alpha$ surfactant A and $n(1-\alpha)$ surfactant B molecules. Substituting Eqs. (4.6), (4.9), and (4.10) in

Eq. (4.11), we obtain the following expression for the equilibrium micellar size and composition distribution

$$X_{n\alpha} = \frac{1}{e} X_{1A}^{n\alpha} X_{1B}^{n(1-\alpha)} e^{-n[\beta g_{mic}(\alpha)-1]} = \frac{1}{e} X_1^n e^{-n\beta g_m(\alpha,\alpha_1)}, \qquad (4.12)$$

where $\beta = 1/kT$, $\beta g_m = [\beta g_{mic} - 1 - \alpha \ln\alpha_1 - (1-\alpha)\ln(1-\alpha_1)]$ is a modified dimensionless free energy of mixed micellization per monomer, $X_1 = X_{1A} + X_{1B}$ is the total mole fraction of free monomers in solution, and $\alpha_1 = X_{1A}/X_1$ is the composition of free monomers in solution. Eq. (4.12) indicates that a delicate balance between two opposing factors determines the nature of the micellar size and composition distribution $\{X_{n\alpha}\}$. The first is the Boltzmann factor, $e^{-n\beta g_{mic}}$, representing the energetic advantage (recall that $g_{mic} < 0$) of assembling the various surfactant molecules in a mixed micelle, which favors micelle formation. The second factor, $X_{1A}^{n\alpha} X_{1B}^{n(1-\alpha)}$, represents the large entropic disadvantage associated with localizing $n\alpha$ surfactant A molecules (each with probability X_{1A}) and $n(1-\alpha)$ surfactant B molecules (each with probability X_{1B}) in a single mixed micelle, and opposes micelle formation. It is noteworthy that with the choice of mean-field interaction potentials adopted in Eq. (4.3) (see also Appendix A), the interaction free energy does not affect the micellar size and composition distribution.

The composition $\alpha^*(n)$, at which $X_{n\alpha}$ exhibits a maximum for a given micellar aggregation number n, is referred to as the optimum composition. Note that, in general, $\alpha^*(n)$ is a function of the aggregation number n, and can be obtained by setting the

derivative of $X_{n\alpha}$ with respect to α equal to zero. Specifically, implementing this procedure with Eq. (4.12) leads to the following implicit equation

$$\beta \frac{\partial g_{mic}(n,\alpha)}{\partial \alpha}\bigg|_{\alpha^*} = \ln\left(\frac{\alpha_1}{1-\alpha_1}\right). \qquad (4.13)$$

Using Eq. (4.13), the optimum composition for all aggregation numbers can be determined from a knowledge of α_1, and $g_{mic}(n,\alpha)$. In addition, note that, for large n, $X_{n\alpha}$ will exhibit a sharp maximum at $\alpha=\alpha^*$ because n appears as a multiplicative factor in the exponential of Eq. (4.12), and consequently any small deviations of α from α^* will be magnified significantly. This implies that, to leading order in α, the mole fraction of micelles having compositions $\alpha \neq \alpha^*$ will be negligible, and, accordingly, $\Sigma_\alpha X_{n\alpha}$ can be approximated by $X_{n\alpha^*}$.

Equation (4.12) for the micellar size and composition distribution is applicable to mixed micelles of all shapes, sizes, and compositions. However, as shown clearly in Eq. (4.12), to determine the distribution one needs to know: (i) the free energy of micellization $g_{mic}(n,\alpha)$ as a function of n and α, or, equivalently, g_m as a function of n, α, and α_1, (ii) the equilibrium solution monomer mole fraction X_1, and (iii) the equilibrium solution monomer composition α_1. Note that conditions (ii) and (iii) are equivalent to knowing $X_{1A}=\alpha_1 X_1$, and $X_{1B}=(1-\alpha_1)X_1$. Note also that X_1 and α_1 (or equivalently X_{1A} and X_{1B}) can be found by using Eq. (4.12) in the two constraints imposed by the conservation of the total number of surfactant A and surfactant B molecules in solution, that is, $N_A = \Sigma_{n\alpha} n\alpha N_{n\alpha}$ and $N_B = \Sigma_{n\alpha} n(1-\alpha)N_{n\alpha}$, or equivalently,

$$X_A = \alpha_{soln} X = \alpha_1 X_1 + \sum_{n,\alpha} n\alpha X_{n\alpha}, \tag{4.14}$$

$$X_B = (1-\alpha_{soln})X = (1-\alpha_1)X_1 + \sum_{n,\alpha} n(1-\alpha)X_{n\alpha} . \tag{4.15}$$

Given g_{mic} (or equivalently g_m), and on inserting Eq. (4.12) into Eqs. (4.14) and (4.15), one obtains two implicit equations for X_1 and α_1 as a function of X and α_{soln}. Solving these two equations simultaneously one can, in principle, obtain $X_1(X,\alpha_{soln},T,P)$ and $\alpha_1(X,\alpha_{soln},T,P)$, which can then be inserted back into Eq. (4.12) to calculate the entire micellar size and composition distribution $\{X_{n\alpha}\}$ as a function of X, α_{soln}, T, P, and other solution conditions. Note that, in general, the free energy of micellization $g_{mic}(n,\alpha)$ will depend on the type and molecular structure of the two surfactants in the mixture, as well as on solution conditions such as temperature, pH, and ionic strength. A detailed molecular model to evaluate g_{mic} has been developed, and will be presented in Chapter 5. However, to illustrate some general features and prediction capabilities of the thermodynamic framework, in the present chapter we develop a simple analytical phenomenological model for g_{mic} (see Sec. 4.2.4).

Having derived an expression for the micellar size and composition distribution $\{X_{n\alpha}\}$, we describe next how the various moments of the distribution are related to one another. We define the moment of order k by $M_k = \Sigma_{n\alpha} n^k X_{n\alpha}$. Note that the first moment is given by $M_1 = X$, and the zeroth moment $M_0 = \Sigma_{n\alpha} X_{n\alpha}$ is proportional to the total number of mixed micelles and free monomers in the solution. Note also that the zeroth

moment plays an important role in determining the value of colligative properties such as the osmotic pressure (for example, see Eq. (4.23) below). In general, using Eq. (4.12), the kth moment can be expressed as

$$M_k = \sum_{n\alpha} \frac{1}{e} n^k (X_1)^n e^{-n\beta g_m(\alpha,\alpha_1)}. \tag{4.16}$$

The total derivative of M_k with respect to X_1 is given by

$$\frac{dM_k}{dX_1} = \frac{M_{k+1}}{X_1} - \sum_{n\alpha} n^{k+1} X_{n\alpha} \left[\frac{\alpha-\alpha_1}{1-\alpha_1}\right] \frac{1}{X_1} . \tag{4.17}$$

Since, as stated above, we assume that for values of $\alpha \neq \alpha^*$, $X_{n\alpha}$ is negligible, it can be shown (see Appendix B) that to a very good approximation

$$\frac{dM_k}{M_{k+1}} \approx \frac{dX_1}{X_1}\left[\frac{1-\alpha_{soln}}{1-\alpha_1}\right]. \tag{4.18}$$

By applying the chain rule to Eq. (4.18) we obtain

$$\frac{dM_k}{dM_j} \approx \frac{M_{k+1}}{M_{j+1}}, \tag{4.19}$$

and by setting k = 1 in Eq. (4.18) we obtain

$$\frac{dlnX_1}{dX} \approx \frac{1}{M_2}\left(\frac{1-\alpha_1}{1-\alpha_{soln}}\right). \tag{4.20}$$

Eqs. (4.19) and (4.20) show that with our choice of Gibbs free energy, Eqs. (4.1)-(4.3), all the moments of the distribution can be expressed solely in terms of the second moment M_2 of the distribution. Note that M_2 can be related to the weight-average aggregation number $<n>_w$ of the mixed micelles through

$$\langle n \rangle_w(X,\alpha_{soln},T,P) = M_2(X,\alpha_{soln},T,P)/X. \tag{4.21}$$

In addition, the relative variance of the distribution is given by the following expression

$$\sigma(X,\alpha_{soln},T,P) = \frac{\langle (n-\langle n \rangle_w)^2 \rangle_w}{(\langle n \rangle_w)^2} = \frac{X}{\langle n \rangle_w}\left(\frac{d\langle n \rangle_w}{dX}\right). \tag{4.22}$$

It is noteworthy that both the weight-average mixed micelle aggregation number and the relative variance can be measured experimentally, and through a comparison with Eqs. (4.21) and (4.22) can therefore serve as useful indicators of the applicability of our thermodynamic framework to specific solutions of surfactant mixtures. Note also that Eqs. (4.19)-(4.22), describing the various moments in the mixed micellar case, are very similar to those developed for single-surfactant solutions (Blankschtein et al., 1985 and 1986).

4.2.3 Phase Behavior and Phase Separation

Having derived expressions for the micellar size and composition distribution and its moments, the thermodynamic framework is used next to describe the phase behavior and phase equilibria of mixed micellar solutions. In particular, the osmotic pressure π can be related to the water chemical potential by $\pi = (\mu_w^o - \mu_w)/\Omega_w$, where as stated earlier Ω_w is the effective volume of a water molecule. Using Eq. (4.5) we obtain

$$-\beta\pi\Omega_w = \ln(1-X) + X - M_o(T,P,X,\alpha_{soln}) + C_{eff}(\alpha_{soln})\frac{\phi^2}{2\gamma_{eff}}. \qquad (4.23)$$

The osmotic compressibility of the solution $(\partial\pi/\partial X)^{-1}_{T,P,\alpha_{soln}}$ can be obtained by differentiating Eq. (4.23) with respect to X, at constant T, P, and α_{soln}. This yields

$$\left(\frac{\partial\pi}{\partial X}\right)^{-1}_{T,P,\alpha_{soln}} = \beta\Omega_w\left[\frac{X}{1-X} + \frac{X}{M_2} - \frac{\beta\gamma_{eff}C_{eff}X}{(1+(\gamma_{eff}-1)X)^3}\right]^{-1}. \qquad (4.24)$$

It is noteworthy that the mathematical structures of Eqs. (4.23) and (4.24) for the osmotic pressure and the osmotic compressibility are identical to those obtained earlier for single-surfactant solutions (Blankschtein et al, 1986).

When solution conditions such as temperature, pressure, or ionic strength are altered in a ternary solution consisting of two surfactants and water, stability criteria could be violated, and the solution may separate into two or more phases in thermodynamic

equilibrium with each other. In this chapter, we restrict our discussions to two-phase equilibria.

The boundary between the stable and unstable regions of a ternary solution is known as the spinodal surface, while that between the two-phase and one-phase regions is known as the coexistence surface. Note that a binary system at fixed pressure will have a single temperature versus concentration spinodal line and coexistence curve. However, a ternary system at fixed pressure will have a family of spinodal lines constituting a spinodal surface, and a family of coexistence curves constituting a coexistence surface in the three-dimensional temperature, total concentration, composition coordinate system.

In general, the spinodal surface in a ternary system is described (Lupis, 1983) by the following stability condition

$$\psi = \left(\frac{\partial^2 G}{\partial N_w^2}\right)\frac{\partial G}{\partial N_A} - \left(\frac{\partial^2 G}{\partial N_w \partial N_A}\right)\frac{\partial G}{\partial N_w} = 0, \qquad (4.25)$$

where G is the Gibbs free energy of the system. On the spinodal surface, the locus of points where the two coexisting phases become indistinguishable is the line of critical points. Note that, at a fixed pressure, there is a single critical point in a binary solution, whereas in a ternary solution there is a line of critical points. Note also that the critical line is the line of tangency between the spinodal surface and the coexistence surface. Thus, at the critical line, in addition to $\psi = 0$, a second stability condition,

$$\phi = \left(\frac{\partial^2 G}{\partial N_w^2}\right)\frac{\partial \psi}{\partial N_A} - \left(\frac{\partial^2 G}{\partial N_w \partial N_A}\right)\frac{\partial \psi}{\partial N_w} = 0, \qquad (4.26)$$

needs to be satisfied (Lupis, 1983). A simultaneous solution of the two stability conditions, $\psi=0$ and $\phi=0$, yields the entire critical line.

As described earlier, the coexistence surface bounds the unstable two-phase region within which a solution spontaneously separates into two isotropic phases. The lines connecting the two coexisting phases in the phase diagram are called tie lines, and the critical line corresponds to the locus of points at which the length of the tie lines vanishes. The conditions of phase equilibria (Guggenheim, 1952) require that the temperature, the pressure, and the chemical potentials of each of the components in the solution be the same in the two coexisting phases. Specifically, for the ternary water, surfactant A and surfactant B system, $\mu_w(T,P,Y,\alpha_Y)=\mu_w(T,P,Z,\alpha_Z)$, $\mu_A(T,P,Y,\alpha_Y)=\mu_A(T,P,Z,\alpha_Z)$, and $\mu_B(T,P,Y,\alpha_Y)=\mu_B(T,P,Z,\alpha_Z)$, where Y and Z are the total surfactant mole fractions in each coexisting phase, respectively, and α_Y and α_Z are the corresponding surfactant compositions. The three chemical potentials μ_w, μ_A, and μ_B can be expressed as derivatives of the Gibbs free energy per particle, $g = G/(N_w+N_A+N_B)$, and the resulting expressions are given by

$$\mu_w = g - X\frac{\partial g}{\partial X}, \qquad (4.27)$$

$$\mu_A = g + (1-X)\frac{\partial g}{\partial X} + \frac{1-\alpha_{soln}}{X}\frac{\partial g}{\partial \alpha_{soln}}, \qquad (4.28)$$

$$\mu_B = g + (1-X)\frac{\partial g}{\partial X} - \frac{\alpha_{soln}}{X}\frac{\partial g}{\partial \alpha_{soln}}. \qquad (4.29)$$

Using Eqs. (4.27)-(4.29), the three conditions of phase equilibria can be reexpressed in the following mathematically useful forms

$$\frac{1}{Y}\frac{\partial g(T,P,Y,\alpha_Y)}{\partial \alpha_Y} = \frac{1}{Z}\frac{\partial g(T,P,Z,\alpha_Z)}{\partial \alpha_Z}, \qquad (4.30)$$

$$\frac{\partial g(T,P,Y,\alpha_Y)}{\partial Y} - \frac{\partial g(T,P,Z,\alpha_Z)}{\partial Z} = \frac{(\alpha_Y-\alpha_Z)}{Z}\frac{\partial g(Z,\alpha_Z)}{\partial \alpha_Z}, \qquad (4.31)$$

$$g(T,P,Y,\alpha_Y) - g(T,P,Z,\alpha_Z) = Y\frac{\partial g(T,P,Y,\alpha_Y)}{\partial Y} - Z\frac{\partial g(T,PZ,\alpha_Z)}{\partial Z}. \qquad (4.32)$$

Using the Gibbs phase rule, a two-phase ternary solution in thermodynamic equilibrium has three independent intensive variables. Therefore, fixing temperature, pressure and one additional intensive variable the remaining intensive variables are uniquely specified. Accordingly, by fixing one of the four intensive variables Y, Z, α_Y, and α_Z in Eqs. (4.30)-(4.32), the remaining three can be calculated. In other words, at fixed pressure, the entire family of coexistence curves in the T-X-α_{soln} coordinate system can be generated.

4.2.4 Modelling the Free Energy of Mixed Micellization

4.2.4.1 General Considerations

As described earlier, the free energy of micellization $g_{mic}(sh,n,\alpha)$ summarizes the many physico-chemical factors responsible for mixed micelle formation, and depends on the molecular structure of the surfactants as well as on solution conditions such as temperature, pH, and the presence of any additives. To illustrate some general features and qualitative prediction capabilities of the thermodynamic framework, below we present a simple analytical phenomenological model for $g_{mic}(sh,n,\alpha)$. Although the predictions presented in this chapter will be *qualitative* in nature, a major advantage of utilizing a simplified model for g_{mic} is that it enables us to obtain *analytical* expressions for many of the useful micellar solution properties, as well as to shed light on the physical basis of some of the observed experimental trends. For more detailed and accurate *quantitative* predictions of micellar solution properties, a molecular model of mixed micellization, which takes into account the detailed molecular structure of the surfactants as well as the effect of solution conditions, is required. Such a model has been developed, and will be presented in Chapter 5.

The free energy of micellization is a function of the shape of the micelle sh, the aggregation number n, and the composition α. It is well known that n can range from very small to very large values. Since $g_{mic}(sh,n,\alpha)$ needs to be evaluated for all n and α, the problem becomes computationally intensive. For the purpose of illustration, we can simplify the calculations by making the following physically reasonable two assumptions. First, as

explained in Sec. 4.2.2, we approximate $\Sigma_\alpha X_{n\alpha}$ *by* $X_{n\alpha^*}$, where α^* is the optimum composition of a micelle having aggregation number n. Second, we evaluate g_{mic} only for the three regular shapes of spheres, infinite-sized cylinders, and infinite-sized discs or bilayers. For the non-regular finite-sized mixed micelles, $g_{mic}(n,\alpha^*)$ and $\alpha^*(n)$ are estimated by linearly interpolating between the $g_{mic}(n,\alpha^*)$ and $\alpha^*(n)$ values corresponding to the limiting regular shapes.

4.2.4.2 Illustrative Example: Finite-Sized Cylindrical Mixed Micelles

To describe a finite-sized cylindrical mixed micelle exhibiting one-dimensional growth, $g_{mic}(n,\alpha^*)$ and $\alpha^*(n)$ are estimated by interpolating between the optimum values of these quantities for a spherical micelle and an infinite-sized cylindrical micelle, that is,

$$g_{mic}(n,\alpha^*) = g_{cyl}(\alpha^*_{cyl}) + \frac{n_{sph}}{n}\left[g^{sph}_{mic}(\alpha^*_{sph}) - g^{cyl}_{mic}(\alpha^*_{cyl})\right], \qquad (4.33)$$

and

$$\alpha^*(n) = \alpha^*_{cyl} + \frac{n_{sph}}{n}\left[\alpha^*_{sph} - \alpha^*_{cyl}\right], \qquad (4.34)$$

where n_{sph} and α^*_{sph} are the aggregation number and composition of the optimum spherical micelle, α^*_{cyl} is the composition of the optimum infinite-sized cylindrical micelle, and g^{sph}_{mic}

and g_{mic}^{cyl} are the free energies of micellization of the optimum spherical and the optimum infinite-sized cylindrical micelles, respectively. Substituting Eqs. (4.33) and (4.34) in the expression for $X_{n\alpha}$ given in Eq. (4.12) we obtain

$$X_{n\alpha^*} = \frac{1}{K}\left(\frac{X_1}{X_{cyl}}\right)^n , \tag{4.35}$$

where $K=e^{\beta\Delta\mu}$, with $\Delta\mu = n_{sph}\left[g_m^{sph}-g_m^{cyl}\right]+kT$, and $X_{cyl} = e^{\beta g_m^{cyl}}$. Recall that $\beta g_m = \beta g_{mic} - 1 - \alpha\ln\alpha_1 - (1-\alpha)\ln(1-\alpha_1)$. Note that the parameter $\Delta\mu$ is a growth parameter analogous to the one introduced (Missel et al., 1980; Blankschtein et al., 1985 and 1986) to describe the one-dimensional growth of single-surfactant cylindrical micelles. Clearly, in order to have growth, one expects $\Delta\mu>0$, where an increase in the value of $\Delta\mu$ will result in an increase in micellar size. Note also that the concentration X_{cyl} reflects the propensity to form cylindrical micelles, and that, in the limit of considerable growth, one has $X_{cyl}\approx$CMC.

It is possible to show, following an analysis similar to the one utilized in the case of single-surfactant cylindrical micelles, that in the limit $\langle n\rangle_w >> n_{sph}$, the following remarkably simple result for $X_{n\alpha^*}$ is obtained

$$X_{n\alpha^*} \approx \frac{1}{K}\, e^{-n(KX)^{-1/2}} . \tag{4.36}$$

Equation (4.36) shows that, in the limit of significant micellar growth,the micellar size

distribution, corresponding to the optimum composition α^*, is a monotonically decreasing exponential function of n (for $n > n_{sph}$) whose width is directly proportional to $(KX)^{1/2}$. As stated earlier, if we approximate $\Sigma_\alpha X_{n\alpha}$ *by* $X_{n\alpha^*}$, the second moment M_2 of the distribution (see Eq.(4.16) with k=2) is given by

$$M_2 \approx n_{sph} + 2K^{1/2}X^{3/2}. \tag{4.37}$$

Similarly, the weight-average mixed micelle aggregation number (see Eq. (4.21)) is given by

$$\langle n \rangle_w = M_2 / X \approx n_{sph} + 2(KX)^{1/2}. \tag{4.38}$$

Note that as stated in Sec. 4.1, the analysis of Ben-Shaul et al. (1986) suggests that when the entire size and composition distribution $\{X_{n\alpha}\}$ is utilized, instead of only that corresponding to the optimum composition $\{X_{n\alpha^*}\}$, $\langle n \rangle_w$ varies as $X^{0.4}$ instead of $X^{0.5}$ as predicted by Eq. (4.38). This, of course, does not affect the qualitative conclusions presented in this chapter.

In addition, the relative variance of the distribution (see Eq.(4.22)) is given by

$$\sigma \approx 1/2. \tag{4.39}$$

4.2.4.3 Simple Analytical Phenomenological Model for g_{mic}

Below we introduce a simple analytical phenomenological model to estimate the free

energy of micellization $g_{mic}(sh,\alpha)$ corresponding to the three regular shapes of spheres, infinite-sized cylinders, and infinite-sized discs or bilayers. As illustrated in (b) above, for non-regular finite-sized micelles, g_{mic} is estimated by linearly interpolating between the optimum g_{mic} values corresponding to the limiting regular shapes.

We model g_{mic} as the sum of four primary contributions (see also Chapters 2 and 5): (i) Hydrophobic free energy $g_{w/mic}(sh,\alpha)$, which represents the free-energy gain in transferring the hydrophobic tails from water to the hydrophobic interior of a mixed micelle characterized by a shape sh and composition α. This contribution can be further expressed as $g_{w/mic}(sh,\alpha) = g_{w/hc}(\alpha) + g_{hc/mic}(sh,\alpha)$. The quantity $g_{w/hc}$ reflects the free-energy gain associated with transferring the hydrophobic tails from water to a bulk phase, having composition α, made from the two tails of the surfactants (note that, as expected, this contribution is independent of micellar shape), and can be expressed as $g_{w/hc} = b_1 + (a_1-b_1)\alpha + kT[\alpha\ln\alpha+(1-\alpha)\ln(1-\alpha)] + c_1\alpha(1-\alpha)$, where a_1 and b_1 are the hydrophobic free-energy contributions associated with pure surfactant A tails and B tails, respectively, $kT[\alpha\ln\alpha+(1-\alpha)\ln(1-\alpha)]$ reflects the free energy of mixing the two surfactant tails in the mixed micelle, and c_1 reflects the strength of the interactions between the two surfactant tails based on the regular solution theory. Note that c_1 is typically equal to zero for a mixture of hydrocarbon (or fluorocarbon)-based surfactants (Scamehorn, 1986), but is greater than zero (Mukerjee and Handa, 1981) for mixtures of hydrocarbon-based and fluorocarbon-based surfactants which exhibit repulsive antagonistic interactions. The quantity $g_{hc/mic}(sh,\alpha)$, which reflects the free-energy loss associated with the reduction in conformational degrees of freedom of the two types of surfactant tails (at composition α)

in the constrained environment provided by the micellar core, depends on micellar shape. For computational simplicity, we assume that this contribution is linear in composition, that is, $g_{hc/mic} = d_1 + (e_1-d_1)\alpha$, where e_1 and d_1 are the conformational free-energy contributions associated with pure surfactants A and B, respectively.

(ii) Interfacial free energy $g_\sigma(sh,\alpha)$, which represents the free energy per monomer associated with creating an interface separating the micellar core from the bulk solution. This contribution can be approximated as $g_\sigma = \alpha\sigma_A a_A + (1-\alpha)\sigma_B a_B$, where, σ_A and a_A, and, σ_B and a_B, are the interfacial tensions and interfacial areas corresponding to surfactants A and B, respectively, and a simple average, weighed by the micellar composition α, relates g_σ to the individual interfacial free energies per monomer $\sigma_A a_A$ and $\sigma_B a_B$. Accordingly, $g_\sigma(sh,\alpha)$ can be expressed as $b_2 + (a_2-b_2)\alpha$, where $a_2 = \sigma_A a_A$ and $b_2=\sigma_B a_B$ are functions of micellar shape.

(iii) Steric free energy $g_{st}(sh,\alpha)$, which represents steric interactions between the surfactant headgroups at the micellar surface. These interactions have been shown (see Chapters 2 and 3) to play an important role in the micellization of nonionic surfactants. By treating the headgroups at the micellar surface as an adsorbed localized monolayer, it can be shown (see Chapter 5) that $g_{st} = -kT\left[\alpha\ln(1-a_{hA}/a)+(1-\alpha)\ln(1-a_{hB}/a)\right]$, where a_{hA} and a_{hB} are the average headgroup cross-sectional areas of surfactants A and B, respectively, and a is the available area per monomer. This equation can also be expressed as $g_{st}(sh,\alpha) = b_3+(a_3-b_3)\alpha$, where $a_3 = -kT \ln(1-a_{hA}/a)$, and $b_3 = -kT \ln(1-a_{hB}/a)$ are functions of micellar shape.

(iv) Electrostatic free energy $g_{elec}(sh,\alpha)$, required to describe charged surfactants, which represents the free energy associated with creating a charged interface in a sea of

counterions. From simple electrostatic considerations (Bockris and Reddy, 1977) one expects that, in general, g_{elec} should be proportional to q^2, where q is the net charge per monomer at the micellar surface. Consequently, for a binary surfactant mixture, $q = \alpha z_A + (1-\alpha)z_B$, where z_A and z_B are the valencies of the two surfactants. Thus, $g_{elec} = b_4 + (a_4-b_4)\alpha + c_4\alpha^2$, where $a_4 = K_{elec}(2z_B-z_A)z_B$, $b_4 = K_{elec}z_B^2$, and $c_4 = K_{elec}(z_A-z_B)^2$, and K_{elec} is a numerical constant which can be evaluated from electrostatic theories and depends on micellar shape. In addition, K_{elec} is expected to be a strong function of salt concentration, and should decrease (screening effect) with increasing salt concentration.

Combining the four contributions described above, g_{mic} can be expressed using the following simple relation

$$g_{mic}(sh,\alpha) = B(sh) + [A(sh)-B(sh)]\alpha + C(sh)\alpha^2 + kT[\alpha\ln\alpha + (1-\alpha)\ln(1-\alpha)] , \quad (4.40)$$

where $A(sh) = a_1 + a_2 + a_3 + a_4 + c_1 + e_1$, $B(sh) = b_1 + b_2 + b_3 + b_4 + d_1$, and $C(sh) = c_4-c_1$. Note that A+C and B are the free energies of micellization of pure surfactants A ($\alpha=1$) and B ($\alpha=0$), respectively. The modified free energy of micellization g_m at the optimum composition α^*, namely, $g_m(sh,\alpha^*,\alpha_1)$, can be evaluated by inserting Eq. (4.40) in Eq. (4.13) and using the resulting relation in the definition of g_m. Carrying out this procedure we find that

$$g_m(sh,\alpha^*,\alpha_1) = B(sh) - C(sh)\alpha^{*2} + kT\ln\left(\frac{1-\alpha^*}{1-\alpha_1}\right) - kT , \quad (4.41)$$

where α^* can be obtained by solving Eq. (4.13) with g_{mic} given in Eq. (4.40).

Since the growth parameter, $\Delta\mu = n_{sph}(g_m^{sph} - g_m^{cyl}) + kT$, then upon using Eq. (4.41) for an optimum spherical micelle and an optimum infinite-sized cylindrical micelle in this definition we find that

$$\Delta\mu = n_{sph}\left[B_{sph} - B_{cyl} - C_{sph}(\alpha_{sph}^*)^2 + C_{cyl}(\alpha_{cyl}^*)^2 + kT\ln\frac{(1-\alpha_{sph}^*)}{(1-\alpha_{cyl}^*)}\right] + kT. \qquad (4.42)$$

We turn next to a discussion of the values of A, B, and C which determine the values of g_{mic}. In general, micellization requires that the free energy of micellization g_{mic} be negative. In particular, since for pure surfactant A, $g_{mic}(sh,\alpha=1) = A(sh)+C(sh)$, and for pure surfactant B, $g_{mic}(sh,\alpha=0) = B(sh)$, it follows that both $A(sh)+C(sh)$ and $B(sh)$ should be negative for single-surfactant micelles of that particular shape to form. Typically A+C and B range between -6 to -20kT (Mukerjee and Mysels, 1971).

The parameter $C = c_4 - c_1$ is a strong function of the type of surfactant mixture. In mixtures of hydrocarbon-based (fluorocarbon-based) surfactants the hydrocarbon (fluorocarbon) tails mix ideally, and consequently $c_1 = 0$, which results in $C = c_4 = K_{elec}(z_A - z_B)^2$. Therefore, for nonionic-nonionic surfactant mixtures, where electrostatic interactions can be neglected, C=0. However, in nonionic-ionic surfactant mixtures where the ionic surfactant (B) is monovalent, that is, $z_A = 0$ and $z_B = \pm 1$, the parameter C is equal to K_{elec}. Simple electrostatic calculations, with no added salt, yield a value of K_{elec} in the range of 3-6kT, and the addition of salt further decreases the value of K_{elec}. Thus, for these

nonionic-ionic mixtures, C has a value of approximately 3-6kT at zero salt concentration, which decreases upon the addition of salt due to electrostatic screening effects. For monovalent anionic-monovalent cationic surfactant mixtures ($z_A = +1$, $z_B = -1$), $C = 4K_{elec}$, which is four times the value for nonionic-monovalent ionic mixtures. For mixtures of hydrocarbon-based and fluorocarbon-based nonionic surfactants ($c_4 = 0$), mixing of the surfactant tails is nonideal due to repulsive interactions, and, therefore, $c_1 > 0$, suggesting that $C = -c_1 < 0$. Thus, depending on the nature of the surfactant mixture, C can range from negative values to positive values of up to 25kT. Table 4.2 summarizes typical values of C for various surfactant mixtures.

4.3 RESULTS AND DISCUSSIONS

4.3.1 Critical Micellar Concentration (CMC)

At very low surfactant concentrations most of the surfactant molecules exist as free monomers. However, as the concentration of surfactant is increased, keeping its composition constant, micelles start to form beyond a certain threshold concentration known as the critical micellar concentration (CMC). Beyond the CMC most of the added surfactant remains in the micellar form, and the monomer concentration remains practically constant. Furthermore, the first micelles that form will have a composition close to the optimum value α^*, because at $\alpha = \alpha^*$ the free energy of micellization exhibits a minimum. The mole fraction of these micelles can therefore be expressed, using $\alpha = \alpha^*$ in Eq. (4.12),

as

$$X_{n\alpha^*} = \frac{1}{e}\left(\frac{X_1}{e^{\beta g_m(\alpha^*,\alpha_1)}}\right)^n . \qquad (4.43)$$

From Eq. (4.43), it follows that $X_{n\alpha^*}$ is vanishingly small for $X_1 \ll e^{\beta g_m}$ and infinitely large for $X_1 > e^{\beta g_m}$. However, for $X_1 \approx e^{\beta g_m}$, $X_{n\alpha^*}$ is finite but small. That is, to a very good approximation, the micelles first form when the monomer concentration $X_1 \approx e^{\beta g_m}$. In other words, one can approximate the CMC of the mixed micellar solution by $e^{\beta g_m}$. Using the expression for g_m given in Eq. (4.41) one finds that

$$\ln(CMC) \approx \beta g_m(sh,\alpha^*,\alpha_1) = \beta B - \beta C\alpha^{*2} + \ln\left(\frac{1-\alpha^*}{1-\alpha_1}\right) - 1 , \qquad (4.44)$$

where sh corresponds to the shape of the optimum micelle, and α^* is obtained by inserting Eq. (4.40) for g_{mic} into Eq. (4.13). The resulting implicit equation for α^* is given by

$$\beta(A-B) + 2\beta C\alpha^* + \ln\frac{\alpha^*}{1-\alpha^*} = \ln\frac{\alpha_1}{1-\alpha_1} . \qquad (4.45)$$

Combining Eqs. (4.44) and (4.45), and performing some algebraic manipulations, we obtain

$$\frac{1}{CMC} = \frac{\alpha_1}{f_A CMC_A} + \frac{1-\alpha_1}{f_B CMC_B}, \tag{4.46}$$

where $\ln f_A = -\beta C(1-\alpha^*)^2$, $\ln f_B = -\beta C(\alpha^*)^2$, $CMC_A = e^{\beta(A+C)-1}$ is the CMC of pure surfactant A, and $CMC_B = e^{\beta B-1}$ is the CMC of pure surfactant B. The variables f_A and f_B are equivalent to the micellar activity coefficients of each surfactant, and the parameter $-\beta C$ is equal to the empirical interaction parameter ϵ used in the pseudo-phase separation model (Rubingh, 1979; Holland and Rubingh, 1983) for mixed micelles. Our approach, therefore, enables us to rationalize the physical basis behind Eq. (4.46), an expression which has been utilized extensively to analyze and predict CMC's of mixed surfactant solutions. Furthermore, our approach also allows us to quantitatively predict mixture CMC's from a knowledge of the parameters A, B, and C which can be computed utilizing the molecular model for the free energy of micellization described in Chapter 5. Thus, the mixture CMC can be predicted as a function of surfactant type, surfactant composition, and solution conditions. In this chapter, we will only make general qualitative observations about the CMC behavior based on the simple model for g_{mic} presented in the previous section. A detailed quantitative analysis of mixture CMC's, with particular emphasis on aqueous binary nonionic surfactant mixtures, will be presented in Chapter 5.

We begin by noting that since $\epsilon = -\beta C$, in view of the discussions in Sec. 4.2.4, we would predict that monovalent anionic-monovalent cationic mixtures have a value of ϵ which is four times that of nonionic-monovalent ionic mixtures. Indeed, this is observed experimentally, where ϵ values range between -2.5 to -5 for nonionic-monovalent ionic mixtures, and between -10 to -25 for monovalent anionic-monovalent cationic mixtures

(Rosen, 1986 and 1989).

Our approach also indicates that, at the CMC, the mixed micelles have compositions significantly different from the solution composition. Indeed, Fig. 4.1 shows the predicted optimum micellar composition α^*, at the mixture CMC, as a function of the solution monomer composition α_1. The predicted mixture CMC is also plotted as a function of α_1 in Fig. 4.2. These calculations were performed for the following four sets of typical parameter values: (i) A=-10kT, B=-12kT, C=0kT, (ii) A=-12kT, B=-12kT, C=2kT, (iii) A=-25kT, B=-12kT, C=15kT, and (iv) A=-8kT, B=-12kT, C=-2kT. Based on the C values (see Table 4.2), cases (i) to (iv) correspond to mixtures of nonionic-nonionic, nonionic-monovalent ionic, monovalent anionic-monovalent cationic, and nonionic hydrocarbon-nonionic fluorocarbon surfactants, respectively. Note that for illustrative purposes we have selected values of A, B, and C such that in all cases A+C=-10kT and B=-12kT. Since, as shown earlier, $CMC_A \approx e^{\beta(A+C)-1}$ and $CMC_B \approx e^{\beta B-1}$, this selection implies that in all four cases pure surfactant B has a lower CMC than pure surfactant A (see Fig. 4.2, where $\alpha_1=0(\alpha_1=1)$ corresponds to pure surfactant B (surfactant A)). Below we analyze cases (i)-(iv) separately.

Case (i), corresponding to an aqueous solution of a nonionic-nonionic surfactant mixture (full lines in Figs. 4.1 and 4.2) represents an ideal mixture at the micellar level (C=0). For this system, Fig. 4.1 shows that the solution monomer composition α_1 is always higher than the optimum micellar composition α^*, indicating that the mixed micelles are enriched with surfactant B having the lower CMC. Case (ii), corresponding to a nonionic-monovalent ionic surfactant mixture (dashed lines in Figs. 4.1 and 4.2) represents a nonideal mixture at the micellar level (weak synergism, C=2kT). For this system, Fig. 4.2 shows that

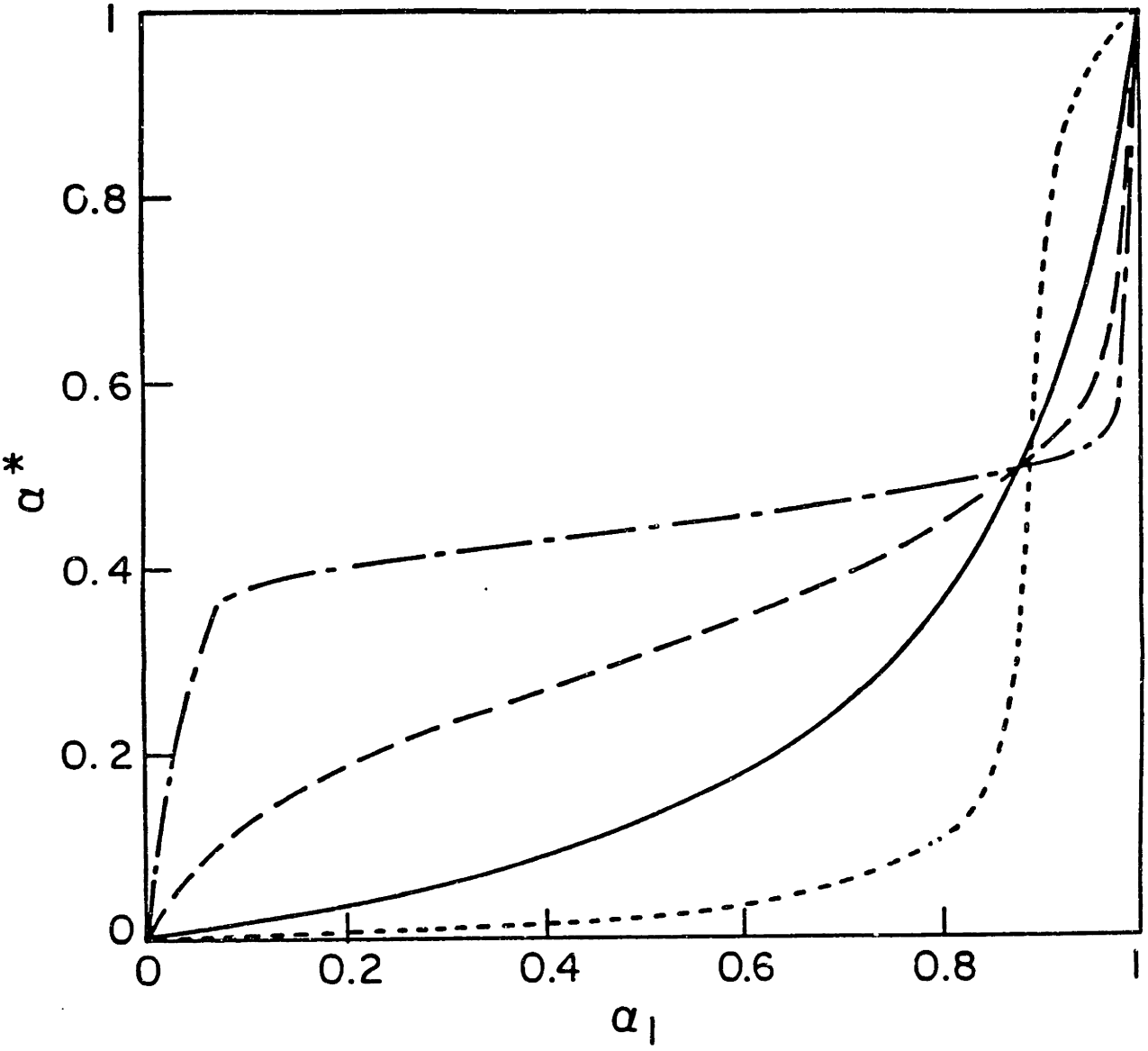

Figure 4.1 Predicted optimum composition of the mixed micelle α^*, at the CMC, as a function of monomer composition α_1 for solutions of: (i) nonionic-nonionic (———), (ii) nonionic-monovalent ionic (— — —); (iii) monovalent anionic-monovalent cationic (— - —), and (iv) nonionic hydrocarbon-nonionic fluorocarbon (- - - -) surfactant mixtures.

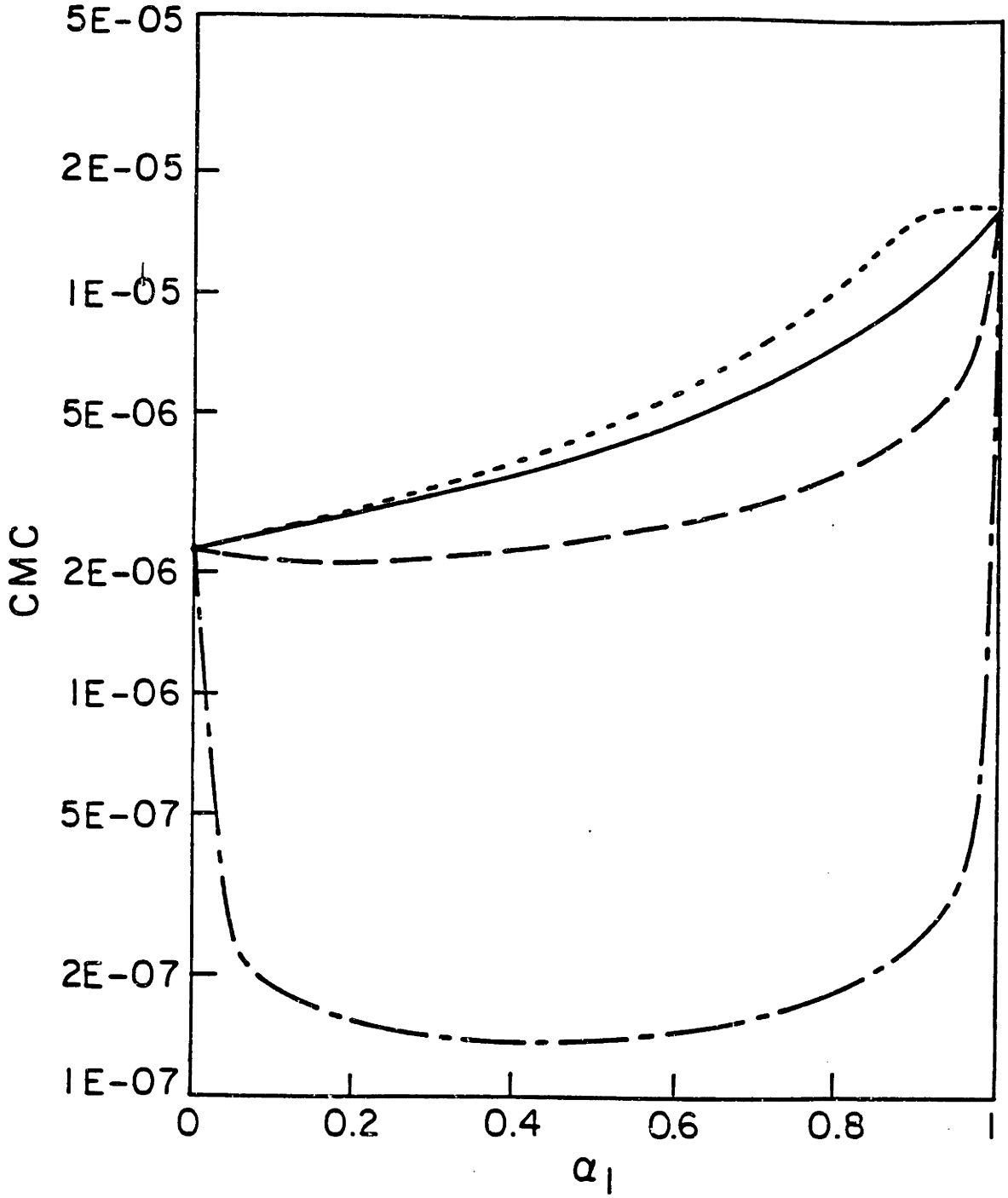

Figure 4.2 Predicted critical micellar concentration (CMC) as a function of monomer composition α_1 for various surfactant mixtures. The notation is the same as in Figure 4.1. Note that for illustrative purposes the CMC's of the pure surfactants ($\alpha_1=0$ and $\alpha_1=1$) are the same in all four cases.

the mixture CMC is lower than in case (i), indicating negative deviations from ideality due to synergistic interactions. Case (iii), corresponding to a monovalent anionic-monovalent cationic surfactant mixture (dashed-dotted lines in Figs. 4.1 and 4.2), represents a highly nonideal mixture at the micellar level (strong synergism, C=15kT). For this system, Fig. 4.2 shows that the mixture CMC is significantly lower than in case (i), indicating large negative deviations from ideality. Furthermore, it is noteworthy that the mixture CMC is considerably lower than the CMC's of the pure surfactants over a broad α_1 range (see Fig. 4.2). Over this α_1 range, Fig. 4.1 shows that the optimum micellar composition α^* is close to 0.5, a composition at which the two opposite surfactant charges would completely neutralize each other. In other words, this suggests that the distribution of the two oppositely charged surfactants between monomers and micelles reflects the tendency to minimize electrostatic repulsions within the micelles, thus leading to strong synergism and associated low CMC values (as compared to the ideal case). It has recently been brought to our attention that under such strong synergistic conditions many surfactants self-assemble to form vesicles rather than micelles (Kaler et al., 1989; Kaler, 1991). However, our theory is applicable only to solutions containing micelles and would therefore be strictly valid for those surfactant mixtures which form micelles rather than vesicles. Case (iv), corresponding to nonionic hydrocarbon-nonionic fluorocarbon surfactant mixtures (dotted lines in Figs. 4.1 and 4.2), represents a nonideal mixture at the micellar level (antagonism, C=-2kT). For this system, Fig. 4.2 shows that the mixture CMC is larger than in case (i), indicating positive deviations from ideality due to antagonistic interactions. As noted in Fig. 4.1, it is noteworthy that over a broad α_1 range, one has $\alpha^* << \alpha_1$, indicating that the mixed micelles

are highly enriched in surfactant B (more than 90%) reflecting the antag[illegible]istic interactions between surfactants A and B.

4.3.3 Characteristics of the Micellar Size and Composition Distribution

For illustrative purposes we consider the case of cylindrical mixed micelles which exhibit significant one-dimensional growth, a case of particular importance for certain aqueous solutions of mixed nonionic-nonionic surfactants. In Sec. 4.2.4 we saw that the weight-average mixed micelle aggregation number is given by Eq. (4.38), which we rewrite here in terms of the growth parameter $\Delta\mu$, namely,

$$\langle n \rangle_w \approx n_{sph} + 2\sqrt{e^{\beta\Delta\mu} X} \,. \tag{4.47}$$

Equation (4.47) indicates a square-root dependence of $<n>_w$ on X, as well as an exponential dependence on $\Delta\mu$. Using Eq. (4.42) for $\Delta\mu$, and Eq. (4.47) for $<n>_w$, in Fig. 4.3 we predict variations of $<n>_w$ (at $X=10^{-3}$) and $\Delta\mu$ with solution composition α_{soln} for two illustrative cases:

(i) $A_{sph}=-9.9kT$, $A_{cyl}=-10kT$, $B_{sph}=-11.6kT$, $B_{cyl}=-12kT$, $C_{sph}=C_{cyl}=0$, and (ii) $A_{sph}=-11.6kT$, $A_{cyl}=-12kT$, $B_{sph}=-11.6kT$, $B_{cyl}=-12kT$, $C_{sph}=1.7kT$, $C_{cyl}=2kT$. Recalling that for pure surfactant A, $g_{mic}(sh,\alpha=1)=A+C$, in cases (i) and (ii) one obtains identical free-energy values of -10kT and -9.9kT for infinite-sized cylindrical and spherical micelles, respectively. Using these values and assuming an aggregation number of 50 for the spherical micelle

(typical values of n_{sph} range between 30-100), the growth parameter for pure A can be computed using $\Delta\mu = n_{sph}(g_m^{sph} - g_m^{cyl}) + kT$, and is found to be equal to 6kT. Note that for pure surfactants (A or B), $g_m = g_{mic} - kT$. Similarly, in cases (i) and (ii), pure surfactant B, for which $g_{mic}(sh, \alpha = 0) = B$, has identical free-energy values of -12kT and -11.6kT for the infinite-sized cylindrical and spherical micelles, respectively. Once again, assuming an aggregation number of 50 for the spherical micelle, we obtain $\Delta\mu = 21kT$ for pure surfactant B. That is, in cases (i) and (ii), pure surfactant B ($\alpha_{soln} = 0$) exhibits significant growth ($\Delta\mu = 21kT$), while pure surfactant A ($\alpha_{soln} = 1$) exhibits moderate growth ($\Delta\mu = 6kT$), see Fig. 3. Based on the C values (see Table 4.2), cases (i) and (ii) would correspond to nonionic-nonionic and nonionic-monovalent ionic surfactant mixtures, respectively. Note that the parameter values in (i) and (ii) were chosen to illustrate the effect of different types of interactions (electrostatic vs steric) on the mixed micellar size. Fig. 4.3 shows that in cases (i) and (ii) $\Delta\mu$ decreases from a value of 21kT (corresponding to pure surfactant B) to a value of 6kT (corresponding to pure surfactant A). However, for small values of α_{soln}, $\Delta\mu$ decreases at a much slower rate in case (ii) (dashed line) than in case (i) (full line). On the other hand, for larger α_{soln} values, $\Delta\mu$ decreases more rapidly in case (ii) reaching a value of 6kT at $\alpha_{soln} = 1$. This decrease in $\Delta\mu$ with α_{soln} is also reflected in the decrease of the weight-average mixed micelle aggregation number with α_{soln}, with $<n>_w$ decreasing more rapidly in case (i) (full line) than in case (ii) (dashed line). Fig. 4.3 clearly shows that $<n>_w$ is larger in case (ii) than in case (i) indicating synergistic interactions in the nonionic-monovalent ionic surfactant mixture. This prediction is in good agreement with experimental measurements (Nilsson and Lindman, 1984) of micellar sizes in the system

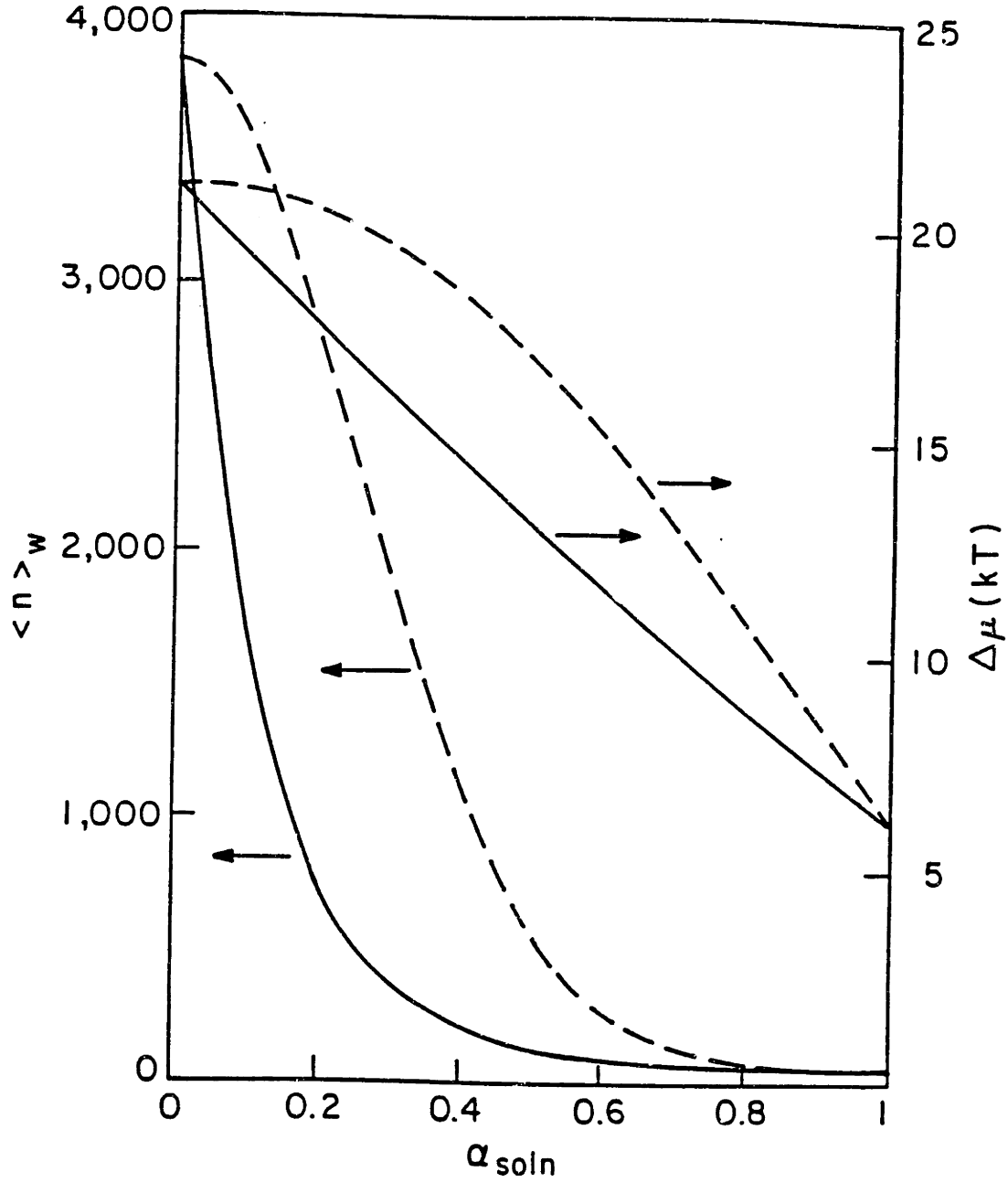

Figure 4.3 Predicted weight-average mixed micelle aggregation number $<n>_w$ (at $X = 10^{-3}$) and growth parameter $\Delta\mu$ as a function of total surfactant composition α_{soln} for solutions of: (i) nonionic-nonionic (———), and (ii) nonionic-monovalent ionic (— — —) surfactant mixtures. Note that in both cases $\Delta\mu$ is the same for the pure surfactants ($\alpha_{soln}=0$ and $\alpha_{soln}=1$).

$C_{12}E_5$-SDS-D_2O, where $C_{12}E_5$ is a nonionic surfactant and SDS is a monovalent anionic surfactant. Specifically, it was found that aqueous solutions of pure $C_{12}E_5$ contain large micelles, and that the addition of small quantities of SDS (up to approximately 20wt%) further increases micellar size (due to the synergistic interactions between the ionic and nonionic surfactants). However, as the amount of SDS is further increased micellar size decreases.

4.3.3 Phase Separation

In this section, we study the influence of adding small amounts of surfactant A ($\alpha_{soln} << 1$) on several aspects of the phase separation of an aqueous solution containing surfactant B. Specifically, we study the influence on the critical temperature, as well as analyze how the added surfactant partitions between the two coexisting micellar-rich and micellar-poor phases.

At the binary critical point of a single-surfactant solution, $(\partial^2 G/\partial N_w^2) = (\partial^3 G/\partial N_w^3) = 0$, suggesting that $(\partial\psi/\partial N_w)=0$ (Lupis, 1983). Consequently, very close to the binary (surfactant B + water) critical point, the condition $\Phi=0$ in Eq. (4.26) can be expressed as

$$\frac{\partial^2 G}{\partial N_w^2} = 0. \qquad (4.48)$$

Substituting the value of the Gibbs free energy, given in Eqs. (4.1)-(4.3), into Eq. (4.48) we find, to leading order in X, that the critical temperature T_c can be expressed as

$$T_c \approx \frac{\gamma_{eff} C_{eff}}{k}. \tag{4.49}$$

Inserting Eq. (4.4) into Eq. (4.49), and expanding the resulting expression to linear order in $\alpha_{soln}(<<1)$ yields

$$kT_c \approx \gamma_B C_{BW} + \left[(\gamma_A-\gamma_B)C_{BW} + \gamma_B[C_{AW}-C_{BW}] - \sqrt{\gamma_A\gamma_B}C_{AB}\right]\alpha_{soln}. \tag{4.50}$$

Note that the critical temperature of an aqueous solution of pure surfactant B (corresponding to $\alpha_{soln}=0$ in Eq. (4.50)) can be expressed as $T_c^\circ = \gamma_B C_{BW}(T_c^\circ)/k$, where we have assumed that C_{BW} can depend on temperature. To estimate the change in T_c of an aqueous solution of surfactant B upon the addition of small quantities of surfactant A ($\alpha_{soln}<<1$), namely, $\Delta T_c = T_c - T_c^\circ$, we expand Eq. (4.50) to leading order in ΔT_c and α_{soln}. This yields

$$k\Delta T_c \approx \frac{\left[(\gamma_A/\gamma_B-1)C_{BW} + (C_{AW}-C_{BW}-\sqrt{\gamma_A/\gamma_B}\,C_{AB})\right]\gamma_B\alpha_{soln}}{1-\frac{\gamma_B}{k}\frac{\partial C_{BW}}{\partial T}}. \tag{4.51}$$

If solution conditions are altered such that the solution enters into the unstable region of the phase diagram, the solution will spontaneously separate into two coexisting

phases, one micellar-poor and the other micellar-rich. Substituting the free-energy contributions given in Eqs. (4.1)-(4.3) into $g=G/(N_w+N_A+N_B)$, we obtain

$$g = (1-X)\mu_w^o + X[\alpha_{soln}\mu_A^o + (1-\alpha_{soln})\mu_B^o] + kT[(1-X)\ln(1-X) + X - M_o + X\ln X_1] \quad (4.52)$$
$$+ kTX[\alpha_{soln}\ln\alpha_1 + (1-\alpha_{soln})\ln(1-\alpha_1)] - \frac{1}{2}C_{eff}\phi X.$$

To derive an expression for the composition difference α_Z-α_Y, when small amounts of surfactant A are added to aqueous solutions of pure surfactant B, we insert Eq. (4.52) in Eq. (4.30). Since the coexisting mole fractions Y and Z are much smaller than 1 (about 10^{-3}) and $\alpha_{soln} << 1$, we expand the resulting expression in powers of Y, Z, α_Y, and α_Z. To linear order in α_Z-α_Y and Z-Y we obtain

$$(\alpha_Z-\alpha_Y) \approx \frac{(Z-Y)}{2}\beta\alpha_Y\gamma_B\left[(\gamma_A/\gamma_B-1)C_{BW} + \left(C_{AW}-C_{BW}-\sqrt{\gamma_A/\gamma_B}\,C_{AB}\right)\right]. \quad (4.53)$$

Combining Eqs. (4.53) and (4.51) we find that the difference in compositions (α_Z-α_Y) between the two coexisting phases is proportional to the change in critical temperature ΔT_c when small quantities of surfactant A are added to aqueous solutions of surfactant B.

Depending on the values of C_{BW}, C_{AW}-C_{BW}, C_{AB}, and γ_A/γ_B, appearing in Eqs. (4.51) and (48), below we consider the following four illustrative cases.

(i) $0 < C_{AW} \leq C_{BW}$, $C_{AB} \approx 0$, and $\gamma_A=\gamma_B$. Since $C_{AB}\approx 0$, this case would represent a mixture of nonionic or zwitterionic surfactants, and since C_{AW} and C_{BW} are both greater than zero, it would represent the addition of a nonionic or zwitterionic surfactant to another nonionic

or zwitterionic surfactant (see Table 4.2). In this case, the critical temperature of the mixture (see Eq. (4.51)) does not change dramatically because the values of C_{AW} and C_{BW} are comparable. If surfactant B is a nonionic surfactant, $(\gamma_B/k)(\partial C_{BW}/\partial T)$ is typically greater than 1 at the lower critical point (see Table 4.1), and the addition of surfactant A raises the lower critical temperature (note that $k\Delta T_c \propto (C_{BW}-C_{AW})/[(\gamma_B/k)(\partial C_{BW}/\partial T)-1] > 0$ in this case). However, at the upper critical point of a nonionic or a zwitterionic surfactant solution, $\partial C_{BW}/\partial T \approx 0$ (see Table 4.1), and consequently since $C_{BW} \geq C_{AW}$, the upper critical temperature will decrease upon the addition of small amounts of surfactant A. In other words, the addition of small quantities of a second surfactant (nonionic or zwitterionic) raises the lower critical temperature of a nonionic surfactant solution and lowers the upper critical temperature of both zwitterionic and nonionic surfactant solutions. In addition, since Z-Y is typically (Blankschtein et al., 1986; Puvvada abd Blankschtein, 1990a) of the order of 10^{-3}, the difference $\alpha_Z-\alpha_Y$ is of order 10^{-5}. This indicates that the composition of surfactant in the two phases is almost identical, and that the added surfactant partitions almost equally between the two phases. Indeed, recent phase separation measurements in aqueous solutions of mixtures of two nonionic surfactants belonging to the alkyl polyethylene oxide family (C_iE_j) appear consistent with this prediction (see Chapter 5).

(ii) $C_{AW} << 0$, $C_{BW}=O(10kT)$, $C_{AB} < 0$, and $\gamma_A=\gamma_B$. Since $C_{AW}<<0$ and $C_{BW}=O(10kT)$ this case would represent (see Table 4.1) the addition of an ionic surfactant (species A) to a solution containing a zwitterionic or nonionic surfactant (species B). If surfactant B is zwitterionic ($\partial C_{BW}/\partial T \approx 0$), then the upper critical temperature decreases more rapidly than

in case (i) with the addition of surfactant A (see Eq. (4.51)). However, if surfactant B is nonionic, then $(\gamma_B/k)(\partial C_{BW}/\partial T)$ is greater than 1 at the lower critical point (see Table 4.1), indicating that the lower critical temperature increases with the addition of surfactant A. In addition, the upper critical point of a nonionic surfactant solution, where $\partial C_{BW}/\partial T \approx 0$, shifts to lower temperatures, thus predicting that the entire closed-loop coexistence curve should shrink upon the addition of an ionic surfactant. All these results, for the addition of an ionic surfactant to both nonionic and zwitterionic surfactants in aqueous solutions, are consistent with experimental data (Valaulikar and Manohar, 1985; Souza et al., 1986; Sadaghiania and Khan, 1991). Since in case (ii) the difference C_{AW}-C_{BW} is large and negative, this suggests that α_Z-α_Y is finite and negative. That is, we predict that the added ionic surfactant preferentially partitions into the dilute phase where the electrostatic repulsions are smaller. Note that in the dilute phase the total surfactant concentration is smaller than in the concentrated phase, and consequently the surfactants are, on average, farther apart from one another thus reducing the net electrostatic repulsions.

(iii) $C_{AB} << 0$, $C_{AW} \approx C_{BW}$ and $\gamma_A = \gamma_B$ which represents strong specific (synergistic because $C_{AB} < 0$) interactions between surfactants A and B, for example, in anionic-cationic surfactant mixtures. In this case, since $\partial C_{BW}/\partial T \approx 0$, Eq. (4.51) indicates that the upper critical point moves to higher temperatures. That is, when there are strong specific attractions between the two surfactants, the addition of the second surfactant increases net intermicellar attractions and thus increases the size of the unstable two-phase region. In this case, Eq. (4.53) indicates that the added surfactant partitions into the concentrated phase. This enhances electrostatic attractions between the two surfactants, and since, on average,

surfactants are closer to each other in the concentrated phase than in the dilute phase, the overall electrostatic repulsion decreases. These interesting predictions remain to be tested experimentally.

(iv) $\gamma_A > \gamma_B$, $C_{AB} = 0$ and $C_{AW} \approx C_{BW} > 0$, which describes mixing two surfactants having similar interactions and different sizes. In this case, we predict that when a larger surfactant (species A) is added to a solution of the smaller surfactant (species B), the upper critical temperature (associated with $\partial C_{BW}/\partial T \approx 0$) increases, while the lower critical temperature (associated with $(\gamma_B/k)(\partial C_{BW}/\partial T) > 1$) decreases, thus increasing the size of the unstable two-phase region (see Eq. (4.51)). Although we are unaware of available experimental data in mixed surfactant solutions to test these predictions, it is noteworthy that a behavior similar to that predicted here has been observed in solutions of polymer mixtures. Specifically, the addition of a high molecular weight polystyrene ($M_w \approx 50 \times 10^4$) to a solution of a low molecular weight polystyrene ($M_w \approx 4.5 \times 10^4$) in cyclohexane raised the upper critical temperature of the solution. In addition, a composition analysis of the two coexisting phases indicated that the high molecular weight polystyrene partitions preferentially into the concentrated phase. (Fujita, 1990; Hashimoto et al., 1984).

4.4 CONCLUDING REMARKS

In this chapter, we have presented a thermodynamic theory of mixed micellar solutions which can be utilized to predict a broad spectrum of micellar solution properties. Our approach represents a generalization of a recently developed thermodynamic theory for

single-surfactant solutions, which has been successfully utilized to predict a wide range of properties of aqueous solutions of pure nonionic surfactants and zwitterionic surfactants with and without added solution modifiers such as salts and urea (Puvvada and Blankschtein, 1989, 1990a and 1990b; Briganti et al., 1991; Carale and Blankschtein, 1992).

In this chapter, the theory has been utilized to make *qualitative predictions* of the critical micellar concentration, the micellar size and composition distribution, and the phase behavior, including phase separation, of solutions containing mixtures of nonionic-nonionic, nonionic-ionic, zwitterionic-ionic, anionic-cationic, and hydrocarbon-fluorocarbon based surfactants. The theory has also clarified the molecular basis of some of the synergistic and antagonistic interactions which were described in earlier works using empirical parameters. For example, the mixture CMC was previously described using an empirical interaction parameter ϵ and the CMC's of the constituent surfactants. In this work, we have derived a similar expression for the mixture CMC (see Eq. (4.46)), in the context of our Gibbs free energy formulation, and thus have provided a clearer understanding of the molecular basis for ϵ. In addition, we have computed the monomer and micellar compositions, including their dependence on the nature of the surfactants present in the mixture.

The theory has also been used to make some qualitative predictions about the variation of micellar size with surfactant composition. The present work predicts that the average micellar size of nonionic micelles in aqueous solution should decrease upon the addition of an ionic surfactant. Interestingly, we also predict that synergistic interactions between nonionic and ionic surfactants ($C>0$) result in larger $<n>_w$ values as compared to those in aqueous solutions of two nonionic surfactants ($C=0$).

In addition to the CMC, the micellar composition, and the average mixed micellar size, the theory is also able to describe the phase behavior of mixed micellar solutions as a function of the composition of the surfactant mixture. Indeed, it successfully predicts that in aqueous nonionic surfactant solutions the lower consolute (critical) temperature will increase, and the upper consolute (critical) temperature will decrease upon the addition of small quantities of an ionic surfactant. On the other hand, it predicts that the upper consolute (critical) temperature of aqueous zwitterionic surfactant solutions will decrease with the addition of small quantities of an ionic surfactant. These predictions are consistent with experimental observations. In addition, the theory can be used to describe the entire two-phase region, where an isotropic mixed surfactant solution spontaneously separates into two isotropic phases having different surfactant concentrations and compositions. We find that the compositions in the two coexisting phases can be significantly different depending on the nature of the two surfactants. Specifically, in nonionic-ionic surfactant mixtures, the ionic surfactant preferentially partitions to the dilute micellar-poor phase in order to minimize electrostatic repulsions. This interesting prediction remains to be tested experimentally. On the other hand, in nonionic-nonionic surfactant mixtures, the compositions of the two coexisting phases are almost identical.

The availability of a molecular model to evaluate the free energy of micellization of mixed surfactant solutions will further enhance the predictive capabilities of the theoretical framework presented in this chapter. In particular, the theory can then be used to make *quantitative predictions* of useful micellar solution properties as a function of (i) the molecular architectures of the surfactants present in the mixture, and (ii) solution conditions,

including the presence of additives such as salts. Progress in this direction is reported in Chapter 5.

4.5 REFERENCES TO CHAPTER 4

Ali, A.A.; Mulley, B.A. *J. Pharm. Pharmac.* **1978**, *30*, 205.

Attwood, D.; Elworthy, P.H.; Kayne, S.B. *J. Phys. Chem.* **1975** *75*, 2212.

Barry, B.W.; Morrison, J.C.; Russel, G.F.J. *J. Colloid Interface Sci.* **1970**, *33*, 554.

Ben-Shaul, A.; Rorman, D.H.; Hartland, G.V.; Gelbart, W.M. *J. Phys. Chem* **1986**, *90*, 5277.

Blankschtein, D.; Thurston, G.M.; Benedek, G.B. *Phys. Rev. Lett.* **1985**, *54*, 955.

Blankschtein,D.; Thurston, G.M.; Benedek, G.B. *J. Chem. Phys.* **1986**, *85*, 7268; and references cited therein.

Blankschtein, D.; Puvvada, S. *MRS Symposium Proceedings* **1990**, *177*,129.

Bockris, J.O'M.; Reddy, A.K.N. *Modern Electrochemistry*, Plenum:New York, **1977**.

Briganti, G.; Puvvada, S.; Blankschtein, D. *J. Phys. Chem.* **1991**, *95*, 8989.

Carale, T.R.; Blankschtein, D. *J. Phys. Chem.* **1990**, (in press).

Carvalho, B.L.; Briganti, G.; Chen, S-H. *J. Phys. Chem.* **1989**, *93*, 4282.

Clint, J.H. *J. Chem. Soc. Faraday Trans. 1*, **1975**, *71*, 1327.

Corkill, J.M.; Goodman, J.F.; Walker, T.; Wyer, J. *Proc. Royal Soc. A*, **1969**, *312*, 243.

Fujita, H. in *Polymer Solutions*, Elsevier:Amsterdam, 1990, p 311.

Funasaki, N.; Hada, S. *J. Phys. Chem.* **1979**, *83*, 2471.

Guggenheim, E.A. *Mixtures: The Theory of the Equilibrium Properties of Some Simple Classes of Mixtures, Solutions and Alloys*; Clarendon: Oxford, **1952.**

Hall, D.G.; Pethica, B.A. in *Nonionic Surfactants*. Shick, M.J. Ed.; Plenum: New York, **1984.**

Handa, T.; Mukerjee, P. *J. Phys. Chem.* **1981**, *85*, 3916.

Hashimoto, T.; Sasaki, K.; Kawai, H. *Macromolecules*, **1984**, *17*, 2812.

Holland, P.M.; Rubingh, D.N. *J. Phys. Chem.* **1983**, *87*, 1984.

Holland, P.M. *In Structure/Performance Relations in Surfactants*; Rosen, M.J., Ed.; ACS Symposium Series: Washington, D.C., **1984**; p. 141.

Holland, P.M. *Adv. Colloid Interface Sci.* **1986**, *26*, 111.

Israelachvili, J. *Intermolecular and Surface Forces*, Academic:London, **1985**; p. 78.

Jost, F.; Lieter, H.; Schwuger, M.J. *Coll. Polym. Sci.* **1988**, *266*, 554.

Kaler, E.W. **1991**, *Personal Communication.*

Kaler, E.W.; Murthy, A.K.; Rodriguez, B.E.; Zasadzinski, J.A.N. *Science*, **1989**, *245*, 1371.

Kamrath, R.F.; Frances, E.I. *Ind. Eng. Chem. Fundam.* **1983**, *22*, 330.

Lange, V.H. *Kolloid Z.* **1953**, *96*, 131.

Lange, V.H.; Beck, K.H. *Kolloid-Z. u. Z. Polymere* **1973**, *251*, 424.

Ljunggren, S.; Eriksson, J.C. *Progr. Colloid & Polymer Sci.* **1987**, *74*, 38.

Lupis, C.H.P. *Chemical Thermodynamics of Materials*; North-Holland:New York, **1983** ch XI.

Marszall, L.; *Langmuir*, **1988**, *4*, 90.

Meroni, A.; Pimpinelli, A.; Reato, L. *Chem. Phys. Lett.*, **1987**, *135*, 137.

Missel, P.J.; Mazer, N.A.; Benedek, G.B.; Young, C.Y.; Carey, M.C. *J. Phys. Chem.* **1980**, *84*, 1044.

Mitchell, D.J.; Tiddy, G.J.T.; Waring, L.; Bostock, T.; McDonald, M.P. *J. Chem. Soc. Faraday Trans. 1* **1983**, *79*, 975; and references cited therein.

Mukerjee, P.; Mysels, K.J. *Critical Micelle Concentration of Aqueous Surfactant Systems*, Natl. Stand. Ref. Data Ser.-Natl. Bur. Stand. No 36, US Dept. of Commerce: Washington, D.C.; **1971**.

Mukerjee, P.; Handa, T. *J. Phys. Chem.* **1981**, *85*, 2298.

Nagarajan, R. *Langmuir*, **1985**, *1*, 331.

Nagarajan, R.; Ruckenstein, E. *J. Colloid Interface Sci.* **1977**, *60*, 221.

Nilsson, P.G.; Lindman, B. *J. Phys. Chem.* **1984**, *88*, 5391.

Nishikido, N.; Moroi, Y.; Matuura, R. *Bull. Chem. Soc. Japan*, **1975**, *48*, 1387.

Puvvada, S.; Blankschtein, D. *J. Phys. Chem.* **1989**, *93*, 7753.

Puvvada, S.; Blankschtein, D. *J. Chem. Phys.* **1990a**, *92*, 3710; and references cited therein.

Puvvada, S.; Blankschtein, D. *Proceedings of the 8th International Symposium on Surfactants in Solution*; Mittal, K.L., Shah, D.O., Eds.; Plenum: New York, **1990b**, in press.

Puvvada, S.; Blankschtein, D. *J. Phys. Chem.* **1991b**, *submitted.*

Reatto, L.; Tau, M. *Chem. Phys. Lett.* **1984**, *108*, 292.

Rosen, M.J.; Hua, X.Y. *J. Colloid Interface Sci.* **1982a**, *86*, 164.

Rosen, M.J.; Hua, X.Y., *JAOCS*, **1982b**, *59*, 582.

Rosen, M.J. In *Phenomena in Mixed Surfactant Systems*, Scamehorn, J.F., Ed.; ACS Symposium Series 311: Washington, D.C. **1986**; p. 144.

Rosen, M.J. In *Surfactants and Interfacial Phenomena 2nd Edition*, John Wiley: New York, **1989**.

Rubingh, D.N. In *Solution Chemistry of Surfactants*, Vol. 1, Mittal, K.L., Ed.; Plenum: New York, **1979**, pp. 337.

Sadaghiania, A. S.; Khan, A. *J. Colloid Interface Sci.* **1991**, *144*, 191.

Scamehorn, J.F. *Phenomena in Mixed Surfactant Systems*, ACS Symposium Series 311, ACS Press, Washington (1986); and references cited therein.

Shinoda, K. *J. Phys. Chem.* **1954**, *58*, 541.

Souza, L.D.S.; Corti, M.; Cantu, L.; Degiorgio, V. *Chem. Phys. Lett.* **1986**, *131*, 160.

Stainsby G.; Alexander A.E. *Trans. of Faraday Soc.* **1950**, *46*, 587.

Stecker, M.M.; Benedek, G.B. *J. Phys. Chem.* **1984**, *88*, 6519.

Valaulikar, B.S.; Manohar, C. *J. Colloid Interface Sci.* **1985**, *108*, 403.

Yoesting, O.E.; Scamehorn, J.F. *Coll. Polym. Sci.* **1986**, *264*, 148.

Zhu, B.Y.; Rosen, M.J. *J. Colloid Interface Sci.* **1985**, *99*, 435.

4.6 APPENDIX A: FREE ENERGY OF INTERACTION FOR MIXED MICELLAR SOLUTIONS

The free energy of interaction reflects interactions between mixed micelles, water molecules, and free monomers in the solution. We adopt a mean-field type approximation to describe these interactions. At the level of a quadratic expansion in the number density, the free energy of interaction takes the following form

$$G_i = \frac{1}{2}N_w U_{ww}\rho_w + \sum_{n,\alpha} N_w U_{w(n\alpha)}\rho_{n\alpha} + \frac{1}{2}\sum_{n_1,\alpha_1}\sum_{n_2,\alpha_2} N_{n_1\alpha_1} U_{(n_1\alpha_1)(n_2\alpha_2)}\rho_{n_2\alpha_2} . \qquad \text{(A1)}$$

Equation (A1) regards the i^{th} particle as interacting with an average local potential U_{ij} produced by other j^{th} particles. For example, $U_{w(n\alpha)}$ represents the average interaction potential between a water molecule (i^{th} particle) and a mixed micelle composed of $n\alpha$ surfactant A molecules and $n(1-\alpha)$ surfactant B molecules (j^{th} particle). In the spirit of a mean-field type approximation, this potential is assumed to be proportional to the number density of the j^{th} particles ρ_j in the solution. The number densities are given by N_j/Ω, where Ω is the total volume of the solution. For dilute solutions, where mixing volume effects are negligible, the total volume of the solution can be modelled as, $\Omega = (N_w\Omega_w + N_A\Omega_A + N_B\Omega_B)$, where Ω_w, Ω_A, and Ω_B are the effective volumes of a water, surfactant A, and surfactant B molecule respectively, and are assumed to be constant. More importantly, we model the interactions contributing to U_{ij} as the sum of pairwise interactions between individual monomers in different mixed micelles, thus neglecting three- and higher-order n-body

interactions. That is,

$$U_{(n_1\alpha_1)(n_2\alpha_2)} = n_1 n_2 \{\alpha_1\alpha_2 U_{AA} + (1-\alpha_1)(1-\alpha_2)U_{BB} + [\alpha_1(1-\alpha_2) + (1-\alpha_1)\alpha_2]U_{AB}\}. \quad \textbf{(A2)}$$

Similarly,

$$U_{w(n\alpha)} = n\alpha U_{WA} + n(1-\alpha)U_{WB} . \quad \textbf{(A3)}$$

In Eqs. (A2) and (A3), U_{AA}, U_{AB}, and U_{BB} denote interaction potentials between two surfactant A molecules, between surfactant A and surfactant B molecules, and between two surfactant B molecules, respectively. Similarly, U_{WA}, U_{WB}, and U_{WW} denote interaction potentials between water and surfactant A, water and surfactant B, and two water molecules, respectively. Using Eqs. (A2) and (A3) in Eq. (A1) we obtain

$$G_i = \Omega \left[\frac{1}{2}U_{WW}\rho_w^2 + \frac{1}{2}U_{AA}\rho_A^2 + \frac{1}{2}U_{BB}\rho_B^2 + U_{WA}\rho_w\rho_A + U_{WB}\rho_W\rho_B + U_{AB}\rho_A\rho_B\right] . \quad \textbf{(A4)}$$

Eliminating $\rho_w = N_w/\Omega$ from Eq. (A4), using $\Omega_w N_w + \Omega_A N_A + \Omega_B N_B = \Omega$, we obtain

$$G_i = N_w\frac{U_{WW}}{2\Omega_W} + \gamma_A N_A\left(\frac{U_{WA}}{\Omega_A} - \frac{U_{WW}}{\Omega_W}\right) + \gamma_B N_B\left(\frac{U_{WB}}{\Omega_B} - \frac{U_{WW}}{\Omega_W}\right)$$
$$- \frac{1}{2}\left(C_{AW}\alpha_{soln} + C_{BW}(1-\alpha_{soln}) - \frac{\sqrt{\gamma_A\gamma_B}}{\gamma_{eff}}C_{AB}\alpha_{soln}(1-\alpha_{soln})\right)(N_A+N_B)(\phi_A+\phi_B), \quad \textbf{(A5)}$$

where, $\phi_A = \Omega_A N_A/\Omega$ and $\phi_B = \Omega_B N_B/\Omega$ are the volume fractions of surfactants A and B,

respectively, $\gamma_A = \Omega_A/\Omega_W$, $\gamma_B = \Omega_B/\Omega_w$, and $\gamma_{eff}=\alpha_{soln}\gamma_A+(1-\alpha_{soln})\gamma_B$. The mean-field interaction parameters C_{AW}, C_{BW}, and C_{AB} are related to the various interaction potentials by the following expressions

$$C_{AW} = \Omega_A\left[\frac{2U_{WA}}{\Omega_W\Omega_A} - \frac{U_{WW}}{\Omega_W^2} - \frac{U_{AA}}{\Omega_A^2}\right], \tag{A6}$$

$$C_{BW} = \Omega_B\left[\frac{2U_{WB}}{\Omega_W\Omega_B} - \frac{U_{WW}}{\Omega_W^2} - \frac{U_{BB}}{\Omega_B^2}\right], \tag{A7}$$

$$C_{AB} = \sqrt{\Omega_A\Omega_B}\left[\frac{2U_{AB}}{\Omega_A\Omega_B} - \frac{U_{AA}}{\Omega_A^2} - \frac{U_{BB}}{\Omega_B^2}\right]. \tag{A8}$$

From Eq. (A6), it is evident that C_{AW} reflects interactions between water molecules and surfactant A only. Similarly, Eq. (A7) indicates that C_{BW} reflects interactions between water molecules and surfactant B only. However, specific interactions between surfactants A and B (captured in U_{AB}), which are not present between two surfactant A molecules, (U_{AA}) or between two surfactant B molecules (U_{BB}), are captured by C_{AB} (see Eq. (A8)). Note, however, that, in general, the interaction potential U_{ij} is expected to be proportional to the product of the number of interaction sites on the two molecules i and j. Thus, if the two molecules interact through electrostatic forces, U_{ij} is proportional to the product of the number of charged sites on each molecule. Similarly, if the two molecules interact through

van der Waals forces, U_{ij} is proportional to the product of the volumes of the two molecules (Israelachvili, 1985). Therefore, if surfactants A and B are nonionic and they interact primarily through van der Waals forces, then $U_{AB}/\Omega_A\Omega_B$ may be approximated by $(U_{AA}/\Omega_A^2+U_{BB}/\Omega_B^2)/2$. In that case, Eq. (A8) indicates that $C_{AB} \approx 0$, suggesting that nonionic surfactants form ideal mixtures. However, if there are synergistic (attractive) interactions between surfactants A and B, $C_{AB} < 0$. Similarly, antagonistic (repulsive) interactions between the two surfactants leads to $C_{AB} > 0$. The magnitude of C_{AB} for various surfactant mixtures can be estimated using similar arguments. In anionic-anionic or cationic-cationic surfactant mixtures, the molecules interact primarily through electrostatic repulsions, and if the two surfactants have the same valency, then $U_{AB} \approx U_{AA} \approx U_{BB} > 0$. In that case, Eq. (A8) indicates that $C_{AB} \approx -U_{AA}(\Omega_A-\Omega_B)^2/(\Omega_A\Omega_B)^{3/2}$, which results in negative C_{AB} values. Since C_{AB} is proportional to $(\Omega_A-\Omega_B)^2$, ionic surfactants having very dissimilar sizes have larger values of C_{AB} than those having similar sizes. In nonionic-ionic mixtures, electrostatic repulsions between the ionic (species A) surfactants leads to very large and positive values of U_{AA}. However, interactions between ionic and nonionic surfactants (present in U_{AB}) or between two nonionic surfactants (present in U_{BB}) are much smaller. Thus nonionic-ionic mixtures will typically have $C_{AB} < 0$. In monovalent anionic-monovalent cationic mixtures, both U_{AA} and U_{BB} are large and positive due to electrostatic repulsions. However, attractive interactions between the oppositely charged surfactant A and B molecules leads to a large but negative value of U_{AB} whose absolute magnitude is of the same order as that of U_{AA} or U_{BB}. Thus, $C_{AB} << 0$, and its value is approximately four times that for nonionic-monovalent ionic surfactant mixtures. For both ionic-nonionic and anionic-cationic

mixtures, the presence of salts screens electrostatic interactions and hence the absolute magnitude of C_{AB} becomes smaller. In hydrocarbon-fluorocarbon mixtures, repulsions between the two surfactants leads to positive C_{AB} values. Table II summarizes expected typical values of C_{AB} for the various surfactant mixtures described above.

The free energy of interaction given in Eq. (A1) reflects interactions between all the components present in the solution. However, we are actually interested only in those interactions which are not already accounted for at the level of the free energy of formation G_f given in Eq. (1). In particular, the first three terms in Eq. (A5), which are proportional to N_W, N_A, and N_B, respectively, reflect interactions between water molecules, surfactant A and water molecules, and surfactant B and water molecules, respectively. Since the standard state chosen in our derivation is pure water, these three contributions have already been captured at the level of G_f. Accordingly, only the last term in Eq. (A5), which is proportional to $(N_A+N_B)\phi$, reflects the excess interactions which should appear in the free energy of interaction G_i. In other words,

$$G_i = -\frac{1}{2}C_{eff}(\alpha_{soln})(N_A+N_B)\phi, \tag{A9}$$

where

$$C_{eff}(\alpha_{soln}) = C_{AW}\alpha_{soln} + C_{BW}(1-\alpha_{soln}) - \frac{\sqrt{\gamma_A\gamma_B}}{\gamma_{eff}}C_{AB}\alpha_{soln}(1-\alpha_{soln}) \tag{A10}$$

reflects the magnitude of the effective mean-field interaction potential.

4.7 APPENDIX B: MOMENTS OF THE MICELLAR SIZE AND COMPOSITION DISTRIBUTION

The kth moment of the micellar size and composition distribution is defined by $M_k = \Sigma_{n\alpha} n^k X_{n\alpha}$. Using Eq. (12) for $X_{n\alpha}$, the kth moment can be expressed as

$$M_k = \sum_{n\alpha} \frac{1}{e} n^k X_1^n e^{-n\beta g_m} , \qquad \text{(B1)}$$

where X_1 is the mole fraction of free monomers in solution, and $g_m(\alpha,\alpha_1)$ is a modified free energy of micellization. Accordingly, M_k is a function of the micellar composition α and the monomer solution composition α_1. Using Eq. (B1), the total derivative of M_k with respect to X_1 is given by

$$\frac{dM_k}{dX_1} = \frac{M_{k+1}}{X_1} - \sum_{n\alpha} n^{k+1} X_{n\alpha} \left[\frac{\alpha-\alpha_1}{1-\alpha_1}\right] \frac{1}{X_1} . \qquad \text{(B2)}$$

As discussed in Sec. IIB, $X_{n\alpha}$ exhibits a sharp maximum at $\alpha=\alpha^*(n)$, and, therefore, to leading order in α, $\Sigma_\alpha X_{n\alpha}$ can be approximated by $X_{n\alpha^*}$. Thus, Eq. (B2) can be rewritten as

$$\frac{dM_k}{dX_1} \approx \frac{M_{k+1}}{X_1} - \sum_{n} n^{k+1} X_{n\alpha^*} \left[\frac{\alpha^*-\alpha_1}{1-\alpha_1}\right] \frac{1}{X_1} . \qquad \text{(B3)}$$

To perform the summation in Eq. (B3) one needs to know how α^* depends on the aggregation number n. Below, we consider two important different limiting cases: (i) monodisperse micelles in equilibrium with monomers, and (ii) polydisperse micelles which exhibit significant one-dimensional growth.

For micelles which do not exhibit growth, one can describe the solution as one containing monodisperse micelles, having an aggregation number m, in equilibrium with the monomers. In that case, the two material balance equations can be expressed as $X = X_1 + mX_{m\alpha^*}$ and $\alpha_{soln}X = \alpha_1 X_1 + m\alpha^* X_{m\alpha^*}$. A simultaneous solution of these equations yields $\alpha^* = (\alpha_{soln}X - \alpha_1 X_1)/(X - X_1)$. Substituting this value of α^* in Eq. (B3) we obtain (for the experimentally relevant range $X >> X_1$)

$$\frac{dM_k}{dX_1} \approx \frac{M_{k+1}}{X_1}\left[\frac{1-\alpha_{soln}}{1-\alpha_1}\right]. \qquad \textbf{(B4)}$$

For micelles which exhibit one-dimensional growth into large cylindrical micelles, the optimum composition α^* can be estimated by modelling the micelles as spherocylinders and linearly interpolating the optimum compositions α^*_{sph} and α^*_{cyl} associated with the corresponding sphere and infinite-sized cylinder, respectively. That is,

$$\alpha^*(n) = \alpha^*_{cyl} + \frac{n_{sph}}{n}(\alpha^*_{sph} - \alpha^*_{cyl}), \qquad \textbf{(B5)}$$

where n_{sph} is the aggregation number of the sphere. Substituting Eq. (B5) in Eq. (B3) we

obtain

$$\frac{dM_k}{dX_1} = \frac{M_{k+1}}{X_1}\left[\frac{1-\alpha^*_{cyl}}{1-\alpha_1}\right] - \frac{n_{sph}M_k}{X_1}\left[\frac{\alpha^*_{sph}-\alpha^*_{cyl}}{1-\alpha_1}\right]. \qquad \textbf{(B6)}$$

In surfactant solutions containing micelles having large average aggregation numbers, it has been shown that $M_{k+1} >> M_k$ (Blankschtein et al., 1986). Consequently, to a very good approximation, the second term in Eq. (B6) can be neglected. In addition, using the expression for $\alpha^*(n)$ given in

Eq. (B5) in the material balance equation for surfactant A, $\alpha_{soln}X = \Sigma_n n\alpha^* X_{n\alpha^*}$, we obtain

$$\alpha_{soln}X = \alpha_1 X_1 + \alpha_{cyl}(X-X_1) + n_{sph}(M_0-X_1)(\alpha_{sph}-\alpha_{cyl}). \qquad \textbf{(B7)}$$

Since $M_k << M_{k+1}$, it follows that $M_0 << X$. Therefore for $X >> X_1$, Eq. (B7) indicates that $\alpha_{cyl} \approx \alpha_{soln}$, and therefore Eq. (B6) reduces to Eq. (B4).

Thus, in both limiting cases, one where micelles remain small and monodisperse, and the other where micelles exhibit one-dimensional growth into large polydisperse cylindrical structures, one finds that

$$\frac{dM_k}{M_{k+1}} \approx \frac{dX_1}{X_1}\left[\frac{1-\alpha_{soln}}{1-\alpha_1}\right]. \qquad \textbf{(B8)}$$

CHAPTER 5

MOLECULAR MODEL OF MICELLIZATION FOR MIXED SURFACTANT SOLUTIONS

5.1 INTRODUCTION

Solutions containing mixtures of surfactants (mixed micellar solutions) are currently a subject of considerable practical importance because they can exhibit properties which are superior to those of solutions containing the constituent single surfactants (Scamehorn, 1986; Rosen, 1989). For example, it is well known that in aqueous solutions of binary surfactant mixtures synergistic (attractive) interactions between the two surfactant species result in critical micellar concentrations (CMC's) which can be substantially lower than those in solutions containing the constituent single surfactants. Moreover, in general, synergistic interactions between different surfactant species can be, and have been, exploited by the surfactant technologist in designing solutions of surfactant mixtures which display unique desirable properties. Accordingly, developing a fundamental understanding of the behavior of mixed micellar solutions, including a rationalization of the nature of synergistic interactions, constitutes a problem of great practical importance. Indeed, such an understanding can assist the surfactant technologist in the rational design and property

control of solutions containing surfactant mixtures. Specifically, in order to tailor solutions of surfactant mixtures to a particular application, the surfactant technologist has to be able to predict and manipulate (i) the tendency of surfactant mixtures to form mixed micelles and other self-assembling microstructures, (ii) the distribution of surfactant species between mixed micelles and monomers, (iii) the nature of the mixed micelles such as their shape, size, composition, and size and composition distribution, and (iv) the phase behavior and phase equilibria of mixed micellar solutions.

In spite of their considerable practical relevance, as well as the challenging theoretical issues associated with the description of these complex fluids, solutions of surfactant mixtures have not been studied sufficiently. In particular, previous theoretical studies of mixed micellar solutions have evolved along two very different, seemingly unrelated, fronts. On the one hand, significant efforts have been devoted to understand the mixture CMC (Lange, 1953; Shinoda, 1954; Clint, 1975; Rubingh, 1979; Holland and Rubingh, 1983; Nagarajan, 1985), as well as the micellar size and composition distribution (Ben-Shaul et al., 1987; Stecker and Benedek, 1984). On the other hand, very little effort has been devoted to understand the solution behavior at higher surfactant concentrations where intermicellar interactions become increasingly important and control the phase behavior and phase separation phenomena (Meroni et al., 1987). In view of this, it is quite clear that there is an immediate need to develop a theoretical description of mixed micellar solutions capable of *unifying* the previously disconnected treatments of micellization and phase behavior, including phase separation, into a *single coherent computational framework.*

To contribute to this much desired *theoretical unification*, in Chapter 4 we have formulated a molecular-thermodynamic theory of mixed micellar solutions capable of describing and predicting self-consistently a broad spectrum of micellar solution properties, ranging from the CMC and the micellar size and composition distribution to the phase behavior and phase separation of solutions containing mixtures of surfactants. The molecular-thermodynamic theory consists of blending a thermodynamic description of mixed micellar solutions, which captures the salient features of the micellar solution at the macroscopic level, with a molecular model of mixed micellization, which incorporates the essential driving forces for micellization. More specifically, the theoretical formulation incorporates the following salient features of the mixed micellar solution in the context of a Gibbs free energy model: (i) the free energy of mixed micellization g_{mic}, computed using the molecular model of micellization (see below and Sec. 5.3), (ii) a distribution of mixed micelles in chemical equilibrium with each other and with the free monomers in solution, (iii) the entropy of mixing mixed micelles, monomers, and water, and (iv) mean-field type interactions between the various solution components. By applying the methods of equilibrium thermodynamics to the Gibbs free energy model, it is possible to self-consistently predict micellar solution properties ranging from the CMC, through characteristic features of the micellar size and composition distribution, to the phase behavior and liquid-liquid phase separation phenomena. It is noteworthy that these property predictions span a concentration range of about 2-3 decades over a wide range of surfactant compositions and temperatures.

As stated above, a molecular model of micellization is utilized to evaluate the free energy of mixed micellization g_{mic}. In Chapter 4, we introduced a simple *analytical* phenomenological model for g_{mic}, which was utilized in conjunction with the thermodynamic theory to make *qualitative predictions* of micellar properties of aqueous solutions containing mixtures of nonionic-nonionic, nonionic-ionic, zwitterionic-ionic, and anionic-cationic surfactants, as well as hydrocarbon-fluorocarbon based surfactants. Although the predictions presented in Chapter 4 (Puvvada and Blankschtein, 1991b) were qualitative in nature, a major advantage of utilizing a simple model for g_{mic} is that it enabled us to obtain *analytical* expressions for many of the useful micellar solution properties, as well as to shed light on the physical basis of some of the observed experimental trends. As stated in Chapter 4, for more accurate *quantitative predictions* of micellar solution properties, a molecular model of mixed micellization, which takes into account the molecular structure of the surfactants present in the mixture as well as the effect of solution conditions, is needed. Accordingly, in the present chapter, we develop a molecular model of mixed micellization to evaluate g_{mic} as a function of the type of surfactants present in the mixture, micelle composition, and solution conditions such as temperature. Utilizing these more accurate computed values of g_{mic}, in the context of the thermodynamic theory developed in Chapter 4, the resulting molecular-thermodynamic framework is utilized to make *quantitative predictions* of micellar properties of aqueous solutions containing *binary mixtures of nonionic surfactants*.

The proposed molecular model of mixed micellization is inspired by the molecular model of micellization developed in Chapter 2 (Puvvada and Blankschtein, 1990a and 1990b) for solutions containing a single surfactant species, as well as by the molecular model

of mixed micellization introduced by Nagarajan (1985). In Nagarajan's model, many of the relevant contributions to g_{mic} were evaluated, using simple analytical expressions, as a function of the micellar composition. Subsequently, the computed values of g_{mic} were utilized in the context of ideal-solution expressions for the mixed micelle and monomer chemical potentials to predict the mixture CMC, as well as the micellar size and composition distribution of solutions containing various binary surfactant mixtures. This approach was able to successfully describe the observed nonidealities in the mixed micellar solution CMC without the use of any empirical interaction parameters. However, an empirical correction factor, obtained by fitting to pure surfactant CMC data, was utilized to account for contributions associated with hydrocarbon-chain packing in the micellar core. The same correction factor was used regardless of the shape, core minor radius, and composition of the mixed micelle, although it has been shown (Szleifer et al., 1987; Puvvada and Blankschtein, 1990a) that these variables can affect the value of the packing free-energy contribution. In addition, it is important to emphasize that the approach developed by Nagarajan (1985) was aimed primarily at describing individual mixed micellar properties in the vicinity of the CMC. Consequently, the micellar solution was modelled as being ideal, that is, intermicellar interactions were neglected. Therefore, this approach cannot be used to predict the phase behavior and phase separation of mixed micellar solutions at higher surfactant concentrations, where intermicellar interactions play a dominant role.

The molecular model of micellization for single-surfactant solutions, which was introduced in Chapter 2, utilizes molecular information, which is readily available or can be estimated using simple scaling-type arguments, about surfactant molecules and water. The

molecular information includes the chemical nature and size of the surfactant hydrophilic and hydrophobic moieties, values of interfacial tensions between hydrocarbon and water, and values of transfer free energies of hydrocarbons from water to bulk hydrocarbon. A numerically calculated value of the free-energy contribution associated with hydrocarbon-chain packing in the micellar core is also needed. In Chapter 2, the molecular model was used in conjunction with the thermodynamic theory of single-surfactant micellar solutions to predict quite accurately a rich variety of micellar properties of aqueous solutions of single nonionic surfactants, belonging to the alkyl polyethylene oxide (C_iE_j) and glucoside families, as a function of surfactant molecular architecture, surfactant concentration, temperature, and the addition of solution modifiers such as urea. The predicted properties include (i) the CMC, (ii) the micellar shape, (iii) the micellar size distribution and its characteristics, (iv) the liquid-liquid phase separation coexistence curve, including the critical surfactant concentration, and (v) other thermodynamic properties such as the osmotic pressure and the osmotic compressibility.

The molecular model of mixed micellization presented in this chapter extends previous work (Nagarajan, 1985) by including a number of important new elements which we summarize below (see also Chapter 2):

(1) A detailed thought process to *visualize* micellization as a series of reversible steps, each associated with a well-defined physico-chemical factor (see Fig. 5.1). This convenient scheme permits a calculation of the free energy of mixed micellization through a clear identification of the basic underlying assumptions, as well as an unambiguous account of the free-energy contributions associated with each step of the thought process.

(2) A systematic quantitative account of the effect of curvature on the interfacial component of the free energy of micellization.

(3) A numerically computed packing free-energy contribution as a function of micellar shape sh, core minor radius l_c, and composition α. As stated above, in previous quantitative studies of micellization this contribution was either ignored or assumed to be independent of sh, l_c, and α, and parametrized empirically by fitting it to experimentally measured CMC values.

(4) An evaluation of the *optimum* micellar-core minor radius l_c^*, and the optimum micellar composition α^* for a given micellar shape sh.

(5) Identification of the *optimum* micellar shape sh^* which can vary with solution conditions. Specifically, given a surfactant mixture and its composition, as well as a set of solution conditions, this enables us to predict whether the mixed micelles that form exhibit two-dimensional, one-dimensional, or no growth under these conditions.

When blended with the thermodynamic theory of mixed micellar solutions developed in Chapter 4, the proposed molecular model of mixed micellization is utilized to predict micellar properties of aqueous solutions of three binary mixtures of C_iE_j nonionic surfactants: $C_{12}E_6$-$C_{12}E_8$, $C_{12}E_6$-$C_{10}E_6$, and $C_{12}E_6$-$C_{10}E_4$. We have chosen these mixtures because they offer a number of convenient experimental features which are described in Sec. 5.5. The predicted properties include (i) the mixture CMC as a function of surfactant composition, (ii) the evolution of micellar shape and size with surfactant composition and temperature, and (iii) the liquid-liquid phase separation coexistence curve as a function of

surfactant composition. The theoretical predictions compare very favorably with the experimentally measured properties.

The remainder of the chapter is organized as follows. In Sec. 5.2 we briefly review the thermodynamic theory presented in Chapter 4, and discuss the computational procedures to evaluate the mixed micellar solution CMC signalling the onset of micellization, the weight-average mixed micelle aggregation number, and the coexistence curve delineating the boundary between the one- and two-phase regions of the phase diagram. In Sec. 5.3 we present the molecular model of mixed micellization for aqueous solutions of binary surfactant mixtures. In Sec. 5.4 we discuss the computational procedure to evaluate g_{mic} for non-regular micellar shapes. In Sec. 5.5 we present a description of the surfactant mixtures utilized in our studies, as well as the experimental methods used to measure the CMC, the micellar size, and the coexistence curve. In Sec. 5.6 we compare the theoretical predictions with the experimental data. Finally, in Sec. 5.7 we present some concluding remarks.

5.2. REVIEW OF THERMODYNAMIC THEORY

In Chapter 4 we developed a thermodynamic theory to describe micellization, phase behavior and phase separation of binary mixed micellar solutions. For completeness, below we briefly review some elements of the theoretical framework which are particularly relevant to the present chapter. Consider a solution of N_A surfactant A molecules, N_B surfactant B molecules, and N_w water molecules in thermodynamic equilibrium at temperature T and pressure P. If the surfactant concentration exceeds the mixed micellar solution CMC, the

surfactant molecules will self-assemble to form a distribution of mixed micelles $\{N_{n\alpha}\}$, where $N_{n\alpha}$ is the number of mixed micelles having aggregation number n and composition α. Note that in such a mixed micelle there are $n\alpha$ surfactant A molecules and $n(1-\alpha)$ surfactant B molecules, such that $N_A = \Sigma_{n\alpha} n\alpha N_{n\alpha}$, and $N_B = \Sigma_{n\alpha} n(1-\alpha) N_{n\alpha}$. The total Gibbs free energy of the mixed micellar solution G is given by

$$G = N_w\mu_w^o + N_A\mu_A^o + N_B\mu_B^o + \sum_{n,\alpha} nN_{n\alpha}g_{mic}(sh,n,\alpha,l_c) + kT\left[N_w lnX_w + \sum_{n,\alpha} N_{n\alpha}\ln X_{n\alpha}\right] \quad (5.1)$$
$$- \frac{1}{2}C_{eff}(\alpha_{soln})(N_A+N_B)\phi \ ,$$

where μ_i^o (i=W,A,B) are the standard-state chemical potentials, $X_w = N_w/(N_w+N_A+N_B)$, $X_{n\alpha} = N_{n\alpha}/(N_w+N_A+N_B)$, k is the Boltzmann constant, g_{mic} is the free energy of mixed micellization, $\alpha_{soln} = N_A/(N_A+N_B)$ is the composition of the surfactant mixture, $\phi = \phi_A + \phi_B$ is the sum of the volume fractions, ϕ_A and ϕ_B, of surfactants A and B, respectively, and C_{eff} is an effective mean-field interaction parameter for the mixture which is given by

$$C_{eff} = C_{AW}\alpha_{soln} + C_{BW}(1-\alpha_{soln}) - C_{AB}\alpha_{soln}(1-\alpha_{soln})\sqrt{\gamma_A\gamma_B}/\gamma_{eff} \ , \quad (5.2)$$

where C_{AW} and C_{BW} reflect the magnitudes of the interaction potentials in aqueous solutions of single surfactants A and B, respectively, and C_{AB} reflects the magnitude of the specific interaction potential between surfactants A and B. In Eq. (5.2), γ_A (γ_B) is the ratio of the molecular volumes of surfactant A (B) and a water molecule, and $\gamma_{eff} = \alpha_{soln}\gamma_A + (1-\alpha_{soln})\gamma_B$.

All thermodynamic properties of the micellar solution are governed by the proposed Gibbs free energy model through the chemical potential of water μ_w, and the chemical potential of a mixed micelle, having aggregation number n and composition α, $\mu_{n\alpha}$, which are obtained from Eq. (5.1) by simple differentiation, that is, $\mu_w = (\partial G/\partial N_w)_{T,P,N_{n\alpha}}$ and $\mu_{n\alpha} = (\partial G/\partial N_{n\alpha})_{T,P,N_w,N_{n'\alpha'}}$. Note that the chemical potentials of a surfactant A monomer μ_A and of a surfactant B monomer μ_B are obtained by setting n=1, and α=1 (for A) or 0 (for B), respectively, in the expression for $\mu_{n\alpha}$.

When the mixed micellar solution is in thermodynamic equilibrium, the chemical potential $\mu_{n\alpha}$ is related to the chemical potentials μ_A and μ_B by the condition of chemical equilibrium, that is, $\mu_{n\alpha}=n\alpha\mu_A+n(1-\alpha)\mu_B$. Using the expressions for $\mu_{n\alpha}$, μ_A, and μ_B obtained from Eq. (5.1) in this condition, the following expression for the micellar size and composition distribution $\{X_{n\alpha}\}$ is obtained

$$X_{n\alpha} = \frac{1}{e} X_1^{\,n} e^{-n\beta g_m(n,\alpha,\alpha_1)} , \tag{5.3}$$

where $\beta=1/kT$, $X_1=X_{1A}+X_{1B}$ is the total mole fraction of free monomers in the solution, and g_m is a modified free energy of micellization per monomer which is related to the conventional free energy of micellization per monomer g_{mic} by

$$\beta g_m(n,\alpha,\alpha_1) = \beta g_{mic}(n,\alpha) - 1 - \alpha\ln\alpha_1 - (1-\alpha)\ln(1-\alpha_1) , \tag{5.4}$$

where $\alpha_1 = X_{1A}/X$ is the composition of free monomers in the solution. Given g_m (or equivalently g_{mic}, see Eq. (5.4)), the two unknowns X_1 and α_1 in Eq. (5.3) can be evaluated by substituting $X_{n\alpha}$ in the material balance equations for surfactants A and B, $X_A = \alpha_{soln} X = \alpha_1 X_1 + \Sigma_{n,\alpha} n\alpha X_{n\alpha}$, and $X_B = (1-\alpha_{soln})X = (1-\alpha_1)X_1 + \Sigma_{n,\alpha} n(1-\alpha) X_{n\alpha}$, respectively. Solving these two equations yields $X_1(X,\alpha_{soln},T,P)$ and $\alpha_1(X,\alpha_{soln},T,P)$, which can then be inserted back into Eq. (5.3) to calculate the entire micellar size and composition distribution $\{X_{n\alpha}\}$ as a function of X, α_{soln}, T, P, and other solution conditions not explicitly included above.

Once $\{X_{n\alpha}(X,\alpha_{soln},T,P)\}$ is known, in the context of the Gibbs free-energy formulation, all equilibrium properties of the mixed micellar solution can be evaluated. These properties include the CMC, characteristic features of the distribution such as the weight-average mixed micelle aggregation number, and the phase behavior including phase separation.

In the micellar literature, the CMC has been defined using a variety of theoretical criteria (Tanford, 1974; Ruckenstein and Nagarajan, 1975; Hamann, 1978; Warr and White, 1985; Everett, 1986, Moroi, 1991) which yield slightly different CMC values. Two extensively used criteria include (i) identifying the CMC as that surfactant concentration where a plot of the total monomer concentration X_1 versus the total surfactant concentration X exhibits a break, and (ii) identifying the CMC as that surfactant concentration where monomers constitute 95% of the total surfactant, that is, where $X_1/X=0.95$. For single-surfactant solutions, we have found that these two criteria yield very similar CMC values. In the case of solutions of mixed surfactants, we have found that although criteria (i) and

(ii) yield similar results, the first criterion is computationally more intensive. Consequently, for computational simplicity, in this chapter we utilize criterion (ii) to calculate the CMC of the mixed micellar solution as a function of surfactant composition α_{soln}.

We have also evaluated the weight-average mixed micelle aggregation number $<n>_w$ as a function of α_{soln}, X, and T using the following relation

$$\langle n \rangle_w = \frac{\sum_{n\alpha} n^2 X_{n\alpha}}{\sum_{n\alpha} n X_{n\alpha}} . \qquad (5.5)$$

An interesting feature of mixed micellar solutions is that, at concentrations which exceed the CMC, they can exhibit liquid-liquid phase separation into micellar-rich and micellar-poor phases upon changes in solution conditions such as temperature and surfactant composition. We have shown in Chapter 4 that, depending on the nature of the surfactant mixture, the compositions of the two coexisting micellar phases can be markedly different. For example, when aqueous solutions of nonionic-monovalent ionic surfactant mixtures phase separate, we find that the added ionic surfactant partitions preferentially into the dilute micellar-poor phase in order to minimize electrostatic repulsions. In general, the entire coexistence surface can be calculated by imposing the conditions of phase equilibria which require that the temperature T, the pressure P, and the chemical potentials μ_w, μ_A and μ_B be the same in the two coexisting micellar phases, that is,

$$\mu_w(T,P,Y,\alpha_Y) = \mu_w(T,P,Z,\alpha_Z), \tag{5.6a}$$

$$\mu_A(T,P,Y,\alpha_Y) = \mu_A(T,P,Z,\alpha_Z), \tag{5.6b}$$

$$\mu_B(T,P,Y,\alpha_Y) = \mu_B(T,P,Z,\alpha_Z), \tag{5.6c}$$

where Y and Z are the total surfactant mole fractions of the two coexisting micellar phases, and α_Y and α_Z their respective compositions. Note that since $\mu_{n\alpha}=n\alpha\mu_A+n(1-\alpha)\mu_B$, Eqs. (5.6b) and (5.6c) imply that $\mu_{n\alpha}(T,P,Y,\alpha_Y)=\mu_{n\alpha}(T,P,Z,\alpha_Z)$ for all n and α. Note also that the Gibbs phase rule (Prigogine and Defay, 1954) indicates that in a two-phase ternary solution, consisting of water, surfactant A and surfactant B, in thermodynamic equilibrium one can vary independently three intensive variables. Therefore, in our calculations, we have evaluated Y, Z, and α_Y, using Eqs. (5.6a)-(5.6c), for various values of T and α_Z at a fixed pressure of 1 atm.

5.3. MOLECULAR MODEL OF MIXED MICELLIZATION

As discussed in Sec. 5.2, the free energy of mixed micellization g_{mic} constitutes a central element in the evaluation of micellar solution properties such as the CMC, the micellar size and composition distribution, and the phase behavior including phase separation of mixed micellar solutions. We have also shown in Chapter 4 that g_{mic} captures,

at the micellar level, specific interactions between different surfactant species. Consequently, g_{mic} determines the observed nonidealities in the CMC, as well as in the distribution of the various surfactant species between monomers and mixed micelles, in solutions containing surfactant mixtures. The free energy of mixed micellization $g_{mic}(sh,n,\alpha,l_c)$ represents the free-energy change (per monomer) associated with creating a micelle, having shape sh, aggregation number n, composition α, and core minor radius l_c, from $n\alpha$ A-type and $n(1-\alpha)$ B-type surfactant monomers. The magnitude of g_{mic} reflects many complex physico-chemical factors such as the hydrophobic effect, interfacial effects, conformational free-energy changes associated with restricting the hydrophobic chains inside the micellar core, steric and electrostatic interactions between the hydrophilic moieties at the micellar core-water interface, and entropy effects associated with mixing the two surfactant species in a mixed micelle.

To evaluate the free-energy contributions associated with the various physico-chemical factors mentioned above, we have developed a thought process to *visualize* the reversible formation of a mixed micelle having shape sh, aggregation number n, composition α, and core minor radius l_c (final state) from $n\alpha$ surfactant A monomers and $n(1-\alpha)$ surfactant B monomers (initial state) in water, as shown in Fig. 5.1. Since the numerical magnitude of the free-energy change associated with a reversible process should be independent of the path connecting the initial and final states, we have chosen a series of convenient intermediate states to calculate g_{mic}. Each individual step, connecting these intermediate states, contributes to g_{mic} a free-energy change that can be evaluated using a simple statistical-thermodynamic approach, and/or available experimental data. Below, we

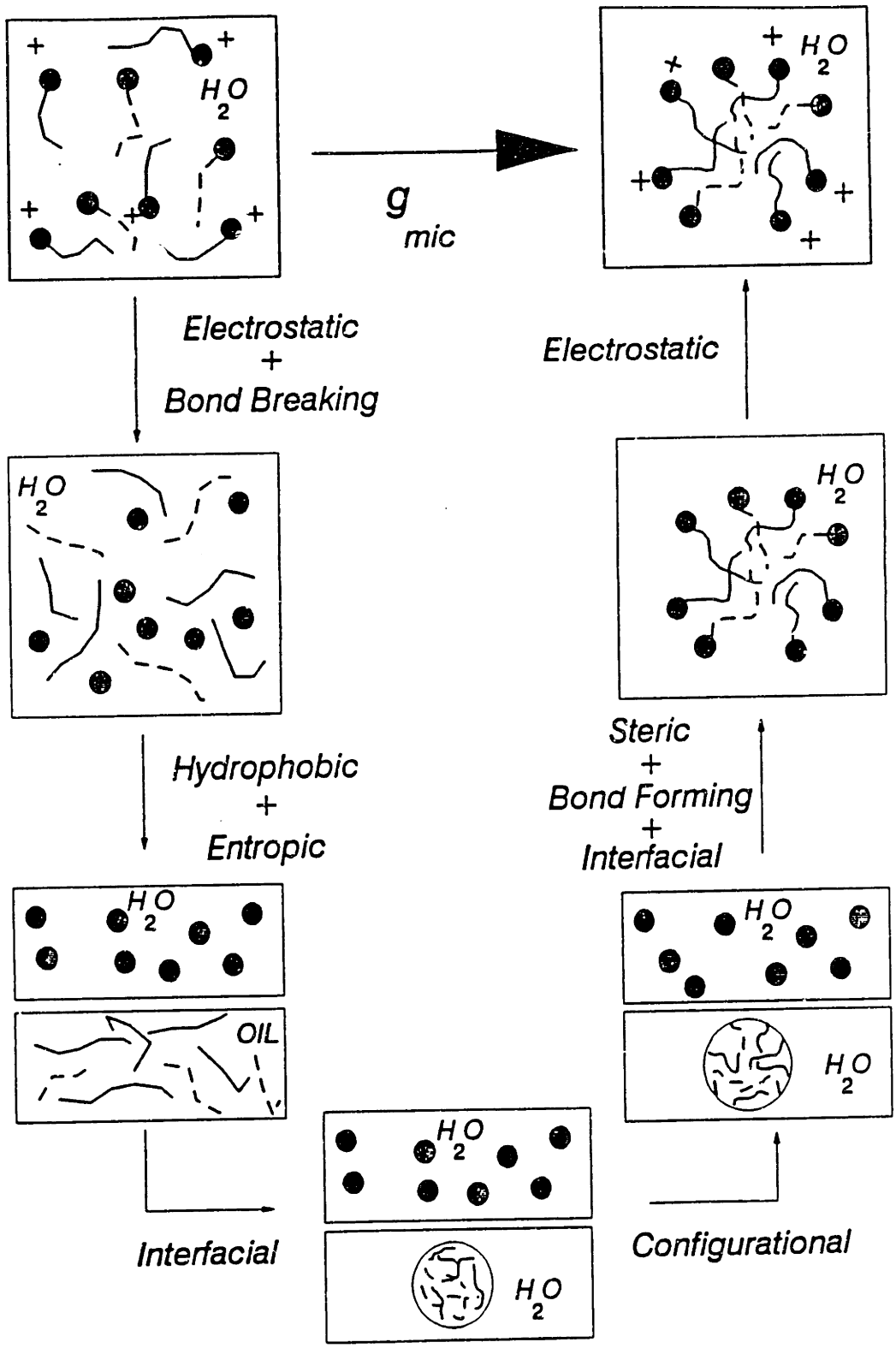

Figure 5.1 Schematic representation of thought process to *visualize* the various physico-chemical factors involved in the formation of a mixed micelle. Surfactant A is represented by a black head and a full tail, and surfactant B by a grey head and a dashed tail.

describe (see also Chapter 2) the various steps of the thought process needed to estimate g_{mic} for a mixed micelle characterized by a shape sh, aggregation number n, micellar composition α, and micellar-core minor radius l_c. As described in Chapter 2, the CH_2 group adjacent to the hydrophilic moiety lies within the hydration shell of this moiety, and therefore does not possess any hydrophobic properties. Accordingly, in the remainder of this chapter, we denote by *head*, the hydrophilic moiety and the CH_2 group adjacent to it, and by *tail*, the rest of the surfactant molecule comprising (n_c-2) CH_2 groups and a terminal CH_3 group, that is, a total of (n_c-1) carbon atoms.

In the first step of the thought process, the heads, if charged, are discharged along with the counterions. Subsequently, in the second step, the bond between the head and the tail of each surfactant molecule is broken. In the third step, the hydrocarbon tails of surfactants A and B are transferred from water to a mixture of hydrocarbons A and B whose composition is equal to the micellar composition α. In the fourth step, an hydrocarbon droplet having shape sh and core minor radius l_c is created from the hydrocarbon mixture having composition α. That is, in this step, an interface separating the hydrocarbon mixture from water is created. Note that within this hydrocarbon droplet the tails are unrestricted and can move freely. However, in a micelle, each tail is bonded to a head and therefore one of the tail ends is restricted to lie in the vicinity of the micellar core-water interface. Accordingly, in the fifth step, this restriction is imposed on the tails. Therefore, at the end of the fifth step, the creation of the micellar core has been completed. The creation of the micellar corona of heads follows next. Accordingly, in the sixth step, the discharged heads are reattached to the tails at the micellar core-water interface. This

involves three operations: recreating the bond between the head and the tail, screening part of the micellar core-water interface from contact with water, and introducing steric repulsions between the heads. Note that the free-energy change associated with reforming the bond is assumed to be equal and opposite in sign to that associated with breaking the bond in the second step, and consequently these two contributions cancel each other. Finally, in the seventh step, the heads, if charged, are recharged along with the associated counterions. This completes the creation of the micellar corona, and hence of the entire mixed micelle.

The resulting free-energy contributions can be related to the various physico-chemical factors associated with micellization. These include (i) the hydrophobic free energy $g_{w/hc}$ associated with transferring the hydrocarbon tails from water to an hydrocarbon mixture in the third step, (ii) the interfacial free energy g_σ associated with creating the micellar core-water interface in the fourth step, as well as with shielding part of that interface in the sixth step, (iii) the configurational (packing) free energy $g_{hc/mic}$ arising from the loss in configurational degrees of freedom in the fifth step, (iv) the steric free energy g_{st} associated with repulsive steric interactions between the heads in the sixth step, and (v) the electrostatic free energy g_{elec} associated with the first and the seventh steps. The total free energy of mixed micellization $g_{mic}(sh,n,\alpha,l_c)$ is then computed by summing these five free-energy contributions, that is,

$$g_{mic}(sh,n,\alpha,l_c) = g_{w/hc} + g_\sigma + g_{hc/mic} + g_{st} + g_{elec} \ . \qquad (5.7)$$

Using Eq. (5.7) and the various contributions to g_{mic}, described in more detail below, the free energy of mixed micellization can be calculated for the three regular micellar shapes of spheres, infinite-sized cylinders, and infinite-sized discs or bilayers (note that the use of a mean-field approximation implies that $g_{hc/mic}$ can only be computed rigorously for these three regular shapes, for details see the discussions in Secs. 5.3.3 and 5.4). In addition, in Sec. 5.4 we present a computational scheme to estimate g_{mic} for the case of non-regular micellar shapes. Note that the various contributions to g_{mic} are evaluated for a particular micellar shape sh, micellar-core minor radius l_c, and micellar composition α. The resulting optimum values sh^*, l_c^*, and α^* are then determined by a minimization procedure which is described in Sec. 5.4.

Below, we discuss in more detail the five free-energy contributions in Eq. (5.7).

5.3.1 Hydrophobic Free Energy

The hydrophobic free energy $g_{w/hc}$ reflects the contribution of the hydrophobic effect (Tanford, 1980), associated with interactions between the nonpolar hydrocarbon tails and water, to g_{mic}. More specifically, $g_{w/hc}$ represents the free-energy change associated with transferring the hydrocarbon tails of surfactants A and B from water to a mixture of hydrocarbons A and B whose composition is equal to the micellar composition α. As such, $g_{w/hc}$ constitutes the largest attractive contribution to g_{mic} and is the main driving force for micellization. We have estimated $g_{w/hc}$ using available solubility data (Abraham, 1984; Abraham and Matteoli, 1988) of pure hydrocarbons in water, and an ideal expression for

the entropy of mixing the hydrocarbon tails of surfactants A and B in the hydrocarbon mixture. Since the mixing process involves two hydrocarbon species, nonidealities associated with specific interactions between hydrocarbon A and hydrocarbon B tails are not expected to be significant. Accordingly,

$$g_{w/hc}(\alpha) = \alpha g_{w/hc}^{A} + (1-\alpha) g_{w/hc}^{B} + kT[\alpha \ln\alpha + (1-\alpha)\ln(1-\alpha)], \tag{5.8}$$

where

$$g_{w/hc}^{A} = \left[(4.09 - 1.05 n_{cA})\frac{298}{T} - (4.62 + 0.44 n_{cA})\right] kT, \tag{5.9a}$$

and

$$g_{w/hc}^{B} = \left[(4.09 - 1.05 n_{cB})\frac{298}{T} - (4.62 + 0.44 n_{cB})\right] kT, \tag{5.9b}$$

are the temperature-dependent hydrophobic free-energy contributions of pure hydrocarbons A and B, consisting of n_{cA} and n_{cB} carbon atoms, respectively. The last term in Eq. (5.8), $kT[\alpha\ln\alpha + (1-\alpha)\ln(1-\alpha)]$, reflects the entropic contribution associated with mixing the two types of hydrocarbons, and captures the increase in the number of available configurations resulting from mixing the two species in the hydrocarbon mixture. In this chapter, we have modelled this entropic contribution using an ideal mixing-entropy expression. This will be most appropriate when the two hydrocarbon tails are of a similar size. However, as the

dissimilarity in size increases, it may prove useful to investigate other entropy models which account better for the size difference, such as, the Flory-Huggins model (Flory, 1986).

5.3.2 Interfacial Free Energy

The interfacial free energy g_σ reflects the contribution to g_{mic} associated with creating a micellar core-water interface. It is a repulsive contribution and therefore opposes micelle formation. We have estimated g_σ using the concept of a macroscopic interfacial free energy of an hydrocarbon-water interface, including its dependence on interfacial curvature. The free-energy change (per monomer) can be approximated as

$$g_\sigma = \alpha\sigma_A(a-a_{oA}) + (1-\alpha)\sigma_B(a-a_{oB}), \qquad (5.10)$$

where σ_A and σ_B are the curvature-dependent interfacial tensions between water and hydrocarbons A and B, respectively, a_{oA} and a_{oB} are the corresponding interfacial areas per surfactant molecule screened by the heads (approximately equal to 21Å^2 each for single-tail surfactants), and $a = Sv/l_c$ is the available interfacial area per surfactant molecule, where S is a shape factor (3 for spheres, 2 for cylinders, and 1 for discs or bilayers), $v = \alpha v_A + (1-\alpha)v_B$ is an average tail volume, where $v_A = 27.4 + 26.9(n_{cA}-1)$ (in Å^3) is the volume of tail A, and $v_B = 27.4 + 26.9(n_{cB}-1)$ is the volume of tail B, and l_c is the micellar-core minor radius. Note that in Eq. (5.10) a simple linear average, weighed by the micellar composition α, relates g_σ to the interfacial free energies per monomer $\sigma_A(a-a_{oA})$ and $\sigma_B(a-a_{oB})$.

Since micelles are small objects (typically the minor radius of the micellar core l_c is 10-20Å) it is necessary to incorporate the curvature dependence of σ_A and σ_B. We approximate this dependence, as in the molecular model for single-surfactant solutions presented in Chapter 2, by the Tolman equation (Tolman, 1949), that is, we take

$$\sigma_A = \sigma_{oA}[1 - (S-1)\delta_A/l_c], \tag{5.11a}$$

and

$$\sigma_B = \sigma_{oB}[1 - (S-1)\delta_B/l_c], \tag{5.11b}$$

where σ_{oA} and σ_{oB} are the interfacial tensions at a planar interface between water and hydrocarbons A and B, respectively, and δ_A and δ_B are the Tolman distances corresponding to hydrocarbons A and B, respectively. In Chapter 2, δ was taken to scale as the fully-extended length l_{max} of the tail, and to obtain best agreement with experimental results a value of $\delta = 2.25$Å was chosen for a C_{11} tail (or $n_c = 12$). The Tolman distance δ for other C_n tails was then estimated using the simple scaling-type assumption $\delta(n) = \delta(11)\, l_{max}(n)/l_{max}(11)$, where $l_{max}(n) = 1.54 + 1.265n$ (in Å). In this chapter, we implement this approach to estimate the values of δ_A and δ_B.

5.3.3 Packing Free Energy

In a mixed micelle, the nonpolar hydrocarbon tails are bonded to the heads, and therefore the tail ends which are attached to the heads are restricted to lie in the vicinity of the micellar core-water interface. This results in a loss of conformational degrees of freedom, and the associated free-energy change $g_{hc/mic}$ is evaluated using a single-chain mean-field model, originally developed for single-surfactant chains (Ben-Shaul et al., 1985; Szleifer et al., 1985) and subsequently generalized to mixed-surfactant chains (Szleifer et al., 1987). Note, however, that the earlier treatments were concerned primarily with calculating the bond-order parameter of the tails, and not with predicting thermodynamic properties, such as, the packing free-energy contribution, which is our main goal here.

To evaluate the free-energy contribution associated with restricting one end of the tail at the micellar core-water interface, all possible conformations of the various chains inside the micellar core need to be generated. Due to the large number of available conformations, this problem constitutes a formidable computational challenge. However, the problem is considerably simplified in the mean-field single-chain approach, where only the conformations of a single central chain are generated. The effect of the neighboring chains on the central chain is modelled as a mean-field which can be self-consistently evaluated from the partition function of the central chain. The resulting field is typically a function of the distance from the micellar interface, and at each point it can be visualized as a lateral pressure which tends to squeeze out the central chain from that point. That is, the larger the value of the field, the more stretched is the central chain. This mean-field

assumption implicitly assumes that the micellar interior is isotropic, and that the interface has a uniform curvature. Such a condition is only satisfied by the three regular shapes of spheres, infinite-sized cylinders, and infinite-sized discs or bilayers. Therefore, we have only evaluated the conformational (packing) free-energy contribution for these three regular shapes. To describe the non-regular shapes, in Sec. 5.4 we introduce a simple interpolation scheme to compute g_{mic}. In addition, in the case of mixed micelles containing surfactants A and B, the mean-field description implies that the two types of surfactant tails should mix homogeneously in the micellar core. The central elements of the packing computational procedure are described below.

For computational purposes, the entire micellar core is divided into L imaginary layers, having equal widths, each parallel to the micellar interface. Note that the magnitude of the mean-field F_i can vary from layer to layer, but is assumed to be constant within each layer. The probability P_A of chains A being in conformation $\boldsymbol{a}$ is related to the energy $E_A(\boldsymbol{a})$ associated with conformation $\boldsymbol{a}$, the number of CH_2 groups in each layer corresponding to conformation $\boldsymbol{a}$, $n_{iA}(\boldsymbol{a})$, and the mean-field F_i in each layer, and is given by

$$P_A(\boldsymbol{a}) = \frac{1}{Z_A} \exp\left[-\beta E_A(\boldsymbol{a}) - \beta \sum_{i=1}^{L} F_i n_{iA}(\boldsymbol{a})\right], \qquad (5.12)$$

where $Z_A = \Sigma_{\boldsymbol{a}} P_A(\boldsymbol{a})$ is the partition function associated with a single chain of type A. The configurational free energy of chain A is then calculated using

$$A_A = \sum_a P_A(a)E_A(a) + kT\sum_a P_A(a)\,lnP_A(a). \qquad (5.13)$$

Using a similar procedure, analogous expressions can be derived for P_B and A_B. The configurational free energy A of the mixed micelle is related to the single-chain configurational free energies A_A and A_B through

$$A = \alpha A_A + (1-\alpha)A_B \ . \qquad (5.14)$$

Using the expressions for P_A and P_B, it is possible to evaluate the average number of CH_2 groups in each layer i, $\overline{n_i}$, as follows

$$\overline{n_i} = \alpha\sum_a P_A n_{iA}(a) + (1-\alpha)\sum_b P_B n_{iB}(b) \ , \qquad i=1,2,..,L. \qquad (5.15)$$

If one assumes (see Chapter 2) that the density of CH_2 groups inside the micellar core is uniform and equal to that in bulk hydrocarbon ρ_{hc}, the L relations in Eq. (5.15) can be utilized to compute the L unknown mean-field values F_i. Note that the average number of CH_2 groups in layer i, $\overline{n_i}$, is related to the volume of the layer V_i, and to ρ_{hc} through $\overline{n_i} = \rho_{hc}V_i$. Combining Eqs. (5.12)-(5.15), one obtains

$$-\frac{A}{kT} = \alpha lnZ_A + (1-\alpha)lnZ_B + \rho_{hc}\sum_{i=1}^{L} F_i V_i \ . \qquad (5.16)$$

As explained earlier, the packing or configurational free energy is the free-energy difference between the micellar state, characterized by one end of the tail being restricted to lie in the vicinity of the micellar core-water interface, and the droplet state, characterized by unrestricted freely-moving tails. In the unrestricted-droplet state, the partition function of a free chain of type A, Z_A^{free}, is related to the free energy of that chain A_A^{free} by

$$A_A^{free} = -kT\ln Z_A^{free} , \tag{5.17}$$

where all generated conformations are used in computing $Z_A^{free} = \sum_a e^{-\beta E_A(a)}$. Recall that in the micellar state some of the generated conformations (those that involve chains which lie partially or totally outside the micellar core) are excluded. A similar expression for the free energy of a free chain of type B in the unrestricted droplet state can also be derived. The resulting free energy (per monomer) of an unrestricted free chain in the droplet state having composition α is given by $A^{free} = \alpha A_A^{free} + (1-\alpha)A_B^{free}$. Subtracting this expression for A^{free} from A, given in Eq. (5.16), yields the following expression for $g_{hc/mic}$

$$-\frac{g_{hc/mic}}{kT} = \alpha\ln(Z_A/Z_A^{free}) + (1-\alpha)\ln(Z_B/Z_B^{free}) + \rho_{hc}\sum_{i=1}^{L} F_i V_i . \tag{5.18}$$

The conformations of the central chain are generated in the context of the rotational isomeric state approximation (Flory, 1969). Each conformation is specified by the bond sequence (the number of gauche and trans bonds and their positions), the overall rotational orientation of the chain, and the distance of the first CH_2 group in the tail (the one attached

to the head) from the interface. For each bond sequence that is generated, the first CH_2 group in the tail is placed randomly over three different positions in a layer 1.53Å (the length of a C-C bond) from the interface, and then the entire chain is rotated randomly over 12 different orientations. For each one of these conformations, we determine the positions of the CH_2 groups and the terminal CH_3 group, and then exclude all conformations in which some of the groups are exposed to water outside the micellar core. The energy of each conformation is then evaluated from the number of gauche-trans bonds present, and the excess energy of a gauche bond over that of a trans bond (approximately 1 kT). Once all conformations and their corresponding energies have been generated for the two chains, the free energy $g_{hc/mic}$ is evaluated using Eqs. (5.12)-(5.18) as described above.

To illustrate some aspects of the packing calculations, in Fig. 5.2 we present predictions of the variation of the field strength F_i as a function of the distance from the micellar interface for a mixture of C_7-C_{11} chains contained within the core of a cylindrical mixed micelle having a core minor radius $l_c = 15.4$Å (corresponding to the length of a fully extended C_{11} chain). The predictions are made for various micellar compositions α, where α is defined as the fraction of C_7 chains in the mixture. An examination of Fig. 5.2 reveals that, close to the micellar interface, the field-strength values are large (~3.6 kT) for a pure C_{11} chain (curve a). However, upon addition of small amounts of the shorter C_7 chains (curves b and c having α values of 0.1 and 0.3, respectively), the field-strength values decrease dramatically to a value close to zero. As the fraction of C_7 chains is further increased to higher values (curves d and e having α values of 0.5 and 0.7, respectively), the F_i values increase once again. In other words, the chains are considerably stretched with

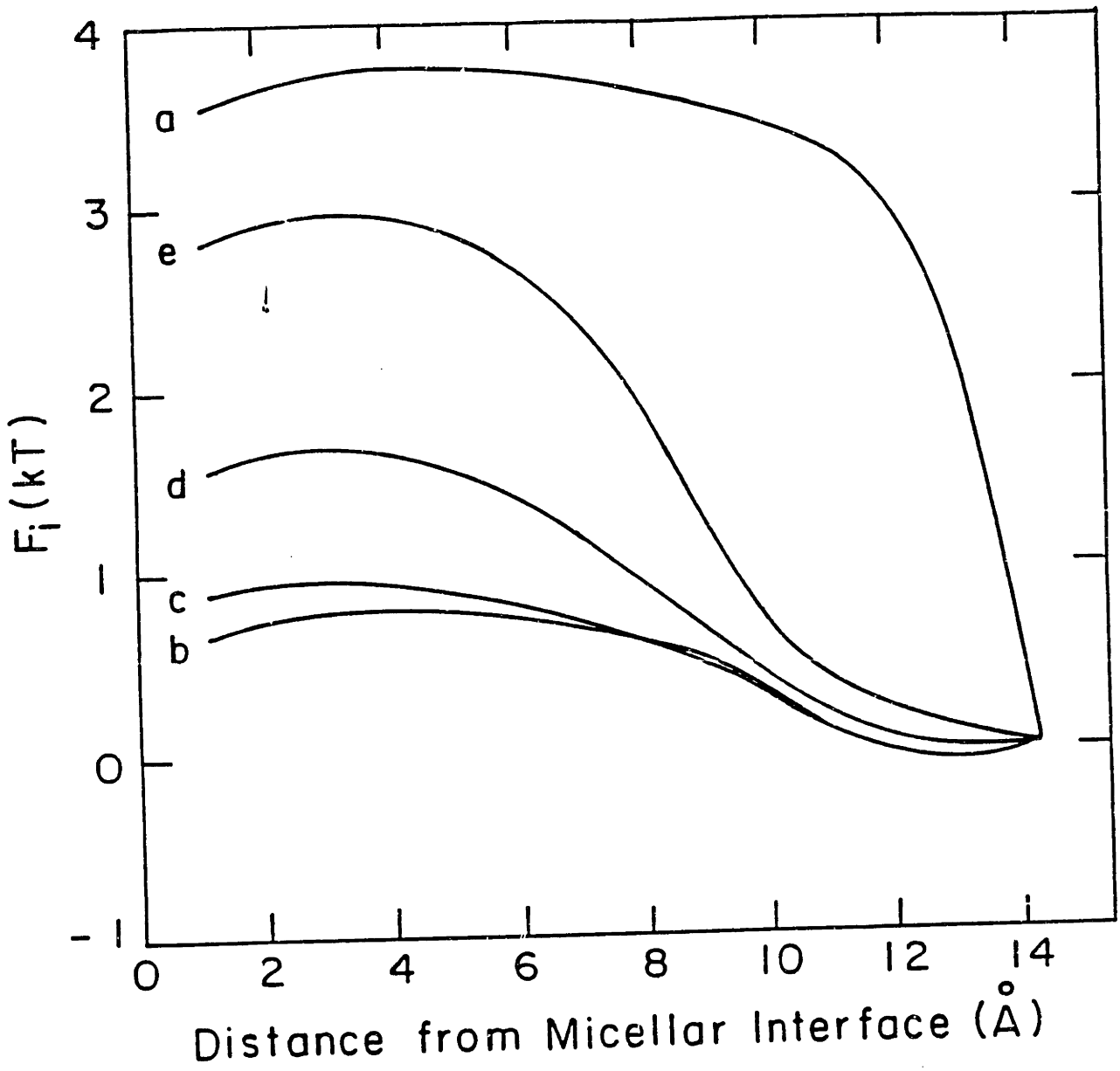

Figure 5.2 Predicted variation of the field strength F_i as a function of the distance from the micellar interface for a mixture of C_7-C_{11} chains contained within the micellar core of a cylindrical mixed micelle having a core minor radius $l_c = 15.4$Å at 25°C. The predictions correspond to the following fractions of C_7 chains in the mixture: a ($\alpha = 0.0$, pure C_{11}), b ($\alpha = 0.1$), c ($\alpha = 0.3$), d ($\alpha = 0.5$), and e ($\alpha = 0.7$).

respect to their conformations in the unrestricted-droplet state (where $F_i=0$) at $\alpha=0$ and for $\alpha\geq0.5$, while they are close to their unrestricted-state conformations for α between 0.1 and 0.3. Indeed, we find that, in the unrestricted state, the longer C_{11} chain backtracks to the micellar interface more often than the shorter C_7 chain. Thus, for a C_{11} chain ($\alpha=0$), the density of CH_2 groups near the interface is larger than ρ_{hc} (the density of CH_2 groups in bulk hydrocarbon), and the chains have to be squeezed (larger field values) into the micellar interior to satisfy the uniform-density requirement. However, upon the addition of a small fraction of C_7 chains ($\alpha\leq0.3$), the density near the micellar interface is closer to ρ_{hc} and the chains need not be stretched as much (smaller field values) to satisfy the uniform-density requirement. If the fraction of C_7 chains is further increased ($\alpha\geq0.5$), the density of CH_2 groups near the micellar center is smaller than ρ_{hc} (because the shorter chains cannot reach the center), and consequently the longer C_{11} chains have to be squeezed once again towards the center of the micelle (larger field values) to satisfy the uniform-density requirement.

The corresponding values of the predicted packing free energy $g_{hc/mic}$ as a function of the micellar composition α for the C_7-C_{11} mixture are presented in Fig. 5.3, where α corresponds to the fraction of C_7 chains in the mixture. The predicted values of $g_{hc/mic}$ follow the behavior of F_i reported in Fig. 5.2. At $\alpha=0$, corresponding to pure C_{11} chains, both $g_{h/mic}$ and F_i values are large ($g_{hc/mic}\approx2.2kT$). However, upon the addition of small amounts of C_7 chains, the value of $g_{hc/mic}$ decreases monotonically to a minimum value of approximately 1.8 kT at $\alpha\approx0.14$ (reflecting the decrease in the F_i values reported in Fig. 5.2). As the fraction of C_7 chains is further increased, $g_{hc/mic}$ increases once again reflecting the increase in F_i values reported in Fig. 5.2. Note that the maximum value of $\alpha=0.7$ in Fig.

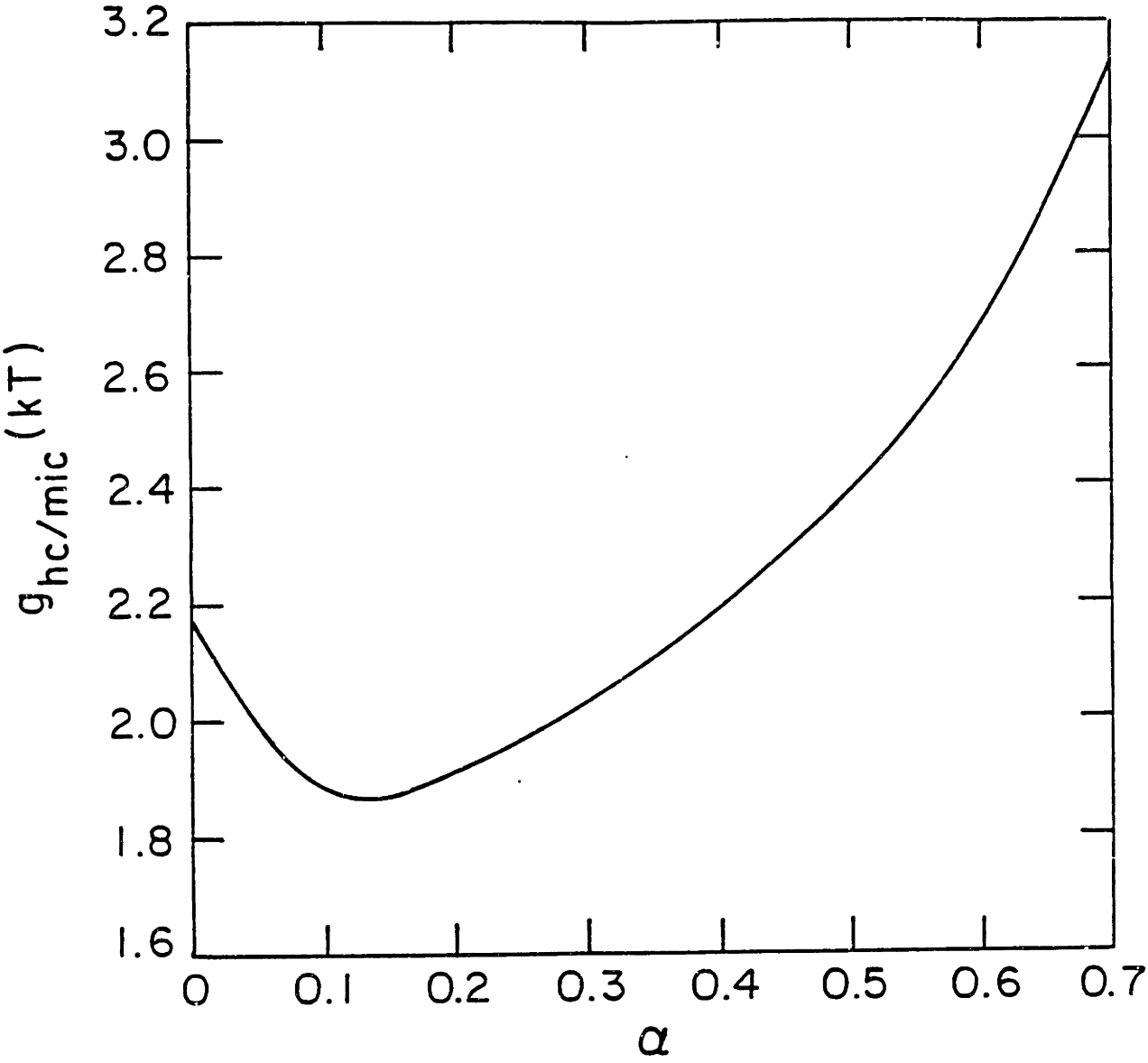

Figure 5.3 Predicted variation of the packing free energy $g_{hc/mic}$, corresponding to a C_7-C_{11} mixture contained within the core of a cylindrical mixed micelle having a core minor radius $l_c = 15.4$Å, as a function of α, the fraction of C_7 chains in the mixture at 25°C. Note that no predictions are presented for $\alpha > 0.7$, because in this α range the uniform-density requirement is no longer satisfied (see Sec. 5.3.3).

5.3 reflects the fact that, beyond $\alpha = 0.7$, the number of the longer C_{11} chains (for the chosen value of $l_c = 15.4$Å) is inadequate to satisfy the constant-density requirement at the micellar center where a hole begins to form.

5.3.4 Steric Free Energy

The presence of the surfactant heads at the micellar core-water interface results in steric repulsions between them. These repulsive steric interactions oppose micellization and have been shown (Puvvada and Blankschtein, 1990a and 1990b) to play an important role in the formation and growth of some nonionic micelles in aqueous solutions. The free-energy contribution associated with these steric repulsions g_{st} is calculated by treating the heads present at the interface as a localized monolayer, which reflects the fact that each head is physically attached to a tail at the interface. We have estimated the steric free energy using two different approaches which are discussed below.

In the first approach, the entire micellar interface, consisting of $n\alpha$ surfactant A heads and $n(1-\alpha)$ surfactant B heads, is divided into n lattice spaces each occupying an area a. It is further assumed that each lattice space can be occupied by a single head. If the average cross-sectional area of head A is denoted by a_{hA}, the single-particle partition function associated with head A, z_A, which reflects the fraction of available free lattice area, is given by $(a-a_{hA})/a$. Similarly, the single-particle partition function associated with head B, z_B, is given by $(a-a_{hB})/a$. If all single-particle partition functions are assumed to be independent of each other, the micellar partition function associated with steric interactions

(corresponding to nα surfactant A heads and n(1-α) surfactant B heads) can be expressed as the product of the single-particle partition functions, that is, $Z_{steric} = z_A^{n\alpha} z_B^{n(1-\alpha)}$. The resulting free-energy change (per monomer), $g_{st}=-(1/n)kT\ln Z_{steric}$, is given by

$$g_{st} = -\alpha kT\ln\left(1-\frac{a_{hA}}{a}\right) - (1-\alpha)kT\ln\left(1-\frac{a_{hB}}{a}\right). \qquad \textbf{(5.19a)}$$

As noted earlier, Eq. (5.19a) for g_{st} assumes that the single-particle partition functions are independent of each other. This assumption is most appropriate when the values of a_{hA} and a_{hB} are similar. However, if the values of a_{hA} and a_{hB} differ considerably, the larger head could occupy more than one lattice space, that is, it could partially occupy some of the lattice spaces occupied by the smaller heads. In that case, Eq. (5.19a) is expected to overpredict the value of g_{st}.

In the second approach, g_{st} is calculated using the test-particle approach (Allen and Tildesley, 1989; Shing and Gubbins, 1981) originally developed to compute chemical potentials using Monte-Carlo simulations. In the spirit of this approach, a "test" particle is introduced to an interface having an area na containing nα surfactant A heads and n(1-α) surfactant B heads. Note that the test particle is not a real particle in the sense that the real particles in the system are not affected by its presence, although the test particle can sense their presence. The excess chemical potential, $\mu^{ex}=\mu-\mu^{id}$ (where μ^{id} is the ideal contribution), has been shown to be equal to $-kT\ln\langle\exp(-U_{test})\rangle$, where U_{test} is the potential-energy change (associated with interactions between the test particle and the real

particles) which would result from the addition of the test particle to the interface at random. If the particles interact only through hard-core steric repulsions, U_{test} is equal to infinity (when the test particle occupies a region already occupied by a real particle), or equal to zero (when the test particle occupies a region unoccupied by any real particles). That is, μ_{ex} is related to the number of ways in which the test particle can be introduced into the system without occupying a region already occupied by another particle. Indeed, assuming additivity of excluded volumes, the number of ways of introducing the test particle should be proportional to the fractional available area $(na\text{-}n\alpha a_{hA}\text{-}n(1\text{-}\alpha)a_{hB})/na$. In other words, $\mu^{ex} = -kT\ln(1-a_h^{eff}/a)$, where $a_h^{eff} = \alpha a_{hA} + (1-\alpha)a_{hB}$. The excess chemical potential μ^{ex} computed above is equal to the steric free-energy contribution , that is,

$$g_{st} = -kT\ln\left[1-\frac{\alpha a_{hA}+(1-\alpha)a_{hB}}{a}\right]. \qquad \textbf{(5.19b)}$$

It is interesting to point out that although Eqs. (5.19a) and (5.19b) reflect somewhat different underlying physical pictures, we have found that both expressions lead to almost identical quantitative predictions of micellar solution properties. Since the conditions leading to Eq. (5.19b) appear to be of a more general nature, the theoretical predictions presented in Sec. 5.6 were made utilizing Eq. (5.19b).

5.3.5 Electrostatic Free Energy

In solutions of surfactant mixtures containing ionic or zwitterionic surfactants, electrostatic interactions can play a very important role in the micellization process. For example, in Chapter 4, we have shown that in aqueous solutions containing mixtures of anionic and cationic surfactants electrostatic interactions can result in mixture CMC's being lower than the CMC's of the constituent single surfactants. However, in this chapter, we focus on mixtures of nonionic surfactants where electrostatic interactions (primarily of the dipole-dipole type) are vanishingly small.

5.4 FREE ENERGY OF MIXED MICELLIZATION FOR NON-REGULAR SHAPES

By adding the various contributions to the free energy of mixed micellization (see Eq. (5.7) and Sec. 5.3), $g_{mic}(sh,n,\alpha,l_c)$ can be evaluated. However, as emphasized in Sec. 5.3, the packing or configurational free energy can only be computed for the three regular shapes of spheres, infinite-sized cylinders, and infinite-sized discs or bilayers. For each of these three regular shapes, we evaluate $g_{mic}(\alpha)$ as a function of l_c. Subsequently, we minimize the computed g_{mic} with respect to l_c to obtain the optimum free-energies $g_{mic}^{sph}(\alpha)$, $g_{mic}^{cyl}(\alpha)$, and $g_{mic}^{disc}(\alpha)$, for a micellar composition α, corresponding to the three regular shapes of spherical, infinite-sized cylindrical and infinite-sized discoidal micelles, respectively. Furthermore, g_{mic} for the non-regular finite-sized cylindrical and discoidal mixed micelles

are then estimated by linearly interpolating between the optimum free energies corresponding to the two limiting regular shapes. For example, for finite-sized cylindrical mixed micelles, we linearly interpolate between the free-energy values corresponding to an optimum infinite-sized cylindrical mixed micelle, having a composition α_{cyl}, and an optimum spherical mixed micelle, having a composition α_{sph}, that is, we take

$$g_{mic}(n,\alpha) = g_{mic}^{cyl}(\alpha_{cyl}) + \frac{n_{sph}}{n}\left[g_{mic}^{sph}(\alpha_{sph}) - g_{mic}^{cyl}(\alpha_{cyl})\right], \qquad \textbf{(5.20)}$$

where n_{sph} is the aggregation number of the optimum spherical mixed micelle. Note that, for the sake of generality, α_{sph} and α_{cyl} are allowed to be different. The composition of a non-regular finite-sized cylindrical mixed micelle α is given by an analogous linear interpolating expression, that is,

$$\alpha = \alpha_{cyl} + \frac{n_{sph}}{n}(\alpha_{sph} - \alpha_{cyl}) . \qquad \textbf{(5.21)}$$

Using Eq. (5.20) in Eq. (5.4), and utilizing the resulting expression for g_m, as well as Eq. (5.21), in the expression for $X_{n\alpha}$ given in Eq. (5.3) we obtain

$$X_{n\alpha} = \frac{1}{K}\left(\frac{X_1}{X_{cyl}}\right)^n , \qquad \textbf{(5.22)}$$

where $X_{cyl} = \exp[\beta g_m^{cyl}]$, *and* $K=\exp[\beta n_{sph}(g_m^{sph} - g_m^{cyl})+1]$, *where* g_m^{cyl} *and* g_m^{sph} are the

modified free energies of mixed micellization corresponding to an optimum infinite-sized cylindrical and an optimum spherical micelle, respectively (see Eq. (5.4)). Eq. (5.22) yields the mole fractions of finite-sized cylindrical mixed micelles as a function of n and α. For all aggregation numbers, the optimum compositions α^*_{cyl} and α^*_{sph}, at which $X_{n\alpha}$ exhibits a maximum, can be obtained by setting the derivatives of $X_{n\alpha}$ (in Eq. (5.22)) with respect to α_{sph} and α_{cyl} equal to zero. This leads to

$$\beta \frac{\partial g_{mic}^{sph}(\alpha)}{\partial \alpha}\bigg|_{\alpha^*_{sph}} = \beta \frac{\partial g_{mic}^{cyl}(\alpha)}{\partial \alpha}\bigg|_{\alpha^*_{cyl}} = \ln \frac{\alpha_1}{1-\alpha_1} \,. \qquad (5.23)$$

For large n, $X_{n\alpha}$ exhibits a sharp maximum at $\alpha_{sph}=\alpha^*_{sph}$ and $\alpha_{cyl}=\alpha^*_{cyl}$ because n appears as a large multiplicative factor in the exponential of Eq. (5.22), and consequently any small deviations of α_{sph} and α_{cyl} from their optimum values will be magnified by this exponential factor. This implies that, to leading order in α, we can approximate $\Sigma_\alpha X_{n\alpha}$ *by* $X_{n\alpha^*}$, where α^* is the optimum composition of a micelle having an aggregation number n, and is obtained by inserting α^*_{cyl} and α^*_{sph} in Eq. (5.21).

Using Eq. (5.23), the optimum compositions α^*_{sph} and α^*_{cyl} and the corresponding optimum free energies of micellization $g_{mic}^{sph}(\alpha^*_{sph})$ *and* $g_{mic}^{cyl}(\alpha^*_{cyl})$ for spherical and infinite-sized cylindrical mixed micelles can be determined. If $g_{mic}^{sph}(\alpha^*_{sph}) < g_{mic}^{cyl}(\alpha^*_{cyl})$, then the optimum micellar shape sh* corresponds to a sphere, and finite-sized spherical mixed micelles will be favored. In that case, the micellar size is assumed to range from that

corresponding to the smallest spherical mixed micelles, having aggregation numbers of approximately 20, to that corresponding to mixed micelles having a core minor radius equal to l_c^{max}, where $l_c^{max} = l_{max}^A$ (*if* $l_{max}^A > l_{max}^B$), and $l_c^{max} = l_{max}^B$ (*if* $l_{max}^A < l_{max}^B$), where l_{max}^i(i=A,B) is the fully-extended tail length introduced in Sec. 5.3.2. The free energy of mixed micellization is then evaluated for all aggregation numbers within this range.

On the other hand, if $g_{mic}^{sph}(\alpha_{sph}^*) > g_{mic}^{cyl}(\alpha_{cyl}^*)$, then the optimum micellar shape sh* corresponds to an infinite-sized cylinder. Under such conditions, infinite-sized (n=∞) cylinders will be favored. However, when entropy of mixing contributions are included (in addition to the g_{mic} considerations presented so far, see also Ref. 8), the surfactant solution will typically consist of a distribution of finite-sized micelles, since a large number of small micelles is entropically favored over a small number of larger ones. Consequently, even if sh* corresponds to an infinite-sized cylinder, the solution will actually consist of a distribution of finite-sized cylindrical mixed micelles (*one-dimensional growth*). The optimum free energy of micellization $g_{mic}(n,\alpha^*)$ and the optimum composition α^* of such non-regular finite-sized cylindrical mixed micelles can be estimated using Eqs. (5.20) and (5.21). In other words,

$$g_{mic}(n,\alpha^*) = g_{mic}^{cyl}(\alpha_{cyl}^*) + \frac{n_{sph}}{n}\left[g_{mic}^{sph}(\alpha_{sph}^*) - g_{mic}^{cyl}(\alpha_{cyl}^*)\right], \qquad (5.24)$$

and

$$\alpha^*(n) = \alpha^*_{cyl} + \frac{n_{sph}}{n}(\alpha^*_{sph} - \alpha^*_{cyl}). \qquad (5.25)$$

Analogous expressions for the free energy of mixed micellization corresponding to non-regular finite-sized discoidal mixed micelles can also be derived. To summarize, we compute g_{mic} for the three regular micellar shapes of spheres, infinite-sized cylinders, and infinite-sized discs or bilayers, and then identify sh^*, which determines if the mixed micelles exhibit *two-dimensional, one-dimensional, or no growth.*

5.5 MATERIALS AND EXPERIMENTAL METHODS

For the experimental investigations presented in this chapter, we have chosen aqueous solutions containing binary mixtures of nonionic surfactants belonging to the alkyl polyethylene oxide (C_iE_j) family, where i denotes the number of carbon atoms in the hydrocarbon moiety and j denotes the number of ethylene oxide groups in the hydrophilic moiety. A convenient feature of these surfactants is that both i and j, and thus the surfactant hydrophobic-hydrophilic character, can be easily manipulated. In particular, the binary surfactant mixtures used in this study include (i) $C_{12}E_6$-$C_{12}E_8$, (ii) $C_{12}E_6$-$C_{10}E_5$ and (iii) $C_{12}E_6$-$C_{10}E_4$, where in case (i) we have changed the nature of the hydrophilic moiety, in case (ii) we have changed the nature of the hydrophobic moiety, and in case (iii) we have changed the nature of both the hydrophobic and the hydrophilic moieties. Our selection of systems i-iii also reflects the fact that aqueous solutions of these surfactant mixtures exhibit a number of interesting experimentally accessible phenomena which can be utilized to test

the validity and range of applicability of the theoretical framework developed in this chapter. Specifically, these phenomena include (1) relatively low CMC's (mole fractions below 10^{-5}), thus providing a broad dilute concentration range, for all compositions, to study mixed micellar solution properties in the absence of significant intermicellar interactions, (2) liquid-liquid phase separation, which varies with surfactant composition, over a convenient temperature range between 0-100°C, and for total surfactant mole fractions below 5wt%, and (3) a "sphere-to-cylinder" shape transition as a function of temperature, between 0-50°C, and of surfactant composition. In each case, the shape transition temperature T^* occurs sufficiently below the critical temperature for phase separation T_c (T_c-T^*≈35°C), such that shape transitions can be studied using scattering techniques (light, neutrons) with minimal critical-fluctuation effects.

5.5.1 Materials and Sample Preparation

Homogeneous surfactants $C_{12}E_6$ (Lot 9011), $C_{12}E_8$(Lot 9054), $C_{10}E_6$(Lot 9030), and $C_{10}E_4$(Lot 9004) were obtained from Nikko Chemicals, Tokyo, and used without any further purification. The high purity of the surfactants was confirmed by the absence of any detectable minimum in the measured surface tension versus surfactant concentration curves of aqueous solutions of each surfactant. In addition, to ensure uniformity in the results, all our measurements were conducted using the same lot for each surfactant. All solutions were prepared using deionized water which had been fed through a Milli-Q ion-exchange system.

5.5.2 Critical Micellar Concentration Measurement

The critical micellar concentration (CMC) of the mixed micellar solution, corresponding to a given surfactant composition α_{soln}, was obtained by the surface-tension method. This method is based on the fact that the surface tension decreases quite rapidly with increasing total surfactant concentration until the CMC, beyond which it remains practically constant. Therefore, we have measured the surface tension σ of the mixed surfactant solution, for a given α_{soln}, as a function of the total surfactant mole fraction X using a Wilhelmy-plate tensiometer (Kruss 10T). Subsequently, for a given α_{soln}, σ was plotted as a function of log(X), and the CMC was estimated from the break in the resulting σ versus log(X) curve with an accuracy of 5%. All measurements were carried out in a thermostated device maintained at a constant temperature of 25°C. Before use, all the glassware was washed in a 1N NaOH-ethanol bath, then in a nitric acid bath, followed by thorough rinsing with milli-Q water, and baking in an oven. The Wilhelmy platinum plate was washed using acetone, rinsed in Milli-Q water, and flamed until red hot before each surface tension measurement.

5.5.3 Cloud-Point Curve and Coexistence-Curve Determinations

As discussed in Sec. 5.2, the Gibbs phase rule indicates that in a two-phase ternary solution, consisting of water and two surfactants, in thermodynamic equilibrium one can vary independently three intensive variables. Accordingly, at a fixed pressure (1 atm) and for a

given surfactant composition α_{soln}, there is a unique temperature T for each total surfactant concentration X at which the ternary solution first exhibits liquid-liquid phase separation. The resulting T-X curve, at a given α_{soln} and P = 1atm, represents a boundary between the one-phase and the two-phase regions of the phase diagram. In general, there are two commonly used experimental methods to determine this boundary. The first method yields the cloud-point curve, while the second method yields the coexistence curve. Below, we discuss and contrast the two methods.

The cloud-point temperature T_{cloud} is determined by visually identifying that temperature at which a solution of known composition α_{soln} and total surfactant mole fraction X (at a fixed pressure P) becomes cloudy as the temperature is varied (raised (lowered) for solutions exhibiting a lower (upper) critical point). The resulting T_{cloud}-X boundary is the cloud-point curve corresponding to that α_{soln}. The method is quite fast and accurate, taking approximately 30 min for each T_{cloud} measurement.

The coexistence curve is typically measured by allowing the phase separation to reach completion, that is, by obtaining two physically separated phases in equilibrium with each other. Consequently, although generally quite precise, this method is very slow and tedious since equilibration times can be very long (6-8 hours). In this method, one measures the equilibrium total surfactant concentrations Y and Z of the two coexisting phases, as well as the corresponding surfactant compositions α_Y and α_Z as a function of temperature T (see Sec. 5.2). Surfactant concentrations and compositions are typically determined by density measurements, differential refractometry, or chromatographic analysis.

It is important to emphasize that in the case of binary solutions, such as, single-surfactant aqueous solutions, the cloud-point curve and the coexistence curve should be identical within experimental error (Fujita, 1990). However, in the case of multicomponent solutions, such as, the ternary mixed micellar systems considered in this chapter, this need not be the case. In general, the compositions of the two coexisting phases (α_Y and α_Z) can be different. This indicates that, in general, the two coexisting phases can lie on two different cloud-point curves, one corresponding to a composition α_Y and the other corresponding to a composition α_Z. Indeed, the cloud-point and coexistence curves are expected to be identical only if $\alpha_Y = \alpha_Z$, that is, if the solute species partition equally between the two phases.

Below, we discuss in some detail some of the important experimental aspects associated with each method.

(a) Cloud-Point Curve Determination: In the case of nonionic surfactants, which exhibit a lower consolute (critical) point, T_{cloud} is determined by visually identifying that temperature at which solutions of known surfactant concentration X and composition α_{soln} become cloudy upon raising the temperature of the sample. For this purpose, each sample was placed in a transparent thermo-regulated cell whose temperature was controlled to within 0.01°C. Initially, each sample was cooled to a temperature low enough so that it exhibited a single, clear, homogeneous phase. The temperature was then raised in small steps until the solution started to cloud at a temperature T_u. As soon as clouding was observed, the temperature was lowered in small steps until the cloudiness disappeared at a temperature T_d. T_{cloud} was then determined by taking the average of T_u and T_d. Note that at each step

the sample was first stirred thoroughly, using a magnetic stirrer, to ensure temperature and concentration homogeneity, and subsequently observed for any signs of cloudiness with the stirrer shut off. The entire procedure was repeated several times with smaller steps in temperature. This cycling procedure was adopted to ensure reproducibility and reversibility in the observed clouding behavior. All measurements were reproducible to within 0.05°C.

(b) Coexistence-Curve Determination: Solutions of known composition α_{soln} and concentration X were prepared in a test tube, and the solution temperature was subsequently raised until the solution entered the two-phase region of the phase diagram. The sample was then allowed to equilibrate for a period of 6-8 hours after which two physically separated phases in equilibrium with each other formed. Samples from each coexisting phase were then carefully extracted using a syringe for surfactant concentration analysis. In this step, great care was taken to avoid any mixing of the two separated phases. The extracted samples where then analyzed using reverse phase high performance liquid chromatography (HPLC), where the surfactants were separated by passing the solution through a Waters C_{18} column with a 60:40 acetone-water mobile phase at a flow rate of 1.0 ml/min. The eluted components were detected using a Waters 320 refractive index (RI) detector maintained at a constant temperature of 35°C. This temperature is sufficiently above room temperature so as to minimize the effects of fluctuations in the room temperature on the measured refractive index. We found the response factor of the RI detector to be linear up to a surfactant mole fraction of about 10^{-2}, and to be independent of surfactant composition. By comparing the response factor with a previously measured

calibration curve, the concentration of each surfactant in the two coexisting phases could then be determined. The accuracy of this method is about 2.5%.

5.5.4 Dynamic Light Scattering Measurements

Dynamic light scattering measurements were performed using a vertically polarized argon ion laser operating at λ = 4880 Å at a 90° configuration. The homodyne autocorrelation function was collected using a 128 channel Langley Ford model 1096 correlator and interpreted using a cumulants analysis (Koppel, 1972; Mazer et al., 1976). The mean-micellar hydrodynamic radius was calculated, in the context of the Stokes-Einstein relation, from the first cumulant using available (Weas. 1987) temperature dependent viscosity data for water. These measurements were performed as a function of temperature (5-55°C) at a fixed surfactant mole fraction of 10^{-3}. At this surfactant concentration scattering-correlation functions have been shown (Brown and Rymden, 1987) to be independent of scattering angle in $C_{12}E_6$-D_2O solutions.

5.6 THEORETICAL PREDICTIONS AND COMPARISON WITH EXPERIMENTS

5.6.1 Estimation of Molecular Parameters

The molecular-thermodynamic framework presented in Secs. 5.2, 5.3, and 5.4 enables us to predict a broad spectrum of micellar properties of aqueous solutions containing binary

surfactant mixtures. All these predictions depend on the values of the free energy of mixed micellization g_{mic}, and the effective mean-field interaction parameter C_{eff} (see Eq. (5.2)). The value of g_{mic} can be computed using the molecular model of mixed micellization presented in Secs. 5.3 and 5.4. Specifically, the values of the two molecular parameters a_{hA} and a_{hB}, reflecting the average cross-sectional areas of the hydrophilic heads and hence determining g_{st} (see Sec. 5.3.4), are needed. All other four free-energy contributions to g_{mic} (see Eq. (5.7)) can be estimated using readily available information as described in Sec. 5.3.

On the other hand, we currently do not have a similar molecular description to evaluate the interaction parameter C_{eff}. Nevertheless, it is interesting to note that, in the context of the proposed molecular-thermodynamic framework, the value of C_{eff} is not actually needed to predict many of the useful properties of the mixed micellar solution, which include the CMC and the weight-average mixed micelle aggregation number (see Sec. 5.2). Furthermore, even in cases where C_{eff} is important, such as, in controlling the phase separation phenomena, one can estimate its value from knowledge of the interaction parameters, C_{AW} and C_{BW}, associated with the corresponding aqueous solutions of pure surfactants A and B, respectively, as well as of the specific interaction parameter C_{AB} (see Eq. (5.2) and the accompanying discussion).

As stated earlier, in this chapter we focus on experimental aspects of aqueous solutions containing binary mixtures of C_iE_j nonionic surfactants. For these systems, we have shown in Chapter 4 that the specific interaction parameter $C_{AB}\approx 0$. Furthermore, we have also shown in Chapter 2 that the parameters C_{AW} and C_{BW} should be temperature dependent, and that the molecular parameters a_{hA} and a_{hB} (hereafter denoted as a_{hj}) should

also vary with temperature. The temperature variation of a_{hj} reflects the fact that the E_j moieties of C_iE_j surfactants are hydrated, with the hydration number decreasing with increasing temperature. In particular, we proposed that a_{hj} varies linearly with temperature according to $a_{hj} = a_{hj}^{o}[1-H(T-298)]$, where a_{hj}^{o} is the average cross-sectional area of a E_j head at 298K, and H reflects the decrease in hydration (per EO group) with increasing temperature. In particular, for $C_{12}E_6$, we found that $a_{hj}^{o}=38.1\text{Å}^2$ and $H=0.0075K^{-1}$. In addition, we proposed the following simple scaling-type relation to relate the variation of a_{hj} with j at a given temperature, that is, $a_{hj}\sim j^{0.8}$. In the present study, we adopt the same expressions for a_{hj}, that is, we take $a_{hj}(T)=a_{h6}(T)(j/6)^{0.8}$, with $a_{h6}=38.1[1-0.0075(T-298)]$ (in Å^2). Table 5.1 lists values of a_{hj} (at 25°C) for the C_iE_j surfactants used in the present study.

As mentioned earlier, we have shown that the interaction parameters, C_{AW} and C_{BW}, are temperature dependent. In particular, the values of C_{AW} and C_{BW} and their temperature variations can be obtained by fitting the theoretically predicted coexistence curves to the experimentally measured ones in aqueous solutions of single surfactants A and B, respectively. Over a range of about 2°C (which is the typical accessible temperature range associated with the coexistence curves of aqueous solutions of the C_iE_j surfactants considered in this chapter), C_{AW} and C_{BW} are found to be linear functions of temperature. Table 5.1 lists the value of C_{AW} (or C_{BW}) and its temperature derivative C'_{AW} (or C'_{BW}), evaluated at the critical temperature T_{cA} (or T_{cB}) corresponding to aqueous solutions of surfactant A (or surfactant B), for the C_iE_j surfactants used in the present study. Since the deduced linear temperature variations of C_{AW} and C_{BW} result from fits to the experimentally

Table 5.1. Typical values of T_c, C_{AW}/k, and C'_{AW}/k (both evaluated at T_c), δ, and a_{hj} for the various C_iE_j nonionic surfactants used in the present study.

Surfactant	T_c (°C)	C_{AW}/k (K)	C'_{AW}/k	δ (Å)	a_{hj} (Å^2) at 25°C
$C_{12}E_6$	51.14	14.48	0.776	2.25	38.1
$C_{12}E_8$	78.39	14.45	1.121	2.25	48.0
$C_{10}E_6$	62.18	18.45	1.6	1.90	38.1
$C_{10}E_4$	19.51	16.5	1.0	1.90	27.0

measured coexistence curves of aqueous solutions of single surfactants A and B, respectively, where in each case the coexistence curve spans only about a 2°C range, we anticipate that deviations from linearity will presumably arise at temperatures which are sufficiently different from T_c^A and T_c^B. Clearly, a situation like that will arise in the mixed micellar systems for certain values of α_{soln}. For example, in the $C_{12}E_6$-$C_{12}E_8$-H_2O system, $T_{cA}\approx 51$°C (for $C_{12}E_6$-H_2O) and $T_{cB}\approx 78$°C (for $C_{12}E_8$-H_2O), and, therefore, we anticipate that as α_{soln} varies from 1 (corresponding to pure $C_{12}E_6$) to 0 (corresponding to pure $C_{12}E_8$) the linear variation of C_{AW} and C_{BW} will probably not hold over the entire temperature range (51-78°C). In view of this, in this chapter, we have estimated the value of $C_{eff}(\alpha,T)$ as,

$$C_{eff}(\alpha) + (T-T_{mix})\,C'_{eff}(\alpha), \text{ where } C_{eff}(\alpha) = \alpha C_{AW}(T_{cA}) + (1-\alpha)C_{BW}(T_{cB}),$$

$$C'_{eff}(\alpha) = \alpha C'_{AW}(T_{cA}) + (1-\alpha)C'_{BW}(T_{cB}), \text{ and } T_{mix} = \alpha T_{cA} + (1-\alpha)T_{cB}.$$

Using these values in the molecular-thermodynamic framework described in Secs. 5.2, 5.3, and 5.4, below we predict and compare with experimental measurements the CMC as a function of α_{soln}, the weight-average mixed micelle aggregation number as a function of

T for various values of α_{soln}, and the coexistence curves, including the compositions of the two coexisting micellar phases, for aqueous solutions of the three binary surfactant mixtures (i) $C_{12}E_6$-$C_{12}E_8$, (ii) $C_{12}E_6$-$C_{10}E_6$, and (iii) $C_{12}E_6$-$C_{10}E_4$. Note that in what follows, $C_{12}E_6$ corresponds to surfactant A and the other surfactant corresponds to surfactant B. In addition, as discussed is Sec. 5.3.4, in the predictions that follow we have utilized Eq. (5.19b) to estimate the steric contribution to the free energy of mixed micellization (recall that utilization of Eq. (5.19a) yields almost identical results).

5.6.2 Critical Micellar Concentration

Using the computational procedures discussed in Secs. 5.2-5.4, and the values of $a_{hj}(T)$ presented in Sec. 5.6.1, the predicted CMC variation at 25°C for aqueous solutions of $C_{12}E_6$-$C_{12}E_8$ (full line) and $C_{12}E_6$-$C_{10}E_4$ (dashed line) as a function of α_{soln}, the fraction of $C_{12}E_6$ in each mixture, is presented in Fig. 5.4. The two symbols in Fig. 5.4 represent experimentally measured CMC values using the surface-tension method described in Sec. 5.5.2. Overall, the theoretical predictions are in good agreement with the experimental CMC values. An examination of Fig. 5.4 reveals that, as expected from the hydrophobic-hydrophilic surfactant balance, the CMC values follow the sequence $C_{10}E_4 > C_{12}E_8 > C_{12}E_6$. As $C_{12}E_6$ is added to either a solution of $C_{12}E_8$-H_2O or $C_{10}E_4$-H_2O, that is, as α_{soln} increases, the CMC of each mixed micellar solution decreases monotonically approaching the CMC value of the $C_{12}E_6$-H_2O solution at $\alpha_{soln} = 1$.

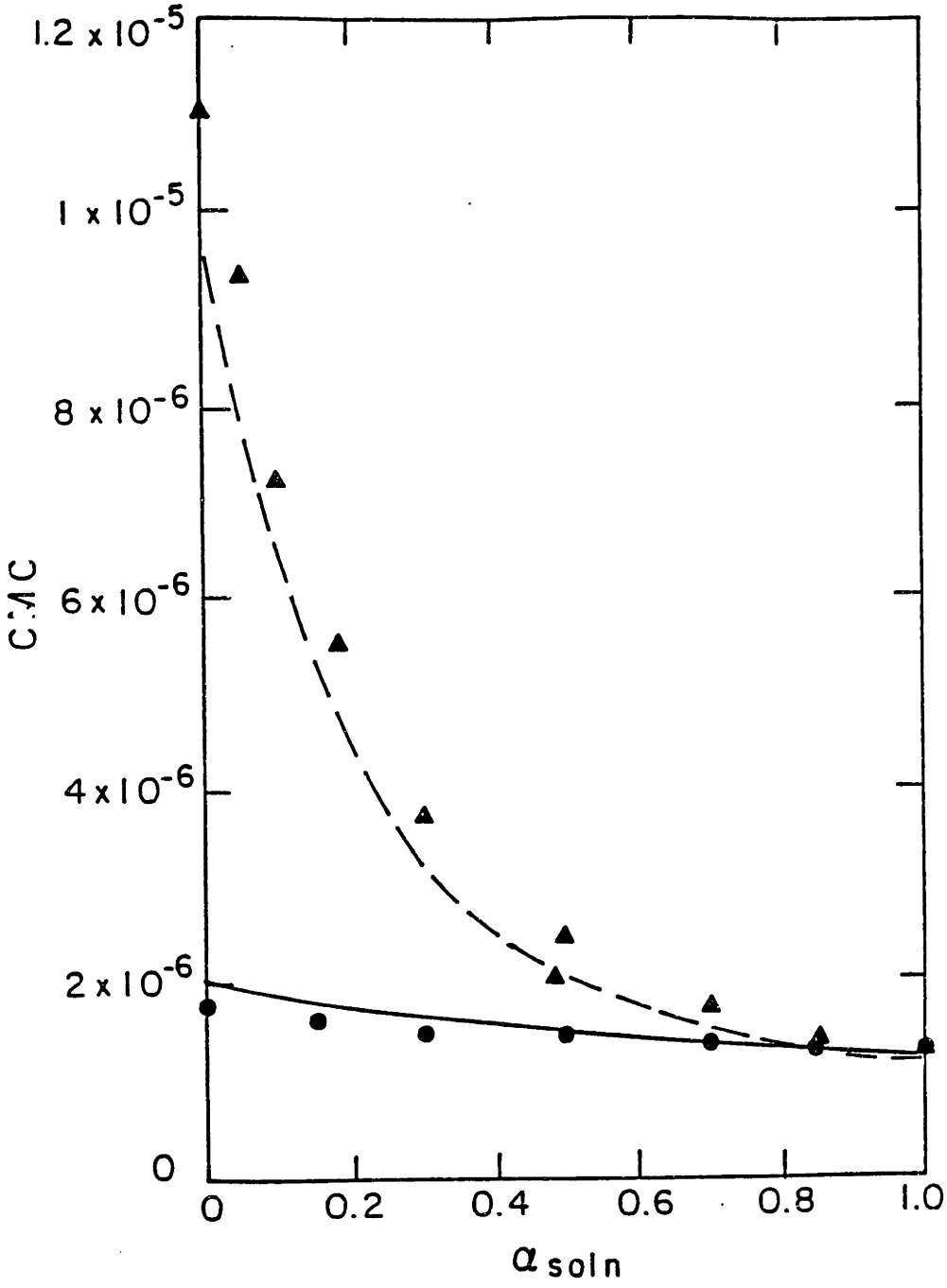

Figure 5.4 Predicted variation of the critical micellar concentration (CMC) of aqueous solutions of $C_{12}E_6$-$C_{12}E_8$ (full line) and $C_{12}E_6$-$C_{10}E_4$ (dashed line) at 25°C as a function of α_{soln}, the fraction of $C_{12}E_6$ in each mixture. The two symbols represent experimentally measured CMC values using the surface-tension method: (●) $C_{12}E_6$-$C_{12}E_8$, and (▲) $C_{12}E_6$-$C_{10}E_4$.

Figure 5.5 shows the predicted variation of the average mixed micellar composition $\alpha_{mic} = (\alpha_{soln}X - \alpha_1 X_1)/(X - X_1)$, at the CMC, for aqueous solutions of $C_{12}E_6$-$C_{12}E_8$ (solid line) and $C_{12}E_6$-$C_{10}E_4$ (dashed line) as a function of α_{soln}, the fraction of $C_{12}E_6$ in each mixture. The figure indicates that, for both surfactant mixtures, the mixed micelles are enriched with $C_{12}E_6$ ($\alpha_{mic} > \alpha_{soln}$). This is due to the fact that, as explained above, $C_{12}E_6$ has the lowest CMC, and consequently exhibits the highest propensity to form micelles. Furthermore, since $C_{10}E_4$ has a higher CMC than $C_{12}E_8$, micelles are considerably more enriched with $C_{12}E_6$ in the $C_{12}E_6$-$C_{10}E_4$ mixture, than in the $C_{12}E_6$-$C_{12}E_8$ mixture. To the best of our knowledge there is no available experimental data to test the predictions presented in Fig. 5.5.

5.6.3 Weight-Average Mixed Micelle Aggregation Number

Fig. 5.6 shows the predicted variation of the weight-average mixed micelle aggregation number $<n>_w$ as a function of temperature for aqueous solutions of $C_{12}E_6$-$C_{12}E_8$ (at $X = 10^{-3}$) having various surfactant compositions α_{soln}. Curve a corresponds to a solution of $C_{12}E_6$-H_2O ($\alpha_{soln} = 1$), and, as we proceed from curve a to curve f, the value of α_{soln} decreases to zero, corresponding to a solution of $C_{12}E_8$-H_2O. For all compositions, Fig. 6 clearly shows that the mixed micelles remain small ($<n>_w \approx 50$) below a certain temperature T^* which depends on α_{soln}. For temperatures higher than T^*, $<n>_w$ increases quite dramatically. In this respect, we have shown in Chapter 2 that pure C_iE_j surfactants in aqueous solutions can exhibit varying degrees of one-dimensional growth, from spheroidal to cylindrical structures, as a function of temperature. In particular, the transition

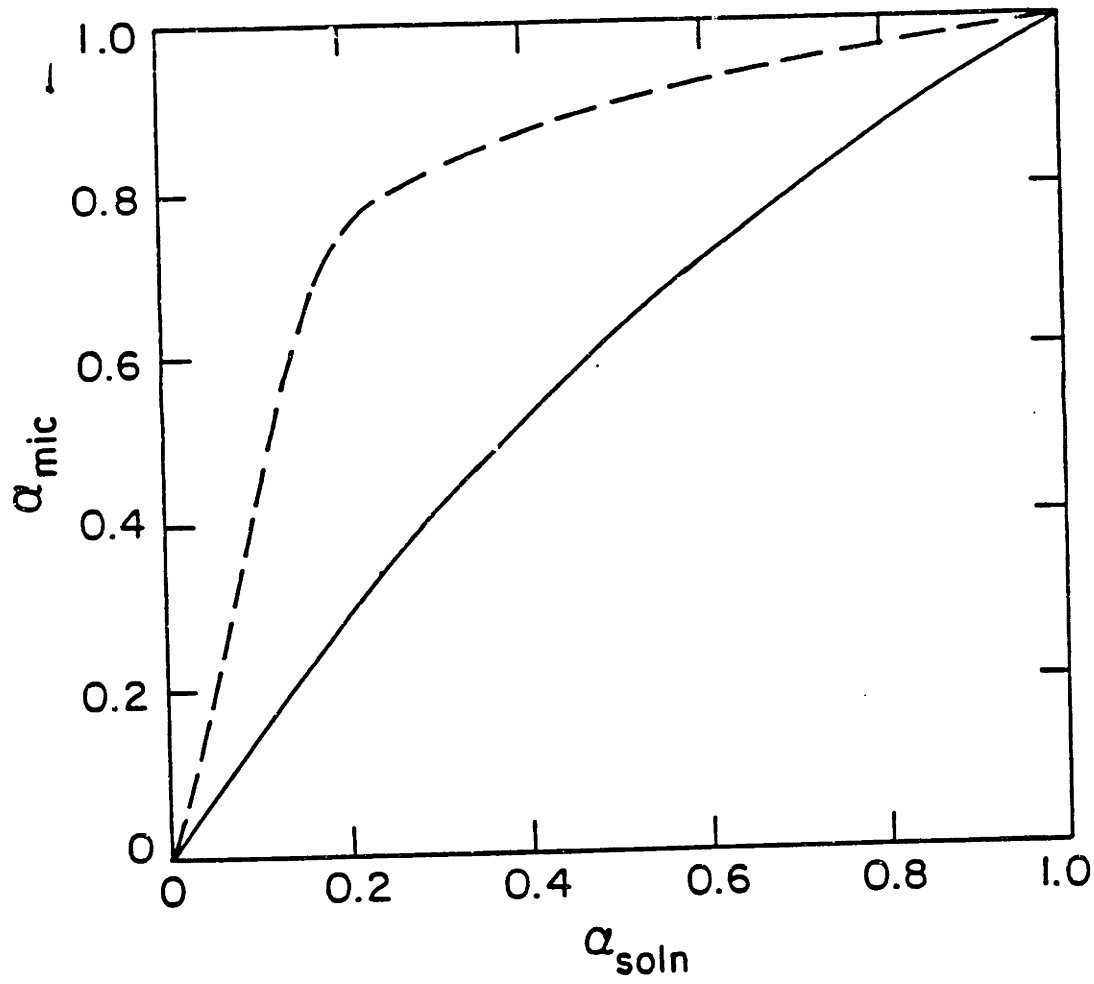

Figure 5.5 Predicted variation of the average mixed micellar composition α_{mic}, at the CMC, for aqueous solutions of $C_{12}E_6$-$C_{12}E_8$ (full line), and $C_{12}E_6$-$C_{10}E_4$ (dashed line) at 25°C as a function of α_{soln}, the fraction of $C_{12}E_6$ in each mixture.

temperature T^* increases from about 15°C for pure $C_{12}E_6$ to about 50°C for pure $C_{12}E_8$ (at a total surfactant concentration of 1 wt%). In this spirit, it is reasonable to suggest that the predictions in Fig. 5.6 are consistent with a "sphere-to-cylinder" shape transition of the mixed micelles which occurs over a narrow temperature range (captured by T^*) which increases as α_{soln} decreases from 1 (corresponding to pure $C_{12}E_6$, $T^* \approx 13°C$) to 0 (corresponding to pure $C_{12}E_8$, $T^* \approx 47°C$). Note that the small differences in the T^* values reported in Chapter 2 and those predicted in the present study reflect the difference in the total surfactant concentrations at which the two predictions were made (in Chapter 2, a value of X = 1wt% (approximately equal to 4×10^{-4}) was used, while in this chapter $X = 10^{-3}$). Since micellar size increases with increasing surfactant concentration, it is reasonable to expect that, the shape transition should occur at a lower T^* value for the higher X values utilized in the this chapter.

The predicted transition temperatures T^* compare very favorably with experimentally deduced transition temperatures, indicated by the various arrows in Fig. 5.6, obtained using dynamic light scattering measurements. Fig. 5.7 shows a plot of the measured average mixed micellar hydrodynamic radius as a function of temperature for various values of α_{soln}. The figure clearly indicates that for $T < T^*$ micelles are small, while for $T > T^*$ micelle size increases rapidly. The figure also indicates that T^* shifts to higher values as the fraction of $C_{12}E_6$ in the mixture is decreased from $\alpha_{soln} = 1$ to $\alpha_{soln} = 0$.

Fig. 5.8 shows predictions of $\langle n \rangle_w$ as a function of total surfactant mole fraction X for aqueous solutions of $C_{12}E_6$-$C_{12}E_8$ at 25°C (unfilled symbols) and 50°C (filled symbols), and for two compositions $\alpha_{soln} = 0.25$ (circles) and $\alpha_{soln} = 0.75$ (squares). Recall that $\alpha_{soln} = 1$

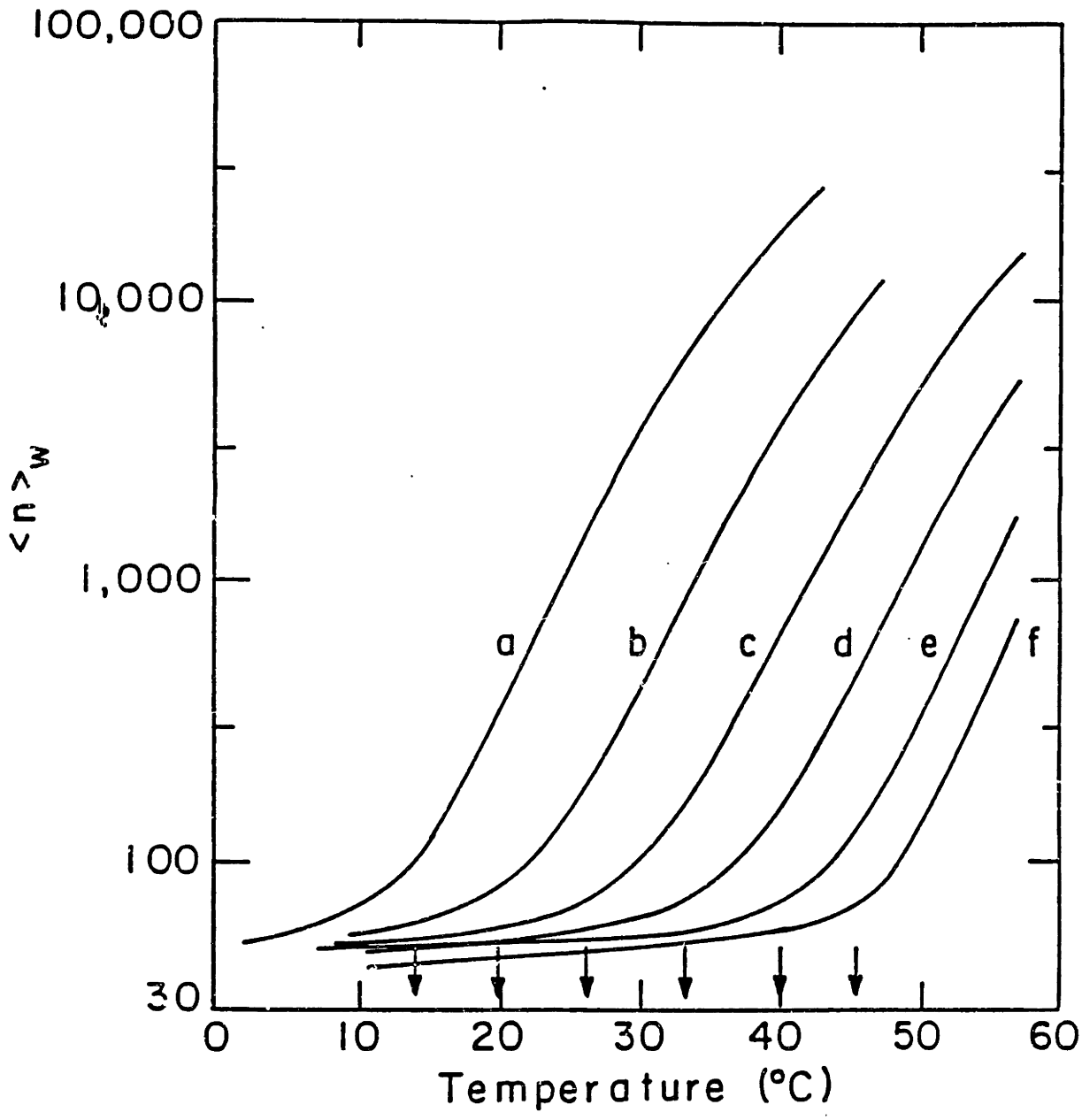

Figure 5.6 Predicted variation of the weight-average mixed micelle aggregation number $<n>_w$ as a function of temperature for aqueous solutions of $C_{12}E_6$-$C_{12}E_8$ having the following compositions: a ($\alpha_{soln}=1.0$, pure $C_{12}E_6$), b ($\alpha_{soln}=0.8$), c ($\alpha_{soln}=0.6$), d ($\alpha_{soln}=0.4$), e ($\alpha_{soln}=0.2$), and f ($\alpha_{soln}=0.0$, pure $C_{12}E_8$). The predictions were made at a total surfactant mole fraction $X=10^{-3}$. The various arrows denote shape transition temperatures deduced from dynamic light scattering measurements in Fig. 5.7.

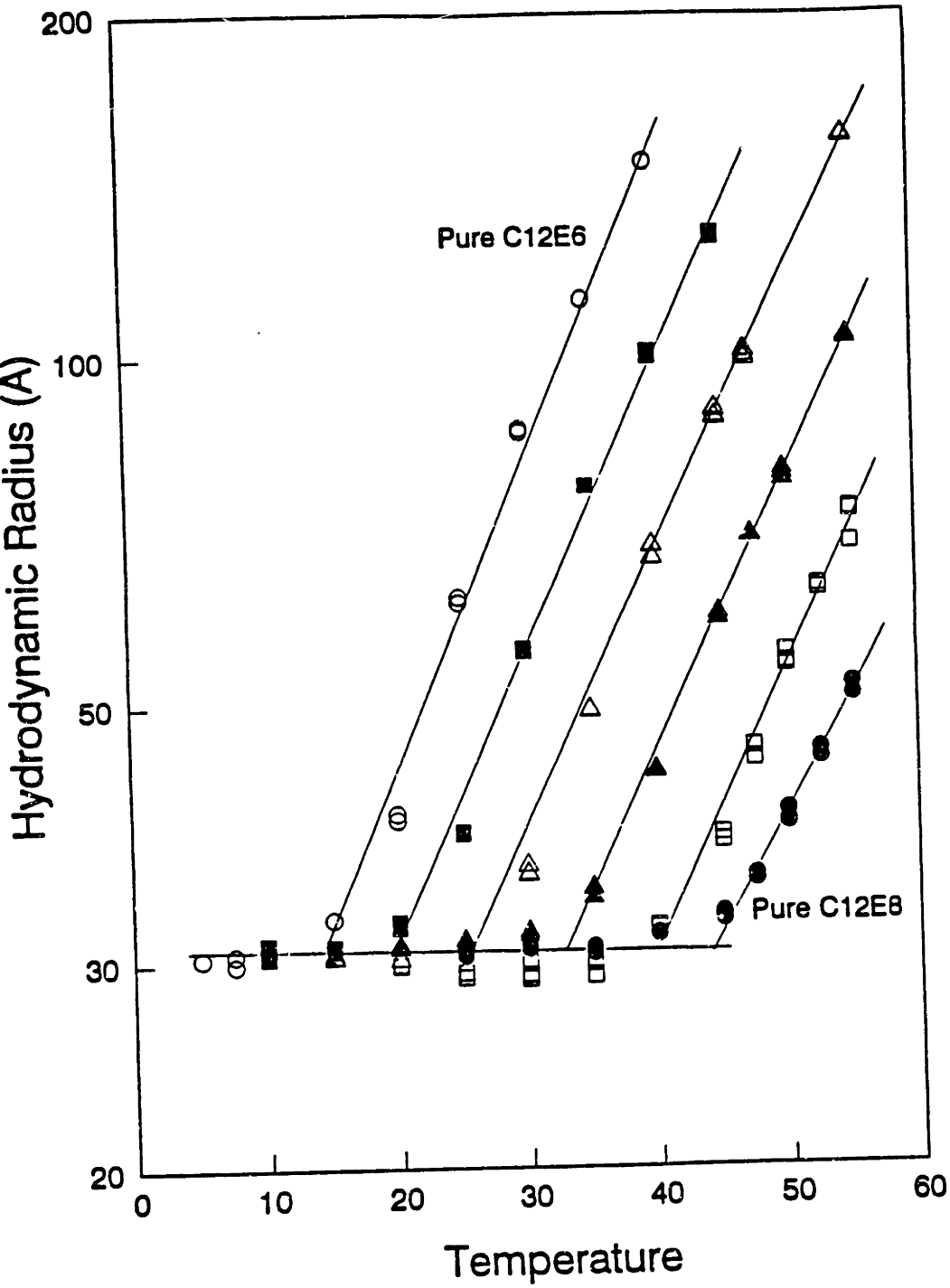

Figure 5.7 Experimental values of the average micellar hydrodynamic radius as a function of temperature for aqueous solutions of $C_{12}E_6$-$C_{12}E_8$ at $X=10^{-3}$ and at surfactant compositions of (○) 1.0, pure $C_{12}E_6$, (■) 0.8, (△) 0.6, (▲) 0.4, (□) 0.2, and (●), pure $C_{12}E_8$.

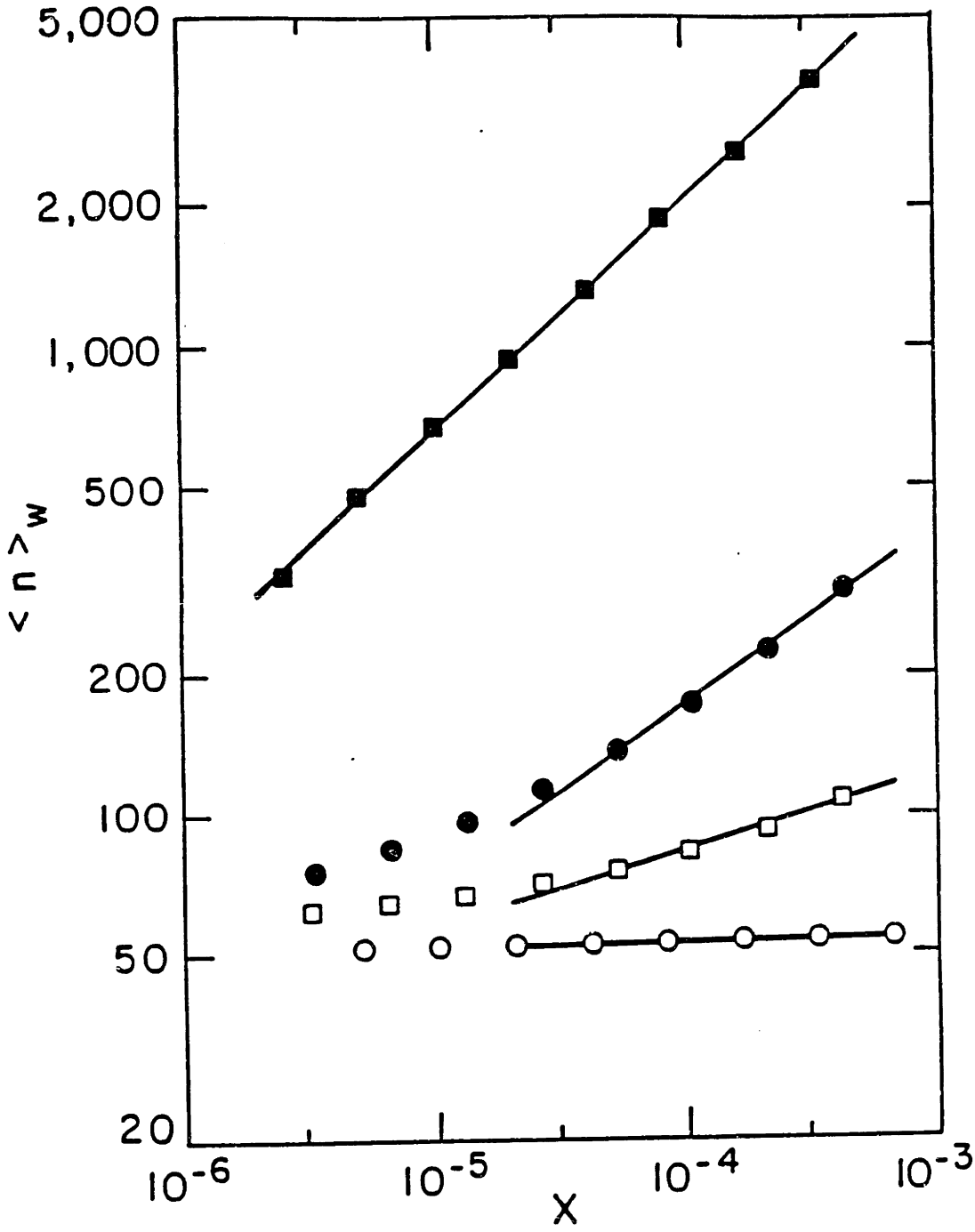

Figure 5.8 Predicted variation of the weight-average mixed micelle aggregation number $\langle n \rangle_w$ as a function of total surfactant mole fraction X for aqueous solutions of $C_{12}E_6$-$C_{12}E_8$ at 25°C (unfilled symbols) and 50°C (filled symbols), and for two surfactant compositions (fraction of $C_{12}E_6$): α_{soln}=0.25 (circles) and α_{soln}=0.75 (squares). The various straight lines are drawn to guide the eye, with the slopes equal to the exponent r (see Sec. 5.6.3 for details).

corresponds to pure $C_{12}E_6$. Fig. 5.8 reveals that the mixed micelles are much smaller at 25°C than at 50°C. In addition, we find that in all four cases, for large X, $<n>_w$ scales as X^r, as suggested by the straight lines in Fig. 5.8. The exponent r is small at 25°C (r= 0.01 for α_{soln}=0.25, and r=0.17 for α_{soln}=0.75), but is larger at 50°C (r=0.35 for α_{soln}=0.25 and r=0.5 at α_{soln}=0.75). This suggests that the average mixed micellar size increases more rapidly upon the addition of surfactant (increasing X) at the higher temperatures than at the lower ones. It is noteworthy that the predicted exponent value r=0.5, at 50°C and α_{soln}=0.75, is similar to that observed experimentally in single-surfactant solutions containing large cylindrical micelles (Missel et al., 1980). This result is also consistent with our prediction in Chapter 4 that $<n>_w \sim X^{0.5}$ for mixed micelles which exhibit *significant growth* into cylindrical aggregates. It is interesting to note that a value of r=0.4 was recently proposed theoretically by Ben-Shaul et al. (1986). Clearly, a precise experimental determination of the exponent r, utilizing scattering techniques (light, neutrons), is needed to test these predictions. Work along these lines is in progress and will be reported elsewhere (Puvvada et al., 1991c).

5.6.4 Coexistence Curve and Cloud-Point Curve

As described in Sec. 5.5.3, the cloud-point curve and the coexistence curve are expected to be identical only if the two surfactant species partition equally between the two coexisting micellar phases. That is, the two curves should coincide if the composition of the micellar-poor phase α_Y is equal to that of the micellar-rich phase α_Z. Since coexistence-

curve measurements are tedious and time consuming, we first tested whether $\alpha_Y = \alpha_Z$, which, if satisfied, would imply that it is sufficient to measure cloud-point curves (a simpler and less time consuming task) rather than coexistence curves. To test this possibility, we performed coexistence-curve measurements of aqueous solutions of $C_{12}E_6$-$C_{10}E_6$ at $\alpha_{soln} = 0.7$. Note that the $C_{12}E_6$-$C_{10}E_6$ mixture was chosen because we expected, based on the theoretically predicted coexistence curve, that the largest difference in α_Z-α_Y (if any) should occur for this system. The conducted measurements (using chromatographic analysis described in Sec. 5.5.3.2) did show that α_Y and α_Z are equal within experimental error. Specifically, the composition of the micellar-rich phase α_Z was found to be 0.7 ± 0.005 and the composition of the micellar-poor phase α_Y was found to be 0.7 ± 0.01. As emphasized above, this equality of α_Y and α_Z suggests that the cloud-point curve and the coexistence curve should be identical. Accordingly, below we present results of cloud-point curve measurements (for various values of α_{soln}) for the three surfactant mixtures considered earlier.

Figs. 5.9, 5.10, and 5.11 show the measured cloud-point curves of aqueous solutions of the three surfactant mixtures $C_{12}E_6$-$C_{12}E_8$, $C_{12}E_6$-$C_{10}E_6$ and $C_{12}E_6$-$C_{10}E_4$, respectively, for various values of α_{soln}, the fraction of $C_{12}E_6$ in each mixture, indicated by the number next to each curve. As expected, for all three mixtures, the cloud-point curves lie between those corresponding to the constituent pure surfactant solutions. Thus, in Figs. 5.9 and 5.10, as the fraction of $C_{12}E_6$ in the mixture is increased (note that $\alpha_{soln} = 1$ corresponds to pure $C_{12}E_6$), the cloud-point curves move to lower temperatures. In Fig. 5.11, for the system $C_{12}E_6$-$C_{10}E_4$, the cloud-point curves move to higher temperatures as the fraction of $C_{12}E_6$ is increased.

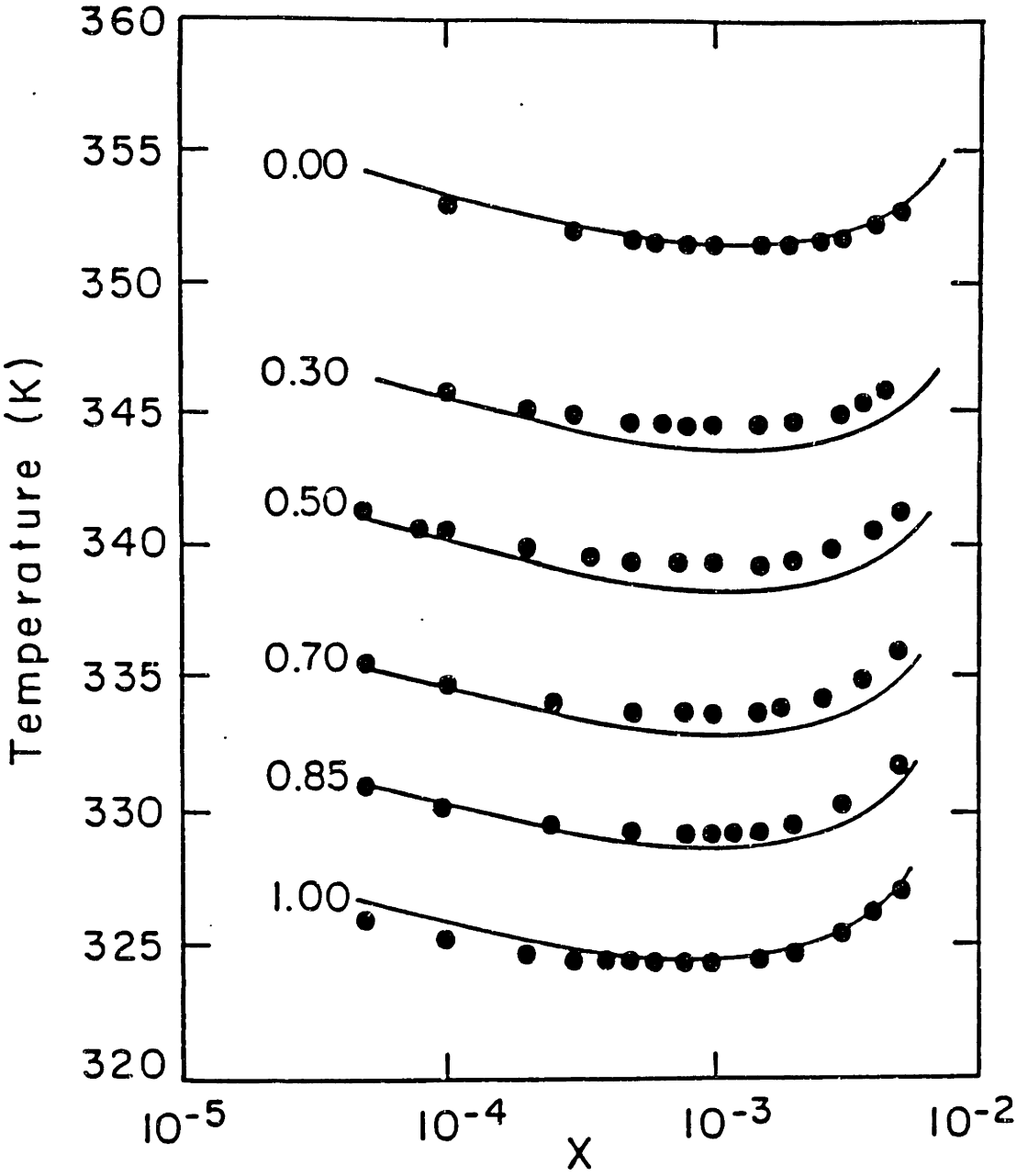

Figure 5.9 Predicted coexistence curves (lines) and experimentally measured cloud-point temperatures (●), corresponding to various total surfactant mole fractions X, of aqueous solutions of $C_{12}E_6$-$C_{12}E_8$ for various values of α_{soln}, the fraction of $C_{12}E_6$ in the mixture. The number next to each theoretical line denotes both the value of α_{soln}, corresponding to the measured cloud-point temperatures, as well as of the composition of the micellar-rich phase α_Z used to predict each coexistence curve.

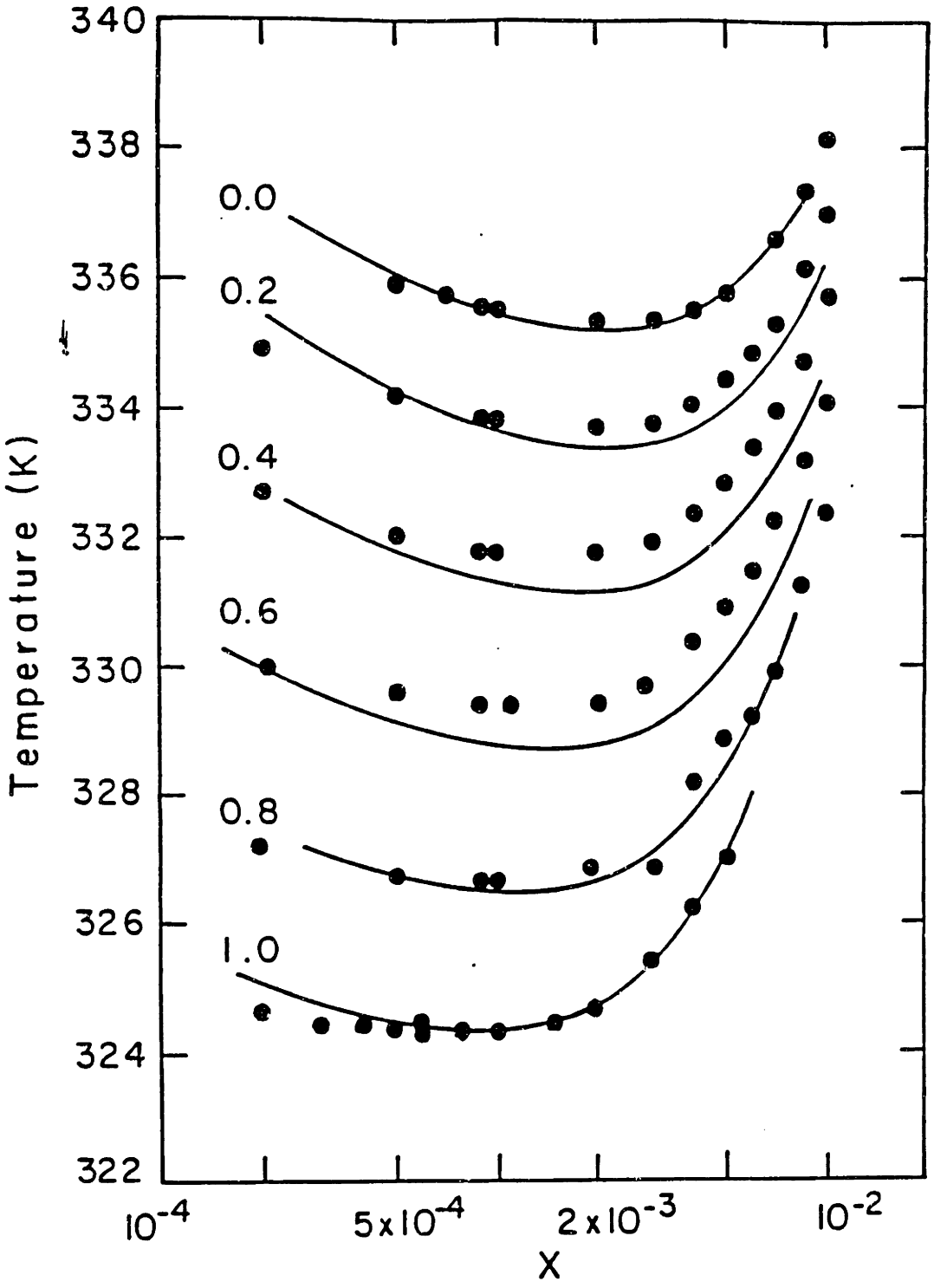

Figure 5.10 Predicted coexistence curves (lines) and experimentally measured cloud-point temperatures (●), corresponding to various total surfactant mole fractions X, of aqueous solutions of $C_{12}E_6$-$C_{10}E_6$ for various values of α_{soln}, the fraction of $C_{12}E_6$ in the mixture. The rest of the notation is the same as that in Fig. 5.9.

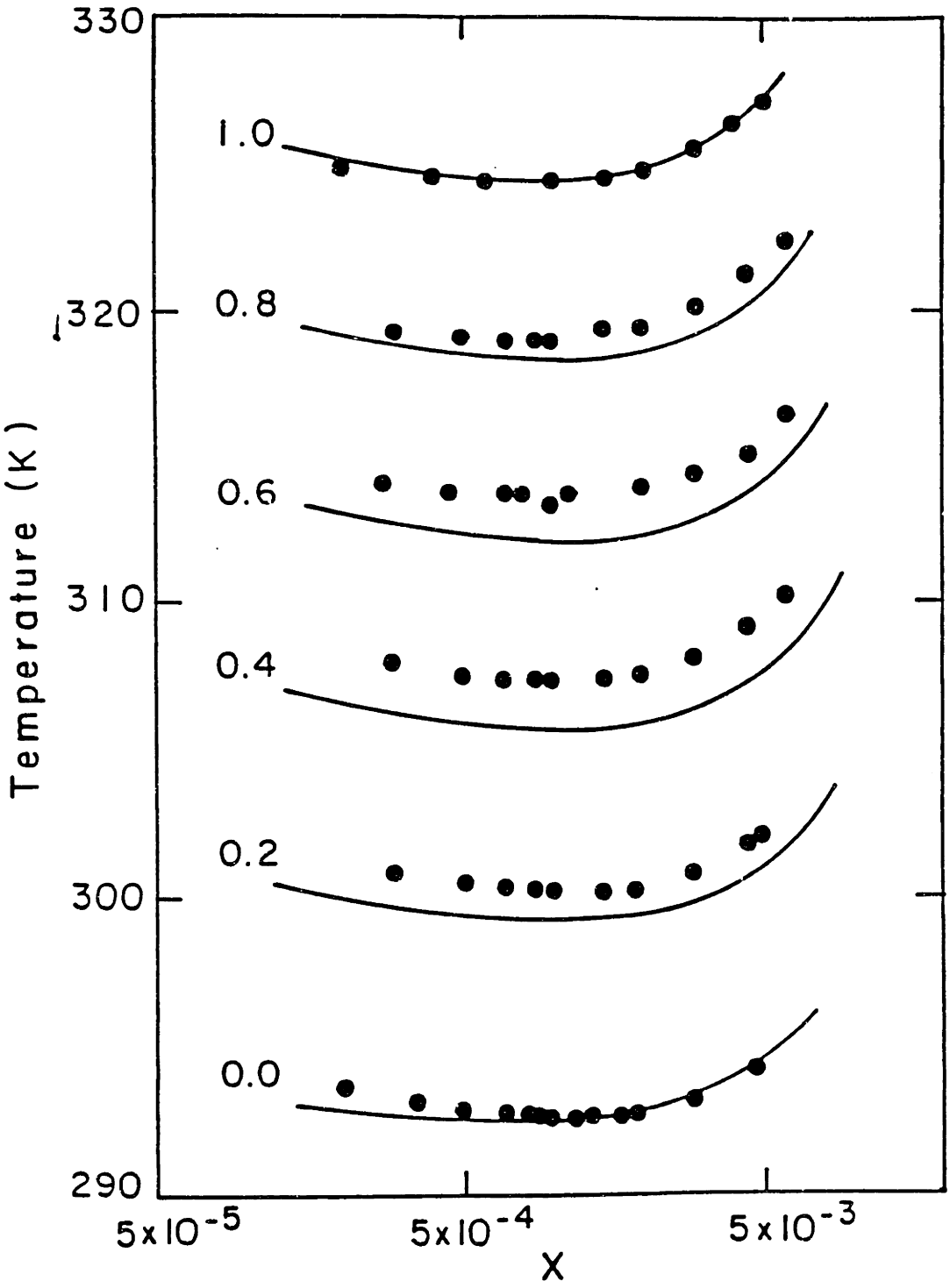

Figure 5.11 Predicted coexistence curves (lines) and experimentally measured cloud-point temperatures (●), corresponding to various total surfactant mole fractions X, of aqueous solutions of $C_{12}E_6$-$C_{10}E_4$ for various values of α_{soln}, the fraction of $C_{12}E_6$ in the mixture. The rest of the notation is the same as that in Fig. 5.11.

As discussed in Sec. 5.2, the Gibbs phase rule indicates that in a two-phase ternary solution one van vary independently three intensive variables. Therefore, we have computed the values of Y, Z, and α_Y using Eqs. (5.6a)-(5.6c) for various values of T and α_Z at a fixed pressure of 1 atm. The solid lines in Figs. 5.9, 5.10, and 5.11 are the theoretical predictions of the coexistence curves for various values of α_Z (indicated by the number next to each curve, where $\alpha_Z = 1$ corresponds to pure $C_{12}E_6$). Overall, from Figs. 5.9-5.11, it is clear that the theoretical predictions capture quite accurately the essential features of the experimentally measured cloud-point curves.

In Table 5.2, we list the predicted values of α_Z and α_Y as a function of $T-T_{cloud}^{min}$ for aqueous solutions of $C_{12}E_6$-$C_{10}E_6$, where T_{cloud}^{min} is the minimum value of T_{cloud} for a solution having a surfactant composition $\alpha_{soln} = \alpha_Z$. The values in Table 5.2 clearly show that $\alpha_Y \approx \alpha_Z$, for $T-T_{cloud}^{min} \leq 1°C$. However, as $T-T_{cloud}^{min}$ increases, the difference $\alpha_Z-\alpha_Y$ becomes larger. This suggests that when an aqueous solution of $C_{12}E_6$-$C_{10}E_6$ is allowed to phase separate, $C_{12}E_6$ partitions preferentially into the micellar-rich phase, and that the difference $\alpha_Z-\alpha_Y$ increases with increasing temperature. Note that, as emphasized earlier, $C_{12}E_6$ has a higher propensity to form micelles, and consequently a smaller fraction of $C_{12}E_6$ remains in the monomeric state. This implies, in turn, that since the micelle to monomer ratio is higher in the micellar-rich phase, $C_{12}E_6$ should partition preferentially into the micellar-rich phase as the difference between the two coexisting phases increases, that is, as $T-T_{cloud}^{min}$ increases. However, note that most of the experimental T_{cloud} measurements reported in Figs. 5.9-5.11

Table 5.2. Predicted values of α_Z and α_Y as a function of ΔT.

ΔT	0.1°C			0.5°C			1.0°C		
α_Z	0.200	0.500	0.800	0.200	0.500	0.800	0.200	0.500	0.800
α_Y	0.200	0.497	0.798	0.199	0.492	0.794	0.198	0.487	0.790

were conducted for $T-T_{cloud}^{min} < 1°C$. In other words, in the temperature range of interest, $T-T_{cloud}^{min} < 1°C$, α_Y is approximately equal to α_Z, and consequently, as emphasized earlier, a comparison of the predicted coexistence curves (solid lines in Figs. 5.9, 5.10 and 5.11) with the experimentally measured cloud-point curves is indeed appropriate.

5.7 CONCLUDING REMARKS

Solutions of surfactant mixtures provide the surfactant technologist with convenient new degrees of freedom, such as mixture type and composition, to tune and thus control micellar solution properties. In this respect, mixed micellar solutions can exhibit properties which are often substantially different, as well as more desirable, than those corresponding to solutions of the constituent single surfactants. In view of their considerable practical relevance, it has become increasingly necessary to develop a theoretical framework capable of self-consistently describing and predicting quantitatively the properties of mixed micellar solutions.

In Chapter 4, we developed a thermodynamic framework to describe and model mixed micellar solutions. A central element of this theoretical framework is the free energy of mixed micellization g_{mic}, which in Chapter 4 was treated at a simple phenomenological level. Accordingly, in Chapter 4 we could only make *qualitative* predictions of micellar solution properties. In order to provide more detailed *quantitative* predictions of mixed micellar solution properties, in the present chapter we presented a molecular model of mixed micellization to compute more accurately the contributions of the various physico-chemical factors which determine the value of g_{mic}. By blending this molecular model of mixed micellization with the thermodynamic framework, we were able to make *quantitative predictions* of a broad spectrum of mixed micellar solution properties as a function of surfactant molecular architecture, surfactant composition, and solution conditions. The predicted properties range from individual micellar characteristics, such as the CMC and the weight-average mixed micelle aggregation number, to collective properties reflected in the phase separation phenomena. These predictions have been made for aqueous solutions containing binary mixtures of nonionic surfactants belonging to the alkyl polyethylene oxide (C_iE_j) family. Specifically, the surfactant mixtures studied in this chapter include $C_{12}E_6$-$C_{12}E_8$, $C_{12}E_6$-$C_{10}E_6$, and $C_{12}E_6$-$C_{10}E_4$. The theoretical predictions of the various micellar properties described above were found to be in very good agreement with the experimentally measured properties over a wide range of solution conditions. Indeed, the theoretical framework was utilized to make predictions which compare very favorably with the experimental values over surfactant mole fractions ranging from 10^{-6} to 10^{-2},

temperatures ranging from 20-80°C, and surfactant mixture compositions ranging from pure surfactant A ($\alpha=1$) to pure surfactant B ($\alpha=0$).

A number of important issues need further clarification and development. First, the value of the exponent r, describing the variation of the weight-average mixed micelle aggregation number $<n>_w$ with total surfactant mole fraction X, deserves further attention. Is the exponent equal to 0.5 or 0.4 when the solution consists of large cylindrical mixed micelles. In this chapter, we predict that, for the $C_{12}E_6$-$C_{12}E_8$-H_2O system, r has a value of 0.5 when the mixed micelles exhibit *significant growth*. It is noteworthy that the predicted CMC's, shape transition temperatures, and coexistence curves reported in this chapter, which are all based on the same theoretical framework which leads to a value of $r=0.5$, were found to be in very good agreement with the experimental data. This seems to suggest that a value of $r=0.5$, rather than 0.4, may indeed be more appropriate for a self-consistent description of a wide range of micellar solution properties in the systems investigated. Nevertheless, an accurate independent measurement of the precise value of r is needed to further substantiate our finding. Work along these lines is in progress and will be reported elsewhere (Puvvada et al., 1991c). Second, the values of C_{AW} and C_{BW}, including their temperature dependence, were obtained by fitting the theoretical predictions to the experimentally measured coexistence curves of aqueous solutions of the constituent single surfactants. Clearly, a quantitative molecular estimation of these parameters would further enhance the predictive capabilities of the molecular-thermodynamic approach presented in this chapter. Such a molecular model should also incorporate the experimentally observed

hydration characteristics of the ethylene oxide moieties of C_iE_j nonionic surfactants. Work along these lines is also in progress.

The theoretical framework presented in this chapter can also be extended to treat *quantitatively* similar phenomena in aqueous solutions of other binary mixtures, including nonionic-ionic, nonionic-zwitterionic, zwitterionic-zwitterionic, zwitterionic-ionic, and anionic-cationic, with or without added solution modifiers such as salts and urea. The theory can also be extended to describe other more complex self-assembling surfactant systems. In particular, one could extend the theoretical formulation to describe the spontaneous formation of vesicles observed in solutions of some anionic-cationic surfactant mixtures (Kaler et al., 1989).

5.8 REFERENCES TO CHAPTER 5

Abraham, M.H. *J. Chem. Soc. Faraday Trans. 1*, **1984**, *80*, 153.

Abraham, M.H.; Matteoli, E. *J. Chem. Soc. Faraday Trans. 1*, **1988**, *84*, 1985.

Allen, M.P.; Tildesley, D.J. *Computer Simulation of Liquids*, Sec. 2.4, Oxford: Oxford, **1989**; and references cited therein.

Ben-Shaul, A.; Szleifer, I.; Gelbart, W.M. *J. Chem. Phys.* **1985**, *83*, 3597.

Ben-Shaul, A.; Rorman, D.H.; Hartland, G.V.; Gelbart, W.M. *J. Phys. Chem.* **1986**, *90*, 5277.

Ben-Shaul, A.; Szleifer, I.; Gelbart, W.M. *J. Chem. Phys.* **1987**, *86*, 1044.

Blankschtein, D.; Thurston, G.M.; Benedek, G.B. *Phys. Rev. Lett.* **1985**, *54*, 955.

Blankschtein, D.; Thurston, G.M.; Benedek, G.B. *J. Chem. Phys.* **1986**, *85*, 7268.

Briganti, G.; Puvvada, S.; Blankschtein, D. *J. Phys. Chem.* **1991**, *95*, 8989.

Carale, T.R.; Blankschtein, D. *J. Phys. Chem. in press.*

Clint, J.H. *J. Chem. Soc. Faraday Trans. 1*, **1975**, *71*, 1327.

Everett, D.H. *Colloids and Surfaces* **1986**, *21*, 41.

Flory, P.J.; in *Statistical Mechanics of Chain Molecules*, Wiley:New York, **1969**.

Flory, P.J. *Principles of Polymer Chemistry*, Cornell:Ithaca; **1986.**

Fujita, H. *Polymer Solutions*, Elsevier:Amsterdam, **1990**, p. 287.

Hamann, S.D. *Aust. J. Chem.* **1978**, *31*, 919.

Holland, P.M.; Rubingh, D.N. *J. Phys. Chem.*, **1983**, *87*, 1984.

Kaler, E.W.; Murthy, A.K.; Rodriguez, B.E.; Zasadzinski, J.A.N. *Science*, **1989**, *245*, 1371.

Lange, V.H.; *Kolloid Z.* **1953**, *96*, 131.

Meroni, A.; Pimpinelli, A.; Reato, L. *Chem. Phys. Lett.*, **1987**, *135*, 137.

Missel, P.J.; Mazer, N.A.; Benedek, G.B.; Young, C.Y.; Carey, M.C. *J. Phys. Chem.* **1980**, *84*, 1044.
Moroi, Y. *J. Colloid Interface Sci.* **1991**, *141*, 581.

Nagarajan, R. *Langmuir*, **1985**, *1*, 331.

Prigogine, I.; Defay, R. *Chemical Thermodynamics*, Longmans Green: London, **1954**.

Puvvada, S.; Blankschtein, D. *J. Phys. Chem.* **1989**, *93*, 7753.

Puvvada, S.; Blankschtein, D. *J. Chem. Phys.* **1990a** *92*, 3710; and references cited therein;

Puvvada, S.; Blankschtein, D. *Proceedings of the 8th International Symposium on Surfactants in Solution*; Mittal, K.L., Shah, D.O., Eds.; Plenum: New York, in press.

Puvvada, S.; Blankschtein, D. *submitted to J. Phys. Chem.* **1991**.

Puvvada, S.; Chung, D.S.; Thomas, H.G.; Blankschtein, D.; Benedek, G.B. *to be published.*

Rosen, M.J. *Surfactants and Interfacial Phenomena* second ed. Wiley: New York, **1989** and references cited therein.

Rubingh, D.N. *In Solution Chemistry of Surfactants,* Vol. 1, Mittal, K.L, Ed.; Plenum: New York, **1979**, p. 337.

Ruckenstein, E.; Nagarajan, R. *J. Phys. Chem.* **1975**, *79*, 2622.

Scamehorn, J.F. *Phenomena in Mixed Surfactant Systems*, ACS Symposium Series 311, ACS:Washington, **1986** and references cited therein.

Shing, K.S.; Gubbins, S.T. *Mol. Phys.* **1981**, *43*, 717.

Shinoda, K. *J. Phys. Chem.* **1954**, *58*, 541.

Stecker, M.M.; Benedek, G.M. *J. Phys. Chem.* **1984**, *88*, 6519.

Szleifer, I.; Ben-Shaul, A.; Gelbart, W.M. *J. Chem. Phys.* **1985**, *83*, 3612.

Szleifer, I.; Ben-Shaul, A.; Gelbart, W.M. *J. Chem. Phys.* **1987**, *86*, 7095.

Tanford, C. *J. Phys. Chem.* **1974**, *78*, 2469.

Tanford, C., *The Hydrophobic Effect*, Wiley:New York, **1980**.

Tolman, R.C. *J. Chem. Phys.* **1948**, *16*, 758; **1949**, *17*, 333.

Warr, G.G.; White, L.R. *J. Chem. Soc. Faraday Trans. 1*, **1985**, *81*, 549.

CHAPTER 6

REEXAMINATION OF OSMOTIC PRESSURE MEASUREMENTS OF MICELLAR SOLUTIONS

6.1 INTRODUCTION

It is universally accepted (Tombs and Peacocke, 1974) that measurements of solution osmotic pressure yield, in the limit of dilute solutions, the *number-average solute molecular weight*, $\overline{M}_n$. In this chapter, we show that due to the unique nature of micellar solutions and special features characterizing membrane osmometry in these self-assembling systems (Coll, 1970), osmotic pressure measurements can yield the *weight-average micellar molecular weight*, $\overline{M}_w$, instead of the generally accepted *number-average micellar molecular weight*, $\overline{M}_n$.

We also examine the implications of this surprising new result for the interpretation of osmotic pressure measurements aimed at determining the extent of micellar-size (molecular-weight) polydispersity. In particular, we have reevaluated available osmotic pressure data (Attwood et al., 1970) of aqueous solutions of the nonionic surfactant $C_{12}E_6$ and have found that, contrary to the original interpretation indicating the presence of monodisperse micelles, the data are consistent with the presence of large polydisperse

micelles.

6.2 CONVENTIONAL OSMOTIC PRESSURE MEASUREMENT

In a conventional osmotic pressure measurement, a *test* solution is contacted with *pure* solvent through a membrane which ideally is permeable only to the solvent. Under such conditions, the solvent will permeate through the membrane until thermodynamic equilibrium is attained, that is, until the solvent chemical potential is equal on both sides of the membrane. At fixed temperature, the solvent chemical potentials will be equal if the side containing the test solution is maintained at a pressure exceeding that of the side containing the pure solvent by the osmotic pressure, π. If π is expressed as a virial expansion in powers of the total solute concentration, c, one obtains, to quadratic order in concentration, the well-known result

$$\pi = \frac{RT}{\overline{M}_n} c + B_2 c^2, \qquad (6.1)$$

where c is the total solute concentration in units of weight/volume, B_2 is the second-virial coefficient reflecting solution non-idealities, T is the absolute temperature, and R is the gas constant.

Typically, the measured osmotic pressure data are analyzed (Tombs and Peacocke, 1974) by plotting the reduced osmotic pressure, $(\pi/RT)/c$, against c and extrapolating the resulting straight line (see Eq. (6.1)) to zero concentration. The intercept at $c=0$ yields

$1/\overline{M}_n$, and the slope yields B_2. This extrapolation procedure is meaningful only when there is no association or dissociation reaction occurring in the solution, so that $\overline{M}_n$ does not vary with concentration, c. However, in micellar solutions $\overline{M}_n$ can vary with concentration and therefore this extrapolation procedure must be implemented with great care (see Sec. 6.4).

6.3 UNIQUE CHARACTERISTICS OF MICELLAR SOLUTIONS

As described earlier, a salient feature of micellar solutions is that micelles are often present in a broad distribution of sizes, $\{X_m\}$, where X_m denotes the mole fraction of micelles composed of m surfactant monomers (m-mer). It is also essential to recognize that the entire micellar size distribution, $\{X_m\}$, and any property derived from it, for example, $\overline{M}_n$ *and* $\overline{M}_w$, necessarily respond in a reversible manner to changes in total surfactant concentration, X, and other solution conditions.

Utilizing the laws of multiple chemical equilibrium to model the reversible association of surfactant monomers into m-mers, the following expression for $\{X_m\}$ can be obtained (see Chapter 2)

$$X_m = X_1^m e^{-\beta m g_{mic}(m)} \tag{6.2}$$

where $\beta = 1/kT$ with k the Boltzmann constant, X_m and X_1 are the mole fractions of m-mers and free monomers, respectively, and $g_{mic}(m)$ is the free energy of micellization representing

the free-energy change associated with transferring a surfactant monomer from bulk water into an m-mer (see Chapter 2). Note that $g_{mic}(m)$ is not a function of X, but can depend on other solution conditions such as temperature, ionic strength, and pH.

Equation (6.2) has been widely used to predict various aspects of micellization (Mittal, 1977), and is recognized to be valid in dilute micellar solutions where intermicellar interactions are negligible. In addition, Eq. (6.2) was found to be valid for certain types of intermicellar interactions (see Chapter 2 and Blankschtein et al., 1986), suggesting that its range of applicability may in fact be quite broad.

It is possible to show that Eq. (6.2) leads to a simple mathematical relation between the weight-average micellar molecular weight,

$$\overline{M}_w = \frac{\sum_m m^2 X_m}{\sum_m m X_m} M_1 , \tag{6.3}$$

and the number-average micellar molecular weight,

$$\overline{M}_n = \frac{\sum_m m X_m}{\sum_m X_m} M_1 , \tag{6.4}$$

that is,

$$\frac{1}{M_w} = \frac{d(X/M_n)}{dX} \qquad (6.5)$$

where M_1 is the molecular weight of a surfactant monomer. Equation (6.5) is of central importance to the discussions which follow.

6.4 OSMOTIC PRESSURE MEASUREMENTS OF MICELLAR SOLUTIONS

The typical membranes used in osmotic pressure measurements are permeable to surfactant monomers, and as a result the measured pressure decreases with time as monomers permeate through the membrane into the solvent side. Under such non-equilibrium conditions the osmotic pressure is usually determined by extrapolating the measured pressure to zero-time (Coll, 1970). However, in micellar solutions the decline of pressure with time becomes rapid and concentration dependent, thus making the procedure unreliable. These non-equilibrium complications can be reduced to tolerable levels by contacting (Coll, 1970) the *test* solution with a *reference* solution having approximately the same monomer concentration as the test solution. In practice (Coll, 1970), this is achieved by choosing the reference solution to be a micellar solution having a total surfactant concentration, X', of about three times the CMC. Under this unique experimental configuration the measured pressure $\Delta\pi$ is given by

$$\Delta\pi = \pi(X) - \pi(X') , \qquad (6.6)$$

where $\pi(X)$ and $\pi(X')$ are the osmotic pressures (measured against pure solvent) of the test and reference solutions, respectively.

For the sake of brevity, we will omit hereafter second and higher-order virial corrections which are negligible in the limit of interest. Using Eq. (6.1), expressed for convenience in mole-fraction units, in Eq. (6.6) one obtains

$$\frac{\Delta\pi\Omega_s}{M_1RT} = \frac{X}{\overline{M}_n(X)} - \frac{X'}{\overline{M}_n(X')} ,$$

where Ω_s is the partial molar volume of the solvent. In micellar solutions (Coll, 1970; Attwood et al., 1970), the reduced osmotic pressure, $\overline{\Delta\pi} = (\Delta\pi\Omega_s/M_1RT)/(X-X')$, is usually plotted against $(X-X')$, and the resulting fitted line is extrapolated to $X=X'$ to obtain the average micellar molecular weight. Indeed, if one measures $\overline{\Delta\pi}$ as a function of $(X-X')$ *sufficiently close to* $X=X'$, then using Eqs. (6.5) and (6.7) at $X=X'$, one obtains

$$\lim_{X\to X'} \overline{\Delta\pi} = \frac{1}{\overline{M}_w(X')} , \qquad \textbf{(6.8)}$$

Equation (6.8) constitutes a surprising new result since it indicates that membrane osmometry in micellar solutions, conducted under the conditions stated above and analyzed

using the procedures described above[1], yields the *weight-average micellar molecular weight*, $\overline{M}_w(X')$, instead of the universally accepted *number-average micellar molecular weight*, $\overline{M}_n$.

It is of interest to examine the implications of this result on the experimental determination of average-micellar sizes and micellar-size polydispersity using membrane osmometry (Coll, 1970; Attwood et al., 1970; Birdi, 1972). A convenient measure of micellar-size polydispersity is provided by the polydispersity index, $\alpha = \overline{M}_w/\overline{M}_n$. For micellar solutions, a value of $\alpha \approx 1$ would indicate the presence of monodisperse micelles, whereas a value of $\alpha \approx 2$ would indicate the presence of large polydisperse micelles which exhibit one-dimensional growth. Typically, $\overline{M}_w$ is obtained from measurements of the absolute intensity of scattered light (Attwood et al., 1970), and $\overline{M}_n$ is obtained from colligative methods such as membrane osmometry. However, if osmotic pressure measurements, conducted as described above, are correctly interpreted as indicated above, then, it would follow that both experimental methods (light scattering and osmometry) should yield the *same* property, $\overline{M}_w$. Consequently, *a deduced value of $\alpha \approx 1$ should not be interpreted as indicating the presence of monodisperse micelles, but rather as a manifestation of experimental consistency.*

---

[1] Note that if $X' < CMC$ (including $X' = 0$), then as $X \rightarrow X'$ the test solution will only consist of monomers dispersed in water (recall that no micelles are present below the CMC). Therefore, in this case Eq.(8) will yield the monomer molecular weight, M_1.

6.5 REEXAMINATION OF AVAILABLE OSMOTIC PRESSURE DATA

The determination of the extent of micellar growth in aqueous solutions of nonionic surfactants belonging to the polyoxyethylene glycol monoether family (C_iE_j) constitutes a very important and still controversial problem (see Sec. 2.4.3). Therefore, it is of considerable interest to examine the implications of the observations made in the previous paragraph in the context of this problem.

To this end, we have reexamined available osmotic pressure data (Attwood et al., 1970) of aqueous solutions of $C_{12}E_6$. Attwood et al. (1970), measured $\Delta\pi$ in the concentration range, $1.2\text{x}10^{-3} \leq X \leq 2.5\text{x}10^{-3}$, using a reference solution having a concentration, $X' \approx 3\text{CMC} \approx 6\text{x}10^{-6}$. Subsequently, a linear fit of $\overline{\Delta\pi}$ versus $(X-X')$ was obtained and extrapolated to $X=X'$. Following common practice, the intercept at $X=X'$ was interpreted as corresponding to $1/\overline{M}_n$. Note that the experimental measurements and the subsequent linear fit were conducted at concentrations X much larger than X'. Consequently, the intercept at $X=X'$ cannot be obtained from Eq.(6.8), since, as explained above, this equation is only valid when the actual $\overline{\Delta\pi}$ measurements are performed sufficiently close to $X=X'$. Indeed, in the context of a linear extrapolation, the intercept at $X=X'$ *does not*, in general, yield $1/\overline{M}_n$ or $1/\overline{M}_w$, but instead a more complicated quantity (see Eq.(6.9) below). A careful analysis of the linear-extrapolation procedure, which accounts for the possible dependence of $\overline{M}_n$ on surfactant concentration, indicates

that for $X=X^{\bullet}$ (where $X^{\bullet} >> X'$ is an arbitrarily chosen value in the measured concentration range) this intercept is approximately given by

$$\frac{1}{\overline{M}_{eff}(X^{\bullet})} \approx \frac{2}{\overline{M}_{n}(X^{\bullet})} - \frac{1}{\overline{M}_{w}(X^{\bullet})} - 2\left[\frac{1}{\overline{M}_{n}(X^{\bullet})} + \frac{1}{\overline{M}_{n}(X')}\right]\frac{X'}{X}, \qquad (6.9)$$

Equation (6.9) clearly shows that $\overline{M}_{eff}$ depends explicitly on $X^{\bullet}$ and, in general, is different from $\overline{M}_{n}$.

Consequently, any conclusions based on the assumption that the intercept at X' is equal to $1/\overline{M}_{n}$, for example, that the micelles are monodisperse, should be carefully reexamined. For this purpose, we have calculated the osmotic pressure as a function of X and T, *allowing for micellar-size polydispersity and growth*, and have compared the predicted values with the original experimental data (Attwood et al., 1970). As can be seen from Figure 6.1, the agreement is very good suggesting that the data are in fact consistent with micellar-size polydispersity and growth.

The theoretical predictions were made in the context of the thermodynamic theory of micellar solutions presented in Chapter 2. As shown in Chapters 2 and 3, this theory has been successfully used to self-consistently predict the experimentally observed coexistence curve, average-micellar size, polydisperse micellar size distribution, and osmotic compressibility of aqueous solutions of $C_{12}E_6$ as a function of surfactant concentration and temperature, as well as the presence of solution modifiers such as urea.

In the context of this theory, the dimensionless osmotic pressure is given by

$$\beta\pi\Omega_w = -\ln(1-X) - X + M_1\frac{X}{\overline{M}_n(X)} - \frac{1}{2}\frac{C\phi^2}{\gamma}, \qquad (6.10)$$

where Ω_w is the partial molar volume of water, γ is the ratio between the molar volumes of $C_{12}E_6$ and water (approximately equal to 25), ϕ is the total volume fraction of surfactant, and C is a phenomenological interaction parameter. Utilizing results from Chapter 2, we have computed $\overline{M}_n(X,T)$ and deduced that $\gamma C/k \approx 14.3T-4220$. Using this information in Eq. (6.10) we have been able to predict, $\pi\Omega_w/RT$, as a function of surfactant concentration, X, at the three temperatures: 25°C, 30°C and 36°C (see Figure 6.1). The favorable comparison with the original data (Attwood et al., 1970) adds further support to the central claim of this chapter, that, in general, osmotic pressure measurements of micellar solutions, performed and analyzed as described above, *do not yield the number-average micellar molecular weight.*

6.5 REFERENCES TO CHAPTER 6

Attwood, D.; Elworthy, P.H.; Kayne, S.B. *J. Phys. Chem.* **1970**, *74*, 3529.

Birdi, K.S. *Kolloid-Z. u. Z. Polymere* **1972**, *250*, 731.

Blankschtein, D.; Thurston, G.M.; Benedek, G.B. *J. Chem. Phys.* **1986**, *85*, 7268

Coll, H. *J. Phys. Chem.* **1970**, *74*, 520

Mittal, K.L., Ed.; *Micellization, Solubilization and Microemulsions*, Plenum: New York, 1977,

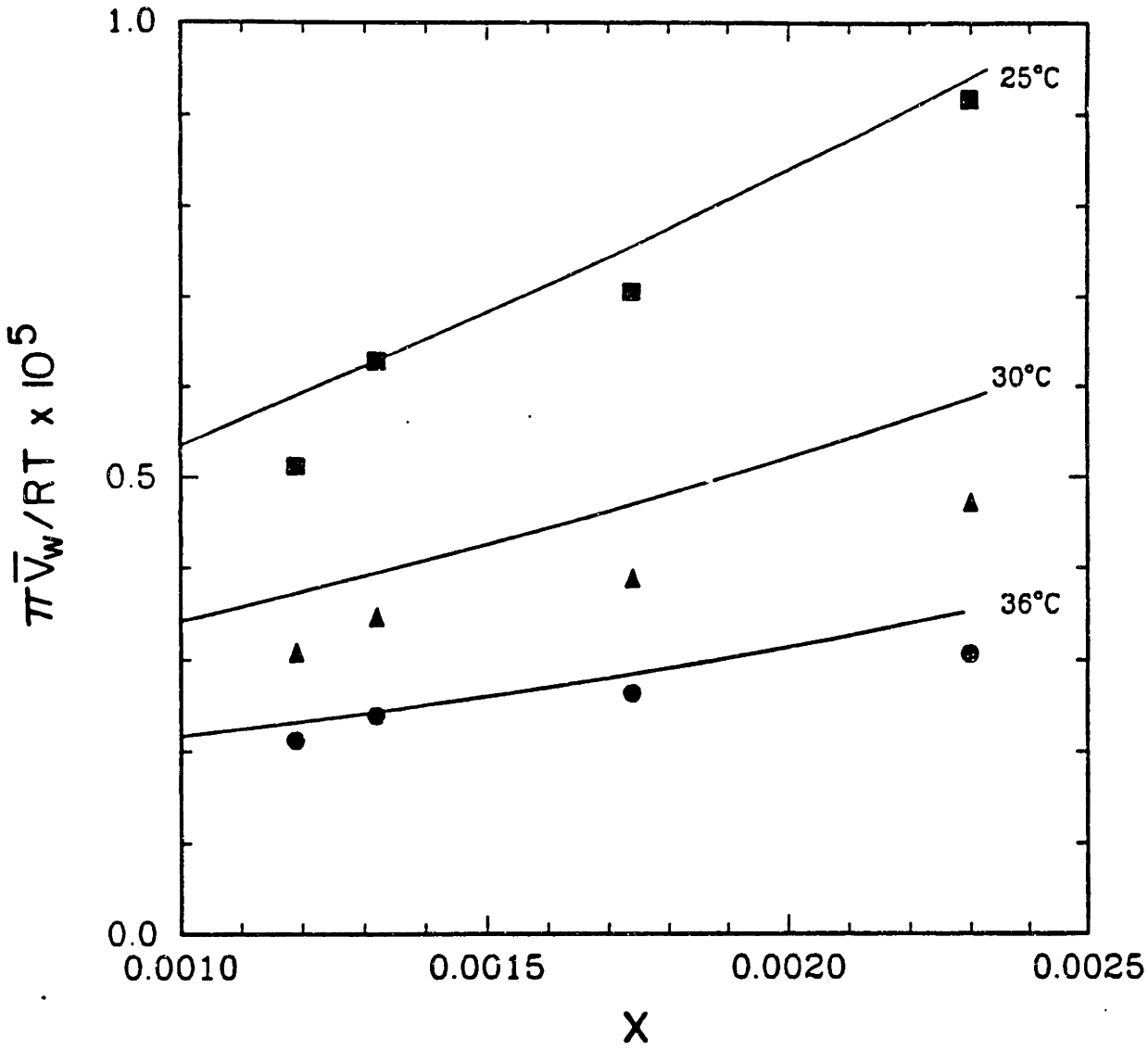

Figure 6.1 Predicted (full line) dimensionless osmotic pressure, $\pi\Omega_w/RT$, as a function of surfactant mole fraction, X, and temperature for an aqueous micellar solution of the nonionic surfactant ($C_{12}E_6$). The experimental points are from Attwood et al. (1970), and correspond to 25°C (■), 30°C (▲), and 36°C (●).

Vols. 1 and 2.

Tombs, M.P.; Peacocke, A.R. *The Osmotic Pressure of Biological Macromolecules*; Clarendon Press: Oxford, 1974.

CHAPTER 7

CONCLUDING REMARKS

Aqueous micellar solutions of single and mixed surfactants are currently the subject of intense experimental study. Consequently, a growing body of detailed information is becoming available on micelle formation and growth, micellar size and composition distribution, critical micellar concentration, and micellar phase behavior including phase separation. In view of these experimental developments it becomes increasingly necessary to develop a theoretical approach capable of unifying the rich variety of seemingly unrelated experimental findings into a single coherent computational framework. It has been the purpose of this thesis to contribute to this much needed theoretical unification.

In spite of recent significant advances in our understanding of the nature of intermolecular forces, we do not yet possess all the required microscopic information to carry out a purely statistical mechanical calculation of the partition function and associated free energy of a micellar solution. Needless to say, such a calculation would also involve formidable computational challenges.

Instead of following a purely microscopic approach, in this thesis, we have developed a new approach which consists of blending a thermodynamic theory of micellar solutions, which reflects the salient features of these complex fluids at the macroscopic level, with a

molecular model of micellization, which captures the numerical magnitude of the essential physical forces responsible for micelle formation and growth. The resulting theoretical approach has been utilized to *describe and predict self-consistently* a broad spectrum of micellar solution properties which include the CMC, the micellar shape, size and composition, the osmotic pressure and osmotic compressibility, and the phase separation phenomena.

In particular, in Chapter 2, we have applied the molecular-thermodynamic approach to predict micellar properties of single-surfactant solutions consisting of nonionic surfactants belonging to the alkyl polyethylene oxide (C_iE_j) and glucoside families. The predictions range from individual micellar properties such as the CMC and the micellar size distribution to the collective properties of the solution such as the phase behavior and phase separation. The predictions were made for surfactant mole fractions ranging from 10^{-6} to 10^{-2}, and temperatures ranging from 0-100°C for a number of surfactants.

In Chapter 3, the theory was utilized to describe the effect of urea on the properties of aqueous solutions of the nonionic surfactant $C_{12}E_6$. In particular, the theory successfully predicted the following experimentally observed effects of adding urea: (i) increase in the value of the CMC, (ii) smaller average micellar aggregation number, (iii) increase in the value of the sphere-to-cylinder transition temperatures, and (iv) shift in the critical point to higher temperatures and surfactant concentrations.

In Chapters 4 and 5, the theoretical approach was generalized to describe aqueous solutions of surfactant mixtures. The generalized thermodynamic theory developed in Chapter 4 was used in conjunction with a simple phenomenological model of mixed

micellization to *qualitatively predict* the critical micellar concentration, the micellar size and composition distribution, and the phase behavior and phase separation of solutions containing mixtures of nonionic-nonionic, nonionic-ionic, zwitterionic-ionic, anionic-cationic, and hydrocarbon-fluorocarbon based surfactants. The theory has also clarified the molecular basis of some of the synergistic and antagonistic interactions which were described in earlier works using empirical parameters. The theory also predicts that the same synergistic interactions which result in smaller CMC values, as compared to those of the constituent single surfactants, also lead to larger micellar sizes. Regarding the phase separation, the theory successfully predicts that in aqueous nonionic surfactant solutions the entire two-phase region should shrink with the addition of small amounts of ionic surfactants. In addition, it predicts that the compositions of the coexisting phases can be significantly different depending on the nature of the two surfactants. Specifically, in nonionic-ionic surfactant mixtures, the ionic surfactant preferentially partitions into the dilute micellar-poor phase in order to minimize electrostatic repulsions. In Chapter 5, we presented a detailed molecular model of mixed micellization to compute more accurately the contributions of the various physico-chemical factors which control micelle formation. By blending the molecular model of mixed micellization with the thermodynamic theory of mixed micellar solutions, we were able to make *quantitative predictions* of a broad spectrum of properties of aqueous solutions containing binary mixtures of nonionic surfactants belonging to the C_iE_j family. The theoretical predictions were found to be in very good agreement with the experimentally measured properties for binary surfactant mixtures of $C_{12}E_6$-$C_{12}E_8$, $C_{12}E_6$-$C_{10}E_5$, and $C_{12}E_6$-$C_{10}E_4$.

In Chapter 6, we presented a rather unusual manifestation of the self-assembling nature of micellar solutions. In particular, we showed that the conventional method of measuring and analyzing the osmotic pressure of a micellar solution yields the weight-average micellar molecular weight rather than the conventionally expected number-average micellar molecular weight.

The theoretical approach developed in this thesis can be extended to treat similar phenomena in other, more complex, self-assembling surfactant systems. It is clear that by including electrostatic interactions our analysis can be extended to predict properties of surfactant solutions containing ionic and zwitterionic surfactants, with or without added salts. The presence of other solution modifiers, both organic and inorganic, can also be incorporated into the theoretical framework. The theory can also be extended to describe more complex self-assembling microstructures. In particular, one could extend the formulation presented in this thesis to describe the spontaneous formation of vesicles in solutions containing anionic-cationic surfactant mixtures.

A number of important issues need further clarification and development. First, the microscopic origin and the associated theoretical modelling of the intermicellar interaction parameter C introduced in Chapters 2 and 3, as well as the parameters C_{AW}, C_{BW}, and C_{AB} introduced in Chapter 4, deserve further attention. In this thesis, we obtained the values of these parameters from the measured coexistence curves, without providing a detailed molecular description of the various intermolecular forces. Clearly, a more quantitative molecular estimation of these parameters would further enhance the predictive capabilities of the molecular-thermodynamic approach presented in this thesis. Such a molecular model

should also incorporate the experimentally observed hydration characteristics, including the effect of temperature and solution modifiers such as urea, of the ethylene oxide moieties of C_iE_j nonionic surfactants.

Second, the temperature-dependent conformations adopted by the hydrated ethylene oxide heads of C_iE_j nonionic surfactants represents another outstanding unresolved problem. In this thesis, we have developed simple scaling-type arguments, in conjunction with an assumed linear temperature dependence, to model these complex conformational effects. What is the molecular origin of hydration and how does temperature and solution modifiers (urea, salts) affect it are some of the important challenging issues which need to be resolved.

Finally, the statistical-mechanical calculations associated with evaluating the conformational free energy of the surfactant tails in the micellar interior are computationally intensive. The single-chain approach utilized in this thesis is only feasible for linear hydrocarbon chains shorter than C_{20}. For longer or branched chains, less numerically intensive approaches need to be developed.

In conclusion, we would like to reiterate that the molecular-thermodynamic formulation developed in this thesis is *predictive* in nature. As such, we believe that beyond its fundamental value, this theoretical framework can be utilized effectively by the surfactant technologist to identify, select, and possibly even tailor new surfactants for a particular application without the need of performing routine and expensive measurements of a large number of equilibrium micellar solution properties. These possibilities appear particularly relevant in times when the search for new biodegradable and environmentally-safe surfactants is being vigorously pursued.

CHAPTER 8

CUMULATIVE REFERENCES

Abraham, M.H. *J. Chem. Soc., Faraday Trans. 1*, **1984**, *80*, 153.

Abraham, M.H.; Matteoli, E. *J. Chem. Soc. Faraday Trans. 1*, **1988**, *84*, 1985.

Abu Hamdiyyah, M.; Al Mansour, L. *J. Phys. Chem.* **1979**, *17*, 2236.

Ali, A.A.; Mulley, B.A. *J. Pharm. Pharmac.* **1978**, *30*, 205.

Allen, M.P.; Tildesley, D.J. *Computer Simulation of Liquids*, Sec. 2.4, Oxford: Oxford, **1989**; and references cited therein.

Amidon, G.L.; Yalkowsky, S.H.; Anik, S.T.; Valvani, S.C. *J. Phys. Chem.* **1975**, *79*, 2239.

Attwood, D.; Elworthy, P.H.; Kayne, S.B. *J. Phys. Chem.* **1970**, *74*, 3529.

Attwood, D.; Elworthy, P.H.; Kayne, S.B. *J. Phys. Chem.* **1975**, *75*, 2212.

Aveyard, R.; Briscoe, B.J.; Chapman, J. *J. Chem. Soc. Faraday Trans. 1*, **1972**, *68*, 10.

Barry, B.W.; Morrison, J.C.; Russel, G.F.J. *J. Colloid Interface Sci.* **1970**, *33*, 554.

Baglioni, P.; Ferroni, E.; Kevan, L. *J. Phys. Chem.* **1990**, *94*, 4296.

Becher, P. *in Nonionic Surfactants*, Shick, M.J., Ed.; Arnold: London, **1967**, p. 478.

Ben-Shaul A.; Gelbart, W.M. *J. Phys. Chem.* **1982**, *86*, 316.

Ben-Shaul, A.; Gelbart, W.M. *An ev. Phys. Chem.* **1985**, *36*, 179.

Ben-Shaul, A.; Szleifer, I.; Gelbart, W.M. *J. Chem. Phys.* **1985**, *83*, 3597.

Ben-Shaul, A.; Rorman, D.H.; Hartland, G.V.; Gelbart, W.M. *J. Phys. Chem* **1986**, *90*, 5277.

Ben-Shaul, A.; Szleifer, I.; Gelbart, W.M. *J. Chem. Phys.* **1987**, *86*, 1044.

Birdi, K.S. *Kolloid-Z. u. Z. Polymere* **1972**, *250*, 731.

Blankschtein, D.; Thurston, G.M.; Benedek, G.B. *Phys. Rev. Lett.* **1985**, *54*, 955.

Blankschtein, D.; Thurston, G.M.; Benedek, G.B. *J. Chem. Phys.* **1986**, *85*, 7268.

Blankschtein, D.; Puvvada, S. *MRS Symposium Proceedings* **1990**, *177*, 129.

Bockris, J.O'M.; Reddy, A.K.N. *Modern Electrochemistry*, Plenum:New York, **1977**.

Bordi, F.; Cametti, C.; Di Biasio, A. *J. Phys. Chem.* **1988**, *92*, 4772.

Briganti, G.; Puvvada, S.; Blankschtein, D. *J. Phys. Chem.* **1991**, *95*, 8989.

Brown, W.; Rymden, R. *J. Phys. Chem.* **1987**, *91*, 3565.

Buff, F.P. *J. Chem. Phys.* **1951**, *19*, 1591.

Buff, F.P. *in Handbuch der Physik*, Flugge, S. Ed.; Springer:Berlin, **1960**, vol 10, p. 1.

Cabane, B. *J. Physique.* **1981**, *42*, 847 1981.

Carale, T.R.; Blankschtein, D. *J. Phys. Chem.* **1990**, *in press*.

Carvalho, B.L.; Briganti, G.; Chen, S-H. *J. Phys. Chem.* **1989**, *93*, 4282.

Clint, J.H. *J. Chem. Soc. Faraday Trans. 1*, **1975**, *71*, 1327.

Coll, H. *J. Phys. Chem.* **1970**, *74*, 520

Corkill, J.M.; Goodman, J.F.; Harrod, S.P.; Tate, J.R. *Trans. Faraday Soc.* **1967**, *63*, 2460.

Corkill, J.M.; Goodman, J.F.; Walker, T.; Wyer, J. *Proc. R. Soc. London Ser. A* **1969**, *312*, 243.

Corkill, J.M.; Walker, T. *J. Colloid Interface Sci.* **1972**, *39*, 621.

Corti M.; Degiorgio, V. *J. Phys. Chem.* **1981**, *85*, 711.

Corti, M.; Minero, C.; Degiorgio, V. *J. Phys. Chem.* **1984**, *88*, 309.

Corti, M.; Degiorgio, V.; Cantu, L. *in Physics of Complex and Supermolecular Fluids*, Safran, S., Clark, N., Eds.; Wiley: New York **1987**, p. 463.

Das Gupta, P.K.; Moulik, S.P. *Coll. Polym. Sci.* **1989**, *267*. 246.

Defay R.; Prigogine, I. *Surface Tension and Adsorption*, Longmans: London, **1966**.

Degiorgio, V.; Corti, M., Eds.; *Proceedings of the International School of Physics Enrico Fermi - Physics of Amphiphiles: Micelles, Vesicles and Microemulsions*, North-Holland Physics Publishing: The Netherlands, **1985**.

Degiorgio, V. *in Proceedings of the International School of Physics Enrico Fermi - Physics of Amphiphiles: Micelles, Vesicles and Microemulsions*, Degiorgio, V.; Corti, M. Eds.; North-Holland Physics Publishing: The Netherlands, **1985**. p. 303.

Dietler, G.; Cannell, D.S. *Phys. Rev. Lett.* **1988**, *60*, 1852.

Emerson, M.F.; Holtzer, A. *J. Phys. Chem.* **1967**, *71*, 3320.

Enea, O.; Jolicoeur, C. *J. Phys. Chem.* **1982**, *86*, 3370.

Eriksson, J.C.; Ljunggren, S.; Henriksson, U. *J. Chem. Soc. Faraday Trans. 2*, **1985a**, *81*, 833.

Eriksson, J.C.; Ljunggren, S. *J. Chem. Soc. Faraday Trans. 2*, **1985b**, *81*, 1209.

Evans, H.; Tildesley, D.J.; Leng, C.A. *J. Chem. Soc. Faraday Trans.* **1987**, *83*, 1525.

Farrell, R.A. *Ph.D. Dissertation*, University of Florida **1988**.

Fisher, M.P.A.; Wortis, M. *Phys. Rev. B* **1984**, *29*, 6252.

Flory, P.J. *Statistical Mechanics of Chain Molecules*, Wiley: New York, **1969**.

Flory, P.J. *Principles of Polymer Chemistry*, Cornell:Ithaca; **1986**.

Franks, F., Ed.; *Water: A Comprehensive Treatise*; Plenum: New York, **1978**; Vol. 4; and references therein.

Franks, H.S.; Franks, F. *J. Chem. Phys.* **1968**, *48*, 4746.

Fowler R.; Guggenheim, E.A. *Statistical Thermodynamics*, Cambridge: London, **1965**.

Fujimatsu, H.; Ogasawara, S.; Kuroiwa, S. *Coll. Polym. Sci.* **1988**, *266*, 594.

Fujita, H. in *Polymer Solutions*, Elsevier:Amsterdam, 1990, p. 287 and 311.

Funasaki, N.; Hada, S. *J. Phys. Chem.* **1979**, *83*, 2471.

Gabrielli, G. *Personal Communication.*

Gibbs, J.W. *The Scientific Papers of J.W. Gibbs,* Dover: New York, **1961**, Vol. 1, p. 219-258.

Goldstein, R.E. *J. Chem. Phys.* **1986**, *84*, 3367.

Goodrich, F.C. *Trans. Faraday Soc.* **1968**, *64*, 3403.

Grant, E.H.; Keefe, S.K.; Shack, R. *Advan. Mol. Relaxation Processes* **1972**, *4*, 217.

Gruen, D.W.R. *J. Phys. Chem.* **1985**, *89*, 146, 153.

Guggenheim, E.A. *Mixtures: The Theory of the Equilibrium Properties of Some Simple Classes of Mixtures, Solutions and Alloys*, Clarendon: Oxford, **1952**.

Hall, D.G.; Pethica, B.A. in *Nonionic Surfactants*. Shick, M.J. Ed.; Plenum: New York, **1984**.

Hamann, S.D. *Aust. J. Chem.* **1978**, *31*, 919.

Han, S.K.; Lee, S.M.; Schott, H. *J. Colloid Interface Sci.* **1988**, *126*, 393.

Han, S.K.; Lee, S.M.; Kim, M.; Schott, H. *J. Colloid Interface Sci.* **1989**, *132*, 444.

Handa, T.; Mukerjee, P. *J. Phys. Chem.* **1981**, *85*, 3916.

Hashimoto, T.; Sasaki, K.; Kawai, H. *Macromolecules*, **1984**, *17*, 2812.

Henderson J.R.; Rowlinson, J.S. *J. Phys. Chem.* **1984**, *88*, 6484.

Hermann, R.B. *J. Phys. Chem.* **1972**, *76*, 2754.

Holland, P.M.; Rubingh, D.N. *J. Phys. Chem.* **1983**, *87*, 1984.

Holland, P.M. *In Structure/Performance Relations in Surfactants*; Rosen, M.J., Ed.; ACS Symposium Series: Washington, D.C., **1984**; p. 141.

Holland, P.M. *Adv. Colloid Interface Sci.* **1986**, *26*, 111.

Huang, Y.X.; Thurston, G.M.; Blankschtein, D.; Benedek, G.B. *J. Chem. Phys.* **1990**, *92*, 1956.

Israelachvili, J.N.; Mitchell, D.J.; Ninham, B.W. *J. Chem. Soc. Faraday Trans. 2*, **1976**, *72*, 1525.

Israelachvili, J.N. *Intermolecular and Surface Forces*; Academic: New York, **1985.**

Jiding, X.; Zhengyu, H. *in Surfactants in Solution*, Mittal, K.L., Bothorel, p., Eds.; Plenum: New York, **1986**, vol. 5, p. 1055.

Jost, F.; Lieter, H.; Schwuger, M.J. *Coll. Polym. Sci.* **1988**, *266*, 554.

Kaler, E.W. **1991**, *Personal Communication.*

Kaler, E.W.; Murthy, A.K.; Rodriguez, B.E.; Zasadzinski, J.A.N. *Science*, **1989**, *245*, 1371.

Kamrath, R.F.; Frances, E.I. *Ind. Eng. Chem. Fundam.* **1983**, *22*, 330.

Karlstrom, G. *J. Phys. Chem.* **1985**, *89*, 4962.

Kimura, H.; Nakano, H. *J. Phys. Soc. Japan*, **1977**, *43*, 1477.

Kjellander, R.; Florin, E. *J. Chem. Soc., Faraday Trans. 1*, **1981**, *77*, 2053.

Kjellander, R.; *J. Chem. Soc. Faraday Trans. 2*, **1982**, *78*, 2025.

Koenig, F.O. *J. Chem. Phys.* **1950**, *18*, 449.

Koppel, D.E. *J. Chem. Phys.*, **1972**, *57*, 4814.

Kuharski, R.A.; Rossky, P.J. *J. Am. Chem. Soc.* **1984**, *106*, 5786, 5794.

Lang, J.C.; Morgan, R.D. *J. Chem. Phys.* **1980**, *73*, 5849.

Lange, V.H. *Kolloid, Z.* **1953**, *96*, 131.

Lange, V.H.; Beck, K.H. *Kolloid-Z. u. Z. Polymere* **1973**, *251*, 424.

Leng, C.A. *J. Chem. Soc. Faraday Trans. 2* **1985**, *81*, 145.

Lindman, B,; Karlstrom, G. *Z. Phys. Chem. Neue Folge* **1987**, *155*, 199.

Ljunggren S.; Eriksson, J.C. *Prog. Coll. Polym. Sci.* **1987**, *74*, 38.

Lupis, C.H.P. *Chemical Thermodynamics of Materials*; North-Holland:New York, **1983** ch XI.

Marszall, L.; *Langmuir*, **1988**, *4*, 90.

Mazer, N.A.; Benedek, G.B.; Carey, M.C. *J. Phys. Chem.*, **1976**, *80*, 1075.

Mazer, N.A.; Carey, M.C.; Kwasnick, R.F.; Benedek, G.B. *Biochemistry* **1979**, *18*, 3064.

McAuliffe, C. *J. Phys. Chem.* **1966**, *70*, 1267.

Meguro, K.; Takasawa, Y.; Kawahashi, N.; Tabata, Y.; Ueno, M. *J. Colloid Interface Sci.* **1981**, *83*, 50.

Meroni, A.; Pimpinelli, A.; Reato, L. *Chem. Phys. Lett.*, **1987**, *135*, 137.

Missel, P.J.; Mazer, N.A.; Carey, M.C.; Benedek, G.B. In *Solution Behavior of Surfactants*, Vol. 1; Mittal, K.L., Fendler, E.J., Eds.; Plenum: New York, **1982**; pp. 373.

Missel, P.J.; Mazer, N.A.; Benedek, G.B.; Young, C.Y.; Carey, M.C. *J. Phys. Chem.* **1980**, *84*, 1044.

Missel, P.J.; Mazer, N.A.; Carey, M.C.; Benedek, G.B. *to be published.*

Mitchell, D.J.; Tiddy, G.J.T.; Waring, L.; Bostock, T.; McDonald, M.P. *J. Chem. Soc. Faraday Trans. 1* **1983**, *79*, 975; and references cited therein.

Mitchell, D.J.; Ninham, B.W. *J. Phys. Chem.* **1983**, *87*, 2996.

Mittal, K.L., Ed.; *Micellization, Solubilization and Microemulsions*, Plenum: New York, 1977, Vols. 1 and 2.

Mittal, K.L.; Lindman, B. Eds.; *Surfactants in Solution*, Plenum: New York, **1984**, vols. 1, 2, and 3.

Moroi, Y. *J. Colloid Interface Sci.* **1991**, *141*, 581.

Morrison, R.T.; Boyd, R.N. *Organic Chemistry* Allyn and Bacon: Boston, **1983**.

Mukerjee, P.; Mysels, K.J. *Critical Micelle Concentration of Aqueous Surfactant Systems*, NSRDS-NBS 36, U.S. Dept. of Commerce: Washington, D.C. **1971**.

Mukerjee, P. *J. Phys. Chem.* **1972**, *76*, 565.

Mukerjee, P.; Handa, T. *J. Phys. Chem.* **1981**, *85*, 2298.

Muller, N. *J. Phys. Chem.* **1990**, *94*, 3856.

Muller, N. *Acc. Chem. Res.* **1990**, *23*, 23.

Mulley, B.A.; Metcalf, A.D. *J. Colloid Sci.* **1962**, *17*, 523.

Mulley, B. *in Nonionic Surfactants* Shick, M.J., Ed.; Arnold: London, **1967**, p. 421.

Nagarajan, R.; Ruckenstein, E. *J. Colloid Interface Sci.* **1977**, *60*, 221.

Nagarajan, R.; Ruckenstein, E. *J. Colloid Interface Sci.* **1979**, *71*, 580.

Nagarajan, R. *Langmuir*, **1985**, *1*, 331.

Nagle, F.F.; Wilkinson, D.A. *Biophys. J.* **1978**, *23*, 159.

Nilsson, P.G.; Wennerstrom, H.; Lindman, B. *J. Phys. Chem.* **1983**, *87*, 1377.

Nilsson, P.G.; Lindman, B. *J. Phys. Chem.* **1983**, *87*, 4756.

Nilsson, P.G.; Lindman, B. *J. Phys. Chem.* **1984**, *88*, 5391.

Nishikido, N.; Moroi, Y.; Matuura, R. *Bull. Chem. Soc. Japan*, **1975**, *48*, 1387.

Nozaki, Y.; Tanford, C. *J. Biol. Chem.* **1963**, *238*, 4074.

Ono S.; Kondo, S. *in Handbuch der Physik*, Flugge, S. Ed.; Springer:Berlin, **1960**, vol. 10, p. 134.

Podo, F.; Ray, A.; Nemethy, G. *J. Am. Chem. Soc.* **1973**, *95*, 6164 1973.

Prigogine, I.; Defay, R. *Chemical Thermodynamics*, Longmans Green: London, **1954**.

Puvvada, S.; Blankschtein, D. *J. Phys. Chem.* **1989**, *93*, 7753.

Puvvada, S.; Blankschtein, D. *J. Chem. Phys.* **1990a**, *92*, 3710.

Puvvada, S.; Blankschtein, D. *Proceedings of the 8th International Symposium on Surfactants in Solution*; Mittal, K.L., Shah, D.O., Eds.; Plenum: New York, **1990b**, in press.

Puvvada, S.; Blankschtein, D. *J. Phys. Chem.* **1991a**, *submitted.*

Puvvada, S.; Blankschtein, D. *J. Phys. Chem.* **1991b**, *submitted.*

Puvvada, S.; Chung, D.S.; Thomas, H.; Benedek, G.B.; Blankschtein, D. *J. Phys. Chem.* **1991c**, *in preparation.*

Reatto, L.; Tau, M. *Chem. Phys. Lett.* **1984**, *108*, 292.

Reiss, H. *in Advances in Chemical Physics*, Prigogine, I., Ed.; Interscience: London, **1965**,

Vol. 9, p. 1.

Reynolds, J.A.; Gilbert, D.B.; Tanford, C. *Proc. Nat. Acad. Sci. U.S.A.* **1974**, *71*, 2925.

Rosch, M. *in Nonionic Surfactants*, Shick, M.J., Ed.; Arnold: London, **1967**, p. 753.

Roseman, M.; Jencks, W.P. *J. Am. Chem. Soc.* **1975**, *97*, 631.

Rosen, M.J.; Hua, X.Y. *J. Colloid Interface Sci.* **1982**, *86*, 164.

Rosen, M.J.; Hua, X.Y., *JAOCS*, **1982**, *59*, 582.

Rosen, M.J. In *Phenomena in Mixed Surfactant Systems*, Scamehorn, J.F., Ed.; ACS Symposium Series 311: Washington, D.C. **1986**; p. 144.

Rosen, M.J. In *Surfactants and Interfacial Phenomena 2nd Edition*, John Wiley: New York, **1989**; and references cited therein.

Rubingh, D.N. In *Solution Chemistry of Surfactants*, Vol. 1, Mittal, K.L., Ed.; Plenum: New York, **1979**, pp. 337.

Ruckenstein, E.; Nagarajan, R. *J. Phys. Chem.* **1975**, *79*, 2622.

Rowlinson, S.; Widom, B. *Molecular Theory of Capillarity,* Clarendon: Oxford, **1982.**

Sadaghiania, A. S.; Khan, A. *J. Colloid Interface Sci.* **1991**, *144*, 191.

Scamehorn, J.F. *Phenomena in Mixed Surfactant Systems*, ACS Symposium Series 311, ACS Press, Washington (1986); and references cited therein.

Shick, M.J. *J. Phys. Chem.* **1964**, *68*, 3585.

Shick, M.J. *J. Phys. Chem.* **1967**, *68*, 3585.

Shick, M.J. Ed.; *Nonionic Surfactants;* Arnold: London, **1967**; and references cited therein.

Shing, K.S.; Gubbins, S.T. *Mol. Phys.* **1981**, *43*, 717.

Shinoda, K. *J. Phys. Chem.* **1954**, *58*, 541.

Shinoda, K.; Yamanaka, T.; Kinoshita, K. *J. Phys. Chem.* **1959**, *63*, 648.

Shinoda, K.; Yamaguchi, T.; Hori, R. *Bull. Chem. Soc. Japan* **1961**, *34*, 237.

Souza, L.D.S.; Corti, M.; Cantu, L.; Degiorgio, V. *Chem. Phys. Lett.* **1986**, *131*, 160.

Stainsby G.; Alexander A.E. *Trans. of Faraday Soc.* **1950**, *46*, 587.

Stecker, M.M.; Benedek, G.B. *J. Phys. Chem.* **1984**, *88*, 6519.

Stokes, R.H. *Aust. J. Chem.* **1967**, *20*, 2087.

Strey, R.; Pakusch, A. In *Surfactants in Solution*, Vol. 4, Mittal, K.L., Bothorel, P., Eds.; Plenum: New York, **1986**; pp. 465.

Subramanian, S.; Sarma, T.S.; Balasubramanian, D.; Ahulawalia, J.C. *J. Phys. Chem.* **1971**, *75*, 815.

Swenson, C.A. *Arch. Biochem. Biophys.* **1966**, *117*, 494.

Szleifer, I.; Ben-Shaul, A.; Gelbart, W.M. *J. Chem. Phys.* **1985**, *83*, 3612.

Szleifer, I.; Ben-Shaul, A.; Gelbart, W.M. *J. Chem. Phys.* **1987**, *86*, 7095.

Tanford, C. *J. Am. Chem. Soc.* **1964**, *86*, 2050.

Tanford, C. *J. Phys. Chem.* **1974**, *78*, 2649.

Tanford, C. *The Hydrophobic Effect*, Wiley: New York, **1980**.

Tolman, R.C. *J. Chem. Phys.* **1948**, *16*, 758.

Tolman, R.C. *J. Chem. Phys.* **1949**, *17*, 333.

Tombs, M.P.; Peacocke, A.R. *The Osmotic Pressure of Biological Macromolecules*; Clarendon Press: Oxford, 1974.

Thurston, G.M.; Blankschtein, D.; Fisch, M.R.; Benedek, G.B. *J. Chem. Phys.* **1986**, *84*, 4558.

Valaulikar, B.S.; Manohar, C. *J. Colloid Interface Sci.* **1985**, *108*, 403.

Venkatesan, V.K.; Suryanarayana, C.V. *J. Phys. Chem.* **1956**, *60*, 775.

Vikingstad, E.; Hoiland, H. *J. Colloid Interface Sci.* **1978**, *64*, 510.

Warr, G.G.; White, L.R. *J. Chem. Soc. Faraday Trans. 1*, **1985**, *81*, 549.

Weast, R.C., Editor-in-Chief, *CRC Handbook of Chemistry and Physics*, CRC Press:Florida,

Ist Student Edition, **1987**.

Wetlaufer, D.B.; Malik, S.K.; Stoller, L.; Coffin, R.L. *J. Am. Chem. Soc.* **1964**, 86, 508.

Yoesting, O.E.; Scamehorn, J.F. *Coll. Polym. Sci.* **1986**, *264*, 148.

Zana R.; Weiil, C. *J. Physique. Lett.* **1985**, *46*, L-953.

Zhu, B.Y.; Rosen, M.J. *J. Colloid Interface Sci.* **1985**, *99*, 435.